The Dissertation Committee for Rosario Mario Fico Jr. certifies that this is the

approved version of the following dissertation:

Structure Property Relationships in Organic Biradicals

Committee:

_____

Marye Anne Fox, Supervisor

_____

Stephen E. Webber, Supervisor

_____

David A. Shultz

_____

Nathan L. Bauld

_____

Jason B. Shear

Structure Property Relationships in Organic Biradicals

by

Rosario Mario Fico, Jr. B.S., M.S.

Dissertation

Presented to the Faculty of the Graduate School of

the University of Texas at Austin

in Partial Fulfillment

of the Requirements

for the Degree of

Doctor of Philosophy

The University of Texas at Austin

December 2003

Dedication

This dissertation is dedicated to the graduate experience for providing many people with the opportunity to obtain a free graduate education. It is during this time that we truly start to learn our trade.

This dissertation is also dedicated to who ever reads this. Thank you very much.

Abdon turned me on to the world of martial arts and that experience is continually changing me. Dr. Scott Reese was always helpful and friendly in to many ways to count. Both are now unfortunately lawyers. In North Carolina, the wonderful couple of Dr. Kevin and Marina Kittredge are friends that will not be forgotten.

I want to thank all of the members of the Shultz group, both past and present. The stories I have to tell about some of them will not be forgotten. I was lucky to meet both Andy Boal, and Hyoyoung Lee as they were leaving the group. They are two very remarkable chemists. I am thankful for having worked with both Kira Vostrikova and Krishna Kumar. Both entertained me in many useful discussions about chemistry and often about their countries. Krishna Kumar and I have had many non-chemical discussions about politics and world affairs. I am grateful that Scot Bodnar was my lab mate and collaborator. There have been many members of this group since I arrived and I thank them all, but I will not name them all. However, I would like to thank the present group members, because they are the ones who are driving this research group forward: Sofi Bin-Salamon, Joe Bousquet, Candice Brannen, Jessica Queen, and Tashni Coote.

I would like to thank the University of Texas at Austin, for allowing me to come to NCSU to finish my research. The University has been very patient and helpful. I must thank North Carolina State University. They have been very thoughtful in ensuring that I have funding. In addition, their staff is top notch. Especially the electronic shop, they do wonderful job repairing our instruments and keeping everything working.

I am very grateful for the work done by the crystallographers Paul Boyle and Jeff Kampf. Both were always very helpful. In addition, Alan Pinkerton and Kristin Kirschbaum for their work in obtaining the low temperature crystal structure presented in Chapter 6. I would also like to thank all of my other collaborators.

I would also like to thank all of my friends and family who had enough confidence in me to simple say "I know you'll get it done." These words of encouragement and confidence have helped me many, many times.

R. M. F.

Structure Property Relationships in Organic Biradicals

Publication No._____

Rosario Mario Fico, Jr., Ph.D
The University of Texas at Austin, 2003

Supervisors: Marye Anne Fox, Stephen E. Webber

In this work, structure-property relationships of several organic biradical ligands are explored. A basic understanding of these relationships is important in designing new molecular magnetic materials. The utility of studying biradicals is, that they represent the simplest high-spin system with which to build upon. All of the spin groups studied are air stable and are synthetically adaptable organic radicals.

A series of bis(verdazyl) biradicals connected (at the nodal position of the verdazyl) to several different aromatic spacer groups (couplers), has been prepared to compare their properties to those of the non-spaced 1,1′,5,5′-tetramethyl-6,6′-dioxo-3,3′-bisverdazyl (**1**) and 1,1′,5,5′-tetramethyl-6,6′-dithio-3,3′-bisverdazyl (**7**). Cyclic voltammograms of 1,4-bis(1,5-dimethyl-6-oxo-3-verdazyl)benzene (**5**), 2,5-bis(1,5-dimethyl-6-oxo-3-verdazyl)thiophene (**6**), and 1,3-bis(1,5-dimethyl-6-oxo-3-verdazyl)benzene (**4**) show a single two-electron oxidation wave near 700 mV vs. SCE. In contrast **1** and **7** (non-spaced verdazyls) display two one-electron oxidation waves,

with the first oxidative wave appearing also near 700 mV vs. SCE. The absorption spectrum of each of these biradicals is red-shifted from the maximum observed for **1**. Biradicals **4**, **5**, and **6** exhibited linear Curie plots, although a curved Curie plot was observed for **7** with J = -280 cm^{-1}.

A magneto-structural correlation of conformational exchange modulation within an isostructural series of TMM-type bis(semiquinone) biradical complexes is presented. Zero-field splitting parameters, X-ray crystal structures, and variable-temperature magnetic susceptibility measurements were used to evaluate electron spin exchange in this series of molecules. Our combined results indicate that the ferromagnetic portion of the exchange coupling occurs via the cross-conjugated π-system, while the antiferromagnetic portion occurs through space and is equivalent to incipient bond formation. Molecular conformation controls the relative amounts of ferro- and antiferromagnetic contributions to exchange coupling. In fact, the exchange parameter correlates with average semiquinone ring torsion angles *via* a Karplus-Conroy-type relation: J = 213 cos$^2\phi$ - 44. This is the first clear assignment of ferro- *and* antiferromagnetic components of exchange coupling to specific molecular structure features in a series of biradicals.

The molecular structures and magnetic properties of six TMM-type dinitroxide biradicals are also described. Five of the dinitroxides are trimethylenemethane-type (TMM-type) biradicals, *i.e.*, the intramolecular exchange parameter, J, is modulated by a carbon-carbon double bond. However, the efficacy of the carbon-carbon double bond as an exchange coupler is determined by the molecular conformation. Our results show that

the exchange parameters correlate with phenyl-ring torsion angles (ϕ) via a simple Karplus-Conroy-type relation: $J = 44 \cos^2 \phi - 17$. Comparison of these results to those obtained for our isostructural series of bis(semiquinone) biradicals shows that both the magnitude of J and the resistance of ferromagnetic J to bond torsions is proportional to the spin density adjacent to the exchange coupler.

Table of Contents

List of Figures

xv

List of Tables

List of Schemes

Chapter 1. Introduction[1-7]

Magnetism – An Overview

For some, the study of magnetism brings them back to their childhood days seeing the magical flux lines while playing with a bar magnet and an Etch a Sketch[®]. For everyone, magnetism has become an integral part our lives. Magnetic interactions form the basis of most of our daily needs from: sources of electricity, simple motors and generators, medicine, and the increasingly more important information storage.[1,3] As advances in technology drive devices to smaller, faster, and cheaper, magnetic materials must also follow suit. Magnetism however, is a bulk property of a material. To understand and control the bulk magnetic properties of a material one must break the material down into its simplest components and study them. As materials shrink to the molecular level, a molecule based solution to magnetism must be reached.[1,8] The goal of this work is to study intramolecular interactions of organic biradical ligands, to strengthen the foundation for building organic-based molecular magnetic materials.

By some accounts magnetism has been known since 2600 B.C.,[3] by others magnetism was introduced to the Chinese in the 1200s by Arabs or the Italians.[4] There are also reports from 800 B.C. by Magnes the Sheppard, who had rocks that stuck to the soles of his shoes and the tip of his staff.[4] Regardless of when it was discovered, magnetism is a property of the bulk material and the basis (foundation) of magnetism is quantum mechanical in nature. A thorough understanding of magnetism could not arise until the advent of Quantum mechanics.[2,3,7]

An electron has a spin of ½, a negative charge, a mass, and through quantum mechanics we know it has a spin. Any spinning charged particle will produce a magnetic dipole. It is the interaction between the magnetic dipoles of the electrons that are not involved in chemical bonds that gives rise to bulk magnetism. Alignment of the individual magnetic dipoles in the same direction leads to a net magnetic moment. The magnetization of a material, M, is directly proportional to the applied magnetic field, H, times a constant called the magnetic susceptibility, χ, **Eq. 1.1**.[1,4-8]

$$M = c_{exp} H \qquad\qquad\qquad \textbf{Eq. 1.1}$$

A material with a positive value of χ increases the net magnetic field or, in other words, is attracted to the applied magnetic field. A negative value of χ implies that the material is repelled or decreases the magnetic field. The observed magnetic susceptibility, χ_{exp} is a sum of individual susceptibilities including paramagnetic susceptibility, χ_{para}, diamagnetic susceptibility, χ_{dia}, and Pauli susceptibility, χ_{Pauli} **Eq. 1.2**.

$$c_{exp} = c_{dia} + c_{para} + c_{Pauli} \qquad\qquad \textbf{Eq. 1.2}$$

Diamagnetic susceptibility, χ_{dia}, results from the core electrons and the paired valence electrons. Paramagnetic susceptibility, χ_{para}, arises from unpaired electrons. Pauli susceptibility, χ_{Pauli}, is the magnetic susceptibility of the conducting electrons, which does not apply to our molecules.

The molar diamagnetic susceptibility can be approximated by summing up the diamagnetic contributions of all of individual atoms and bonds in the molecule. For large polymeric or biological materials the diamagnetic susceptibility must be approximated

from similar nonparamagnetic material.[1,5,6] Pascal tabulated the diamagnetic contributions of atoms and functional groups in the 1940s.[6] All molecules have a χ_{dia} contribution to the overall susceptibility. The diamagnetic susceptibility contribution to a molecule is much smaller than the paramagnetic contributions, $\chi_{dia}(10^{-6}$ emu$) << \chi_{para}(10^{-4}$ emu$)$. Experimentally we are only concerned with χ_{para}. Since the magnetic susceptibility is our experimentally observed quantity, and χ_{dia} can be calculated **Eq. 1.2** is rewritten as **Eq. 1.3**.

$$c_{para} = c_{exp} - c_{dia} \qquad\qquad \textbf{Eq. 1.3}$$

Magnetic susceptibility is a unitless constant but for our work it will always be considered a molar quantity.

There are many different types of magnetic interactions but we are primarily be concerned with 5 types; diamagnetism, paramagnetism, ferromagnetism, antiferromagnetism, and ferrimagnetism. Diamagnetism and paramagnetism are general terms that describe the magnetic properties of an unordered material, **Figure 1.1**. When χ is negative ($\chi_{dia} < 0$, repelled by a field) a material is diamagnetic. Diamagnetic materials have no magnetic moment.
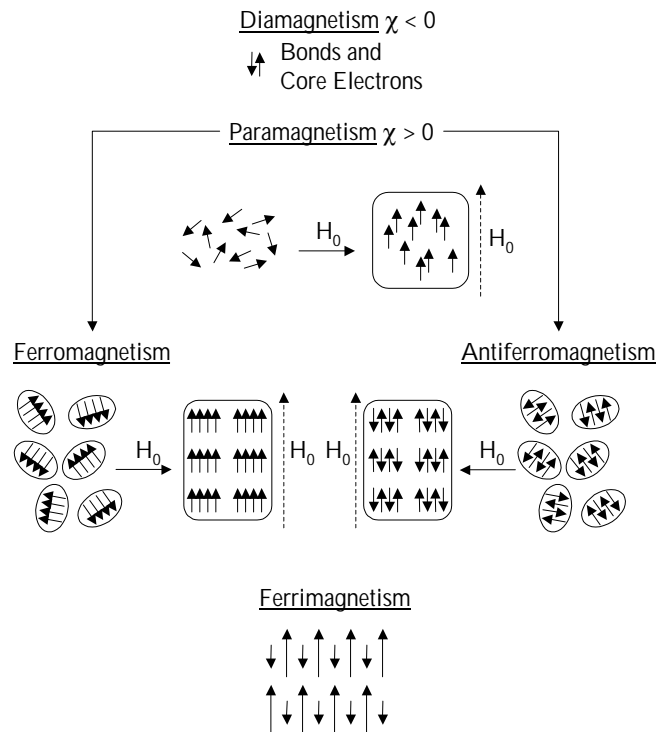
Figure 1.1. The 5 main types of magnetism: diamagnetism, paramagnetism, ferromagnetism, antiferromagnetism, and ferrimagnetism.

If there is at least one unpaired electron in a material, χ will be positive and the material is paramagnetic, **Figure 1.1**. A paramagnetic material is attracted to a magnetic field, $\chi_{para} > 0$. If the material consists of non-interacting spins it will have no net magnetic moment in the absence of an applied field, H. Application of a magnetic field will cause the spins to align. In 1895 Pierre Curie established the law that bears his name for the susceptibility of a paramagnetic substance, **Eq. 1.4**.[4,9]

$$c_{para} = \frac{C}{T} \qquad\qquad \textbf{Eq. 1.4}$$

Where C is the Curie constant and is dependent on the material, and T is temperature. Curie Law however, only explains non-interacting spins. In 1907, in what now can be considered foreshadowing of the changes to come, Pierre Weiss gave the first modern

theory of magnetism.[4,10] Weiss assumed that weak intermolecular interactions could be described by a molecular field approach. The intermolecular interactions would create a small additional magnetic field. That field would act in a similar fashion as the external field, **Eq. 1.5**, where θ is the molecular field correction for weak intermolecular interactions.

$$c = \frac{C}{T - q}$$ **Eq. 1.5**

The remaining three types of bulk magnetic behaviors describe long-range three-dimensional order in a material. A material is ferromagnetic if the individual spins all align in the same direction throughout the material. Note, that there can be domains of local order and that these domains are not necessarily aligned with respect to each other, a manifestation of entropy, **Figure 1.1**. Application of a magnetic field will cause the domains to coalesce into larger domains throughout the material. When a material is antiferromagnetic there is still alignment of nearby spins, but the alignment is opposite in direction. Finally, ferrimagnetism is the case where the spins align in an antiferromagnetic manor, but there is not complete cancellation of the spins, **Figure 1.1**.

Molecular Analogs to Bulk Magnetic Properties

These properties are the bulk properties of a material and that material is made up of domains. As materials shrink we move from observing the bulk properties of a material, to observing the individual domains, to observing the individual molecules. As chemists we consider our 'domain' to be individual molecules and thus study the molecular analogs to these types of behaviors, **Figure 1.2**. Experimentally we observe

5

χ_{para} (> 0). For the simplest system, a biradical, χ_{para} can be related to the exchange

coupling parameter, J, between the two electrons. The exchange coupling parameter is a

measure of the energy separation between the singlet and triplet energy levels, **Figure**

1.2. We are now in the realm of quantum mechanics and we need to introduce the

empirical Hamiltonian, **Eq. 1.6**. This will be discussed further in Chapter 2.

$$\hat{H} = -2J\hat{S}_a \bullet \hat{S}_b$$
Eq. 1.6

Consider the case of two spin containing substituents connected by a "coupler."

If the two spins are coupled so that both are aligned in the same direction they are

considered to be ferromagnetically coupled. By our definition of the exchange coupling

parameter, *J* would be positive indicating a spin triplet ground state. If the two spins are

coupled so that the moment of the spins are aligned opposite to each other they are said to

be antiferromagnetically coupled. The exchange parameter is negative, and the ground

state would be a spin singlet, **Figure 1.2**. An extreme form of antiferromagnetic coupling

is a covalent bond. Of course if the spins are not coupled at all the molecule behaves like

two doublets (monoradicals).

If the spins are not of the same magnitude then ferrimagnetism can result. The

combination of antiferromagnetic coupling and ferromagnetic coupling can lead to an

overall larger spin state, analogous to ferrimagnetism. Consider the case of three spins

where two S = 1 spin containing substituents are coupled by an S = ½ coupler, **Figure**

1.2. Antiferromagnetic exchange between the "coupling" spin and the two S = 1 spin

containing substituents leads to ferromagnetic exchange between the two larger spins and

an overall quartet state.
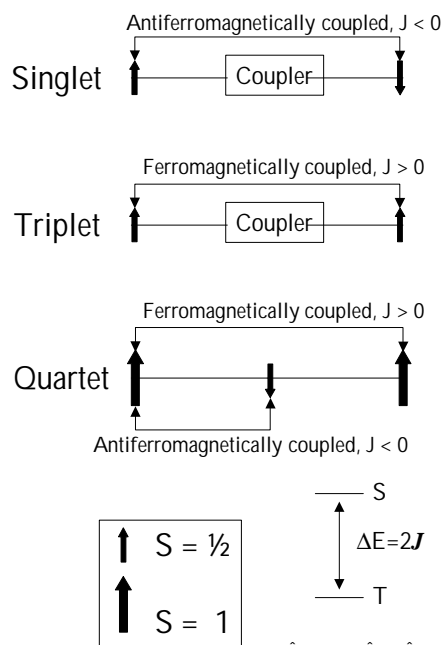
Figure 1.2. Schematic representation of ferromagnetic and antiferromagnetic coupling. The smaller arrows represent S = ½. The larger arrows represent S = 1.

Couplers that promote both ferromagnetic and antiferromagnetic interactions are known.[2,6,11-15] Note, that although the spins are said to be ferromagnetically coupled, the molecule itself is not ferromagnetic, it is just that the ground state is high-spin. Thus, ferromagnetism is a bulk property of a material, exchange coupling parameter is a molecular property.

Approaches to Molecular Magnetism

There are many approaches to studying the design and synthesis of molecular based magnetic materials. One approach is to make large macromolecular assemblies containing a large number of spins. Racja has been a leader in this area for 15 years.[15] Recently he reported a dedrimeric macromolecule with a spin value of ~5000, **Figure 1.3**. This macromolecule exhibits a blocking temperature below 10K.[16] These

macromolecular assemblies are quite challenging synthetically and are air and temperature sensitive. Our approach is to study air stable, room temperature stable biradicals. The information obtained through studying structure property relationships in biradical coupling can be used to help design macromolecular assemblies.
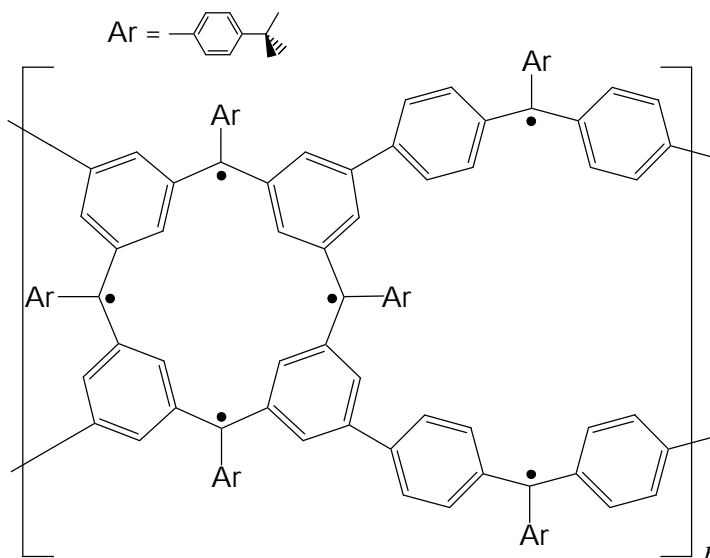
Figure 1.3. Repeating unit in Racja's macrocycle. Total S~5000.

Another approach uses organic ligands in coordination polymers. This approach allows one to study 1-D chains, 2-D sheets and 3-D assemblies. Two leaders using this area are Gatteschi in Florence, Italy,[2,13,17] and Iwamura in Japan.[14,18] These polymers typically consist of an organic coupler and a paramagnetic transition metal. Gatteschi used nitronylnitroxides (NIT) to coordinate $Cu(hfac)_2$ through the oxygens forming a linear chain, **Figure 1.4**.[17,19]
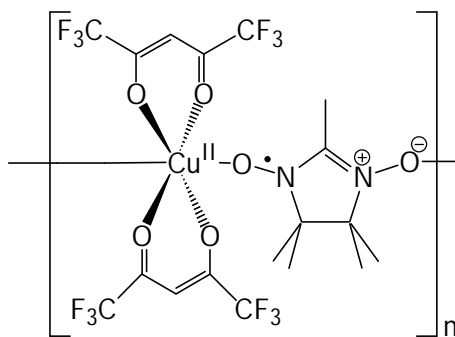
Figure 1.4. Repeating unit in Gatteschi's coordination polymer.

Iwamura used $Mn(hfac)_2$ and a high-spin bis(nitroxide) as the coupler to form his chains.
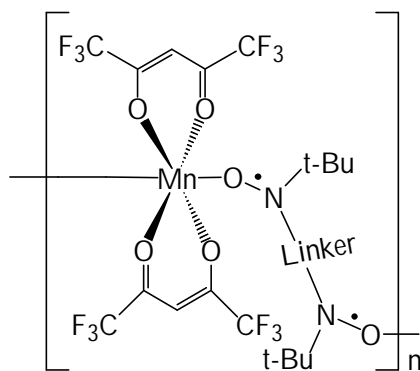
Figure 1.5. Repeating unit in Iwamura's coordination polymer.

Our approach is to study the intramolecular interactions in the biradical ligand to build up on the foundation for making polyradical systems.

We are not studying extended solids, we are taking a basic approach and studying the ligands that can be used to make extended solids.

Dissertation Outline

In discussing biradicals it is useful to discuss the electronic considerations as well as the connectivity or topological considerations in electron-electron coupling. The two electrons in a biradical will interact to form singlet states and triplet states.[6,15,20] In addition to the electronic considerations, the design elements of the organic coupler

9

connecting the two radicals will be discussed. There is a good understanding of the

design elements which promote ferromagnetic interactions in a molecule.[2,11,14,15,20]

Chapter 2 will discuss both the electronic and connectivity considerations for biradicals.

There are two very useful tools for studying radicals and magnetic materials,

Electron Paramagnetic Resonance (EPR) and Super conducting Quantum Interference

device (SQUID). Because electrons are ½ spin particles and have a large gyromagnetic

ratio, magnetic resonance techniques such as Electron Paramagnetic Resonance can be

used to provide information about the spin distribution and electron-electron coupling in

a molecule. The temperature dependence of the magnetic moment can be correlated to χ

and the exchange coupling parameter, $\textbf{\textit{J}}$. A SQUID is very useful in detecting small

magnetic moments. Chapter 3 will describe the design and use of these instruments and

how they aid our work.

Bis(verdazyl) biradicals are analogous to bipyridine rings and can bind to metal

centers through the nitrogens.[21,22] Recently both Hicks and Brook independently studied

metal complexes of the pyridine substituted monoverdazyl **1**.[23,24] Similar to bipyridine,

verdazyls and bis(verdazyl)s might make interesting coordination polymers. Fox and

Brook synthesized Cu(I) coordination polymers of bis(verdazyl) **2**.[25]

1   **2**
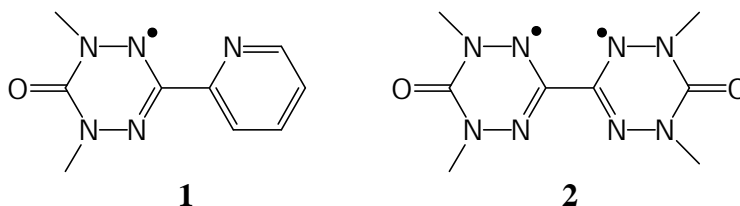
The coupling in **2** is antiferromagnetic. Using **2** as a parent compound, the

electronic characteristics of a series of spaced bis(verdazyl)s that include couplers that are

known to promote ferromagnetic coupling, as well as couplers known to promote antiferromagnetic coupling were studied. In addition, the effect of replacing the oxygens in 2 with sulfur was studied. These results are reported in Chapter 4.

Semiquinones are known to bind to most transition metals through the oxygens.[26-28] Although there are both *para* and *ortho* isomers of semiquinones we are primarily concerned with *ortho*-semiquinones such as **3** and the *ortho-* prefix will be omitted in future discussions. An isostructural series of bis(semiquinone)s that share a common ferromagnetic coupler were synthesized and the ground spin state as well as the magnitude of the exchange coupling parameter was correlated to the structural features. Chapter 5 will discuss how torsions, which modulate the amount of spin density in the coupler, can affect the coupling in TMM-linked bis(semiquinone)s.

3
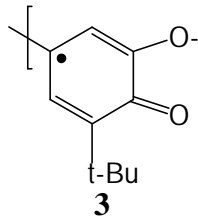
Nitroxides such as **4** can bind to metals and form 1-D or 2-D chains and sheets. Chapter 6 will discuss the effect of torsions on and isostructural series of TMM-linked bis(nitroxide)s. These results are compared to the results of the bis(semiquinone)s in Chapter 5 to provide further elucidation of the parameters affecting the nature of the exchange coupling parameter.

4
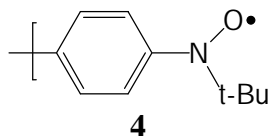
References
(1)   Jakubovics, J. P. *Magnetism and Magnetic Materials*; Second ed.; University Press: Cambridge, 1994.
(2)   Gatteschi, D., Ed. *Molecular Magnetic Materials*; Kluwer Academic Publishers: Amsterdam, 1991.
(3)   Turnbull, M. M.; Sugimoto, T.; Thompson, L. K., Eds. *Molecule-Based Magnetic Materials. Theory, Techniques, and Applications*; ACS: Washington, DC, 1996.
(4)   Mattis, D. C. *The Theory of Magnetism*; Harper & Row: New York, 1965.
(5)   Drago, R. S. *Physical Methods*.
(6)   Kahn, O. *Molecular Magnetism*, 1993.
(7)   *Magnetism I - Fundamentals*; Kluwer Academic Publishers: Norwell, 2002.
(8)   *Magnetic Molecular Materials*; Kluwer Academic Publishers: Boston, 1991; Vol. 198.
(9)   Curie, P. *Ann. Chim. Phys.* **1895**, 289.
(10)   Weiss, P. *J. de Phys.* **1907**, 661.
(11)   Borden, W. T.; Iwamura, H.; Berson, J. A. *Acc. Chem. Res.* **1994**, *27*, 109.
(12)   Borden, W. T., Ed. *Diradicals*; Wiley: New York, 1982.
(13)   Gatteschi, D.; Sessoli, R. *J. Magn. Magn. Mat.* **1992**, *104*, 2092.
(14)   Iwamura, H. *Pure Appl. Chem.* **1987**, *59*, 1595.
(15)   Rajca, A. *Chem. Rev.* **1994**, *94*, 871.
(16)   Rajca, A.; Wongsriratanakul, J.; Rajca, S. *Science* **2001**, *294*, 1503.
(17)   Gatteschi, D.; Caneschi, A.; Laugier, J.; Rey, P. *J. Am. Chem. Soc.* **1987**, *109*, 2191.
(18)   Iwamura, H.; Inoue, K.; Hayamizu, T. *Pure Appl. Chem.* **1996**, *68*, 243.
(19)   Caneschi, A.; Gatteschi, D.; Sessoli, R. *Acc. Chem. Res.* **1989**, *22*, 392.
(20)   Dougherty, D. A. *Acc. Chem. Res.* **1991**, *24*, 88.
(21)   Baclay, T. M.; Hicks, R. G.; Lemaire, M. T.; Thompson, L. K. *Inorg. Chem.* **2003**, *42*, 2261.
(22)   Hicks, R. G. *Aust. J. Chem.* **2001**, *54*, 597.
(23)   Hicks, R. G.; Lemaire, M. T.; Thompson, L. K.; Baclay, T. M. *J. Am. Chem. Soc.* **2000**, *122*, 8077.
(24)   Brook, D. J. R.; Fornell, S.; Stevens, J. E.; Noll, B.; Koch, T. H.; Eisfeld, W. *Inorg. Chem.* **2000**, *39*, 562.
(25)   Brook, D. J. R.; Fox, H. H.; Lynch, V.; Fox, M. A. *J. Phys. Chem.* **1996**, *100*, 2066.
(26)   Pierpont, C. G.; Attia, A. S. *Coll. Czech. Chem. Comm.* **2001**, *66*, 33.
(27)   Pierpont, C. G.; Buchanan, R. M. *Coord. Chem. Rev.* **1981**, *38*, 45.
(28)   Pierpont, C. G.; Lange, C. W. *Prog. Inorg. Chem.* **1994**, *41*, 331.

Chapter 2. Electron Spin-Spin Exchange Coupling in Biradicals

Two Orbital/Two-Electron Approach: Active Electron Approximation[1]

Biradicals are the simplest multi-spin molecular analogs of magnetic materials. Biradicals that are high-spin (S=1) are molecular analogs of ferromagnets, while biradicals that are low-spin (S=0) are molecular analogs of antiferromagnets. Finally, hetero-spin biradicals are molecular analogs of ferrimagnets. Our goal is to study the intramolecular electronic and structural properties of organic biradical ligands to strengthen the foundation for building organic-based molecular magnetic materials.

We can use a simple two-electron/two-orbital approach to demonstrate why electrons orient their spin in either ferromagnetic or antiferromagnetic fashion. The interaction between two electrons is generally called exchange coupling. The exchange coupling parameter, J_{Tot} ($\Delta E_{S-T} = 2J_{Tot})$, is the sum of two components: a ferromagnetic component (J_F), and an antiferromagnetic component (J_{AF}), **Eq. 2.1**.[1]

$$J_{TOT} = J_F + J_{AF}$$ **Eq. 2.1**

The ferromagnetic component (J_F) is positive, while the antiferromagnetic component is negative (J_{AF}). Whichever component dominates will determine whether the overall exchange coupling parameter J_{Tot} is positive or negative, thus whether the biradical is ferromagnetically coupled or antiferromagnetically coupled, respectively.

Using a two-orbital/two-electron model with orthogonal magnetic orbitals,[2] we can demonstrate how preferences for ferromagnetic or antiferromagnetic states arise. The total wavefunction (Ψ_{TOT}) for each spin state is a product of the spatial (ψ) and spin (φ)

wavefunctions. Electrons are fermions and Ψ_{TOT} must be antisymmetric with respect to electron label exchange.[3]

Electrons must be indistinguishable and the two allowed spatial wavefunctions are linear combinations of the two orbitals giving **Eq. 2.2** and **Eq. 2.3**.[3]

$$\psi_+ = \frac{1}{\sqrt{2}}\left[f_A(1)f_B(2) + f_B(1)f_A(2)\right] \qquad \textbf{Eq. 2.2}$$

$$\psi_- = \frac{1}{\sqrt{2}}\left[f_A(1)f_B(2) - f_B(1)f_A(2)\right] \qquad \textbf{Eq. 2.3}$$

Exchange of electron labels ($P_{12}\psi$) in **Eq. 2.2** and **Eq. 2.3** shows that **Eq. 2.2** is a symmetric wavefunctions (ψ_+) and **Eq. 2.3** is an antisymmetric wavefunction (ψ_-).

The allowed spin wavefunctions are described by **Eqs. 2.4 – 2.7**.[3]

$$\varphi_{\uparrow\uparrow,+} = a(1)a(2) \qquad \textbf{Eq. 2.4}$$

$$\varphi_{\downarrow\downarrow,+} = b(1)b(2) \qquad \textbf{Eq. 2.5}$$

$$\varphi_{\uparrow\downarrow,+} = \frac{1}{\sqrt{2}}\left[a(1)b(2) + b(1)a(2)\right] \qquad \textbf{Eq. 2.6}$$

$$\varphi_{\uparrow\downarrow,-} = \frac{1}{\sqrt{2}}\left[a(1)b(2) - b(1)a(2)\right] \qquad \textbf{Eq. 2.7}$$

Eqs. 2.4 – 2.6 are symmetric and **Eq. 2.7** is antisymmetric.

Recall that the total wavefunction must be antisymmetric with respect to electron exchange ($P_{12}\Psi_{TOT} = -\Psi_{TOT}$). Therefore the allowed total wavefunctions are given by **Eqs. 2.8 – 2.11**.

$$\Psi_{TOT} = \psi_- \varphi_{\uparrow\uparrow,+} \qquad \textbf{(antisymmetric spatial, symmetric spin)} \quad \textbf{Eq. 2.8}$$

14

$$\Psi_{TOT} = \psi_- \downarrow\downarrow_{,+} \qquad \textbf{(antisymmetric spatial, symmetric spin)} \quad \textbf{Eq. 2.9}$$

$$\Psi_{TOT} = \psi_- \uparrow\downarrow_{,+} \qquad \textbf{(antisymmetric spatial, symmetric spin)} \quad \textbf{Eq. 2.10}$$

$$\Psi_{TOT} = \psi_+ \uparrow\downarrow_{,-} \qquad \textbf{(symmetric spatial, antisymmetric spin)} \quad \textbf{Eq. 2.11}$$

Eq. 2.8 – 2.10 describe the three microstates of the triplet manifold, while **Eq. 2.11**

represents an open-shell singlet state.

Next, we calculate the energy difference between the triplet and singlet states.

The difference in energy between these to states is due to electron-electron repulsions and

is independent on the spin of the electron. Therefore to calculate the energies of the

states only the spatial wavefunction is used. We should note that the three triplet states

have antisymmetric spatial wavefunctions (triply degenerate) and the singlet state has a

symmetric wavefunction. Also, we must consider the energies of the closed-shell

zwitterionic singlet states ($\Psi_{S+,CS}$ and $\Psi_{S-,CS}$). Altogether, the allowed wavefunctions for

the four states are:[4]

$$\Psi_{T,OS} = \frac{1}{\sqrt{2}}\left[a(1)b(2) - b(1)a(2)\right] \qquad \textbf{Eq. 2.12}$$

$$\Psi_{S,OS} = \frac{1}{\sqrt{2}}\left[a(1)b(2) + b(1)a(2)\right] \qquad \textbf{Eq. 2.13}$$

$$\Psi_{S+,CS} = \frac{1}{\sqrt{2}}\left[a(1)a(2) + b(1)b(2)\right] \qquad \textbf{Eq. 2.14}$$

$$\Psi_{S-,CS} = \frac{1}{\sqrt{2}}\left[a(1)a(2) - b(1)b(2)\right] \qquad \textbf{Eq. 2.15}$$

Equations 2.12 and **2.13** describe the spatial wavefunctions of the open-shell triplet and

singlet states respectively, while **Equations 2.14** and **2.15** represent the closed-shell

zwitterionic singlet states. **Equations 2.14** and **2.15** are linear combinations of the two

orbitals to ensure electron indistiguishability.

The four possible spatial configurations for the electrons are shown in **Figure 2.1**.
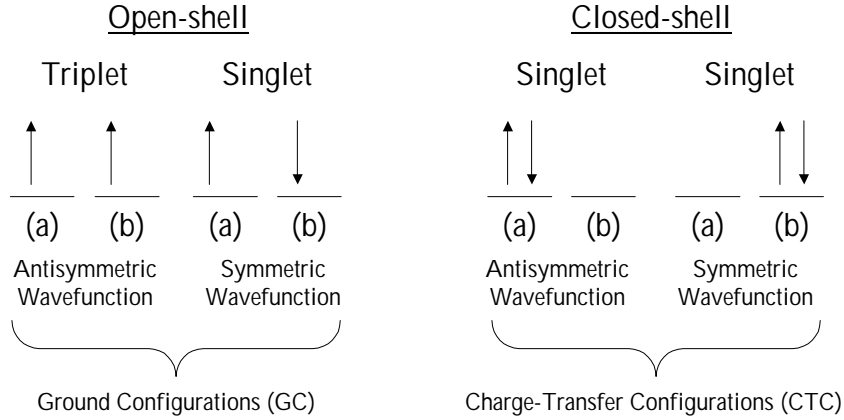
Figure 2.1. Open shell (left) ground-configuration states and closed shell (right) charge-transfer states for a two-electron/two-orbital system.

The zero-order Hamiltonian, **Eq. 2.16**, excludes electron-electron repulsion, is used to

calculate the state energies.

$$H^0 = h(1) + h(2) \qquad\qquad \textbf{Eq. 2.16}$$

Energy of the triplet is:

$$
\begin{aligned}
E^{(0)}\left(\Psi_{T,OS}\right) &= \frac{1}{2}\left\langle a(1)b(2) - b(1)a(2) \middle| h(1) + h(2) \middle| a(1)b(2) - b(1)a(2) \right\rangle \\
&= \frac{1}{2}\Big[\left\langle a(1)b(2) \middle| h(1) + h(2) \middle| a(1)b(2) \right\rangle - \left\langle a(1)b(2) \middle| h(1) + h(2) \middle| b(1)a(2) \right\rangle \\
&\quad - \left\langle b(1)a(2) \middle| h(1) + h(2) \middle| a(1)b(2) \right\rangle + \left\langle b(1)a(2) \middle| h(1) + h(2) \middle| b(1)a(2) \right\rangle \Big] \\
&= \frac{1}{2}\Big[\left\langle b(2) \middle| b(2) \right\rangle\left\langle a(1) \middle| h(1) \middle| a(1) \right\rangle + \left\langle a(1) \middle| a(1) \right\rangle\left\langle b(2) \middle| h(2) \middle| b(2) \right\rangle \\
&\quad - \left\langle b(2) \middle| a(2) \right\rangle\left\langle a(1) \middle| h(1) \middle| b(1) \right\rangle - \left\langle a(1) \middle| b(1) \right\rangle\left\langle b(2) \middle| h(2) \middle| a(2) \right\rangle \\
&\quad - \left\langle a(2) \middle| b(2) \right\rangle\left\langle b(1) \middle| h(1) \middle| a(1) \right\rangle - \left\langle b(1) \middle| a(1) \right\rangle\left\langle a(2) \middle| h(2) \middle| b(2) \right\rangle \\
&\quad + \left\langle a(2) \middle| a(2) \right\rangle\left\langle b(1) \middle| h(1) \middle| b(1) \right\rangle + \left\langle b(1) \middle| b(1) \right\rangle\left\langle a(2) \middle| h(2) \middle| a(2) \right\rangle \Big]
\end{aligned}
$$

$$= \frac{1}{2}[a + a - 0 - 0 - 0 - 0 + a + a] = 2a \qquad \textbf{Eq. 2.17}$$

where α is the coulomb integral. $(\alpha = \langle a(1)|h(1)|a(1)\rangle = \langle b(2)|h(2)|b(2)\rangle)$

Energy of the open shell singlet is:

$$E^{(0)}\left(\Psi_{S,os}\right) = \frac{1}{2}\langle a(1)b(2) + b(1)a(2)|h(1) + H(2)|a(1)b(2) + b(1)a(2)\rangle$$

$$= \frac{1}{2}\left[\langle a(1)b(2)|h(1) + h(2)|a(1)b(2)\rangle + \langle a(1)b(2)|h(1) + h(2)|b(1)a(2)\rangle\right.$$

$$\left. + \langle b(1)a(2)|h(1) + h(2)|a(1)b(2)\rangle + \langle b(1)a(2)|h(1) + h(2)|b(1)a(2)\rangle\right]$$

$$= \frac{1}{2}\left[\langle b(2)|b(2)\rangle\langle a(1)|h(1)|a(1)\rangle + \langle a(1)|a(1)\rangle\langle b(2)|h(2)|b(2)\rangle\right.$$

$$+ \langle b(2)|a(2)\rangle\langle a(1)|h(1)|b(1)\rangle + \langle a(1)|b(1)\rangle\langle b(2)|h(2)|a(2)\rangle$$

$$+ \langle a(2)|b(2)\rangle\langle b(1)|h(1)|a(1)\rangle + \langle b(1)|a(1)\rangle\langle a(2)|h(2)|b(2)\rangle$$

$$\left. + \langle a(2)|a(2)\rangle\langle b(1)|h(1)|b(1)\rangle + \langle b(1)|b(1)\rangle\langle a(2)|h(2)|a(2)\rangle\right]$$

$$= \frac{1}{2}[a + a + 0 + 0 + 0 + 0 + a + a] = 2a \qquad \textbf{Eq. 2.18}$$

Energy of the first closed-shell singlet is:

$$E^{(0)}\left(\Psi_{S+,CS}\right) = \frac{1}{2}\langle a(1)b(2) + b(1)a(2)|h(1) + h(2)|a(1)b(2) + b(1)a(2)\rangle$$

$$= \frac{1}{2}\left[\langle a(1)b(2)|h(1) + h(2)|a(1)b(2)\rangle + \langle a(1)b(2)|h(1) + h(2)|b(1)a(2)\rangle\right.$$

$$\left. + \langle b(1)a(2)|h(1) + h(2)|a(1)b(2)\rangle + \langle b(1)a(2)|h(1) + h(2)|b(1)a(2)\rangle\right]$$

$$= \frac{1}{2}\left[\langle b(2)|b(2)\rangle\langle a(1)|h(1)|a(1)\rangle + \langle a(1)|a(1)\rangle\langle b(2)|h(2)|b(2)\rangle\right.$$

$$+ \langle b(2)|a(2)\rangle\langle a(1)|h(1)|b(1)\rangle + \langle a(1)|b(1)\rangle\langle b(2)|h(2)|a(2)\rangle$$

$$+ \langle a(2)|b(2)\rangle\langle b(1)|h(1)|a(1)\rangle + \langle b(1)|a(1)\rangle\langle a(2)|h(2)|b(2)\rangle$$

$$\left. + \langle a(2)|a(2)\rangle\langle b(1)|h(1)|b(1)\rangle + \langle b(1)|b(1)\rangle\langle a(2)|h(2)|a(2)\rangle\right]$$

$$= \frac{1}{2}[a + a + 0 + 0 + 0 + 0 + a + a] = 2a \qquad \textbf{Eq. 2.19}$$

Energy of the second closed-shell singlet is:

$$E^{(0)}\left(\Psi_{S-,CS}\right)=\frac{1}{2}\left\langle a(1)a(2)-b(1)b(2)\left|h(1)+h(2)\right|a(1)a(2)-b(1)b(2)\right\rangle$$

$$=\frac{1}{2}\Big[\left\langle a(1)a(2)\left|h(1)+h(2)\right|a(1)a(2)\right\rangle-\left\langle a(1)a(2)\left|h(1)+h(2)\right|b(1)b(2)\right\rangle$$

$$-\left\langle b(1)b(2)\left|h(1)+h(2)\right|a(a)a(2)\right\rangle+\left\langle b(1)b(2)\left|h(1)+h(2)\right|b(1)b(2)\right\rangle\Big]$$

$$=\frac{1}{2}\Big[\left\langle a(2)\big|a(2)\right\rangle\left\langle a(1)\big|h(1)\big|a(1)\right\rangle+\left\langle a(1)\big|a(1)\right\rangle\left\langle a(2)\big|h(2)\big|a(2)\right\rangle$$

$$-\left\langle a(2)\big|b(2)\right\rangle\left\langle a(1)\big|h(1)\big|b(1)\right\rangle-\left\langle a(1)\big|b(1)\right\rangle\left\langle a(2)\big|h(2)\big|b(2)\right\rangle$$

$$-\left\langle b(2)\big|a(2)\right\rangle\left\langle b(1)\big|h(1)\big|a(1)\right\rangle-\left\langle b(1)\big|a(1)\right\rangle\left\langle b(2)\big|h(2)\big|a(2)\right\rangle$$

$$+\left\langle b(2)\big|b(2)\right\rangle\left\langle b(1)\big|h(1)\big|b(1)\right\rangle+\left\langle b(1)\big|b(1)\right\rangle\left\langle b(2)\big|h(2)\big|b(2)\right\rangle\Big]$$

$$=\frac{1}{2}\left[a+a-0-0-0-0+a+a\right]=2a \qquad\qquad \textbf{Eq. 2.20}$$

All of the energies when calculated to zero-order come out to be 2α, where α = the Hückel α value, which is the energy of the electron within a single orbital. Therefore, to zero-order, regardless of the orientation of the electrons, the energy will be the same as long as the electrons occupy identical orbitals. This is, of course, neglecting electron-electron repulsion. Electron-electron repulsions for the four states can be calculated by using a first-order Hamiltonian that accounts for electron-electron repulsions, **Eq. 2.21**.

$$H=H^{(0)}+H^{(1)}=H^{(0)}+\frac{1}{r_{12}} \qquad\qquad \textbf{Eq. 2.21}$$

First-order energy of the triplet is:

$$E\left(\Psi_{T,OS}\right)=\frac{1}{2}\left\langle a(1)b(2)-b(1)a(2)\left|H^{(0)}+\frac{1}{r_{12}}\right|a(1)b(2)-b(1)a(2)\right\rangle$$

$$=2a+\frac{1}{2}\left\langle a(1)b(2)-b(1)a(2)\left|\frac{1}{r_{12}}\right|a(1)b(2)-b(1)a(2)\right\rangle$$

$$= 2a + \frac{1}{2}\left[\left\langle a(1)b(2)\left|\frac{1}{r_{12}}\right|a(1)b(2)\right\rangle - \left\langle a(1)b(2)\left|\frac{1}{r_{12}}\right|b(1)a(2)\right\rangle \right.$$

$$\left. - \left\langle b(1)a(2)\left|\frac{1}{r_{12}}\right|a(1)b(2)\right\rangle + \left\langle b(1)a(2)\left|\frac{1}{r_{12}}\right|b(1)a(2)\right\rangle \right]$$

$$= 2a + \frac{1}{2}\left[\left\langle a(1)a(1)\left|\frac{1}{r_{12}}\right|b(2)b(2)\right\rangle - \left\langle a(1)b(1)\left|\frac{1}{r_{12}}\right|a(2)b(2)\right\rangle \right.$$

$$\left. - \left\langle b(1)a(1)\left|\frac{1}{r_{12}}\right|a(2)b(2)\right\rangle + \left\langle b(1)b(1)\left|\frac{1}{r_{12}}\right|a(2)a(2)\right\rangle \right]$$

$$= 2a + \frac{1}{2}\left[j - k - k + 2 \right] = 2a + j - k \qquad \textbf{Eq. 2.22}$$

First-order energy of the open-shell singlet is:

$$E\left(\Psi_{s,os}\right) = \frac{1}{2}\left\langle a(1)b(2) + b(1)a(2)\left|H^{(0)} + \frac{1}{r_{12}}\right|a(1)b(2) + b(1)a(2)\right\rangle$$

$$= 2a + \frac{1}{2}\left\langle a(1)b(2) + b(1)a(2)\left|\frac{1}{r_{12}}\right|a(1)b(2) + b(1)a(2)\right\rangle$$

$$= 2a + \frac{1}{2}\left[\left\langle a(1)b(2)\left|\frac{1}{r_{12}}\right|a(1)b(2)\right\rangle + \left\langle a(1)b(2)\left|\frac{1}{r_{12}}\right|b(1)a(2)\right\rangle \right.$$

$$\left. + \left\langle b(1)a(2)\left|\frac{1}{r_{12}}\right|a(1)b(2)\right\rangle + \left\langle b(1)a(2)\left|\frac{1}{r_{12}}\right|b(1)a(2)\right\rangle \right]$$

$$= 2a + \frac{1}{2}\left[\left\langle a(1)a(1)\left|\frac{1}{r_{12}}\right|b(2)b(2)\right\rangle + \left\langle a(1)b(1)\left|\frac{1}{r_{12}}\right|a(2)b(2)\right\rangle \right.$$

$$\left. + \left\langle b(1)a(1)\left|\frac{1}{r_{12}}\right|a(2)b(2)\right\rangle + \left\langle b(1)b(1)\left|\frac{1}{r_{12}}\right|a(2)a(2)\right\rangle \right]$$

$$= 2a + \frac{1}{2}\left[j + k + k + j \right] = 2a + j + k \qquad \textbf{Eq. 2.23}$$

First-order energy of the first closed-shell singlet is:

$$E\left(\Psi_{S+,CS}\right) = \frac{1}{2}\left\langle a(1)a(2) + b(1)b(2)\middle| H^{(0)} + \frac{1}{r_{12}}\middle| a(1)a(2) + b(1)b(2)\right\rangle$$

$$= 2a + \frac{1}{2}\left\langle a(1)a(2) + b(1)b(2)\middle| \frac{1}{r_{12}}\middle| a(1)a(2) + b(1)b(2)\right\rangle$$

$$= 2a + \frac{1}{2}\left[\left\langle a(1)a(2)\middle|\frac{1}{r_{12}}\middle| a(1)a(2)\right\rangle + \left\langle a(1)a(2)\middle|\frac{1}{r_{12}}\middle| b(1)b(2)\right\rangle\right.$$

$$\left. + \left\langle b(1)b(2)\middle|\frac{1}{r_{12}}\middle| a(1)a(2)\right\rangle + \left\langle b(1)b(2)\middle|\frac{1}{r_{12}}\middle| b(1)b(2)\right\rangle\right]$$

$$= 2a + \frac{1}{2}\left[\left\langle a(1)a(1)\middle|\frac{1}{r_{12}}\middle| b(2)b(2)\right\rangle + \left\langle a(1)b(1)\middle|\frac{1}{r_{12}}\middle| a(2)b(2)\right\rangle\right.$$

$$\left. + \left\langle b(1)a(1)\middle|\frac{1}{r_{12}}\middle| a(2)b(2)\right\rangle + \left\langle b(1)b(1)\middle|\frac{1}{r_{12}}\middle| b(2)b(2)\right\rangle\right]$$

$$= 2a + \frac{1}{2}\left[j^0 + k + k + j^0 \right] = 2a + j^0 + k \qquad\qquad \textbf{Eq. 2.24}$$

First order energy of the second closed-shell singlet is:

$$E\left(\Psi_{S-,CS}\right) = \frac{1}{2}\left\langle a(1)a(2) - b(1)b(2)\middle| H^{(0)} + \frac{1}{r_{12}}\middle| a(1)a(2) - b(1)b(2)\right\rangle$$

$$= 2a + \frac{1}{2}\left\langle a(1)a(2) - b(1)b(2)\middle| \frac{1}{r_{12}}\middle| a(1)a(2) - b(1)b(2)\right\rangle$$

$$= 2a + \frac{1}{2}\left[\left\langle a(1)a(2)\middle|\frac{1}{r_{12}}\middle| a(1)a(2)\right\rangle - \left\langle a(1)a(2)\middle|\frac{1}{r_{12}}\middle| b(1)b(2)\right\rangle\right.$$

$$\left. - \left\langle b(1)b(2)\middle|\frac{1}{r_{12}}\middle| a(1)a(2)\right\rangle + \left\langle b(1)b(2)\middle|\frac{1}{r_{12}}\middle| b(1)b(2)\right\rangle\right]$$

$$\left. - \left\langle b(1)a(1)\middle|\frac{1}{r_{12}}\middle| a(2)b(2)\right\rangle + \left\langle b(1)b(1)\middle|\frac{1}{r_{12}}\middle| a(2)a(2)\right\rangle\right]$$

$$= 2a + \frac{1}{2}\left[j^0 - k - k + j^0 \right] = 2a + j^0 - k \qquad\qquad \textbf{Eq. 2.25}$$

Within **Equations 2.22** through **2.25**, the two-center coulomb integral, **J**

($j = \left\langle a(1)a(1)\middle|\frac{1}{r_{12}}\middle| b(2)b(2)\right\rangle$), is the energy of the electron-electron repulsion between

two electrons in different orbitals ($j^0 \gg j$). The two-center exchange integral, k

($k = \left\langle a(1)b(1) \left| \dfrac{1}{r_{12}} \right| a(2)b(2) \right\rangle$), is the electron-electron repulsion between two electrons

that are within the overlap region of the two orbitals. The one-center coulomb integral, j^0

($j^0 = \left\langle a(1)a(1) \left| \dfrac{1}{r_{12}} \right| b(2)b(2) \right\rangle$), is the electron-electron repulsion between two electrons

that are in the same orbital. A cartoon of the orbitals can bee seen in **Figure 2.2**

j = coulomb integral
  = electron-electron repulsions
    between a and b

k = exchange integral
  = electron-electron repulsion in
    the overlap region (black)

j^0 = one-center coulomb integral
  = electron-electron repulsion with a <u>or</u> b

l = hybrid coulomb integral
  = electron-electron repulsion between a <u>or</u> b
    and the overlap region (black)

a = Orbital a
b = Orbital b
black = overlap between
        a and b
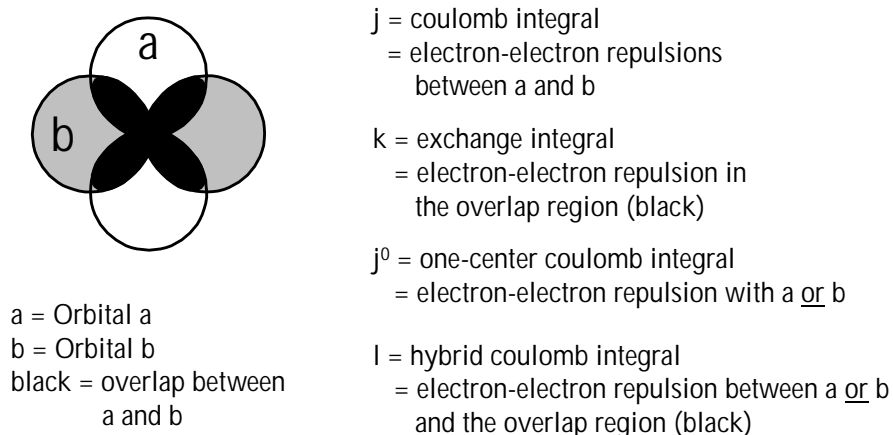
Figure 2.2. A cartoon of the two orbitals described by **Eqs. 2.22 – 2.25**.

We have now described the energy of the states (**Equations 2.12-2.15**) in terms of

the energy of the electron in a single orbital (zero-order Hamiltonian, H^0) and the energy

of the electron-electron repulsions (first-order Hamiltonian, H^1). **Figure 2.3** shows the

energy of the states and the terms describing them thus far. We should also notice that

the lowest energy state is a triplet and that $\Delta E_{S\text{-}T} = 2J_{Tot} = 2k$.

Closed-shell Singlet $\left(\Psi_{S+,CS}\right): E = 2a + j^0 + k$

$2k$

Closed-shell Singlet $\left(\Psi_{S-,CS}\right): E = 2a + j^0 - k$

$j^0 - j$

Open-shell Singlet $\left(\Psi_{S,os}\right): E = 2a + j + k$

$2k$

Open-shell Triplet $\left(\Psi_{T,os}\right): E = 2a + j - k$
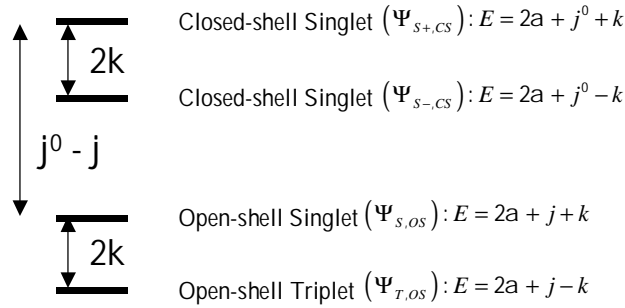
Figure 2.3. The relative energy states of a two-electron, two-orbital system including the energy from the electron in a single orbital (H^0), and electron-electron repulsions (H^1). Notice that without second-order contributions (configuration interaction) the triplet state is lower in energy by 2k compared to that of the open-shell singlet.

Figure 2.3 is over-simplified and configuration interactions must also be included. To do this we will use a second order correction to the Hamiltonian to allow for mixing of the states, **Eq. 2.26**, where Ψ_i and Ψ_j are the two states that interact.

$$E_i^{(2)} = \frac{\left\langle \Psi_i \left| H^{(1)} \right| \Psi_j \right\rangle^2}{E_i - E_j} \qquad \textbf{Eq. 2.26}$$

We begin by calculation the numerator for **Eq. 2.26** with the highest closed-shell singlet mixing into the open-shell singlet:

$$\left\langle \Psi_{S,OS} \left| h(1) + h(2) + \frac{1}{r_{12}} \right| \Psi_{S+,CS} \right\rangle^2$$

$$= \left\langle \frac{1}{\sqrt{2}}\left[a(1)b(2) + b(1)a(2)\right] \left| h(1) + h(2) + \frac{1}{r_{12}} \right| \frac{1}{\sqrt{2}}\left[a(1)a(2) + b(1)b(2)\right] \right\rangle^2$$

$$= \left\{ \frac{1}{2}\left[\left\langle a(1)b(2) + b(1)a(2) \left| h(1) \right| a(1)a(2) + b(1)b(2) \right\rangle \right.\right.$$

$$+ \left\langle a(1)b(2) + b(1)a(2) \left| h(2) \right| a(1)a(2) + b(1)b(2) \right\rangle$$

$$+ \left.\left. \left\langle a(1)b(2) + b(1)a(2) \left| \frac{1}{r_{12}} \right| a(1)a(2) + b(1)b(2) \right\rangle \right]\right\}^2$$

$$= \left\{ \frac{1}{2} \left[\langle a(1)b(2)|h(1)|a(1)a(2)\rangle + \langle a(1)b(2)|h(1)|b(1)b(2)\rangle + \langle b(1)a(2)|h(1)|a(1)a(2)\rangle \right. \right.$$

$$+ \langle b(1)a(2)|h(1)|b(1)b(2)\rangle + \langle a(1)b(2)|h(2)|a(1)a(2)\rangle + \langle a(1)b(2)|h(2)|b(1)b(2)\rangle$$

$$+ \langle b(1)a(2)|h(2)|a(1)a(2)\rangle + \langle b(1)a(2)|h(2)|b(1)b(2)\rangle + \langle a(1)b(2)|\frac{1}{r_{12}}|a(1)a(2)\rangle$$

$$\left. \left. + \langle a(1)b(2)|\frac{1}{r_{12}}|b(1)b(2)\rangle + \langle b(1)a(2)|\frac{1}{r_{12}}|a(1)a(2)\rangle + \langle b(1)a(2)|\frac{1}{r_{12}}|b(1)b(2)\rangle \right] \right\}^2$$

$$= \left\{ \frac{1}{2} \left[\langle b(2)|a(2)\rangle\langle a(1)|h(1)|a(1)\rangle + \langle b(2)|b(2)\rangle\langle a(1)|h(1)|b(1)\rangle \right. \right.$$

$$+ \langle a(2)|a(2)\rangle\langle b(1)|h(1)|a(1)\rangle + \langle a(2)|b(2)\rangle\langle b(1)|h(1)|b(1)\rangle$$

$$+ \langle a(1)|a(1)\rangle\langle b(2)|h(2)|a(2)\rangle + \langle a(1)|b(1)\rangle\langle b(2)|h(2)|b(2)\rangle$$

$$+ \langle b(1)|a(1)\rangle\langle a(2)|h(2)|a(2)\rangle + \langle b(1)|b(1)\rangle\langle a(2)|h(2)|b(2)\rangle$$

$$+ \langle a(1)a(1)|\frac{1}{r_{12}}|a(2)b(2)\rangle + \langle a(1)b(2)|\frac{1}{r_{12}}|b(2)b(2)\rangle$$

$$\left. \left. + \langle b(1)a(1)|\frac{1}{r_{12}}|a(2)a(2)\rangle + \langle b(1)b(1)|\frac{1}{r_{12}}|a(2)b(2)\rangle \right] \right\}^2$$

$$= \left\{ \frac{1}{2} \left[0 + b + b + 0 + b + 0 + 0 + b + l + l + l + l \right] \right\}^2$$

$$= \left\{ \frac{1}{2} \left[4b + 4l \right] \right\}^2 = 4(b + l)^2 \qquad \textbf{Eq. 2.27}$$

Combining with **Eq. 2.26**, the second order energy correction for the highest closed-shell singlet mixing into the open-shell singlet is:

$$E^{(2)} = \frac{4(b + l)^2}{j^0 - j} \qquad \textbf{Eq. 2.28}$$

For the lower closed-shell singlet mixing into the open-shell singlet we obtain:

$$\left\langle \Psi_{S,OS} \left| h(1) + h(2) + \frac{1}{r_{12}} \right| \Psi_{S-,CS} \right\rangle^2$$

$$= \left\langle \frac{1}{\sqrt{2}} [a(1)b(2) + b(1)a(2)] \left| h(1) + h(2) + \frac{1}{r_{12}} \right| \frac{1}{\sqrt{2}} [a(1)a(2) - b(1)b(2)] \right\rangle^2$$

$$= \left\{ \frac{1}{2} \Big[\langle a(1)b(2) + b(1)a(2) | h(1) | a(1)a(2) - b(1)b(2) \rangle \right.$$

$$+ \langle a(1)b(2) + b(1)a(2) | h(2) | a(1)a(2) - b(1)b(2) \rangle$$

$$\left. + \langle a(1)b(2) + b(1)a(2) | \frac{1}{r_{12}} | a(1)a(2) - b(1)b(2) \rangle \Big] \right\}^2$$

$$= \left\{ \frac{1}{2} \Big[\langle a(1)b(2) | h(1) | a(1)a(1) \rangle - \langle a(1)b(2) | h(1) | b(1)b(2) \rangle + \langle b(1)a(2) | h(1) | a(1)a(2) \rangle \right.$$

$$- \langle b(1)a(2) | h(1) | b(1)b(2) \rangle + \langle a(1)b(2) | h(2) | a(1)a(2) \rangle - \langle a(1)b(2) | h(2) | b(1)b(2) \rangle$$

$$+ \langle b(1)a(2) | h(2) | a(1)a(2) \rangle - \langle b(1)a(2) | h(2) | b(1)b(2) \rangle + \langle a(1)b(2) | \frac{1}{r_{12}} | a(1)a(2) \rangle$$

$$\left. - \langle a(1)b(2) | \frac{1}{r_{12}} | b(1)b(2) \rangle + \langle b(1)a(2) | \frac{1}{r_{12}} | a(1)a(2) \rangle - \langle b(1)a(2) | \frac{1}{r_{12}} | b(1)b(2) \rangle \Big] \right\}^2$$

$$= \left\{ \frac{1}{2} \Big[\langle b(2) | a(2) \rangle \langle a(1) | h(1) | a(1) \rangle + \langle b(2) | b(2) \rangle \langle a(1) | h(1) | b(1) \rangle \right.$$

$$- \langle a(2) | a(2) \rangle \langle b(1) | h(1) | a(1) \rangle + \langle a(2) | b(2) \rangle \langle b(1) | h(1) | b(1) \rangle$$

$$- \langle a(1) | a(1) \rangle \langle b(2) | h(2) | a(2) \rangle + \langle a(1) | b(1) \rangle \langle b(2) | h(2) | b(2) \rangle$$

$$- \langle b(1) | a(1) \rangle \langle a(2) | h(2) | a(2) \rangle - \langle b(1) | b(1) \rangle \langle a(2) | h(2) | b(2) \rangle$$

$$+ \langle a(1)a(1) | \frac{1}{r_{12}} | a(2)a(2) \rangle - \langle a(1)b(2) | \frac{1}{r_{12}} | b(2)b(2) \rangle$$

$$\left. + \langle b(1)a(1) | \frac{1}{r_{12}} | a(2)a(2) \rangle - \langle b(1)b(1) | \frac{1}{r_{12}} | a(2)b(2) \rangle \Big] \right\}^2$$

$$= \left\{ \frac{1}{2} [0 - b + b - 0 + b - 0 + 0 - b + l - l + l - l] \right\}^2 = \left\{ \frac{1}{2}[0] \right\}^2 = 0 \quad \textbf{Eq. 2.29}$$

Again combining with **Eq. 2.26**, the second order energy correction for the lower closed-shell singlet mixing into the open-shell singlet is:

$$E^{(2)} = \frac{0}{j^0 - j} = 0 \qquad\qquad \textbf{Eq. 2.30}$$

For the highest closed-shell singlet mixing into the triplet we obtain:

$$\left\langle \Psi_{T,OS} \left| h(1) + h(2) + \frac{1}{r_{12}} \right| \Psi_{S+,CS} \right\rangle^2$$

$$= \left\langle \frac{1}{\sqrt{2}}[a(1)b(2) - b(1)a(2)] \left| h(1) + h(2) + \frac{1}{r_{12}} \right| \frac{1}{\sqrt{2}}[a(1)a(2) + b(1)b(2)] \right\rangle^2$$

$$= \left\{ \frac{1}{2} \left[\langle a(1)b(2) - b(1)a(2) | h(1) | a(1)a(2) + b(1)b(2) \rangle \right.\right.$$

$$+ \langle a(1)b(2) - b(1)a(2) | h(2) | a(1)a(2) + b(1)b(2) \rangle$$

$$\left.\left. + \langle a(1)b(2) - b(1)a(2) | \frac{1}{r_{12}} | a(1)a(2) + b(1)b(2) \rangle \right] \right\}^2$$

$$= \left\{ \frac{1}{2} \left[\langle a(1)b(2) | h(1) | a(1)a(2) \rangle + \langle a(1)b(2) | h(1) | b(1)b(2) \rangle - \langle b(1)a(2) | h(1) | a(1)a(2) \rangle \right.\right.$$

$$- \langle b(1)a(2) | h(1) | b(1)b(2) \rangle + \langle a(1)b(2) | h(2) | a(1)a(2) \rangle + \langle a(1)b(2) | h(2) | b(1)b(2) \rangle$$

$$- \langle b(1)a(2) | h(2) | a(1)a(2) \rangle - \langle b(1)a(2) | h(2) | b(1)b(2) \rangle + \langle a(1)b(2) | \frac{1}{r_{12}} | a(1)a(2) \rangle$$

$$\left.\left. + \langle a(1)b(2) | \frac{1}{r_{12}} | b(1)b(2) \rangle - \langle b(1)a(2) | \frac{1}{r_{12}} | a(1)a(2) \rangle - \langle b(1)a(2) | \frac{1}{r_{12}} | b(1)b(2) \rangle \right] \right\}^2$$

$$= \left\{ \frac{1}{2} \left[\langle b(2) | a(2) \rangle \langle a(1) | h(1) | a(1) \rangle + \langle b(2) | b(2) \rangle \langle a(1) | h(1) | b(1) \rangle \right.\right.$$

$$- \langle a(2) | a(2) \rangle \langle b(1) | h(1) | a(1) \rangle - \langle a(2) | b(2) \rangle \langle b(1) | h(1) | b(1) \rangle$$

$$+ \langle a(1) | a(1) \rangle \langle b(2) | h(2) | b(2) \rangle + \langle a(1) | b(1) \rangle \langle b(2) | h(2) | b(2) \rangle$$

$$- \langle b(1) | a(1) \rangle \langle a(2) | h(2) | a(2) \rangle - \langle b(1) | b(1) \rangle \langle a(2) | h(2) | b(2) \rangle$$

$$+ \langle a(1)a(1) | \frac{1}{r_{12}} | a(2)b(2) \rangle + \langle a(1)b(2) | \frac{1}{r_{12}} | b(2)b(2) \rangle$$

$$\left.\left. - \langle b(1)a(1) | \frac{1}{r_{12}} | a(2)a(2) \rangle - \langle b(1)b(1) | \frac{1}{r_{12}} | a(2)b(2) \rangle \right] \right\}^2$$

$$= \left\{ \frac{1}{2} [0 + b - b - 0 + b + 0 - 0 - b + l + l - l - l] \right\}^2 = \left\{ \frac{1}{2} [0] \right\}^2 = 0 \qquad \textbf{Eq. 2.31}$$

Again combing with **Eq. 2.26**, the second order energy correction for the highest closed-

shell singlet mixing into the triplet is:

$$E^{(2)} = \frac{0}{j^0 - j} = 0$$

Eq. 2.32

For the lower-closed shell singlet mixing into the triplet we obtain:

$$\left\langle \Psi_{T,OS} \left| h(1) + h(2) + \frac{1}{r_{12}} \right| \Psi_{S-,CS} \right\rangle^2$$

$$= \left\langle \frac{1}{\sqrt{2}} [a(1)b(2) - b(1)a(2)] \left| h(1) + h(2) + \frac{1}{r_{12}} \right| \frac{1}{\sqrt{2}} [a(1)a(2) - b(1)b(2)] \right\rangle^2$$

$$= \left\{ \frac{1}{2} \left[\langle a(1)b(2) - b(1)a(2) | h(1) | a(1)a(2) - b(1)b(2) \rangle \right. \right.$$

$$+ \langle a(1)b(2) - b(1)a(2) | h(2) | a(1)a(2) - b(1)b(2) \rangle$$

$$\left. \left. + \langle a(1)b(2) - b(1)a(2) | \frac{1}{r_{12}} | a(1)a(2) - b(1)b(2) \rangle \right] \right\}^2$$

$$= \left\{ \frac{1}{2} \left[\langle a(1)b(2) | h(1) | a(1)a(2) \rangle - \langle a(1)b(2) | h(1) | b(1)b(2) \rangle - \langle b(1)a(2) | h(1) | a(1)a(2) \rangle \right. \right.$$

$$+ \langle b(1)a(2) | h(1) | b(1)b(2) \rangle + \langle a(1)b(2) | h(2) | a(1)a(2) \rangle - \langle a(1)b(2) | h(2) | b(1)b(2) \rangle$$

$$- \langle b(1)a(2) | h(2) | a(1)a(2) \rangle + \langle b(1)a(2) | h(2) | b(1)b(2) \rangle + \langle a(1)b(2) | \frac{1}{r_{12}} | a(1)a(2) \rangle$$

$$\left. \left. - \langle a(1)b(2) | \frac{1}{r_{12}} | b(1)b(2) \rangle - \langle b(1)a(2) | \frac{1}{r_{12}} | a(1)a(2) \rangle + \langle b(1)a(2) | \frac{1}{r_{12}} | b(1)b(2) \rangle \right] \right\}^2$$

$$= \left\{ \frac{1}{2} \left[\langle b(2)|a(2) \rangle \langle a(1)|h(1)|a(1) \rangle - \langle b(2)|b(2) \rangle \langle a(1)|h(1)|b(1) \rangle \right. \right.$$
$$- \langle a(2)|a(2) \rangle \langle b(1)|h(1)|a(1) \rangle + \langle a(2)|b(2) \rangle \langle b(1)|h(1)|b(1) \rangle$$
$$+ \langle a(1)|a(1) \rangle \langle b(2)|h(2)|a(2) \rangle - \langle a(1)|b(1) \rangle \langle b(2)|h(2)|b(2) \rangle$$
$$- \langle b(1)|a(1) \rangle \langle a(2)|h(2)|a(2) \rangle + \langle b(1)|b(1) \rangle \langle a(2)|h(2)|b(2) \rangle$$
$$+ \langle a(1)a(1)|\frac{1}{r_{12}}|a(2)b(2) \rangle - \langle a(1)b(2)|\frac{1}{r_{12}}|b(2)b(2) \rangle$$
$$\left. \left. - \langle b(1)a(1)|\frac{1}{r_{12}}|a(2)a(2) \rangle + \langle b(1)b(1)|\frac{1}{r_{12}}|a(2)b(2) \rangle \right] \right\}^2$$

$$= \left\{ \frac{1}{2}[0 - b - b + 0 + b - 0 - 0 + b + l - l - l + l] \right\}^2 = \left\{ \frac{1}{2}[0] \right\}^2 = 0 \qquad \textbf{Eq. 2.33}$$

Again combing with **Eq. 2.26**, the second order energy correction for the lower-closed shell singlet mixing into the triplet is:

$$E^{(2)} = \frac{0}{j^0 - j} = 0 \qquad \textbf{Eq. 2.34}$$

In **Eqs. 2.27 - 2.34** β is the resonance integral ($b = \langle a(1)|h(1)|b(1) \rangle$), and l is the hybrid two-center coulomb integral ($l = \langle a(1)a(1)|\frac{1}{r_{12}}|a(2)b(2) \rangle$). Based on these equations configuration interactions only occur within the singlet manifold. It makes sense that the singlet states do not mix or interact with the triplet states.

If the higher lying singlet state is low enough in energy relative to the open-shell singlet, the configuration interaction can occur and lower the open-shell singlet below the triplet state to become the ground state. Adding these calculations to **Figure 2.3** we obtain **Figure 2.4**. Through configuration interaction, the singlet state becomes lower in energy then the triplet state.

Closed-shell Singlet $\left(\Psi_{S+,CS}\right): E = 2a + j^0 + k + \left(\dfrac{4(b+l)^2}{j^0 - j}\right)$

$2k$

$j^0 - j$

Closed-shell Singlet $\left(\Psi_{S-,CS}\right): E = 2a + j^0 - k$

$2k$

Open-shell Triplet $\left(\Psi_{T,os}\right): E = 2a + j - k$

Open-shell Singlet $\left(\Psi_{S,os}\right): E = 2a + j + k - \left(\dfrac{4(b+l)^2}{j^0 - j}\right)$

$J > 0$ $J < 0$
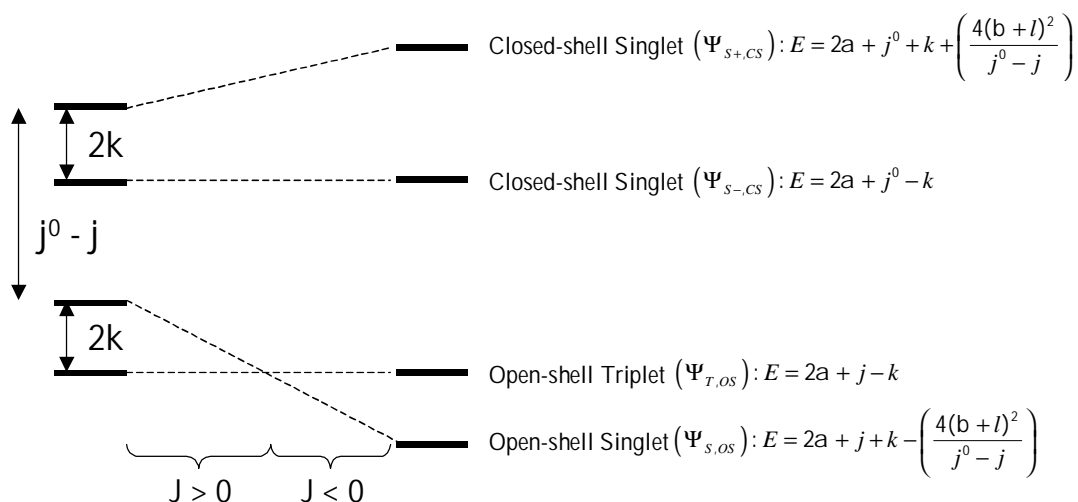
Figure 2.4. The relative energy states of a two-electron, two-orbital system including the energy from the electron in a single orbital (H^0), electron-electron repulsions (H^1), and configuration interaction (E^2). The energy states on the right side are after correcting for configuration interactions that can lead to the open-shell singlet becoming the preferential ground state.

The exchange coupling parameter is a measure of the energy difference between the triplet state and the singlet state. The zero-order and first-order Hamiltonians predict a triplet ground sate, or the ferromagnetic contribution to J_{Tot}, which is twice the exchange integral. So the more overlap between the two orbitals, the stronger the ferromagnetic contribution to J. The second-order correction (configuration interaction) lowers the energy of the singlet state, or contributes to the antiferromagnetic component of J_{Tot}. Thus, J_{Tot} then becomes **Eq. 2.35**.

$$\Delta E_{S-T} = 2J_{TOT} = J_F + J_{AF} = 2k - \left(\frac{4(b+l)^2}{j^0 - j}\right) \qquad \textbf{Eq. 2.35}$$

Depending on which component is greater, J_F or J_{AF}, determines what the ground state will be and the overall exchange coupling.

We are primarily interested in the ferromagnetic component, J_F, because by maximizing J_F we can achieve the greatest positive value of exchange coupling (ferromagnetic interaction).

Biradical Molecules and Hund's Rule

Another way to describe J_F and the overlap region is Hund's Rule.[5] The reasons for the high spin preference in atomic carbon are based in quantum mechanics.[6] The triplet state is lower than the single state in energy by $2k_{ab}$, where k_{ab} is the exchange integral, $k = \left\langle a(1)b(1) \left| \frac{1}{r_{12}} \right| a(2)b(2) \right\rangle$. Simply put, k is the energy the molecule "saves" by avoiding the overlap region between the two orbitals. The size of k_{ab} depends on the overlap density of the two orbitals. The more overlap between the two orbitals, the larger k_{ab} and the preference for a triplet state, **Figure 2.2**. This is Hund's Rule: unpaired electrons are placed into each degenerate orbital to maximize M_s. Extending this to molecules, the size of k_{ab} depends on the overlap density of the Singly Occupied Molecular Orbitals (SOMOs) in other words, it depends on the spin density (coefficients) in the overlapping orbitals that are on common atoms.

This is also based on the Pauli Exclusion Principle. Two electrons with the same spin are not allowed to occupy the same region of space. They avoid the overlap region between the orbitals. Electrons of opposite spin are not spatially constrained by the Pauli Exclusion Principle. There will be some probability of the electrons occupying the overlap region. This will raise the energy of the singlet, compared to the triplet, due to the electron-electron repulsion in the overlap region, k_{ab}.

Disjoint and Non-disjoint Biradicals

In molecules, bond connectivity and the relative energies of the singly occupied molecular orbitals (SOMOs) are important in determining the spin preference of the biradical. There are two theories that have been used to graphically predict the ground state in multi-spin molecules: valence bond (VB) theory,[7] and molecular orbital (MO) theory.[8] The VB approach, developed mainly by Ovchinnikov,[7] is able to predict the ground state in a biradical system, but has difficulty in determining the size of the singlet-triplet gap. The MO approach has the advantage of being able to estimate the size of the singlet-triplet gap qualitatively, but is sometimes unable to determine the ground spin state when the gap is very small.

Three biradicals, **Figure 2.5**, illustrate these theories: trimethylenemetane (TMM), *m*-benzoquinodimethane (MBQDM), and tetramethylenemethane (TME). In the VB approach, one assumes that one electron occupies the p-π AO on each carbon. A π-bond can only form is the p-π electrons on adjacent atoms have opposite spins. This is readily described by the star/non-star method.[9] A star (*) denotes an α or "up" spin and a non-star denotes a β or "down" spin. Stars are arranged on a molecule so that none are adjacent to another starred atom, while maximizing the number of starred atoms. **Eq. 2.36** is than used to determine the ground spin state,

$$S = \frac{\left(N^* - N\right)}{2}$$

Eq. 2.36

where S is the ground spin state of the system, N^* is the number of starred atoms and N is the number of non-starred atoms. **Figure 2.5** demonstrates this approach of our three

example biradicals. Both TMM and MBQDM are predicted to be ground state triplets,

and TME is predicted to be a ground state singlet.[5]

	TMM	MBQDM	TME
	(triplet)	(triplet)	(singlet)
$(N^*-N)/2 = S =$	$(3-1)/2 = 1$	$(5-3)/2 = 1$	$(3-3)/2 = 0$
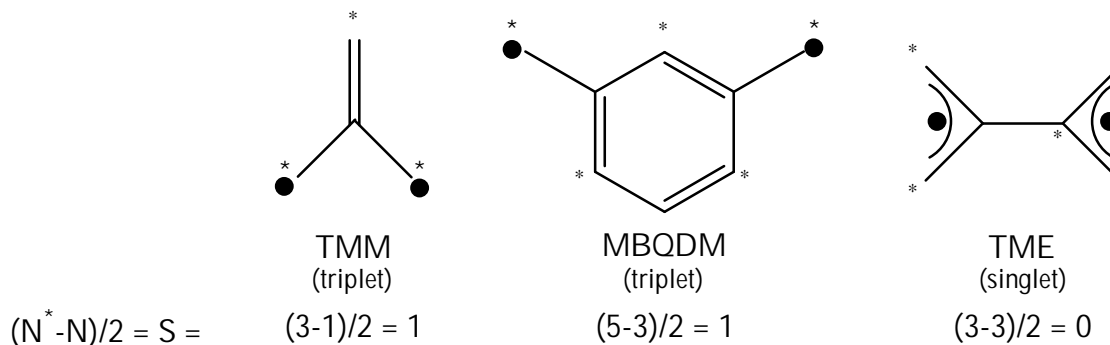
Figure 2.5. VB theory predictions for TMM, MBQDM and TME using the star/non-star approach.

Using an MO approach, Hückel theory can help predict the ground state based on

where the spin density is found in the SOMOs, **Figure 2.6**.

TMM
Non-disjoint
Triplet

MBQDM
Non-disjoint
Triplet

TME
Disjoint
Singlet
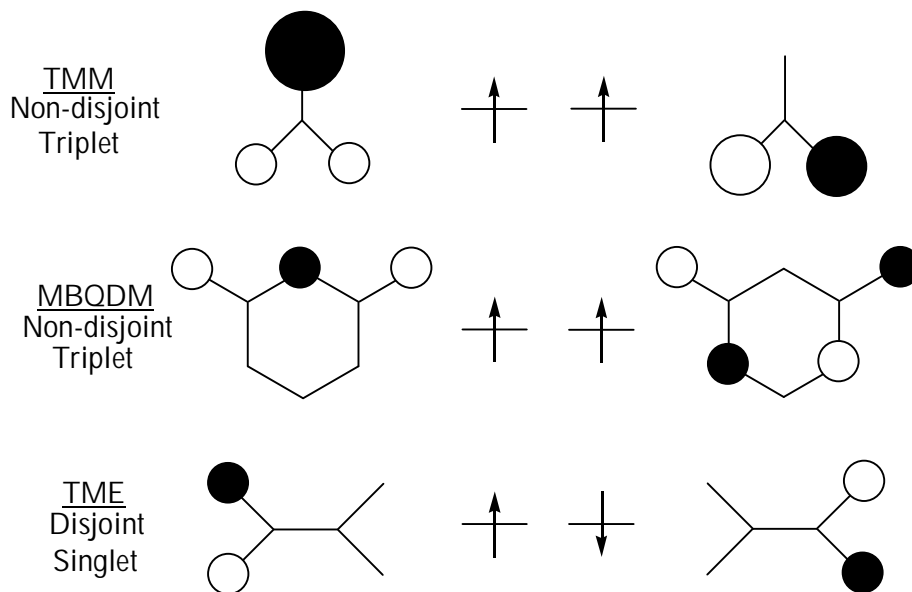
Figure 2.6. Hückel coefficients indicating where the electron density is on the two SOMO's of our three example biradicals.

If the two SOMOs do not share spin density on common atoms, then they are said to be

disjoint.[10] Disjoint molecules have no overlap of orthogonal orbitals with spin density

and the exchange integral, k, is zero. If the two SOMOs have spin density on common atoms then they are said to be non-disjoint.[10] There is overlap of the two orbitals and the exchange integral does not equal zero. As explained at the beginning of the chapter, this favors the triplet state.

Hückel theory does have limitations in describing SOMOs and the coefficients cannot account for geometric configurations and different symmetries of biradical molecules.[10] Often one chooses the Hückel MOs that "work" out of many possible NMBOs, ignoring other equally plausible MOs.

A better method than looking at the overall MO, for predicting whether a system is disjoint or non-disjoint, is based on the connectivity of simpler components and the coefficients of these components.[10] Consider the allyl radical which has two types of atoms: active (A, having spin density), inactive (I, no spin density), **Figure 2.7**. The active atoms are the two atoms on both ends. The inactive atom is the middle carbon. If one attaches an active radical ($\bullet CH_2$) to an inactive site (Case1, A – I), a non-disjoint system, TMM is formed (triplet ground state). If an active radical ($\bullet CH_2$) is attached to another active site (Case 2, A – A), a bond is formed. Finally if two inactive sites are attached (Case 3, I – I), a disjoint system, TME, is formed.
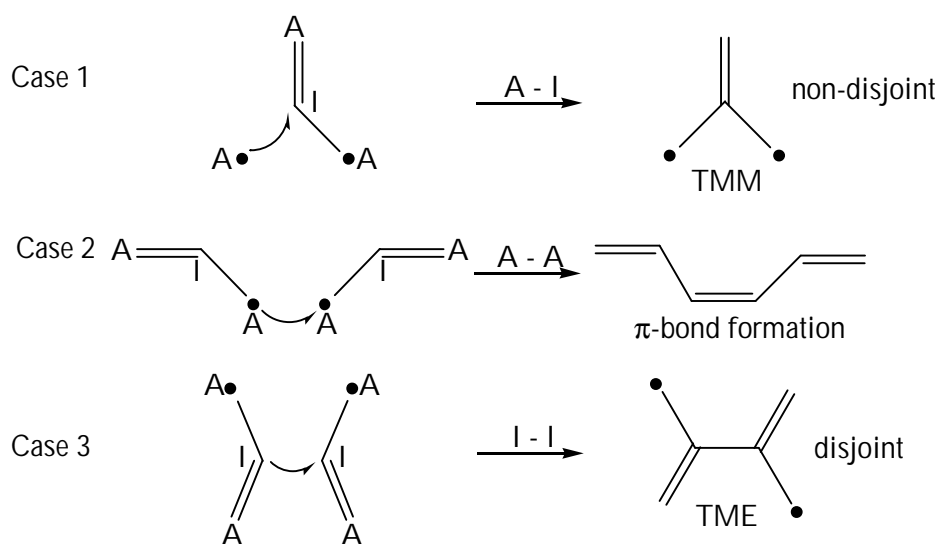
Figure 2.7. Three examples of using simpler components to determine if a molecule is disjoint or non-disjoint. Case 1: active to inactive leads to non-disjoint (high spin); Case 2: active to active leads to bond formation; Case 3: inactive to inactive leads to disjoint.

Both disjoint and non-disjoint molecules are also non-Kekulé hydrocarbons. A

non-Kekulé hydrocarbons is a molecule with a resonance structure that has as many π-

bonds as possible, but at least two atom are not included in a π-bond.[8] In other words,

regardless of what resonance structure is drawn, there will always be two unpaired

electrons in the biradical. Non-disjoint molecules are also called cross-conjugated.[11]

Based on these discussions, ethenylidene and *meta* substituted phenylene are both

cross-conjugated couplers that promote ferromagnetic coupling, **Figure2.8**.
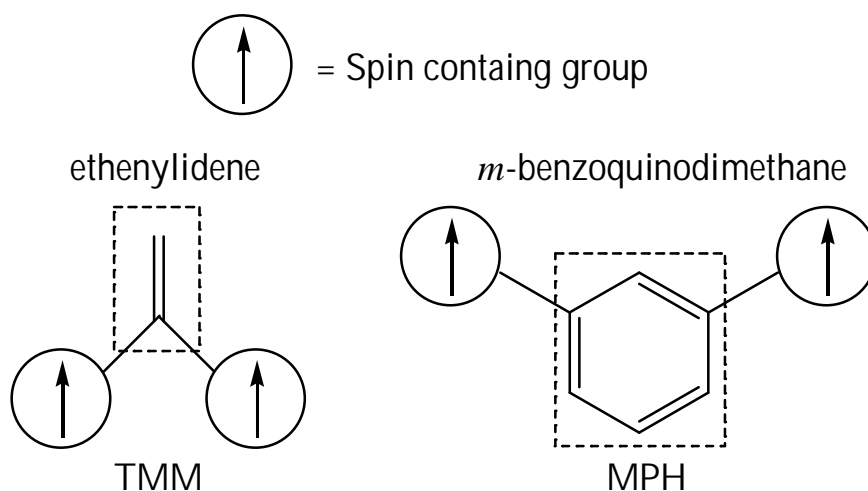
Figure 2.8. Spin coupling units that promote ferromagnetic coupling between two radicals. The coupling unit is highlighted in a dashed box. Ethenylidene biradicals are referred to as TMM-type and phenylene biradicals are referred to as MPH-type (*m*-phenylene).

These biradicals are commonly referred to as TMM-type and MPH-type, based on their parent compounds.[2,8] A basic motif for creating high spin molecules is to connect two "spin containing" groups to a "coupler" that will promote ferromagnetic coupling.

When two spins are exchange coupled, states are created with different multiplicities. These higher lying states can be thermally accessible. The Heisenberg-Dirac-Van Vleck (HDVV) Hamiltonian is used to describe exchange coupled spins, **Eq. 2.36**.[1]

$$\hat{H}_{ab} = -2J_{ab}\hat{S}_a\hat{S}_b \qquad\qquad \textbf{Eq. 2.36}$$

This empirical Hamiltonian describes the spin angular momentum operators ($\hat{S}_a$ and $\hat{S}_b$) and the magnitude of this interaction depends on J_{Tot}, the isotropic exchange parameter. The product of the spin operators can be expressed in terms of the component spin operators and the total spin operator, **Eq. 2.37**.

$$\hat{S}_{Tot} = \hat{S}_a + \hat{S}_b \qquad\qquad \textbf{Eq. 2.37}$$

$$\hat{S}_{Tot}^2 - \left(\hat{S}_a + \hat{S}_b\right)^2 = \hat{S}_a^2 + \hat{S}_b^2 + 2\hat{S}_a\hat{S}_b \qquad \textbf{Eq. 2.38}$$

$$\hat{S}_a\hat{S}_b = \frac{1}{2}\left(\hat{S}_{Tot}^2 - \hat{S}_a^2 - \hat{S}_b^2\right) \qquad \textbf{Eq. 2.39}$$

Since the eigenvalue of S^2 is $S(S+1)$, the energy of the state can easily be determined by substituting in the appropriate terms, **Eq. 2.40**.

$$E_{Tot} = -\boldsymbol{J}_{ab}\left[S_{Tot}(S_{Tot}+1) - S_a(S_a+1) - S_b(S_b+1)\right] \qquad \textbf{Eq. 2.40}$$

Since the final two terms are constants **Eq. 2.40** reduces to **Eq. 2.41**.

$$E_{Tot} = -\boldsymbol{J}_{ab}\left[S_{Tot}(S_{Tot}+1)\right] \qquad \textbf{Eq. 2.41}$$

Thus, the energy of the singlet state, triplet state and the energy gap between them can be determined, **Eq. 2.42 – Eq. 2.44**.

$$E_{Triplet} = -\boldsymbol{J}\left[1(1+1)\right] = -2\boldsymbol{J} \qquad \textbf{Eq. 2.42}$$

$$E_{Singlet} = -\boldsymbol{J}\left[0(0+1)\right] = 0 \qquad \textbf{Eq. 2.43}$$

The singlet-triplet energy gap is then just $2\boldsymbol{J}$, **Eq. 2.43**.

$$\Delta E_{ST} = E_S - E_T = 2\boldsymbol{J} - 0 = 2\boldsymbol{J} \qquad \textbf{Eq. 2.44}$$

By the convention used above, $\boldsymbol{J}_{Tot} > 0$ describes ferromagnetic coupling and $\boldsymbol{J}_{Tot} < 0$ describes antiferromagnetic coupling. The exchange coupling parameter, $\boldsymbol{J}_{Tot}$, can be determined experimentally by either Electron Paramagnetic Resonance (EPR) or by magnetometry.

In EPR spectroscopy the double integrated $\Delta m_s = 2$ signal is typically used. Temperature dependence of this signal can be used to determine $\boldsymbol{J}_{Tot}$ through the expression, **Eq. 2.45**.[12]

$$I = \frac{C}{T}\left(\frac{3e^{\left(-2J_{Tot}/k_BT\right)}}{1+3e^{\left(-2J_{Tot}/k_BT\right)}}\right)$$

Eq. 2.45

When $J < 0$ the magnitude can be determined. When $J \geq 0$ only a linear plot will result.

For molecules with very small magnetic moments a Super Conducting Quantum Interference Device (SQUID) is typically used. The temperature dependence of the magnetic susceptibility for an S=1 system is given by the HDVV equation, **Eq. 2.48**.[1]

$$c = \frac{2Ng^2b^2}{k_BT}\frac{e^{-2J/k_BT}}{1+3e^{-2J/k_BT}}$$

Eq. 2.48

Both instruments, EPR and SQUID magnetometry, are described in detail in Chapter 3.

Spin Containing Groups and Biradicals Studied

From the preceding discussion we can now design high-spin molecules by putting together "coupling units" with "spin containing" groups. In this work, three different spin groups were used. These spin groups also can act as ligands to metals to make extended solids. An important characteristic for the spin group is the electron distribution in the spin group.

Verdazyls were first reported by Kuhn and Trischmann in 1963, **Figure 2.9**.[13,14] They are similar to linear hydrazinyl radicals, but in cyclic form. Verdazyls are heterocyclic analogs to a three π-electron pentadienyl system or three π-electron allyl-type system. Verdazyls can bind through nitrogen to form metal complexes.[15]
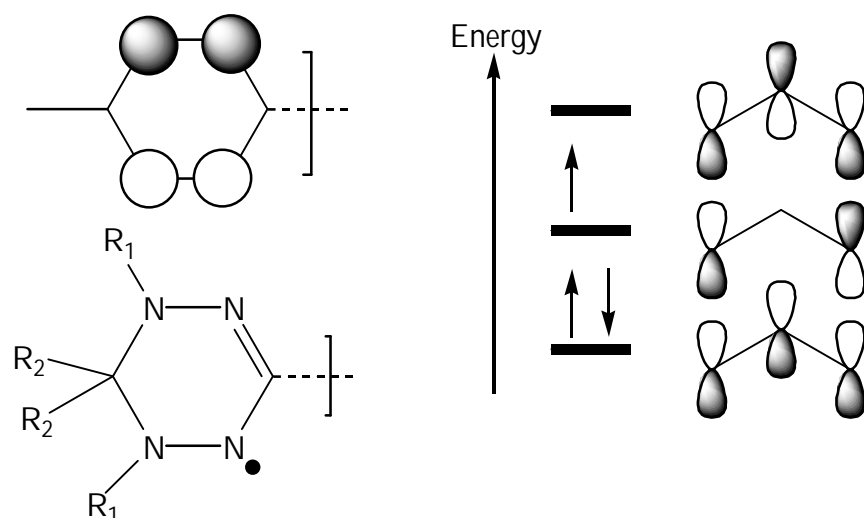
Figure 2.9. MO of verdazyl radical (For our work R_1 = phenyl and R_2 = carbonyl). Molecular orbital diagram for an allyl system with 3 π-electrons. The bis(verdazyl)s studied were connected through the nodal position on the verdazyl ring.

The unpaired electron is in a non-bonding MO. The bis(verdazyl)s studied were all connected through the nodal position. Bis(verdazyl)s are considered disjoint biradicals and are heterocyclic analogs to TME. The MO diagram of bisverdazyl is shown in **Figure 2.10**.[16]
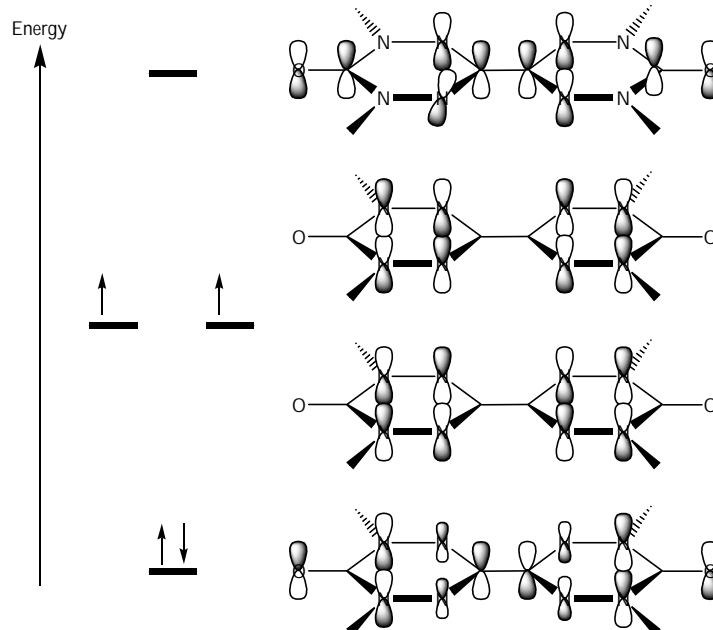
Figure 2.10. MO diagram of the parent bisverdazyl.[16]

This suggests that there will be very little coupling between the two verdazyl groups.

Our studies of bis(verdazyl)s will be reported in Chapter 4.[17]

Semiquinones versatile organic spin carriers that can bind metals.[18-20] Our work

focuses on 3-*tert*-buytlorthoquinones, **Figure 2.11**, and will simply be referred to as

semiquinones.
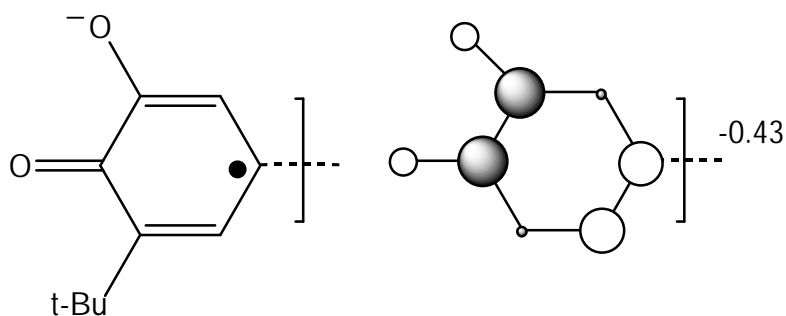
Figure 2.11. 3-*tert*-butylorthoquinone and its SOMO.

This semiquinone anion radical is stericly protected by zinc hydro-tris(pyrazolyl) borate

ancillary ligand, **Figure 2.12**.
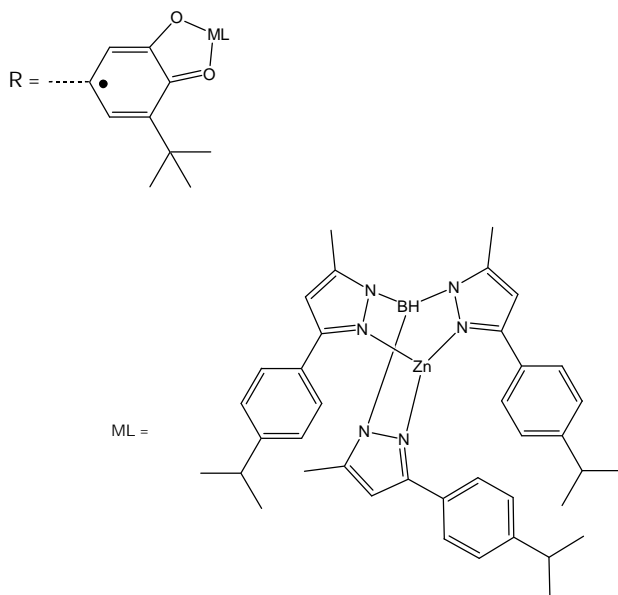
Figure 2.12. Zinc trisperazoylborate ancillary ligand used to sterically protect the semiquinone anion radical.

The semiquinones were connected to an ethene coupler. In essence these are TMM-type biradicals, are non-disjoint and should be ground state triplets. Our studies of bis(semiquinone)s are the subject of Chapter 5.[21]

Nitroxides are very versatile and have found many uses in chemistry and biochemistry.[22] for our purposes we used *t*-butyl nitroxides that were connected *para* on a benzene ring and will be referred to as nitroxide, **Figure 2.13**.
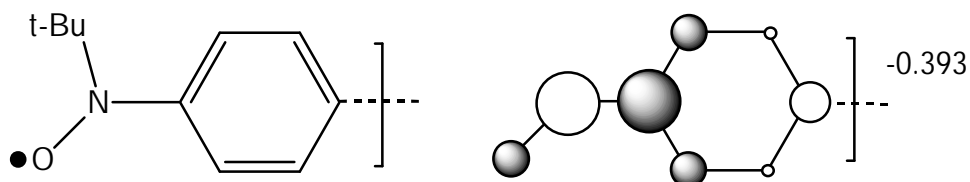
Figure 2.13. Structure of the nitroxide spin containing group used in our studies.

These phenyl nitroxides were connected using to an ethene coupler. In essence these are TMM-type biradicals, are non-disjoint and should be ground state triplets. Our studies of bis(nitroxide)s are the subject of Chapter 6.[23]

References
(1)   Kahn, O. *Molecular Magnetism*, 1993.
(2)   Rajca, A. *Chem. Rev.* **1994**, *94*, 871.
(3)   Lowe, J. P. *Quantum Chemistry*; 2nd ed.; Academic Press: New York, 1993.
(4)   Alberty, R. A.; Silbey, R. J. *Physical Chemistry*; John Wiley & Sons, Inc.: New York, 1992.
(5)   Borden, W. T.; Iwamura, H.; Berson, J. A. *Acc. Chem. Res.* **1994**, *27*, 109.
(6)   Hadfield, D. *Permanent Magnets and Magnetism*; Iliffe Books, LTD.: New York, 1962.
(7)   Lahti, P. M., Ed. *Magnetic Properties of Organic Materials*; Marcel Dekker: New York, 1999.
(8)   Dougherty, D. A. *Acc. Chem. Res.* **1991**, *24*, 88.
(9)   Longuett Higgins, H. C. *J. Chem. Phys.* **1950**, *18*, 265.

(10)   Borden, W. T.; Davidson, E. R. *J. Am. Chem. Soc.* **1977**, *99*, 4587.

(11)   Phelan, N. F. *J. Chem. Ed.* **1968**, *45*, 633.

(12)   Berson, J. A., Ed. *The Chemistry of the Quinonoid Compounds, Vol. II*; John Wiley & Sons: New York, 1988.

(13)   Kuhn, R.; Trischmann, H. *Angew. Chem., Int. Ed. Eng.* **1963**, *2*, 155.

(14)   Kuhn, R.; Neugebauer, F. A.; Trischmann, H. *Angew. Chem., Int. Ed. Eng.* **1964**, *3*, 232.

(15)   Hicks, R. G. *Aust. J. Chem.* **2001**, *54*, 597.

(16)   Brook, D. J. R.; Fox, H. H.; Lynch, V.; Fox, M. A. *J. Phys. Chem.* **1996**, *100*, 2066.

(17)   Fico, R. M., Jr.; Hay, M. F.; Reese, S.; Hammond, S.; Lambert, E.; Fox, M. A. *J. Org. Chem.* **1999**, *64*, 9386.

(18)   Pierpont, C. G.; Lange, C. W. *Prog. Inorg. Chem.* **1994**, *41*, 331.

(19)   Pierpont, C. G.; Attia, A. S. *Coll. Czech. Chem. Comm.* **2001**, *66*, 33.

(20)   Pierpont, C. G.; Buchanan, R. M. *Coord. Chem. Rev.* **1981**, *38*, 45.

(21)   Shultz, D. A.; Fico, R. M., Jr.; Bodnar, S. H.; Kumar, R. K.; Vostrikova, K. E.; Kampf, J. W.; Boyle, P. D. *J. Am. Chem. Soc.* **2003**, *125*, 11761.

(22)   Volodarsky, L. B.; Reznikov, V. A.; Ovvharenko, V. I. *Synthetic Chemistry of Stable Nitroxides*; CRC Press: Boca Raton, 1994.

(23)   Shultz, D. A.; Fico, R. M., Jr.; Lee, H.; Kampf, J. W.; Kirschbaum, K.; Pinkerton, A. A.; Boyle, P. D. *J. Am. Chem. Soc.* **2003**, *in press*.

Chapter 3. Electron Paramagnetic Resonance and Super Conducting Quantum Interference Device

Electron Paramagnetic Resonance (EPR)[1-5]

EPR: The Instrument

Nuclear magnetic resonance (NMR) and electron paramagnetic resonance (EPR) are very similar in that both utilize magnetic resonance techniques. In the presence of a magnetic field there are two spin states, m_s: α (+½) and β (-½), **Figure 3.1**.
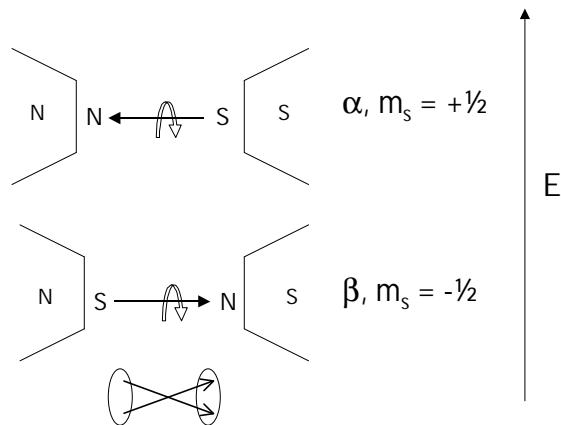
Figure 3.1. Cartoon of the α and β spin states of an electron in the presence of a magnetic field. The arrow represents the magnetic moment of the electron.

The energy of the spin state is described by **Eq. 3.1**,[1-5]

$$E = g_e \mathrm{b} m_S H \qquad\qquad \textbf{Eq. 3.1}$$

where g_e is the electronic g-factor of an electron (Lande's constant), β is the Bohr magneton, m_S is the spin quantum number, and H is the applied magnetic field. The larger the magnetic field, the larger the energy difference between the spin states. The splitting of the spin states in the presence of a magnetic field is known as the Zeeman splitting, **Figure 3.2**.
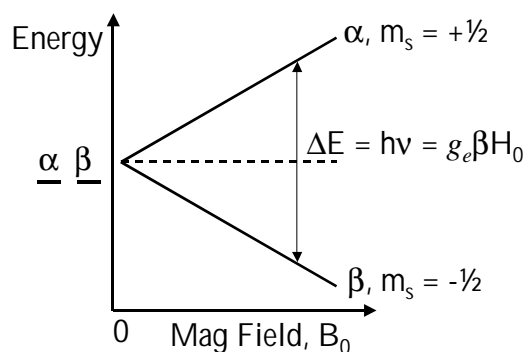
Figure 3.2. Zeeman splitting of an electron in the presence of a magnetic field. The double-headed arrow represents the resonance condition for the absorption of a photon of light.

A magnetic dipole, such as an electron, will precess in a magnetic field. The often-used analogy is that of a top spinning in the presence of the earth's magnetic field. The processional (Larmor) frequency, ω, is directly proportional to the gyromagnetic ratio of the electron, γ_e, and the strength of the applied magnetic field, **Eq. 3.2.**

$$w = g_e H \qquad \qquad \textbf{Eq. 3.2}$$

For X-band EPR the field strength is around 0.33 Tesla, which is approximately 3x greater than a refrigerator magnet. This sets up a resonance condition for the absorption of a quantum of electromagnetic radiation. Electromagnetic radiation of the Larmor frequency will cause the spins to flip, **Eq 3.3**.

$$\Delta E = h\text{n} = hg_e H = g_e \text{b}H \qquad \qquad \textbf{Eq. 3.3}$$

This follows the selection rule for multiplicity 2S + 1. An S=½ system will give rise to a doublet, an S=1 system will be a triplet. The allowed transitions obey the selection rule $\Delta m_S = \pm 1$, $\Delta m_I = 0$, where m_I is the nuclear spin quantum number.

The basic design elements of an EPR spectrometer are shown in **Figure 3.3**.
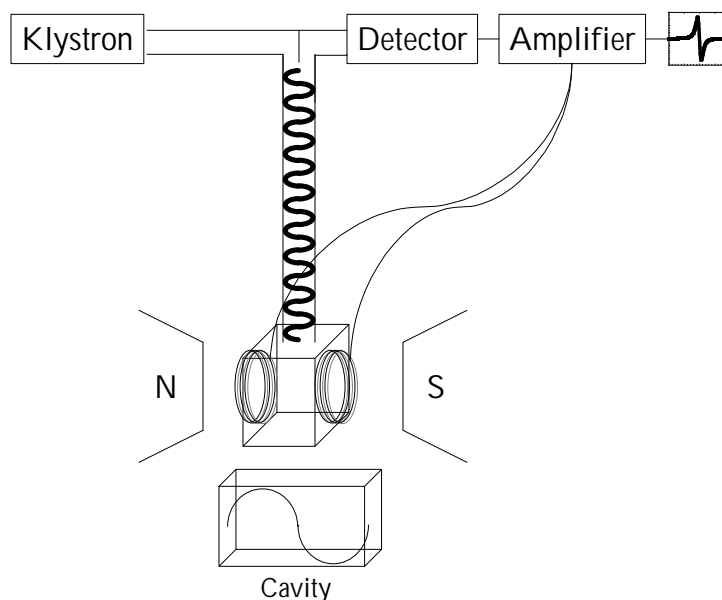
Figure 3.3. The basic design elements of an EPR spectrometer.

Typically for X-band EPR the frequency is held constant and the field is swept. The

source for electromagnetic radiation in an EPR is a klystron. A klystron produces

frequencies in the microwave range (typically 9.5 GHz). The radiation then travels down

a waveguide into the cavity. The cavity is 2-3 cm long, which is the wavelength of the

radiation. The radiation then is reflected back into the detector.

The cavity holds one standing wave of radiation. When the detector "sees" a

change in the intensity of the radiation a signal is sent to an amplifier to be recorded.

Along the sides of the cavity are coils of wire called modulation coils. An alternating

current is passed through these coils producing a small alternating magnetic field. This

AC current produces an alternating shielding/deshielding effect on the external field. The

amplifier is in phase with the alternating current. The only signals from the detector that

are amplified are those that are in frequency with the modulation amplitude. This effectively filters out unwanted noise whose frequency is not the same modulation frequency (typically 100 kHz). This has a secondary effect on recorded spectra. The recorded spectrum is a plot of field vs. signal intensity. Since the modulation coils vary the observed magnetic field, and the detector is recording the change in intensity of the microwave radiation a plot of field (ΔH) versus intensity (ΔI) is really a plot of Δy/Δx. Thus, the signal is recorded as the first derivative of an absorption signal, **Figure 3.4**.

$$y = \frac{1}{1 + ax^2}$$

$$\frac{dy}{dx} = \frac{-2ax}{\left(1 + ax^2\right)^2}$$
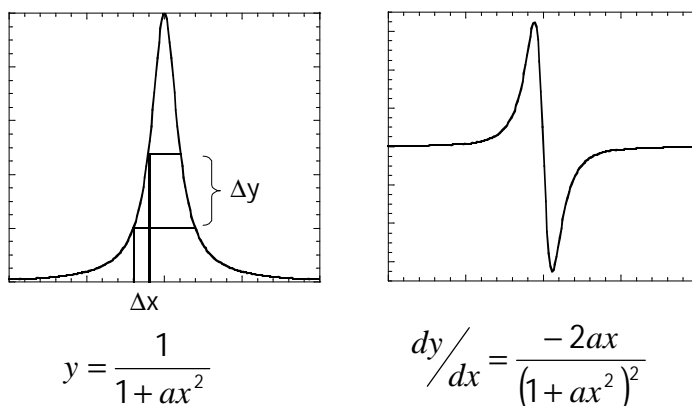
Figure 3.4. Plots a lorenztian line and of the first derivative of a lorentzian line.

EPR: The Spectrum - Solution Phase

Solution phase EPR spectra are very useful for studying radicals. From the preceding discussion one might assume that you would 'see' a single absorption for an S=½ system. However, the spin of an unpaired electron may couple to nuclear spins. Due to the low natural abundance of ^{13}C, and small gyromagnetic ratio this direct coupling is weak. However, a spin centered on a carbon atom, such as that depicted in **Figure 3.5** and **Figure 3.6**, will polarize the spin density on the adjacent protons spin, through the σ framework.[2,4]

Carbon p-orbital

Hydrogen s-orbital

Carbon hybrid orbital
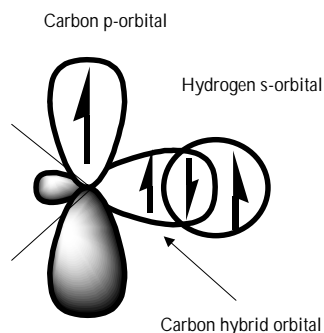
Figure 3.5. Electron Spin Polarization through the σ-framework.
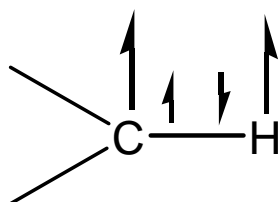
Figure 3.6. Electron Spin Polarization through the σ-framework.

This is called hyperfine coupling and the hyperfine coupling constant (hfcc) is denoted by a_N, where N is the nucleus of interest. The hfcc is related to the spin density through the McConnell relationship, **Eq. 3.4**, where Q is the proportionality constant (approximately the same for all carbon atoms) and ρ_t is the spin density at that nucleus.[2,4]

$$a_i = Q r_i \qquad \textbf{Eq. 3.4}$$

The maximum number of observable transitions is:

$$\text{\# of EPR transitions} = \prod_i 2n_i I + 1 \qquad \textbf{Eq. 3.5}$$

where n is the number of nuclei and I is the spin of the nuclei. For simple systems the intensity and spacing of this lines can be predicted using Pascal's triangle. For illustrative purposes, simple versions of Pascal's triangle for the three different spin carriers were used our studies is shown in **Figure 3.7**. The relative intensity of the transition is listed to the left of each transition. Pascal's triangle is only useful for simple

systems. However, it does serve to illustrate that EPR spectra are typically symmetric, the spectral width is directly related to the magnitude of the coupling constants, and the higher the number of magnetically distinct nuclei the more complex the spectra.
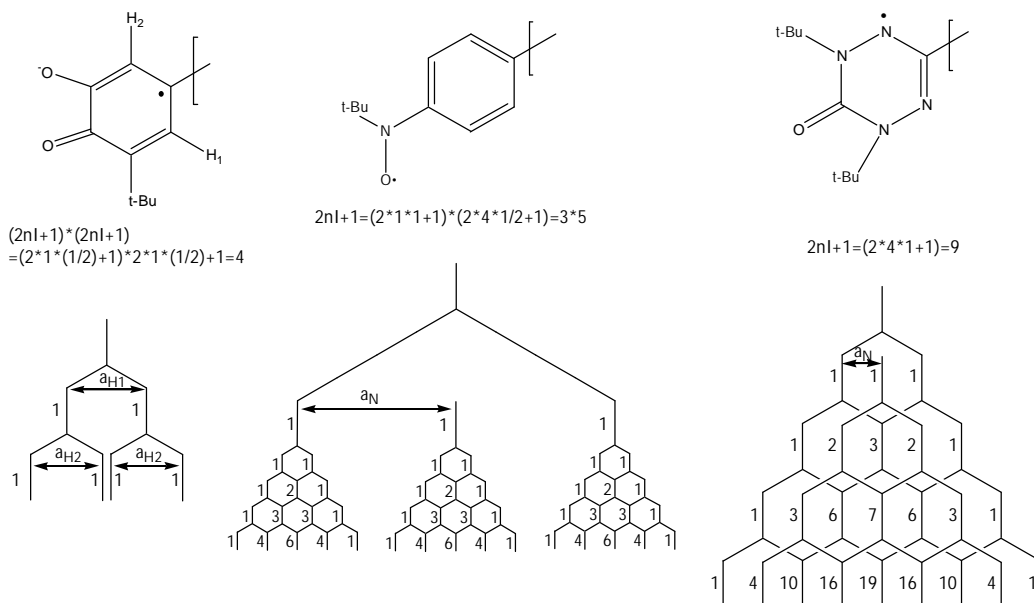
Figure 3.7. Pascal's triangle for monoradicals spin carriers used in the studies. These are presented only as simple pictorials of the spin containing units in these studies and are only used to illustrate EPR spectra. The coupling constants are not drawn to scale with respect to each molecule.

For biradicals if $|J| >> |a_N|$ the spectral width will be half that of the monoradical.[1,2,4,6] As the number of magnetically different nuclei increases, the complexity of the EPR spectrum also increases. Simulation of solution phase EPR spectra is often difficult, but for our systems a readily available free simulation program was used. This program is free and available for download from the National Institute of Environmental Health and Sciences under the Public EPR Software Tools (P.E.S.T.).[7] It provides an iterative fitting routine for optimizing spectral parameters used in fitting the data.

EPR: The Spectrum – Frozen Matrix

Solution phase EPR is very useful for determining the spin distribution in a molecule. For systems where $m_s > \frac{1}{2}$ spectra of randomly oriented molecules (in a powder or a matrix) can be used to determine the zero field splitting parameters to gain insight into the dipolar interactions and the geometry of the molecule.

The exchange coupling between two electrons in a biradical leads to two spin states; a singlet and a triplet. These states were briefly discussed in Chapter 1 and were discussed in further detail in Chapter 2. Suffice to say that the singlet state is EPR silent (no unpaired electrons) and for biradicals only the triplet state is observed by EPR.

The isotropic Heisenberg Hamiltonian can describe the energy separation between these two states $\hat{H} = -2J\hat{S}_1\hat{S}_2$. Spin-spin dipolar interactions within the triplet state lift the degeneracy of the three triplet microstates even in the absence of an applied magnetic field. This energy separation is described by the spin-spin Hamiltonian $\hat{H} = \hat{S}_1 gDg\hat{S}_2$ and the eigenvalues are the Zero Field Splitting (ZFS) parameters D and E.[4] Thus, when two electrons interact, the exchange interaction lifts the degeneracy of the singlet and triplet states and the dipolar (ZFS) interactions lift the degeneracy of the three triplet microstates, **Figure 3.8**.
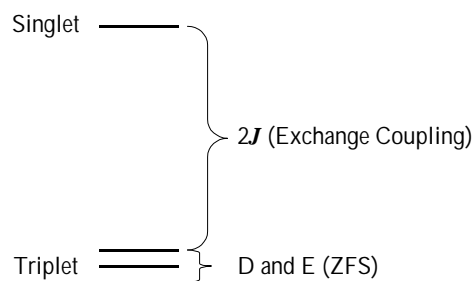
Figure 3.8 Simple energy level diagram describing exchange interaction (2**J**) and ZFS (D and E).

The basis of an EPR experiment was described at the beginning of this chapter.

For an S = ½ system (2S + 1 = 2) this gives rise to a doublet, **Figure 3.2**. In solution,

there is often hyperfine coupling between the electron spin and proton spins that are

alpha. Hyperfine coupling is observable in triplet species in solution because random

tumbling of the molecules averages out dipolar interactions. In a frozen matrix the

dipolar interaction will dominate the spectrum.[4] For an S = 1 system (2S + 1 = 3) this

gives rise to a triplet. As mentioned earlier, the degeneracy of the triplet state is lifted

because of dipolar interactions that give rise to the ZFS parameters. In the presence of a

magnetic field, Zeeman splitting further separates the triplet microstates. The spectrum

follows the selection rule $\Delta m_S = \pm 1$ and transitions that are observed for the $m_S = -1$ to

$m_S = 0$ spin state and $m_S = 0$ to $m_S = +1$ state, **Figure 3.9**.
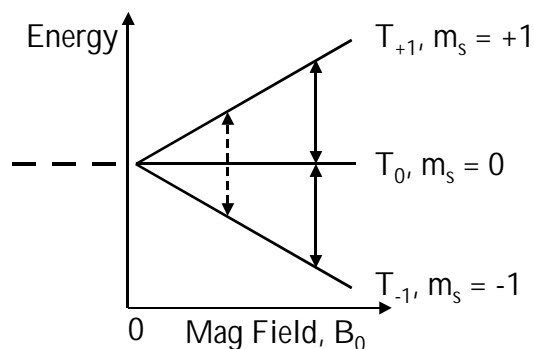
Figure 3.9. Zeeman splitting in a triplet system. The double-headed arrow represents an absorption. The transition depicted by the dashed double headed arrow at lowest field represents the formally forbidden $\Delta m_S = 2$ transition.

48

Figure 3.9 is oversimplified and shows only the Zeeman interaction of the spins and the magnetic field similar to the one electron case (**Figure 3.2**). The triplet microstates are not degenerate. The effective magnetic field experienced by each electron is the vector sum of several magnetic fields. The vector sum includes the magnetic field of the other electron, the magnetic fields of the nuclei and the magnetic field that arises from each electron's own orbital angular momentum.[8] The largest internal magnetic field that we will be concerned about is the field of the other electron. The magnetic moment of an electron is three orders of magnitude grater than that of a nuclei and can be ignored.[9] The contribution from spin-orbit coupling of the spin of the electron with the orbital angular momentum is very small in organic systems. Manifestation of spin-orbit coupling is seen in deviation of the g value for the free electron (g = 2.0023) and for organic system there is very little change.[8] Therefore, the only contribution to the ZFS will be the dipolar interaction between the two electrons.

Dipole-dipole interactions within the triplet state are repulsive in nature and depend upon the geometry of the molecule. **Figure 3.10** depicts how geometry affects the ZFS parameters D and E.
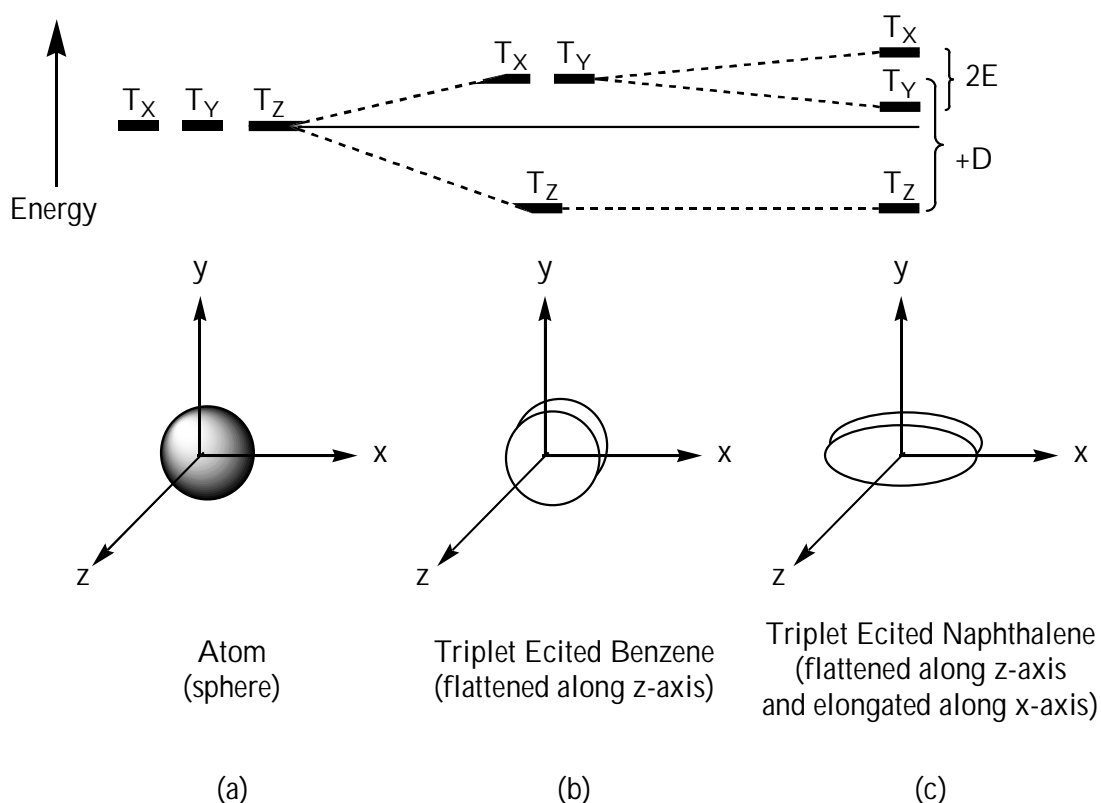
Figure 3.10. Cartoon representation of ZFS and how the geometry of a molecule affects the energy of the triplet microstates.

The T_Z state represents the state in which the spin axis of the two electrons have been quantized so that they are confined to the XY plane, thus the spin angular momentum in the Z direction is zero. The T_X and T_Y states are defined in analogous ways in which the spin angular momentum is zero in the X and Y directions respectively. In **Figure 3.10**, case (a) the two electrons are distributed symmetrically in a sphere. There is no direction in which the electrons can move further apart to decrease the energy. In this case, the three microstates are degenerate (no ZFS). In case (b), with triplet excited benzene as the model, the molecule is compressed along the z-axis. The electrons experience the most repulsions in the microstates that have a z component. The T_X state (yz plane) and the T_Y state (xz plane) will therefore be raised in energy. The T_Z state (xy plane) has no z

component and will be lowered in energy. In case (c), triplet excited naphthalene, the z-axis remains compressed in addition to an elongation along the x-axis. Since the elongation is along the x-axis the T_Z state is unaffected. The T_Y state on the other hand is lowered in energy because the electrons can effectively stay farther apart. The T_X state is raised in energy because the spins are confined to the yz plane. These splittings described, are not the result of an external magnetic field, but they are due to the dipole-dipole interactions between the electrons based on the geometry of the molecule. This energetic difference in the triplet microstates at zero field is due to the anisotropic spin distribution within a molecule and is described by the parameters D and E. D is the difference in energy between the lowest lying microstate and the average of the higher two microstates and is related to the distance between the unpaired electrons ($D \sim 1/r^3$). E is ½ the energy difference between the two highest lying microstates and is related to the ellipicity of the molecule. A positive D arises if an axis is flattened as in **Figure 3.10** but, a negative D is the result if that same axis is elongated. Thus, the geometric shape of the molecule can accurately be predicted based on the D and E parameters of a molecule.[10] These parameters are obtained by simulating the EPR spectrum. For our work, ZFS parameters were estimated by simulation using a program from Brüker EPR.[11] Most EPR ZFS parameters are listed as absolute values because the EPR line positions only depends on the relative signs of D and E.[4]

The simplest triplet EPR spectrum arises from a molecule with a spherical distribution of the spins. If the applied magnetic field is aligned along the z-axis, then the electrons that are in the xy-plane will remain the same in energy (T_0 state) because their

51

spin vectors are perpendicular to the applied magnetic field. The electrons in the yz plane or the xz-plane will either be stabilized or destabilized if their spin vectors are opposed to the applied field (T_{-1} state) or aligned to the applied field (T_{+1} state). **Figure 3.11** depicts the energy diagram for a triplet with spherical geometry.
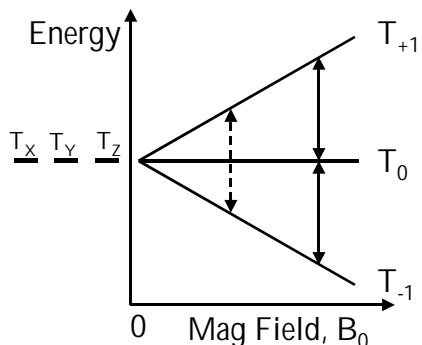
Figure 3.11. Energy diagram for a triplet with spherical geometry. A double-headed arrow represents a transition.

There are two allowable transitions that occur at the same field strength. The EPR spectrum depends on the alignment of the molecule with respect to the applied magnetic field. In this simple case, if the applied field were along the y-axis or x-axis the same spectral pattern would result.

Just as in **Figure 3.10**, the symmetry of the molecule can be lowered from this simple case (a), cubic, to case (b), axial, and finally to case (c), rhombic increasing the complexity of the EPR spectrum. **Figure 3.12** is an example of an axially symmetric triplet EPR energy diagram and the corresponding spectrum. The solid double arrows represent $\Delta m_S = \pm 1$ transitions and the dashed double arrow is the formally forbidden $\Delta m_S = 2$ transition. In this case there would be four observed transitions.
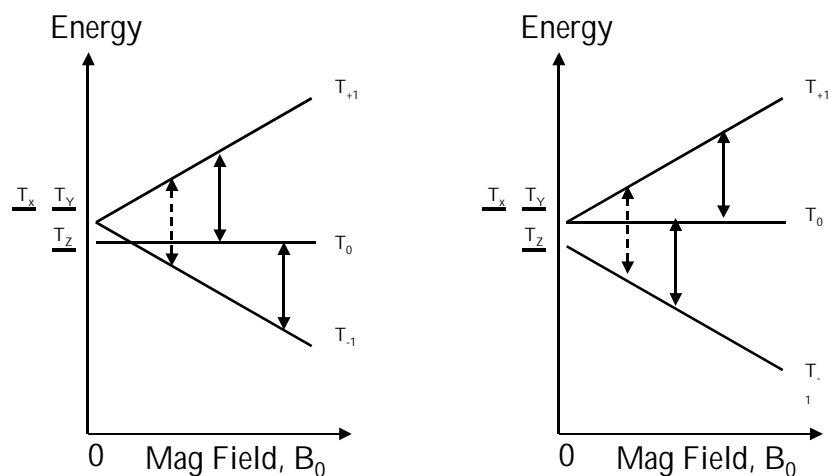
Figure 3.12. Energy diagram for a triplet with axial symmetry. (a) Applied field along the molecular z-axis. (b) Applied field along the molecular y-axis or x-axis (they are degenerate). (c) Simulation of the observed EPR spectrum.

The outermost two occur from molecules with the applied field along the molecular z-axis and are called the z transitions. The inner two transitions result from molecules that have their y-axis or x-axis along the applied molecular field.

The energy level diagram for a molecule with rhombic symmetry is depicted in **Figure 3.13**.
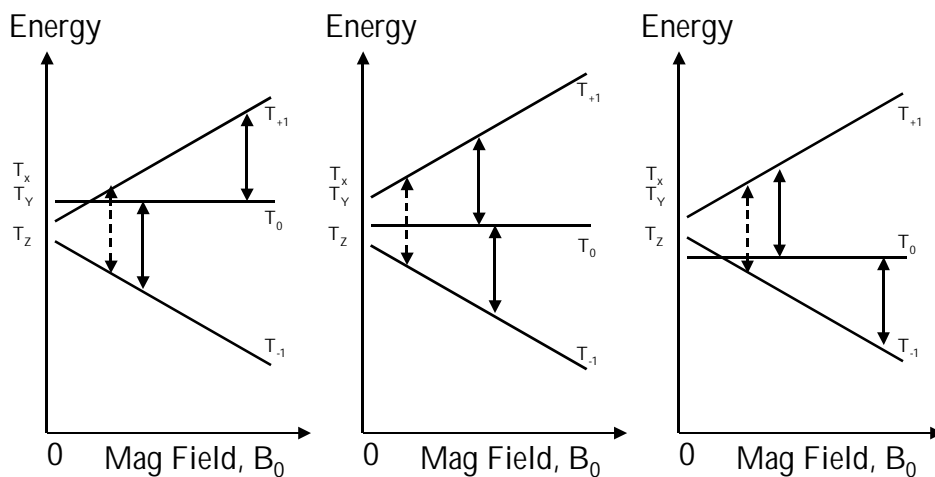
Figure 3.13. Energy level diagram for a triplet with rhombic symmetry. (a) Applied field aligned with the molecular x-axis. (b) Applied field aligned with the molecular y-axis. (c) Applied field aligned with the molecular z-axis.

In this case there would be six total transitions. Again, the outer most two are due to molecules with the applied field along the molecular z-axis and the inner four are a result of alignment of the applied field with the molecular x-axis and y-axis.

Figure 3.14 represents a typical frozen solution EPR spectrum. The outer most z transitions are directly related to D. The number of transition is directly related to the geometry of the molecule. If the molecule is axial the transitions due to the x-axis and y-axis are degenerate and only four total transitions will be observed.
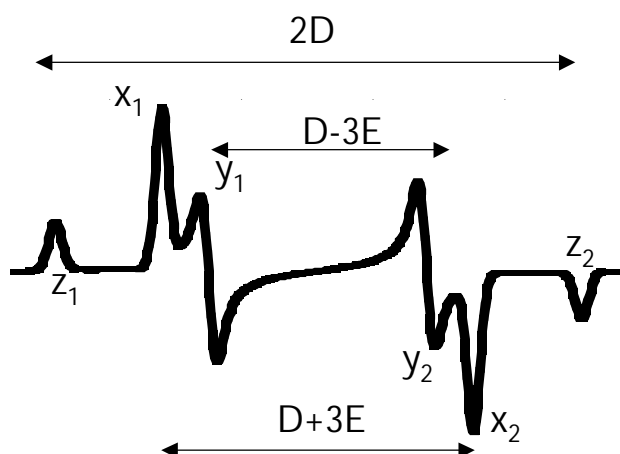
Figure 3.14. Simulated EPR spectrum for a rhombic triplet. The ZFS parameters are shown.

The value of obtaining the ZFS parameters for a triplet is two-fold. First, the ZFS are an indicator to the molecular geometry. Second, since they are due to dipole-dipole interactions between electrons, D will be related to the average distance between the two electrons $(D\sim 1/r^3)$.[4] As this distance becomes smaller, D becomes larger as in **Eq. 3.6**.

Although the singlet state is EPR inactive, doublet impurities occur at the same field as the $\Delta m_S = 1$ transitions of the triplet. Integration of this region can prove difficult due to monoradical impurities. Luckily, there is a transition that occurs only in the triplet that is at half the field of the $\Delta m_S = 1$ transition. This half-field, $\Delta m_S = 2$, transition can

be used as an indicator of a triplet species, and also to use Boltzmann statistics to

determine the energy spacing between the triplet and singlet states.

$$\frac{n_T}{n_T + n_S} = [Triplet]_{rel} = \frac{3e^{-\varepsilon_T/RT}}{3e^{-\varepsilon_T/RT} + 3e^{-\varepsilon_S/RT}} \qquad \textbf{Eq. 3.6}$$

Multiplying the numerator and denominator by $e^{\varepsilon_S/RT}$, and using $\varepsilon_T - \varepsilon_S = \Delta E_{ST}$ give, **Eq. 3.7**.

$$[Triplet]_{rel} = \frac{3e^{-\Delta E_{ST}/RT}}{1 + 3e^{-\Delta E_{ST}/RT}} \qquad \textbf{Eq. 3.7}$$

Substituting $\Delta E_{ST} = -2J$ give **Eq. 3.6**. [12]

$$I = \frac{C}{T}\left(\frac{3e^{\left(2J_{Tot}/k_B T\right)}}{1 + 3e^{\left(2J_{Tot}/k_B T\right)}}\right) \qquad \textbf{Eq. 3.8}$$

Thus, double integration of the half-field signal will yield the area of the peak,

which is related to the number of unpaired spins, or the population of the triplet state, **Eq.

3.8**. **Figure 3.15** shows several plots of **Eq. 3.8** using several *J*-values. This

demonstrates one of the problems with using EPR to determine the ground state.

Antiferromagnetically coupled spin groups (negative *J*-values) show a curved line. This

line can be fit to **Eq. 3.8** to determine *J*. Weakly coupled (*J* < -10 cal) or

ferromagnetically coupled (positive *J*-values) spins cannot be discerned from one

another. Thus, while an EPR Curie plot can be informative for antiferromagnetically

coupled spins, if *J* <-10 or $\geq$ 0 a straight line is the result. We cannot distinguish

ferromagnetically coupled spins from weakly coupled spins.[12]
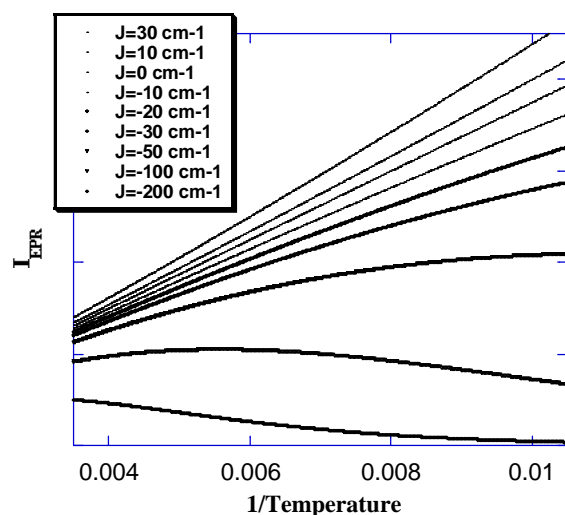
Figure 3.15. EPR Curie plots for various *J* values. Positive *J*-values give a straight line indicating either a ground state triplet, or nearly degenerate singlet/triplet states.

Super Conducting Quantum Interference Device (SQUID)[13,14]

SQUID: The Instrument

A SQUID magnetometer is a very useful tool for studying magnetic properties because it is able to detecting very small magnetic fields. The instrument itself is very interesting, because it required the juxtaposition of three quantum mechanical effects and results from work that led to three Nobel prizes. As the name suggests, a super-conducting quantum interference device (SQUID) magnetometer requires a superconducting material. Two Nobel prizes have been awarded in this respect. The first Nobel prize went to Onnes for his discovery of superconductivity in 1913.[15] The second Nobel prize was awarded in 1972 for an understanding of how superconductivity works. This was awarded jointly to Barden, Cooper and Schrieffer in what is now known as BSC theory.[16] The second quantum mechanical effect, and the third Nobel prize was the result of the work done by Brian Josephson, who was awarded the Nobel prize in 1973. His

work developing the Josephson junction[17] is what makes the SQUID very sensitive. The third quantum mechanical effect is the idea that magnetic flux is quantized.

In a SQUID magnetometer a sample is passed through a superconducting detection coil, which, in our case, is a second derivative gradiometer. This produces a small current that is proportional to the magnetic field of the sample and is detected by the SQUID, which is two Josephson junctions connected in parallel.

The superconducting detection coil is one superconducting wire arranged as a set of three counter-wound coils, **Figure 3.16**. The first coil is wound clockwise, the second coil is a set of two counterclockwise wound coils and the third is a coil wound clockwise. The sample is passed through these coils, which produces a small change in the flux in the detection coil. The Josephson junction detects the change in flux and that change is directly proportional to the moment of the sample.
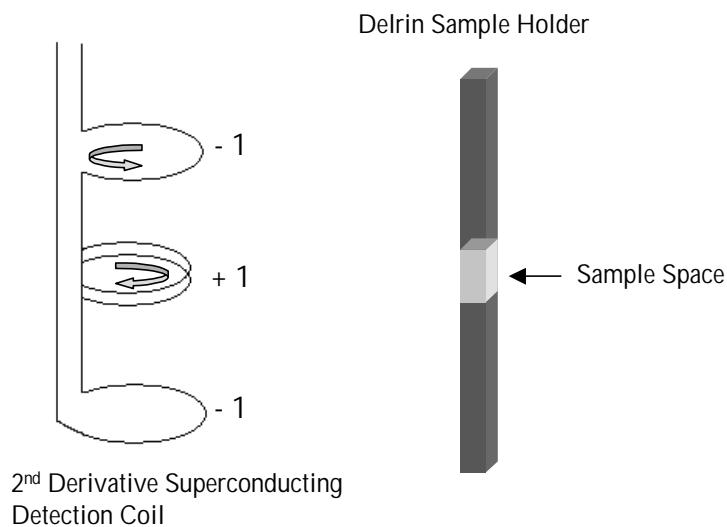
Figure 3.16. The superconducting detection coil in a SQUID magnetometer, which is a second order gradiometer.

This arrangement of the coils offers us a huge advantage, and a disadvantage. Because the detection coils are arranged in a second derivative manor, it is possible to have a sample holder that is not detected by the instrument except in the sample region. If the sample holder has a uniform magnetic susceptibility and passes through the top and bottom detection coils, the change in flux from the sample holder is zero. In our work either a sample holder made of Delrin was used, or a clear plastic drinking straw. This greatly simplifies background subtraction.

Our choice of sample holder can have some interesting consequences. The Delrin holder is a solid rod except for the sample space, **Figure 3.16**. Delrin is a diamagnetic polymer, but our background is of the less dense sample space so it appears as a "paramagnetic" background to the instrument, even though it is the absence of diamagnetic material. Because of this the sample signal is "enhanced" and will not change sign creating a difficult fit for the instrument, **Figure 3.17**. In Chapter 6 we suspend our samples in PVC. PVC has a diamagnetic response. This effectively "shields" the sample, which makes detecting a small, weak signal more difficult.
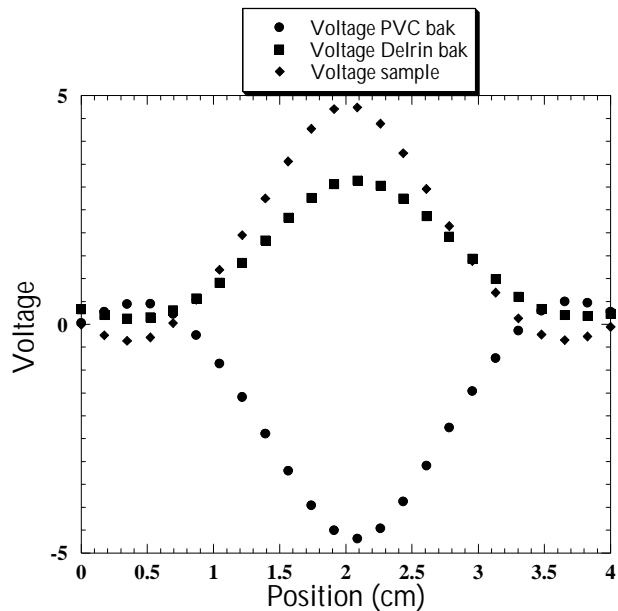
Figure 3.17. Voltage trace (2nd derivative) for a Delrin sample holder, PVC matrix, and for biradical.

The above discussion on sample holders assumes that the magnetic center of the sample holder and the magnetic center of the sample are the same. An example of the importance of centering the sample can bee seen by summing the PVC background and the sample signal and comparing it with the sum of the Delrin background and the sample signal, **Figure 3.18**. The Delrin was centered with the sample and the resulting signal is normal. Close inspection of **Figure 3.17** shows that the center of the sample and the center of the PVC are offset by about 0.1 cm. This small deviation results in a SQUID response that is not a 2nd derivative. As such the fitting routine will give an improper magnetic moment.
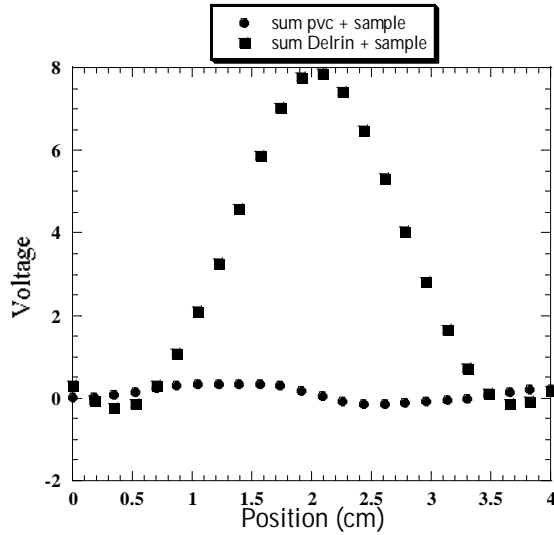
Figure 3.18. The signal response from the sum of the background signal and the sample signal.

SQUID: The Data

In Chapter 1 we learned that the magnetization of a material was directly proportional to the magnetic susceptibility of that material and the applied magnetic field, **Eq. 3.9**.[5,13,18-27]

$$M = c_{exp} H \qquad \textbf{Eq. 3.9}$$

The magnetic susceptibility is a constant that is the sum of the diamagnetic and paramagnetic susceptibilities, **Eq. 3.10**.[5,13,18-27]

$$c_{exp} = c_{dia} + c_{para} \qquad \textbf{Eq. 3.10}$$

The diamagnetic susceptibility of a material can be tabulated from Pascal's constants.[27] The paramagnetic susceptibility of a material is temperature dependent and follows Curie Law, **Eq. 3.11**.[28]

$$c_{para} = \frac{C}{T} \qquad \textbf{Eq. 3.11}$$

We are primarily concerned with exchange-coupled spins. As described in Chapter 2, the Heisenberg-Dirac-Van Vleck (HDVV) Hamiltonian, Eq. 3.12, can predict the energy levels of the system using the Hamiltonian:

$$\hat{H}_{ab} = -2J_{ab}\hat{S}_a g\hat{S}_b$$ **Eq. 3.12**

By this definition, $J > 0$ is ferromagnetic coupling and $J < 0$ is antiferromagnetic coupling. Note, one must always know the definition of the Hamiltonian. If $H_{ab} = 2J_{ab}\hat{S}_a\hat{S}_b$, then $J < 0$ would be antiferromagnetic coupling and ΔE would equal $2J$.

Van Vleck derived a field-independent expression relating magnetic susceptibility and the exchange coupling parameter, J, **Eq. 3.13**[22,29]

$$c = \frac{Ng^2b^2}{3k_BT} \frac{\sum\left\{S(S+1)(2S+1)e^{-E_S/k_BT}\right\}}{\sum\left\{(2S+1)e^{-E_S/k_BT}\right\}}$$ **Eq. 3.13**

where g is the electron g-value, β is the Bohr magneton, E_S is the energy of the exchange-coupled spins determined using the HDVV Hamiltonian and the other constants have their usual meaning. Substituting the energy of the singlet (S=0) and triplet (T=2J) states, Chapter 2, gives **Eq. 3.15**.[22,29]

$$c = \frac{Ng^2b^2}{3k_BT} \frac{\left\{(0)(1)e^{-0/k_BT}\right\}+\left\{(2)(3)e^{-2J/k_BT}\right\}}{\left\{1e^{-0/k_BT}+3e^{-2J/k_BT}\right\}}$$ **Eq. 3.14**

$$c = \frac{2Ng^2b^2}{k_BT} \frac{e^{-2J/k_BT}}{1+3e^{-2J/k_BT}} = \frac{2Ng^2b^2}{k_BT\left(3+e^{-2J/k_BT}\right)}$$ **Eq. 3.15**

Figure 3.19A shows plots of typical χT vs. T for a biradical system using **Eq. 3.15**.
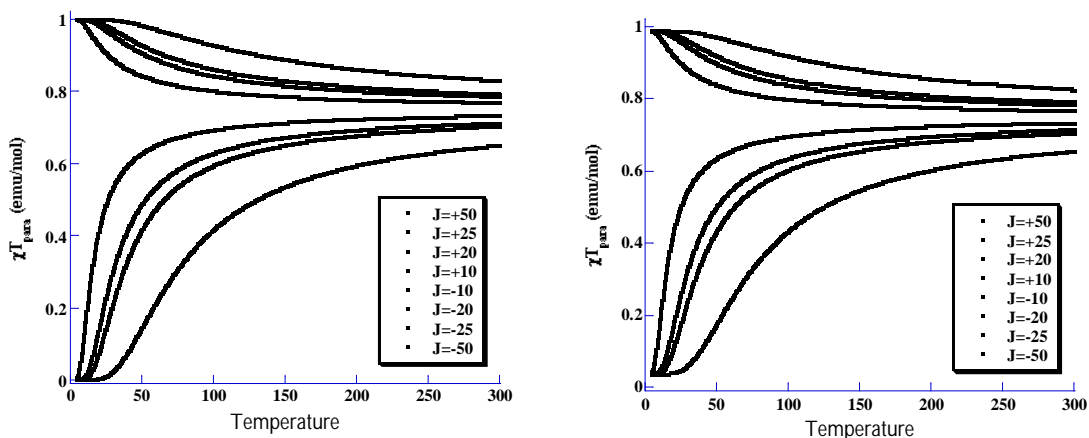
Figure 3.19. Plot of χT vs. T for various *J*-values. A. using **Eq. 3.15**. B. Using **Eq. 3.16**, with 5% monoradical impurity.

Note that for a ferromagnetically coupled biradical χT approaches unity at low

temperatures and for an antiferromagnetically coupled biradical χT approaches zero.

Both tend towards χT = 0.75 emu/mol at high temperatures, which is the expected value

for uncoupled spins.

As with EPR, we can also observe monoradical impurities in the SQUID

magnetometry data. These impurities can be modeled by adding the susceptibility of a

monoradical to the field-independent Van Vleck expression, **Eq. 3.16**, assuming that the

monoradical also displays Curie like behavior.[22]

$$c = (1 - r)\frac{2Ng^2\beta^2}{k_BT\left(3 + e^{-2J/k_BT}\right)} + r\frac{Ng^2\beta^2}{2k_BT} \qquad \textbf{Eq. 3.16}$$

The plot of χT vs T for a monoradical is a straight line. **Figure 3.19B** is a plot of χT vs T

for a biradical with a 5% monoradical impurity. The effect on the χT plot is simple,

ferromagnetically coupled spins approach a value below one, and antiferromangetically

coupled spins approach a value greater than zero at low temperatures.

Figure 3.20A is a plot of χ vs T for a biradical. Note the difference between

ferromagnetic coupling and antiferromangetic coupling. Anti ferromagnetically coupled

spins are typically plotted χ vs. T, **Figure 3.20**, which exhibits a maximum at T_{max} =

1.285 *J/k*.[22] Thus, a maximum in the plot of χ vs. T is a signature of antiferromagnetic
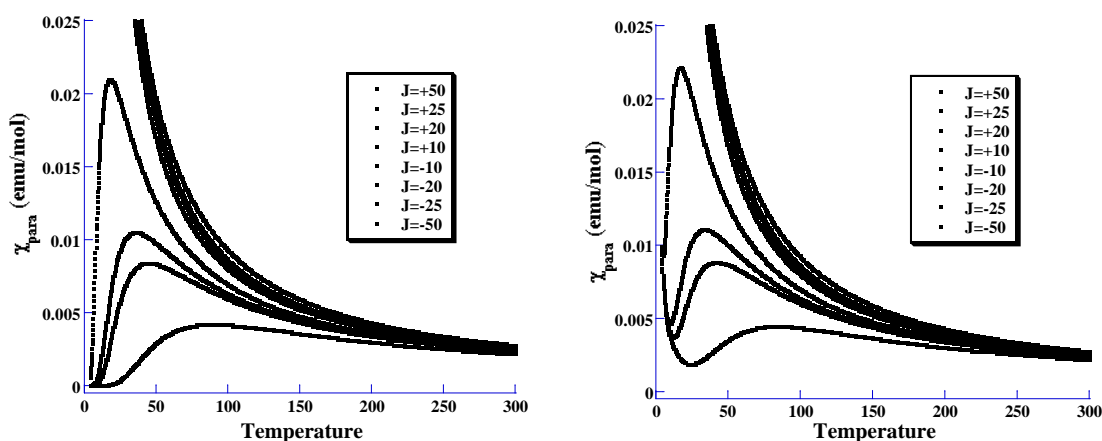
coupling.

Figure 3.20. Plot of χ vs. T for various *J*-values. A. Using **Eq. 3.15**. B. Using **Eq. 3.16**, with 5% monoradical impurity.

Figure 3.20B is a plot of χ vs T for a biradical with a 5% monoradical impurity.

Again, there is very little difference in the plots of the ferromagnetically coupled spins.

A χ vs T for a biradical with a 5% monoradical impurity shows a sharp upturn at low

temperatures.

Our primary concern is *intra*molecular exchange coupling, but in crystalline form

there can also be *inter*molecular exchange coupling. Intermolecular exchange coupling

can be accounted for with a Weiss mean-field correction, using the expression χ_{eff} = χ/(1-

$J\chi$), where $J = 2_zJ\mathfrak{e}/(Ng^2\beta^2)$.[25] The origin of $_zJ\mathfrak{e}$ may be zero-field splitting, intermolecular interaction, saturation effects, or some combination of all three.[30]

References
(1) Gerson, F. *High Resolution E.S.R. Spectroscopy*; John Wiley & Sons Ltd.: New York, 1970; Vol. 1.
(2) Atherton, N. M. *Electron Spin Resonance*; John Wiley & Sons Inc.: New York, 1973.
(3) Assenheim, H. M. *Introduction to Electron Spin Resonance*; Hilget & Watts Ltd.: London, 1966.
(4) Wertz, J. E.; Bolton, J. R. *Electron Spin Resonance*; Chapman and Hall: New York, 1986.
(5) Drago, R. R. *Physical Methods for Chemists*; 2nd ed. ed.; HBJ Saunders: Orlando, 1992.
(6) Rajca, A. *Chem. Rev.* **1994**, *94*, 871.
(7) Duling, D.; Version 0.96 ed.; Public EPR Software Tools, National Institute of Environmental Health Sciences, National Institutes of Health: Triangle Park, NC, 1996.
(8) Hanna, M. *Quantum Mechanics in Chemistry*; Hanna, M. Quantum Mechanics in Chemistry; The Benjamin/Cummings Publishing Company, Inc.: Menlo Park, CA, 1981: Menlo Park, CA, 1981.
(9) Bersohn, M.; Baird, J. C. *An Introduction to Electron Paramagnetic Resonance*; W. A. Benjamin, Inc.: New York, 1966.
(10) Angiolillo, P. J.; Lin, V. S.-Y.; Vanderkooi, J. M.; Therien, M. J. *J. Am. Chem. Soc.* **1995**, *117*, 12514.
(11) Bruker; 1.25, Shareware Version ed.; Brüker Analytische Messtechnik GmbH, 1996.
(12) Berson, J. A., Ed. *The Chemistry of the Quinonoid Compounds, Vol. II*; John Wiley & Sons: New York, 1988.
(13) McElfresh, M. "Fundamentals of Magnetism and Magnetic Measurements," Quantum Design, 1994.
(14) Jacobs, S. J. In *Chemistry*; California Institute of Technology: Pasadena, 1994.
(15) Onnes, H. K. "Nobel Prize in Physics," 1913.
(16) Bardeen, J.; Cooper, N. L.; Schrieffer, J. R. "Nobel Prize in Physics," 1972.
(17) Josephson, B.; Esaki, I.; Giaever, I. "Nobel Prize in Physics," 1973.
(18) *Magnetism I - Fundamentals*; Kluwer Academic Publishers: Norwell, 2002.
(19) Gatteschi, D., Ed. *Molecular Magnetic Materials*; Kluwer Academic Publishers: Amsterdam, 1991.
(20) Gatteschi, D.; Sessoli, R. *J. Magn. Magn. Mat.* **1992**, *104*, 2092.
(21) Jakubovics, J. P. *Magnetism and Magnetic Materials*; Second ed.; University Press: Cambridge, 1994.
(22) Kahn, O. *Molecular Magnetism*; VCH: New York, 1993.

(23)   Lahti, P. M., Ed. *Magnetic Properties of Organic Materials*; Marcel Dekker: New York, 1999.

(24)   Mattis, D. C. *The Theory of Magnetism*; Harper & Row: New York, 1965.

(25)   O'Connor, C. J. *Prog. Inorg. Chem.* **1982**, *29*, 203.

(26)   Turnbull, M. M.; Sugimoto, T.; Thompson, L. K., Eds. *Molecule-Based Magnetic Materials. Theory, Techniques, and Applications*; ACS: Washington, DC, 1996.

(27)   Carlin, R. L. *Magnetochemistry*; Springer-Verlag: New York, 1986.

(28)   Curie, P. *Ann. Chim. Phys.* **1895**, 289.

(29)   Van Vleck, J. H. *The Theory of Electric and Magnetic Susceptibilities*; Oxford University Press: Oxford, 1932.

(30)   Caneschi, A.; Dei, A.; Mussari, C. P.; Shultz, D. A.; Sorace, L.; Vostrikova, K. E. *Inorg. Chem.* **2002**, *41*, 1086.

Chapter 4. Bis(verdazyl)s: Electronic Interactions in Verdazyl Biradicals[1]

Introduction

The electronic interactions in **1** were previously studied in the Fox group.[2] Bisverdazyl **1** is a non-Kekulé disjoint hydrocarbon that exists as a ground state singlet with small contributions of a thermally populated triplet state. The HOMO is analogous to a 7 π-electron pentadienyl system. Bisverdazyl **1** is two verdazyl substituents connected at a nodal position. The HOMO and LUMO are similar to 3,3'-bis(pentadienyl), which like tetramethylenemethane (TME) is disjoint.[3,4] Previous Hückel LCAO-MO calculations of verdazyl biradicals have indicated that the unpaired electrons reside in degenerate molecular orbitals and that the electron density at C_3 is very near zero.[5]

1
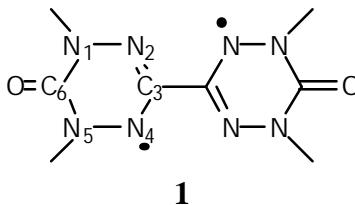
The spaced bis(verdazyl)s **2** and **3** have been reported to be ground state triplets with ZFS parameter D = 0.0050 cm^{-1} and D = 0.0040 cm^{-1} respectively.[6,7] This is contrary to general motifs that promote ferromagnetic coupling. *Meta* through benzene promotes ferromagnetic coupling and *para* through benzene promotes antiferromagnetic coupling. Regardless of the true ground spin state, bisverdazyls connected through the nodal positions are expected to be weakly exchange coupled. Theoretical calculations on TME suggest that it is a ground state singlet.[3] Other TME analogs that have been synthesized suggest that TME might be a ground state triplet.[8-12]

2   **3**
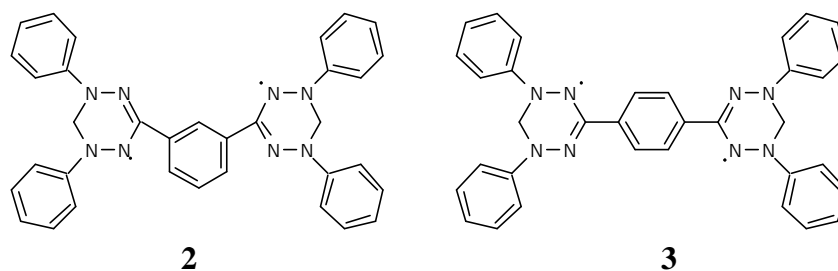
These differences in the ground spin state of linked bis(verdazyl)s prompted us to further study other bisverdazyl derivatives. Using **1** as the parent compound, three bis(verdazyl)s with aromatic spacer units were synthesized: 1,3-bis(1,5-dimethyl-6-oxo-3verdazyl)benzene (**4**), 1,4-bis(1,5-dimethyl-6-oxo-3verdazyl)benzene (**5**), and 2,5-bis(1,5-dimethyl-6-oxo-3-verdazyl)thiophene (**6**).

Furthermore, the carbonyls were substituted with thiones to make the dithione derivative 1,1′,5,5′-tetramethyl-6,6′-dithio-3,3′-bisverdazyl (**7**).

4   **5**

6

7
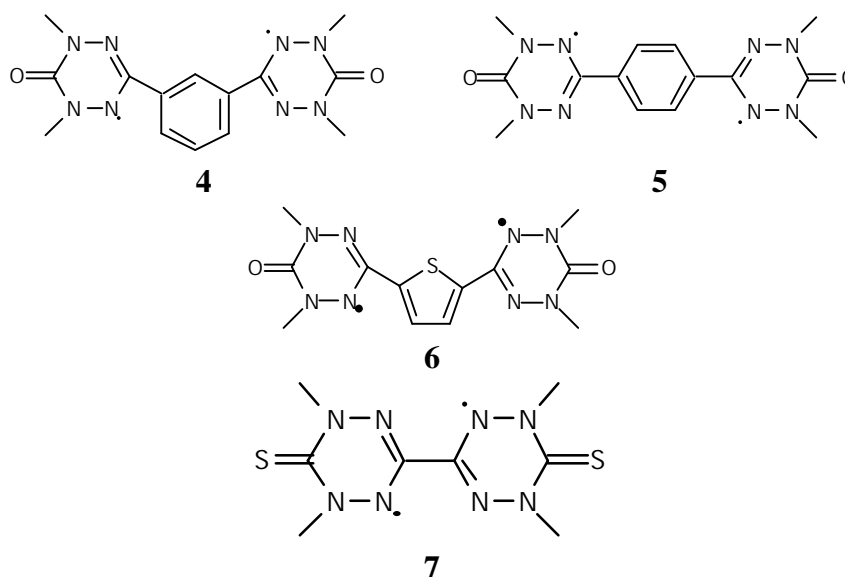
To further understand the intramolecular interaction within these compounds we have investigated the electrochemical properties and the absorption and electron spin resonance spectra of these biradicals.

Results and Discussion

Synthesis and Properties of 4-7. Biradicals **4** – **6** were synthesized by condensing isophthalaldehyde, terephthaldicarboxaldehyde, or 2,5-thiophenedicarboxaldehyde with 2,4-dimethyl carbonohydrazide. Oxidations to the neutral biradical were carried out using potassium ferricyanide for the electrochemical and absorption experiments and with lead oxide or tetraphenylhydrazine for the EPR experiments. The thio analogue **7** was similarly prepared from the thiohydrazide. Compounds **4** – **6** were sufficiently stable to be characterized by chemical ionization high-resolution mass spectra analysis, but compound **7** proved to be too air sensitive for MS analysis and was characterized by other *in situ* spectral methods.

Room temperature EPR spectra of the biradicals **4** – **7** are similar to that of **1** within our experimental determination. Linear Curie plots were observed for **4** – **6** indicating either a ground state triplet of nearly degenerate singlet/triplet energy levels.[13] However, the absorption spectra of **4** – **7** are red-shifted compared with **1**. Electrochemical measurements show that the stability of the dications and dianions derived of these biradicals are also sensitive to structural variation.

The room temperature EPR spectrum of **7** is also almost identical to that of **1**. the observation of a triplet spectrum in frozen chloroform however, reveals ZFS parameters

and substantial changes in electron density and molecular symmetry. The absorption spectrum of **7** is also red-shifted, and electrochemical measurements indicate the thio analogue is less stable and oxidizes and reduces easier than **1**.

Electrochemical Behavior. The electrochemistry was performed by Michael Hay and Scott Reese and is presented here to give further insight to the verdazyl biradicals studied.

Despite the many EPR studies of verdazyls, very few substituted verdazyls have been studied electrochemically.[4,14-23] The available literature reports have focused on the electrochemistry of 1,3,5-triphenylverdazyl in determining the effect of solvent on reaction entropies and disproportionation equilibria.[24,25] Oxidation of 1,3,5-triphenylverdazyl to the cation was reported to be reversible, while reduction to the anion is only quasireversible. It is likely that the stability of the mono and diions of **1** and of **4** – **7** are related to the stability of the analogous monoverdazyl ions. Half-wave potentials were not given, but the peak separation between the anodic and cathodic peaks was given as ΔE_p^{ox} = 60 mV and ΔE_p^{red} = 110 mV, respectively.[24,25]

Cyclic voltammetry of the non-spaced bis(verdazyl)s **1** and **7** in N_2 saturated acetonitrile solutions shows substantially different electrochemical behavior than the spaced bis(verdazyl)s. In **1**, two reversible oxidation waves are observed as the neutral biradical is first converted to the radical cation (803 mV) and then to the dication (1.05 V), **Figure 4.1**. In the reduction, one two-electron wave is observed as the molecule goes from the neutral biradical to the dianion. In **7**, two one-electron oxidation waves are also seen (778 mV, 902 mV), only one of which is reversible, **Figure 4.2**. The return

69

reduction wave of **7** is suppressed, indicating that the two-electron reduction is

irreversible.
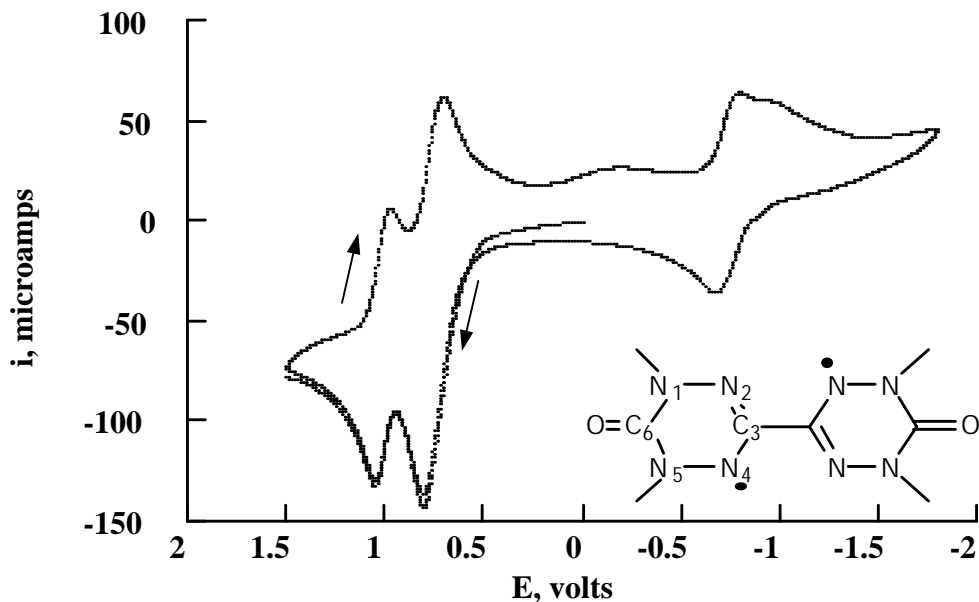
Figure 4.1. Cyclic voltammetry scan of 1.0 mM **1** in degassed CH_3CN containing 0.1 M NBu_4PF_6 with a Pt electrode. Scan rate: 250 mV/s.
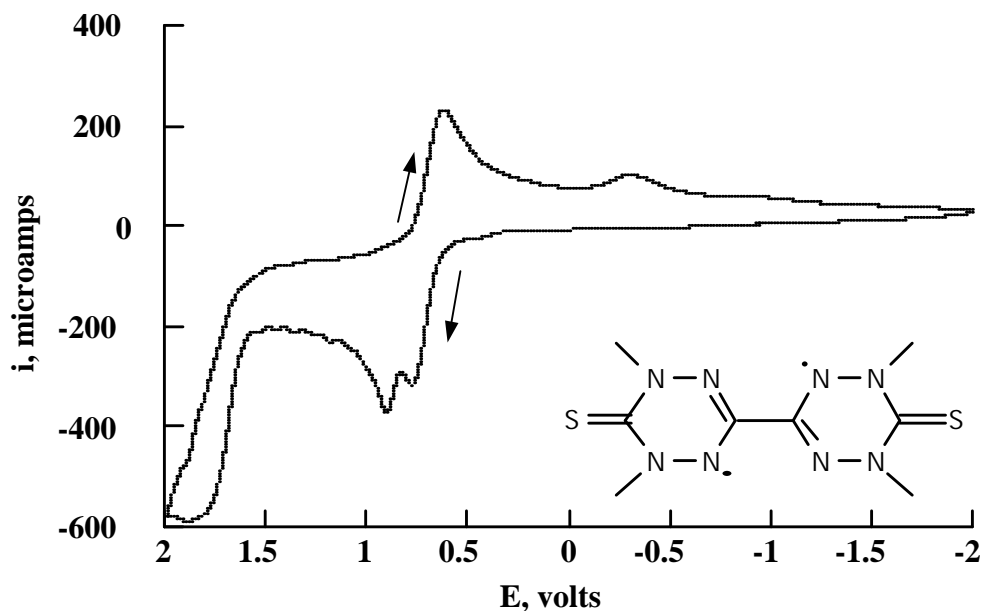
Figure 4.2. Cyclic voltammetry scan of 1.0 mM **7** in degassed CH_3CN containing 0.1 M NBu_4PF_6 with a Pt electrode. Scan rate: 1000 mV/s.

As indicated in **Table 4.1**, the difference between the first one-electron oxidation wave and the second one-electron oxidation wave, ΔE_{ox}, is twice as large in **1** as in **7**. Although reversibility was not established, this suggests greater interaction between the two verdazyl spin groups in **1** than in **7**.

In the spaced biradicals **4**, **5**, and **6**, **Figures 4.3**, **4.4** and **4.5**, cyclic voltammetry shows one two-electron oxidation wave, rather than the two one-electron oxidation waves as observed in **1** and **7**. These waves are found at approximately the same potentials in these biradicals, **Table 4.1**. This indicates that there is less communication between the two unpaired electrons in **4**, **5** and **6** than in **1** and **7**.
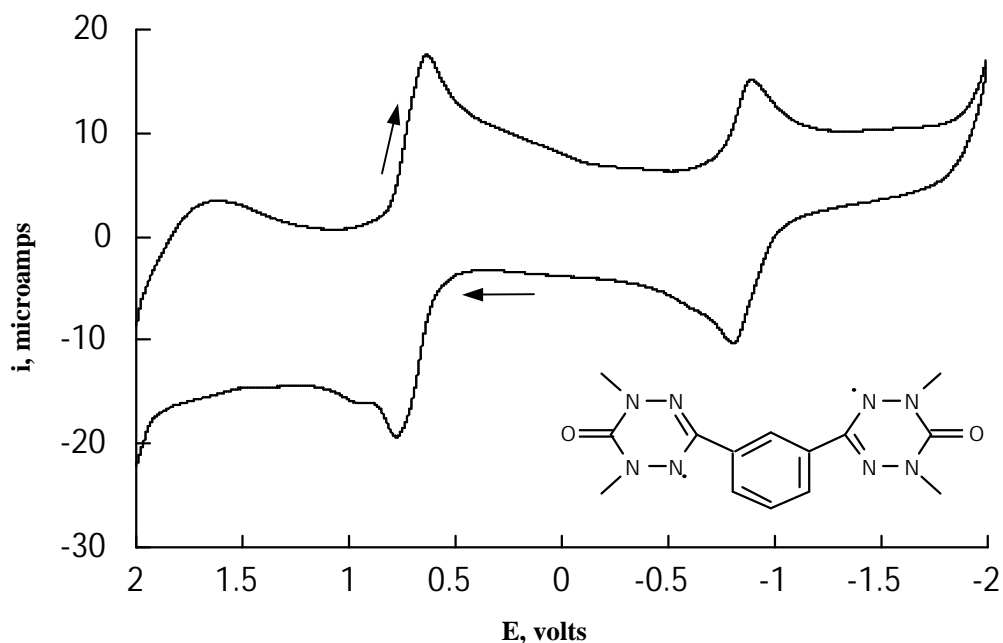
Figure 4.3. Cyclic voltammetry scan of 1.0 mM **4** in degassed CH_3CN containing 0.1 M NBu_4PF_6 with a Pt electrode. Scan rate: 1000 mV/s.
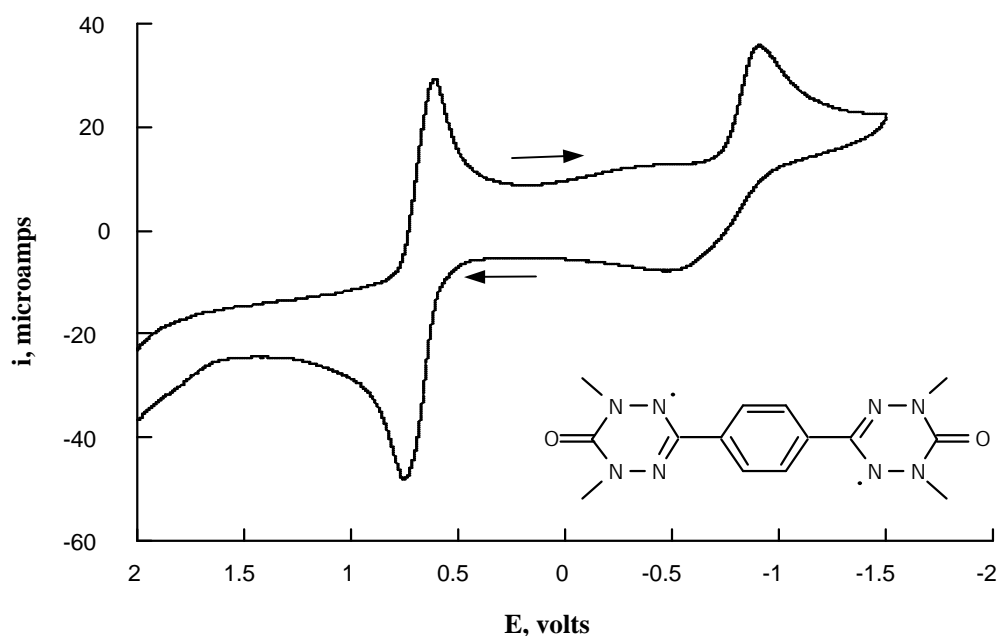
Figure 4.4. Cyclic voltammetry scan of 1.0 mM **5** in degassed CH_3CN containing 0.1 M NBu_4PF_6 with a Pt electrode. Scan rate: 1000 mV/s.
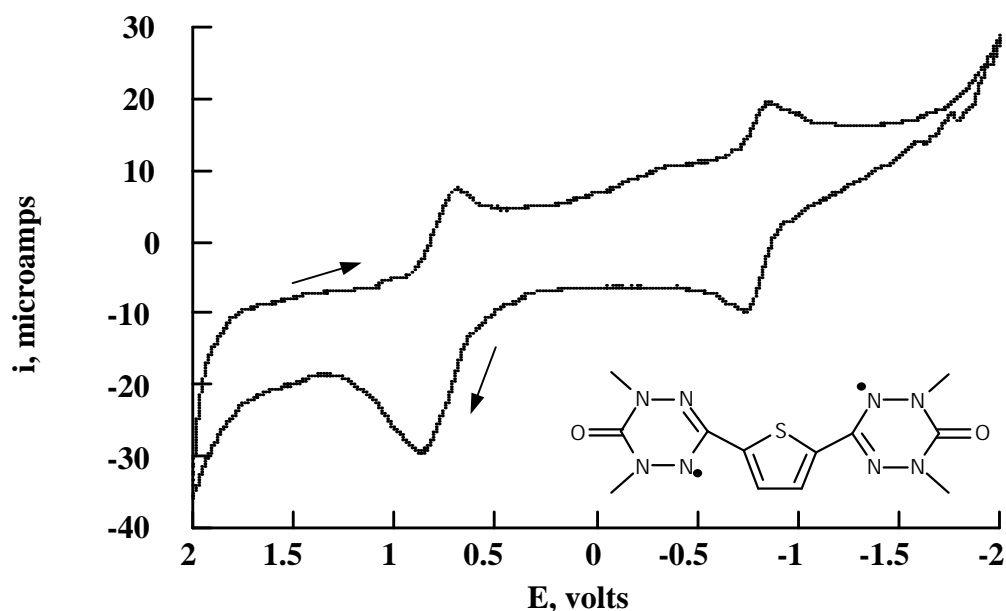
Figure 4.5. Cyclic voltammetric scan on Pt wire of 1.0 mM **6** in degassed CH_3CN containing 0.1 M NBu_4PF_6. Scan rate: 1000 mV/s.

Thus, cyclic voltammetry shows little coupling between radical centers in

bis(verdazyl)s **4**, **5** and **6**, but some coupling in the non-spaced bis(verdazyl)s **1** and **7**.

As would be expected for radical substituent connected at nodal positions.

Table 4.1. Electrochemical Data for Verdazyl Biradicals **1, 4-7.**[a]

	$E_{\frac{1}{2}}$ (0/· +)	DE_p	$E_{\frac{1}{2}}$ (· +/2+)	DE_p	$E_{\frac{1}{2}}$ (0/· -)	DE_p	Dox (mV)
1	**755**	**93**	**1013**	**75**	**-728**	**105**	**248**
7	**701**	**152**	**763**	**275**	**-304**	**irr.**	**123**

	$E_{\frac{1}{2}}$ (0/2+)	DE_p			$E_{\frac{1}{2}}$ (0/2-)	DE_p	
4	**706**	**144**			**-849**	**79**	
5	**685**	**134**			**-800**	**>200**	**-**
6	**749**	**155**			**-815**	**130**	**-**

[a]mV vs SCE

Absorption Spectroscopy. The absorption spectroscopy recorded by Scot Reese and Michael Hay and is briefly presented here. The biradicals (**1**, **4-7**) range in color from yellow to black. Simple MO calculations suggests that in the SOMO the bridging carbons are nodal positions or that the electron density close to zero at C_3.[4,26] However, the absorption spectra of the spaced biradicals are all red-shifted from **1**, **Figure 4.6**, suggesting an increase in conjugation. In the LUMO, the bridging carbons are not at nodal positions and there would be considerable interaction between the verdazyl radical units, and the spacer group. Indeed, from the spacer groups examined here, the degree of red-shift follows the expected path of increased conjugation in the LUMO.

The meta-spaced bisverdazyl **4** is only red-shifted from **1** by 6 nm. *m*-Phenylene permits the least through-• interaction of the spacer groups examined. In **5**, whose connectivity is *para* through benzene, the absorption spectrum is red shifted by 36 nm from **1**. The thiophene group in **6** shifts the absorption maximum by 66 nm from **1**. The absorption spectrum of **7**, **Figure 4.6**, shows that the substitution of oxygen by sulfur at C_6 induces a red shift in the absorption maximum by 46 nm.[21] This suggests that the π system in **7** is more delocalized than in **7**.
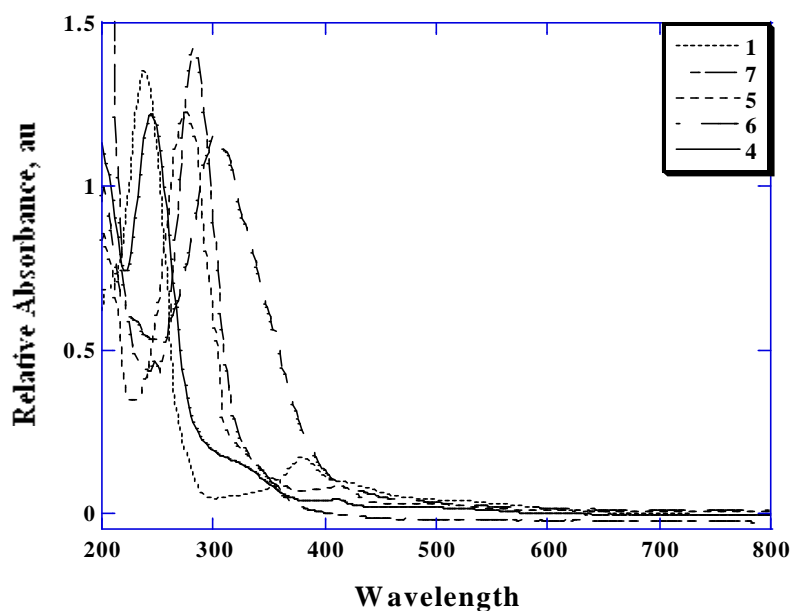
Figure 4.6. Electronic absorption spectra of **1**, **4-7** in degassed acetonitrile solution.

Electron Paramagnetic Spectroscopy. EPR spectra of chloroform solutions of

4-7 are similar to spectra reported previously for the phenyl-substituted monoverdazyl

8.[14]

8
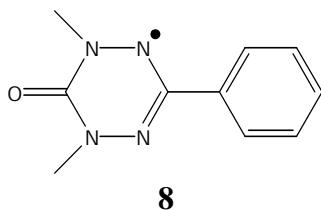
Solution spectra of **4**-**7** show at least 9 lines with a 1:4:10:16:19:16:10:4:1 splitting

pattern consistent with hyperfine coupling constants $a_{N2, N4}$ • 6-5 Hz and $a_{N1, N5}$ • 5 Hz.[17]

Smaller hyperfine coupling constants could not be determined due to large line widths

and underlying monoradical impurities. These splitting patterns indicate the presence of

four nitrogen atoms with nearly the same spin densities.[5] The resolution of these spectra

is considerably poorer than that of **8**, as is consistent with previous studies that show

decreased resolution upon increasing the number of radical centers linked through a

phenyl group.[5,18] The observed line broadening was assigned to intermolecular hyperfine interactions or the intermolecular magnetic dipole-dipole interactions.[5,20]

EPR Frozen Solutions. Curie plots were recorded by Beth Lambert and Steve Hammond. The spectra for compounds **4-7** in frozen solutions are consistent with those of randomly oriented triplets.[27] In all compounds, a trace of a doublet impurity can be found. However, the zero field splitting (ZFS) parameters were still observed and simulated, **Table 4.2**.

Table 4.2. Zero Field Splitting Parameters and Curie Plot Results for Verdazyl Biradicals **1, 4-7**.

	$|D/hc|$ (cm^{-1})	$|E/hc|$ (cm^{-1})	Curie Plot
1^2	0.038	0.0016	J=-380 cm^{-1}
7	0.018	0.0012	J=-280 cm^{-1}
4	0.0063	0.0037	Linear
5	0.0043	0.00042	Linear
6	0.0051	0.00047	Linear

The EPR spectra of frozen solutions of **4**, **5** and **6** are very similar. The simulated ZFS parameters[28] for **5** are $|D/hc|$=0.0043 cm^{-1}, $|E/hc|$=0.00042 cm^{-1}, **Figure 4.7**. The simulated ZFS parameters for **6** are $|D/hc|$=0.0051 cm^{-1} and $|E/hc|$=0.00047 cm^{-1}, **Figure 4.8**. For **4** $|D/hc|$=0.0063 cm^{-1}, $|E/hc|$=0.00037 cm^{-1}, **Figure 4.9**, indicating very little difference in the degree of electronic interaction between radical centers in compounds containing any of the spacers. In fact, since D proportional to $1/r^3$ the values correlate according to the number of bonds between the verdazyls, i.e. **4** > **6** > **5**. These compounds also gave linear Curie plots, indicating either a ground state triplet or a nearly degenerate ground state.[13]
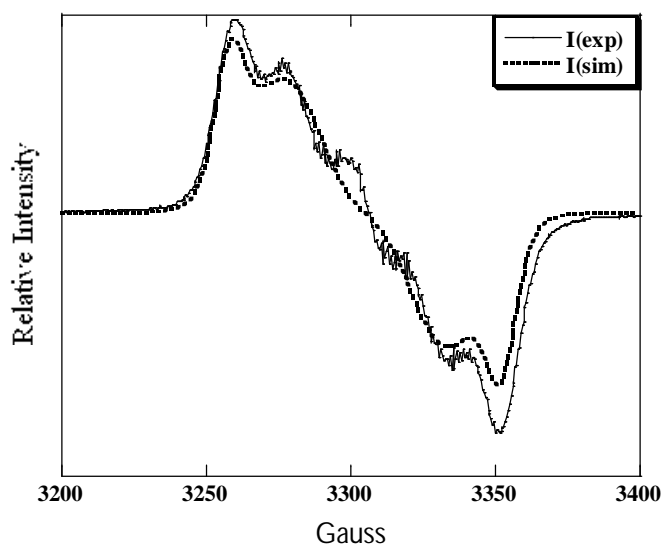
Figure 4.7. EPR spectrum (top) and simulation (bottom) of **5** in a frozen, degassed THF solution.
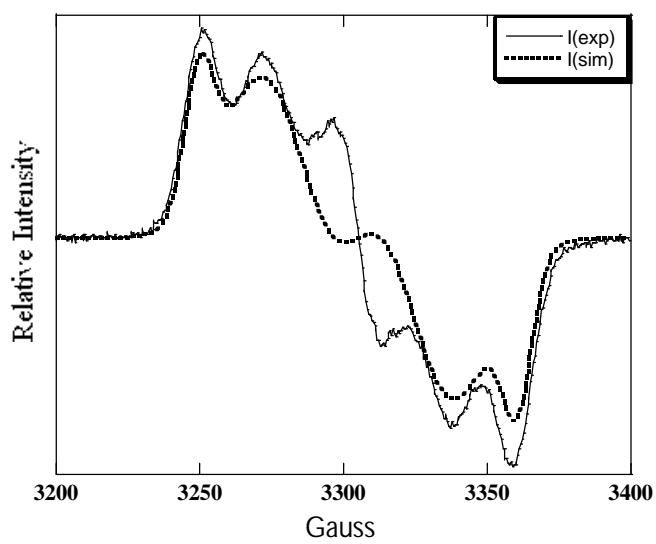
Figure 4.8. EPR spectrum (top) and simulation (bottom) of **6** in a frozen, degassed THF solution.
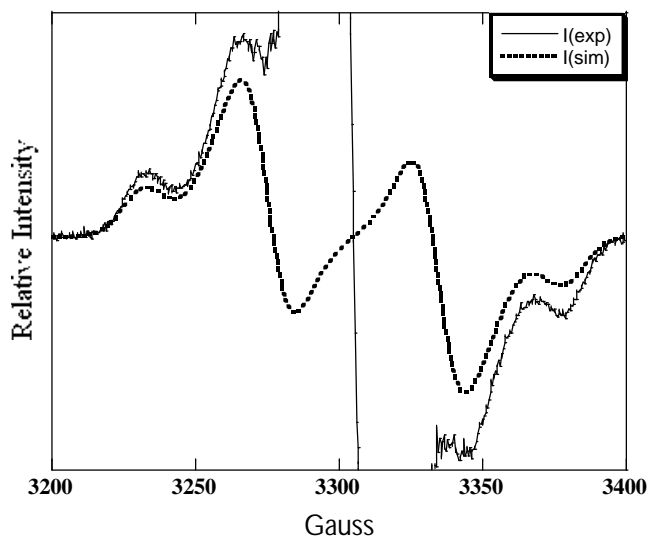
Figure 4.9. EPR spectrum (top) and simulation (bottom) of **4** in a frozen, degassed THF solution.
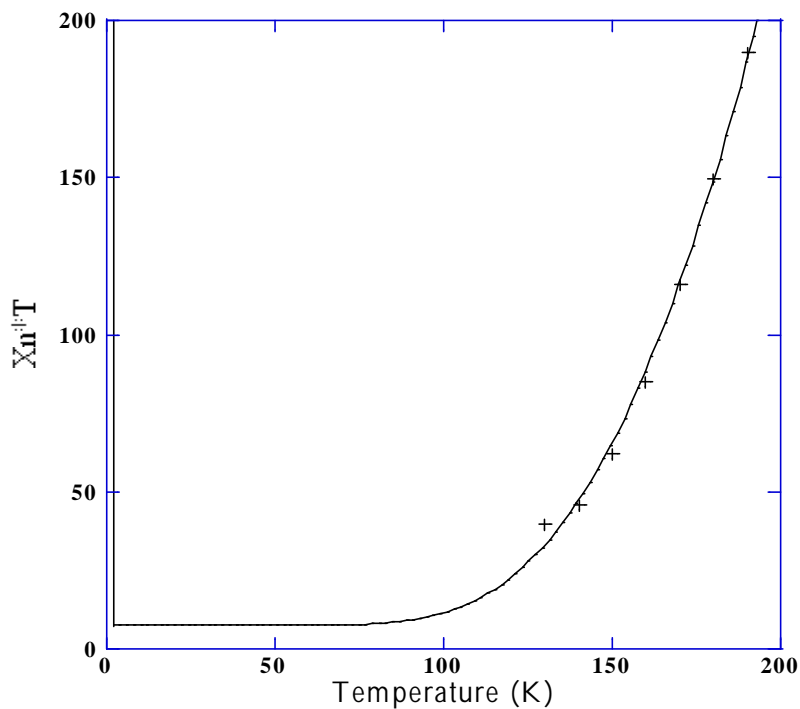
Figure 4.10. Dependence of the product of susceptibility and temperature ($\chi_N T$) on temperature (T) for **7**. The solid line is a best fit to **Eq. 4.**1 with $\Delta E = 0.069$ eV, k = 12200, P = 7.6.

The similarities in **4, 5** and **6** are expected. Recall that cyclic voltammetry revealed one two-electron-oxidation wave, showing little interaction between the two radical spin groups. Since the D value is inversely proportion to the average distance

77

between the two-electrons, the average electron density in these compounds must be farther apart. As such, a lower level of coupling is expected than if they were more strongly interacting as in **1** and **7,** which have two one-electron oxidation waves.

The spectrum of **7** in frozen chloroform is consistent with the hyperfine structure of a randomly oriented triplet,[29] **Figure 4.7**. The large featureless absorption in the middle of the spectrum is identical to that previously attributed to a doublet impurity.[4] Zero field parameters $|D/hc|$ and $|E/hc|$ were determined to be 0.018 cm^{-1} and 0.0012 cm^{-1}, respectively. The ZFS parameters are smaller than those of the previously reported bisverdazyl **1** of $|D/hc|$ = 0.038 cm^{-1} and $|E/hc|$ = 0.0016 cm^{-1}.[4] The D value is smaller in **7** than in **1**, indicating a higher degree of delocalization of the unpaired electrons into the orbitals of the thione. Because the D parameter is a measure of the distance between the two unpaired electrons, and because the value for **7** is approximately half that of **1**, the unpaired electrons are likely localized further apart onto the two sulfur atoms, which is consistent with the cyclic voltammetry peak splitting. Thus, **7** has a peak splitting of about one half of **1**.

Inspection of the half-field region of the spectrum of **7** reveals signals consistent with transitions between the m_S = -1 and m_S = +1 states of the triplet. The temperature dependence of this signal allows for the singlet-triplet energy separation **J** to be determined. The temperature dependence of $\chi_N T$ (where $\chi_N = I/I_{300}$ where I is the integrated signal intensity and I_{300} is the integrated signal intensity at 300K) was determined from the EPR signal intensity for **7**, **Figure 4.10**. Fitting this data to **Eq. 4.1**[4]

$$c_N T = P + ke^{-\Delta E/k_B T}$$ **Eq. 4.1**

gives a singlet-triplet energy gap of 560 cm^{-1} (0.069 eV, J = -280). This value is lower than that found for **1**, where the activation energy has been determined to be 887 cm^{-1} (0.11 eV, J = -444).[4]

Conclusions

Electronic coupling between the radical centers in substituted verdazyl biradicals is affected by substitution at the C_3 position. Aromatic spacers at C_3 in **4-6** decrease the magnitude of coupling between the two unpaired electrons, compared to **1**, as shown by cyclic voltammetry and EPR spectral measurements. This effect is illustrated in the observed electrochemistry, where two one-electron oxidation waves (to produce a dication) are observed for **1**, whereas a single two-electron oxidation wave is evident in **4**, **5** and **6**. Red shifts in the absorption spectra however, indicate structural perturbation by these binding groups, although spectral broadening makes unambiguous assignment of the causes for these differences difficult.

Biradicals **4-6** all gave linear Curie plots with D values ranging from 0.0043 to 0.0063 cm^{-1}. A linear Curie plot suggests that each member of this family exists as a ground state triplet, or as a species with degenerate triplet/singlet energy levels.[13]

Replacement of oxygen at C_6 in **1** with sulfur in **7** does affect the electronic structure of the biradical. The absorption spectrum of **7** is red-shifted by about 50 nm from that of **1**. Electrochemical measurements indicate two one-electron oxidation waves in **7**, but scan reversal reveals only one return wave, suggesting an unstable dication. Room temperature EPR spectra of **7** are nearly identical to those for **1**, but |D/hc| and

|E/hc| parameters derived from spectra of frozen solution suggest a higher degree of electronic delocalization away from the other verdazyl in **7** than in **1**. This is also evident in the smaller singlet-triplet energy gap in 7 than the oxygen analog **1**.

Experimental

General methods. Phosgene (20% from Fluka) and methylhydrazine were used without further purification producing 2,4-dimethylhydrazide.[30] This in turn was condensed with the dialdehyde of the spacer of interest to produce the corresponding tetrahydrazine. The tetrahydrazine was then was then oxidized with either potassium ferricyanide, tetraphenylhydrazine, or lead oxide to produce the desired bisverdazyl biradical.[14]

^{1}H and ^{13}C NMR spectra were recorded on a Varian Gemini Unity Plus NMR spectrometer at 300 and 75.5 MHz, respectively. X-band EPR spectra were recorded on IBM-Bruker E200SRC spectrometer fitted with an Oxford model 900 liquid helium cryostat. Powder EPR spectra were simulated using: WINEPR SimFonia, Shareware Version 1.25. Absorption spectra were recorded on a Shimadzu UV-3101PC scanning spectrophotometer equipped with a near infrared (IR) detector. Electrochemical measurements were carried out on a Bioanalytical Systems BAS/W potentiostat using a Pt wire working electrode, a Pt coil auxiliary electrode and a Ag/AgCl reference electrode. For each electrochemical experiment, the supporting electrolyte was 0.1 M ^{n}Bu$_4$PF$_6$ in acetonitrile. The electrolyte, tetrabutylammonium hexafluorophosphate, was recrystallized three times from absolute ethanol and dried under vacuum. Acetonitrile (Burdick and Jackson) was purified according to previously described methods.[31] All

other reagents were purchased from Aldrich and were used as received. Melting points were recorded on capillary melting point apparatus and are uncorrected.

Synthesis of 1,3-bis(1,5-dimethyl-6-oxo-3-verdazyl)benzene (4). To a solution of 0.42 g (3.1 mmol) isophthaldehyde in 5 mL 100% ethanol, at 80 •C, 0.96 g (8.1 mmol) 2,4-dimethylcarbonohydrazide was added. After heating for 5 min a white precipitate had formed. The mixture was stored at 10 •C for 4 h and the white solid collected by filtration (63%), mp. 181•C(dec.). ^{1}H NMR (d_6-DMSO): δ 7.72 (1 H, s), 7.48 - 7.36 (3 H, m), 5.68 (4 H, d), 4.90 (2 H, t), 2.94 (12 H, s). ^{13}C NMR (d_6-DMSO): δ 154.5, 136.8, 128.1, 126.5, 126.1, 68.6, 37.6. HRMS (CI): (m/z) $C_{14}H_{20}N_8O_2$ (M+H)$^+$: calculated 335.1944, found 335.1938.

Into a small vial, 102.5 mg (0.306 mmol) of 1,3-bis(1,5-dimethyl-hexahydro-6-oxo-1,2,4,5-tetrazin-3-yl)benzene and 732.6 mg (3.27 mmol) lead oxide in 10 mL dry THF were stirred for 24 hr under inert conditions. The lead oxide was removed by filtering an EPR sample through a 0.2 μm teflon syringe filter, yielding a red solution. (CI): (m/z) $C_{14}H_{16}N_8O_2$ (M+H)$^+$: calculated 329.147, found 329.147.

Synthesis of 1,4-bis(1,5-dimethyl-6-oxo-3-verdazyl)benzene (5). In a round bottom flask was placed 100 mg (0.31 mmol) of 1,4-bis(1,5-dimethyl-hexahydro-6-oxo-1,2,4,5-tetrazin-3-yl)benzene[23] in 6 mL water. Na_2CO_3 (3 mL, 2 N) was added together with 600 mg (1.8 mmol) $K_3Fe(CN)_6$ in 5 mL water. The solution was stirred for 4 h and was then extracted with CH_2Cl_2. The solvent was removed under vacuum. The product (50 mg, 0.15 mmol, 48%) was collected as a red solid, mp. 250•C (dec.). Uv-vis (CH_3CN):

81

λ_{max} nm (log ε): 415 (3.17), 277 (4.48), 200 (4.28). HRMS (CI): (m/z) $C_{14}H_{16}N_8O_2$

$(M+H)^+$: calculated 329.3531, found 329.1487. LRMS (CI+): 329 (49%).

Synthesis of 2,5-bis(1,5 dimethyl-6-oxo-3-verdazyl)thiophene (6). To a solution of 1.1

g (8.9 mmol) 2,4-dimethylcarbonohydrazide in 10 mL ethanol was added 0.50 g (3.6

mmol) thiophenedicarboxaldehyde. The solution was heated to reflux for 45 min and

then cooled to rt. A solid formed upon cooling which was separated by filtration,

yielding 0.84 g (69%) as a white powder, mp. 242-3 •C. ^{1}H NMR (d_6-DMSO): δ 6.96 (s,

2 H), 5.83 (d, 4 H, *J* = 5.7 Hz), 5.07 (t, 2 H, *J* = 5.4 Hz), 2.92 (s, 12 H). ^{13}C NMR (d_6-

DMSO): δ 154.0, 140.9, 125.5, 65.5, 37.9. Uv-vis (DMSO): λ_{max} nm (log ε): 318

(3.05). HRMS (CI): (m/z) $C_{12}H_{20}N_8O_2S$ $(M+H)^+$: calculated 341.42, found 341.151.

To a solution of 100 mg (0.30 mmol) 2,5-bis(1,5-dimethyl-hexahydro-6-oxo-

1,2,4,5-tetrazin-3-yl)thiophene in 7 mL water was added to 600 mg $K_3Fe(CN)_6$ (1.8

mmol) in 6 mL water and 3 mL 2N Na_2CO_3. The solution was stirred for approximately

6 h and the resulting brown solution was extracted with $CHCl_3$. The solvent was

removed under vacuum and the resulting yellow-brown solid collected by filtration (48

mg, 0.14 mmol), mp. 245 •C (dec.). Uv-vis (CH_3CN): λ_{max} nm (log ε): 357 (4.70, sh),

343 (4.78, sh), 317 (4.92), 300 (4.98, sh), 194 (5.02). HRMS (CI): (m/z) $C_{12}H_{14}N_8O_2S$

$(M+H)^+$: calculated 335.3773, found 335.103. LRMS (CI+): 335 (100%).

Synthesis of 1,1',5,5'-tetramethyl-6,6'-dithio-3,3'-biverdazyl (7). A solution of 0.67 g

(5.0 mmol) 2,4-dimethylthiohydrazide was combined with 0.60 g (2.3 mmol) glyoxal

sodium bisulfate addition compound in 15 mL distilled water and the resulting solution was heated to reflux for 2 h. The solution was cooled to rt and the product collected by filtration, yielding 0.51 g (1.7 mmol, 34%) of product as a brownish yellow powder, mp. 271•C. ^{1}H NMR (d$_6$-DMSO): δ 5.60 (d, 4 H, J=6.1 Hz), 3.82 (t, 2 H, J=6.6 Hz), 3.31 (s, 12 H). ^{13}C NMR (d$_6$-DMSO): δ 173.7, 66.0, 43.7. HRMS (CI): (m/z) $C_8H_{18}N_8S_2$ (M+H)$^+$: calculated for 291.43, found 291.12. LRMS (CI+): 291 (89%).

A vacuum-sealed solution of 0.024 g (0.087 mmol) 2,2',3,3',4,4',5,5'-octahydro-1,1',5,5'-tetramethyl-3,3'-bis-1,2,4,5-tetrazin-6,6'-thione and 0.072 g (0.25 mmol) tetraphenylhydrazine in 2 mL degassed CHCl$_3$ was heated in an oil bath at 330 K for 48 h, turning first green and then dark purple. UV-VIS (CH$_3$CN) λ$_{max}$ (log ε): 284 (3.56).

References
(1)   Fico, R. M., Jr.; Hay, M. F.; Reese, S.; Hammond, S.; Lambert, E.; Fox, M. A. *J. Org. Chem.* **1999**, *64*, 9386.
(2)   Brook, D. J. R.; Fox, H. H.; Lynch, V.; Fox, M. A. *J. Phys. Chem.* **1996**, *100*, 2066.
(3)   Borden, W. T.; Davidson, E. R. *J. Am. Chem. Soc.* **1977**, *99*, 4587.
(4)   Brook, D. J. R.; Fox, H. H.; Lynch, V.; Fox, M. A. *J. Phys. Chem.* **1996**, *100*, 2066.
(5)   Fischer, H. H. *Tetrahedron* **1967**, *23*, 1939.
(6)   Mukai, K.; Azuma, N.; Shikata, H.; Ishizu, K. *Bull. Chem. Soc. Jpn.* **1970**, *43*, 3958.
(7)   Azuma, N.; Ishizu, K.; Mukai, K. *J. Chem. Phys.* **1974**, *61*, 2294.
(8)   Dowd, P.; Chang, W.; Paik, Y. H. *J. Am. Chem. Soc.* **1987**, *109*, 5284.
(9)   Roth, W. R.; Ruhkamp, J.; Lennartz, H. W. *Chem. Ber.* **1991**, *124*, 2047.
(10)   Roth, W. R.; Kowalczik, U.; Maier, G.; Reisenaur, H. P.; Sustmann, R.; Müller, W. *Angew. Chem., Int. Ed. Eng.* **1987**, *26*, 1285.
(11)   Alies, F.; Luneau, D.; Laugier, J.; Rey, P. *J. Phys. Chem.* **1993**, *97*, 2922.
(12)   Ullmann, E. F.; Boocock, D. G. B. *Chem. Comm.* **1969**, 1161.
(13)   Berson, J. A. *The Chemistry of the Quinonoid Compounds*; Wiley, 1988; Vol. 2, Chapter 10.

(14)   Neugebauer, F. A.; Fischer, H. *Angew. Chem. Int. Ed. Eng.* **1980**, *19*, 724.

(15)   Kuhn, R.; Trischmann, H. *Angew. Chem. Int. Ed. Eng.* **1963**, *2*, 155.

(16)   Katritzky, A. R.; Belyakov, S. A.; Durst, H. D.; Xu, R.; Dalal, N. S. *Can. J. Chem.* **1994**, *72*, 1849.

(17)   Neugebauer, F. A. *Angew. Chem., Int. Ed. Eng.* **1973**, *12*, 455.

(18)   Kuhn, R.; Neugebaur, F. A.; Trischmann, H. *Monatsch.* **1966**, *97*, 525.

(19)   Neugebauer, F. A. *Tetrahedron* **1970**, *26*, 4853.

(20)   Dormann, E.; Winter, H.; Dyakonow, W.; Gotschy, B.; Lang, A.; Naarmann, H.; Walker, N. *Ber. Bunsenges. Phys. Chem.* **1992**, *96*, 922.

(21)   Neugebauer, F. A.; Fischer, H.; Krieger, C. *J. Chem. Soc., Perkin Trans. 2* **1993**, 535.

(22)   Neugebauer, F. A.; Fischer, H.; Siegel, R. *Chem. Ber.* **1988**, *121*, 815.

(23)   Neugebauer, F. A.; Fischer, H.; Krieger, C. *Chem. Ber.* **1983**, *116*, 3461.

(24)   Jaworski, J. S. *Electroanal. Chem.* **1991**, *300*, 167.

(25)   Jaworski, J. S.; Krawczyk, I. *Monatsh. Chem.* **1992**, *123*, 43.

(26)   Forrester, A. R.; Hay, J. M.; Thomson, R. H. *Organic Chemistry of Stable Free Radicals*; Academic Press: London, 1968.

(27)   Wertz, J. E.; Bolton, J. R. *Electron Spin Resonance*.

(28)   Bruker; 1.25, Shareware Version ed.; Brüker Analytische Messtechnik GmbH, 1996.

(29)   Wasserman, E.; Snyder, L. C.; Yager, W. A. *J. Chem. Phys.* **1964**, *41*, 1763.

(30)   Raphaelian, L.; Hooks, H.; Ottmann, G. *Angew. Chem. Int. Ed. Engl.* **1967**, *6*, 363.

(31)   Knorr, A. *Funktionalisierte Fluoreszenzfarbstoffe auf Anthracen-und Pyrenbasis*; University of Regensburg: Regensburg, 1995.

Chapter 5. Trends in Exchange Coupling for Trimethylenemethane-Type Bis(semiquinone) Biradicals.[1,2]

Introduction

The general rules for creating high-spin organic molecules, as described in Chapter 2, involve attaching a spin-containing group to a coupler, such that the SOMOs in the resulting biradical are nondisjoint.[3-6] Several different couplers have been identified and explored.[4,5] There are two factors that effect this scheme for creating high-spin molecules: substituents on either the spin group or the coupler, and the molecular conformation.[7-9] The Shultz group has recently reported the first examples of substituent-modulated exchange coupling in a series of triplet ground-state biradicals **1(SQZnL)₂, Scheme 5.1**.[10] As for conformation-dependent exchange coupling, it has been understood for some time, from a handful of examples, that severe bond torsions between the spin-containing group and the coupling group will attenuate the exchange coupling.[11-19] In this Chapter we explore the first magnetostructural study of conformation-dependent exchange modulation within an isostructural series.

Scheme 5.1. Spin protecting groups used for the TMM-type bis(semiquinone) biradicals.
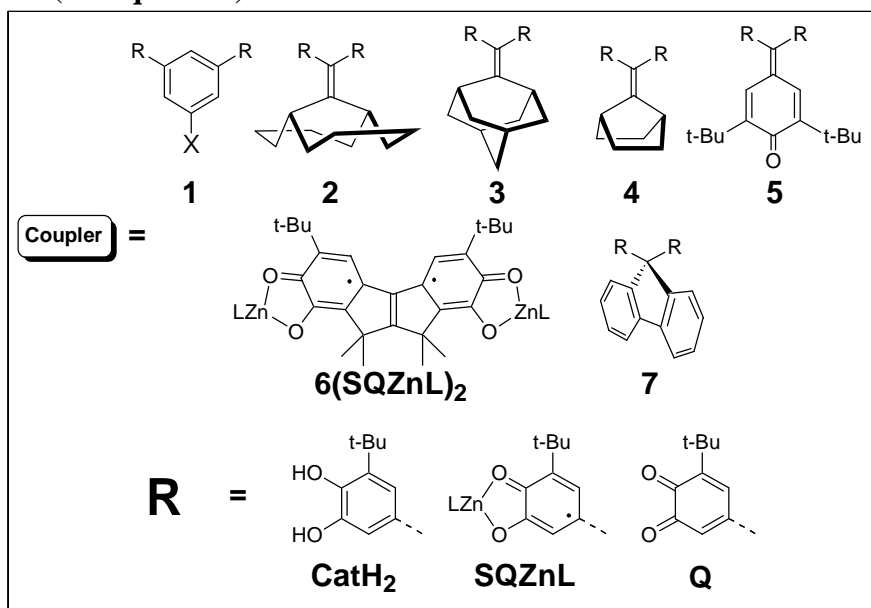
Earlier work in the Shultz group discussed the design elements for creating conformational dependent exchange coupling within a generalized TMM-type biradical and are repeated here, **Figure 5.1**.[20] The TMM-type π-topology is created by attaching spin containing groups geminal to an ethene connector. The spin containing group is any general group that places spin density on a carbon connected to the ethene group. In the case of this Chapter it is semiquinones, for Chapter 6 it is phenyl t-butylnitroxides. Since stable molecules are our desired product there must be some spin-protecting group that will provide steric protection to the spin in the ethene group (R in **Scheme 5.1**). The steric interaction between the spin-protecting group and the spin containing group will disrupt or attenuate the conjugation into the coupling group. Bicyclic spin protecting groups have a unique advantage, since the steric interaction can be modulated by the size of the bicyclic ring. The larger the bicyclic ring the larger the angle θ and therefore ϕ.

86

Our studies then are primarily concerned with the angle ϕ, determined from X-ray

crystallography, and the exchange coupling parameter J, determined by variable

temperature magnetic suceptibility.

Capping groups: steric protection of unparied electrons; provides for variable phenyl torsion (ϕ)

TMM functionality: Ethene Coupler

Spin-Containing Units: organic radicals, metal ions, etc.
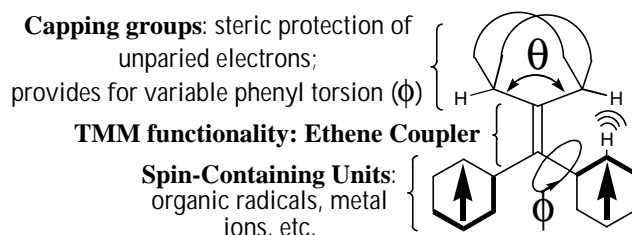
Figure 5.1. Design elements for creating conformation-dependent exchange coupling in a generalized TMM-type biradical.

Results and Analysis

Synthesis. The biradical complexes **2(CatH$_2$)$_2$ – 7(CatH$_2$)$_2$** are shown in

Scheme 5.1. The general procedure for complex formation is shown in **Scheme 5.2**.

Scheme 5.2. General procedure for bis(semiquinone) complex formation.
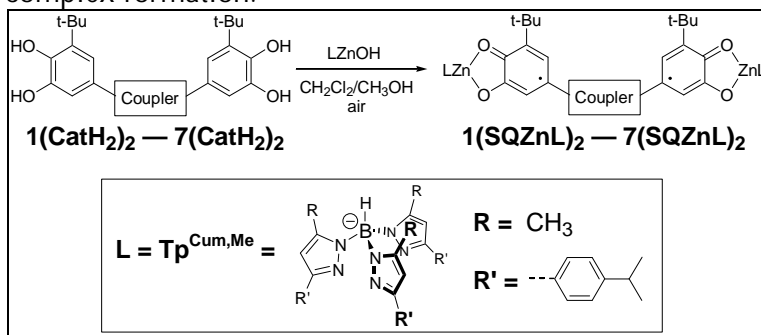
The bis(catechol)s were complexed with LZnOH, where L is the hydo-tris(pyrazolyl)

borate ligand, and then oxidized with air to the corresponding bis(semiquinone). The

bis(catechol) ligands **3(CatH$_2$)$_2$ – 7(CatH$_2$)$_2$** have all been previously prepared.[2,21,22]

Preparation of **2(CatH$_2$)$_2$**, **Scheme 5.3** begins with carbinol **8**[2] which was oxidized to

ketone **9** and subsequently transformed into thione **10** using P_4S_{10}.[23] Reaction of thione

10 with diazo compound **11**,[20] followed by desulfurization with triphenylphosphine gave alkene **12**. Deprotection afforded **2(CatH₂)₂**, and oxidation gave bis(quinone) **2(Q)₂**.

Scheme 5.3. Synthesis of **2(CatH₂)₂**.
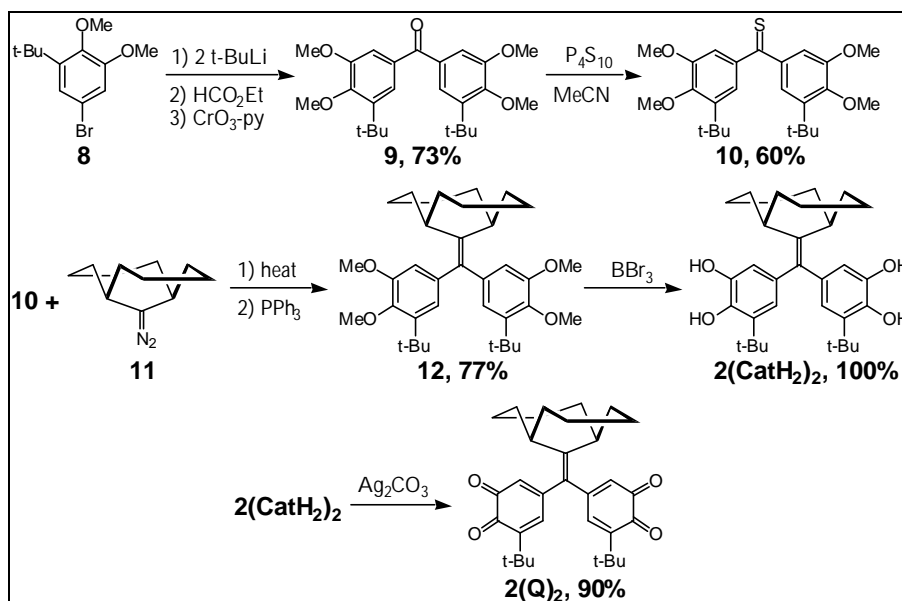
X-ray Data. The molecular structures of **2(CatH₂)₂ – 4(CatH₂)₂**, **6(CatH₂)₂** and **7(CatH₂)₂** were determined by X-ray crystallography and the thermal ellipsoid plots are shown in **Figure 5.2**. The X-ray structure of **5(CatH₂)₂**, has been previously reported.[24]
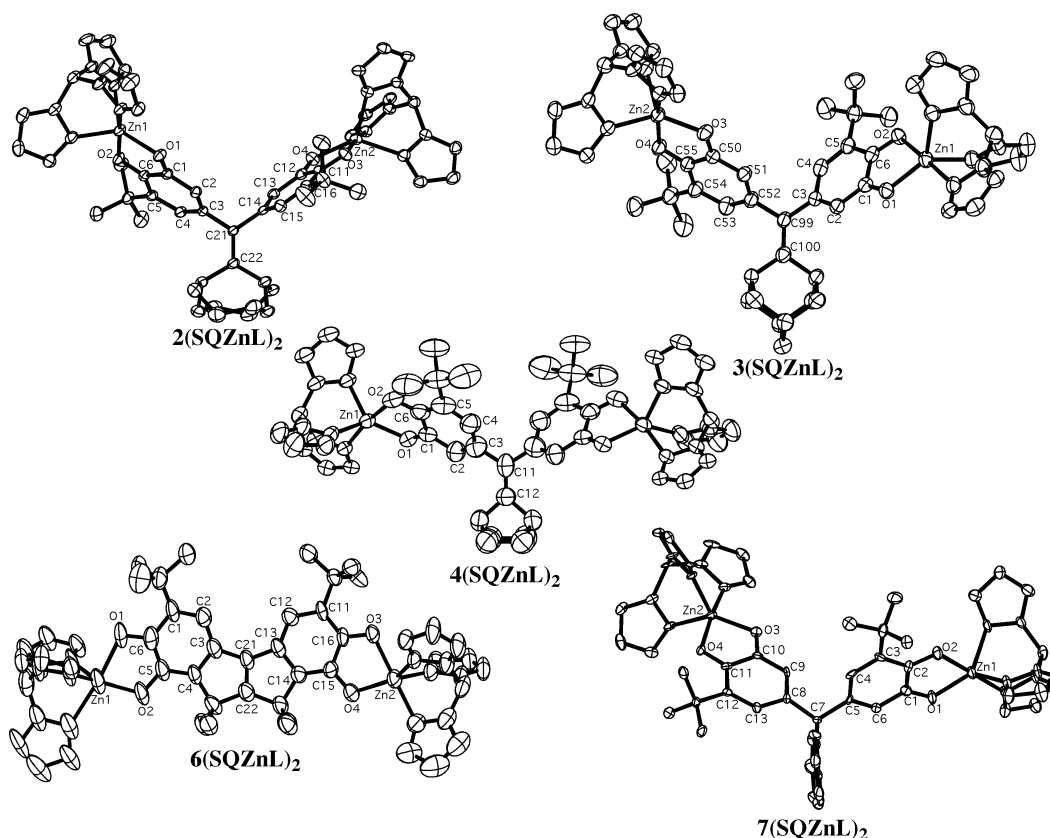
Figure 5.2. Thermal ellipsoid plots of **2(CatH₂)₂** – **4(CatH₂)₂**, **6(CatH₂)₂** and **7(CatH₂)₂**. The ancillary trisperazoyl borate ligand and the hydrogens have been omitted for clarity.

All of the dioxolene bond lengths are consistent with the semiquinone oxidation state as opposed to either Cat or CatH.[25-27] A complete list of the dioxolene bond lengths and all other crystallographic data can be found in **Appendix A**. **Table 5.1** lists the semiquinone ring torsion angle with the TMM coupler.

Table 5.1. Semiquinone Ring Torsion Angles for **2(CatH₂)₂** – **7(CatH₂)₂**.[a-c]

Biradical	Semiquinone Ring Torsion Angles (°)[a]	Average Semiquinone Ring Torsion Angles (°)
2(SQZnL)₂	64.10±0.13, 78.04±0.13	71.1±3.5
3(SQZnL)₂	47.51±0.18, 48.94±0.27	48.23±0.4
4(SQZnL)₂	48.37±0.29	48.37±0.29
5(SQZnL)₂[b]	50.3±0.3, 42.6±0.8	46.5±3.9
6(SQZnL)₂	4.9±0.8, 9.7±0.8	7.3±2.4
7(SQZnL)₂[c]	42.3±0.9, 52.4±0.1	47.4±2.5

[a]Torsion angle defined as the angle between the plane of a semiquinone ring and the plane containing the ethene coupler. [b]Data from ref [24]. [c]**7(SQZnL)₂** torsion angles defined as bond torsion through the sp³ carbon of the fluorenyl group.

Frozen-Solution EPR Spectroscopy. **Figure 5.3** shows the EPR spectra of **2(SQZnL)₂**—**7(SQZnL)₂** recorded at 77 K in 2-MTHF. All spectra are consistent with randomly oriented triplet species[28] along with small amounts of doublet monoradical impurities.[29] The zero-field-splitting parameters for the biradicals[30] are given in **Table 5.2**. The spectral shapes of all biradicals, except **3(SQZnL)₂**, are invariant with temperature changes, suggesting the absence of rotomers.[31] The results for **3(SQZnL)₂** are discussed below.
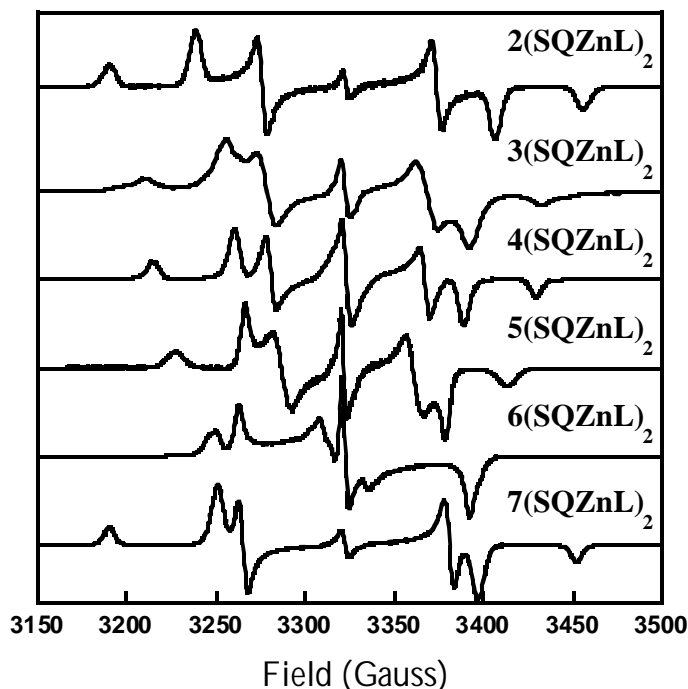
Figure 5.3. Frozen solution EPR spectra of **2(SQZnL)₂**—**7(SQZnL)₂** recorded at 77 K in 2-MTHF.

Table 5.2. Zero Field Splitting Parameters for **2(SQZnL)₂**—**7(SQZnL)₂**.

Biradical	$|D|/hc$ (cm^{-1})	$|E|/hc$ (cm^{-1})	$|E/D|$
2(SQZnL)₂	0.0124	0.0011	0.0887
3(SQZnL)₂	0.0105	0.0008	0.0762
4(SQZnL)₂	0.0098	0.0006	0.0612
5(SQZnL)₂	0.0093	0.0006	0.0645
6(SQZnL)₂	0.0068	0.0017	0.2500
7(SQZnL)₂	0.0123	0.0005	0.0407

Variable-Temperature EPR Spectroscopy. Curie plots for the doubly-integrated $\bullet m_S = 2$ signals of $\mathbf{2(SQZnL)_2}$—$\mathbf{7(SQZnL)_2}$ are shown in **Figure 5.4**, and are summarized in **Table 4**. Biradicals $\mathbf{4(SQZnL)_2}$—$\mathbf{7(SQZnL)_2}$ gave linear responses, consistent with $\boldsymbol{J} > 0$ (ferromagnetic coupling) or $\boldsymbol{J} = 0$,[32] and are in agreement with previous findings on bis(semiquinone)s prepared by electrochemical and chemical reduction.[2,21] The intensity of $\bullet m_S = 2$ signal of $\mathbf{2(SQZnL)_2}$ decreased with decreasing temperature consistent with antiferromagnetic coupling. The data was fit to **Eq. 1**:[32]

$$I_{EPR} = \frac{C}{T} \left| \frac{3\exp\left(\dfrac{-2J}{kT}\right)}{1 + 3\exp\left(\dfrac{-2J}{kT}\right)} \right| \tag{1}$$

where C is a constant and $\boldsymbol{J}$ is the exchange parameter. Best fit results give $\boldsymbol{J} = -35 \text{ cm}^{-1}$.
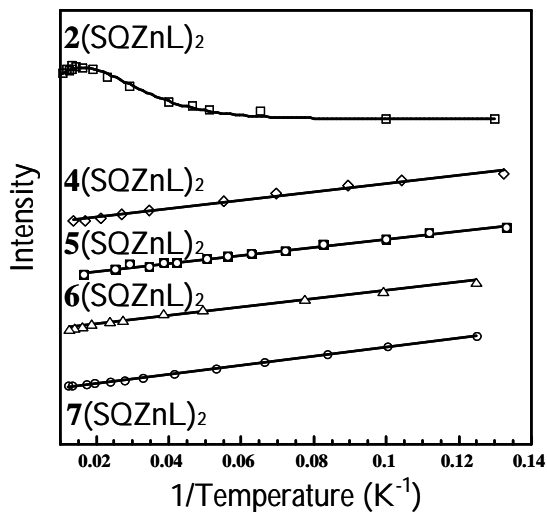
Figure 5.4. EPR Curie plots for biradical complexes $\mathbf{2(SQZnL)_2}$, $\mathbf{4(SQZnL)_2}$ — $\mathbf{7(SQZnL)_2}$.

The $\bullet m_S = 1$ region of the EPR spectrum of biradical $\mathbf{3(SQZnL)_2}$ shows that at least three rotamers characterized by different zero-field splitting parameters are present, **Figure 5.5**.
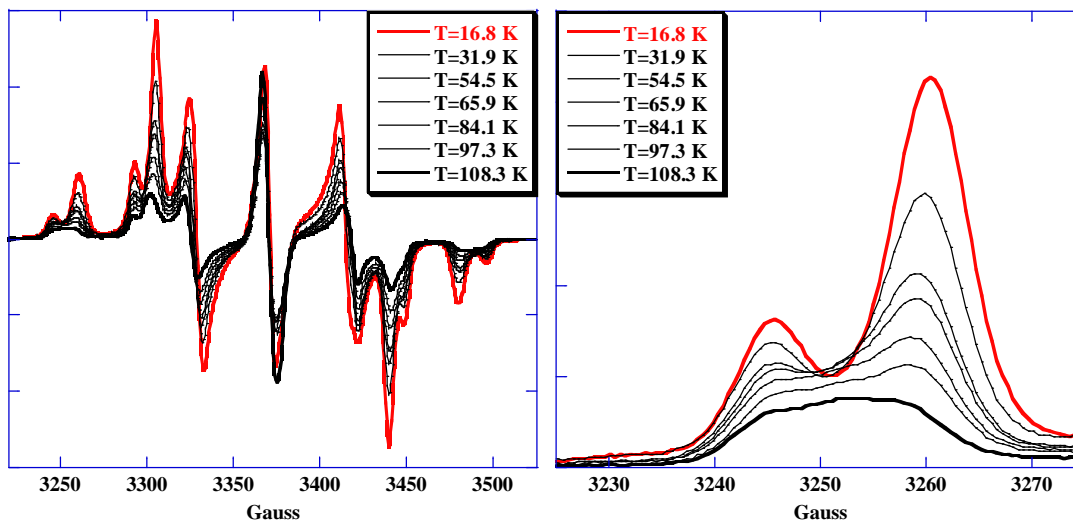
Figure 5.5. Left: $\Delta m_s = 1$ region of the EPR spectrum of **3(SQZnL)$_2$** at various temperatures. Right: Enlargement of the z-transition , which clearly shows at least three peaks. The top line corresponds to T=16.8 K.

The low field z-transition was deconvoluted into three separate peaks using a sum of Gaussian and Lorentzian curves, **Figure 5.6**. Curie plots for each of the three peaks based on the area under the fitted curves yielded best fits for three rotamers having $\textbf{\textit{J}} \bullet$ -3, -10, and -38 cm^{-1}, **Figure 5.7**. This result differs from the linear Curie plot for the sodium salt of the **3(SQ)$_2$**,[33] but parallels the results for the corresponding bis(phenoxy) radical.[31]
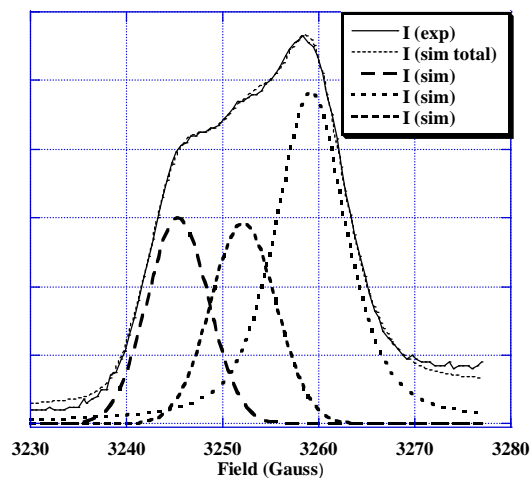
Figure 5.6. An example of the deconvolution of the low field z-transition in **3(SQZnL)$_2$**.
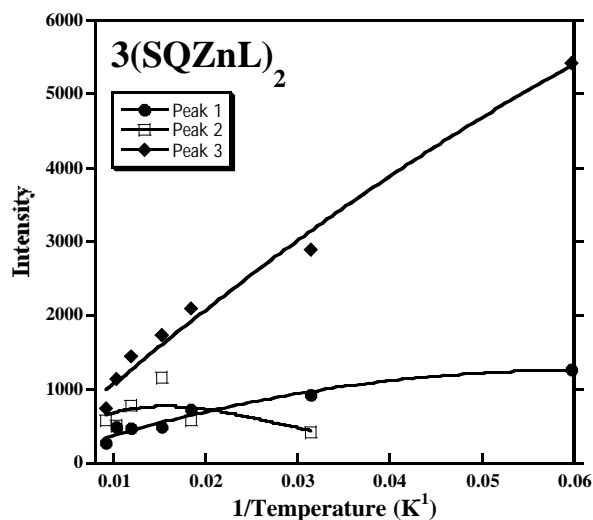
Figure 5.7. Curie plot of the three rotamers in **3(SQZnL)$_2$**.

Solid-State Magnetic Susceptibility Measurements. The magnetic

susceptibility data for **2(SQZnL)$_2$—7(SQZnL)$_2$** are plotted in **Figure 5.8**. The magnetic

susceptibility data was fit using the temperature-dependent χ_{para}T field-independent van

Vleck expression, **Eq. 2**,[34,35]

$$\chi T = \frac{2Ng^2\beta^2}{k\left[3+e^{-2J/kT}\right]} \qquad\qquad \textbf{Eq. 2}$$

where g is the isotropic Landé constant (g = 2.0023), β is the Bohr magneton, T is

temperature in Kelvin, k is Boltzmann's constant, and $\boldsymbol{J}$ is the intramolecular

semiquinone-semiquinone exchange coupling parameter. The relative singlet- and

triplet-state energies were derived using the Hamiltonian, $\mathrm{H} = -2\boldsymbol{J}\hat{S}_1 \cdot \hat{S}_2$, where $\hat{S}_1$ and

$\hat{S}_2$ are the spin operators for the bis(semiquinone)s. The decrease in the χT data at low

temperatures was accounted for with a Weiss correction, using the expression $\chi_{eff} = \chi/(1-$

$J\chi)$, where $J = 2zJ'/(Ng^2\beta^2)$.[36] The origin of zJ' may be zero-field splitting,

intermolecular interaction, saturation effects, or some combination of all three.[37] The

other terms have their usual meanings.[36] All curve fit results are presented in **Table 5.3**.

The results for **2(SQZnL)₂** are displayed as a χ_{para} *vs.* T plot as the inset in **Figure**

5.8. For antiferromagnetically coupled dimers, the χ_{para} *vs.* T plot displays a signature

maximum with T_{max} = 1.285J/k.[34] Despite several attempts, we were unable to

satisfactorily fit the low temperature region. Nevertheless, the J-value from the fit

parameters (-29.5 cm^{-1}) compares well with the value of J determined from T_{max} (J = -31

cm^{-1}). The value for J given in **Table 5.3** represents an average of the values from the fit

and from the value determined from T_{max}.
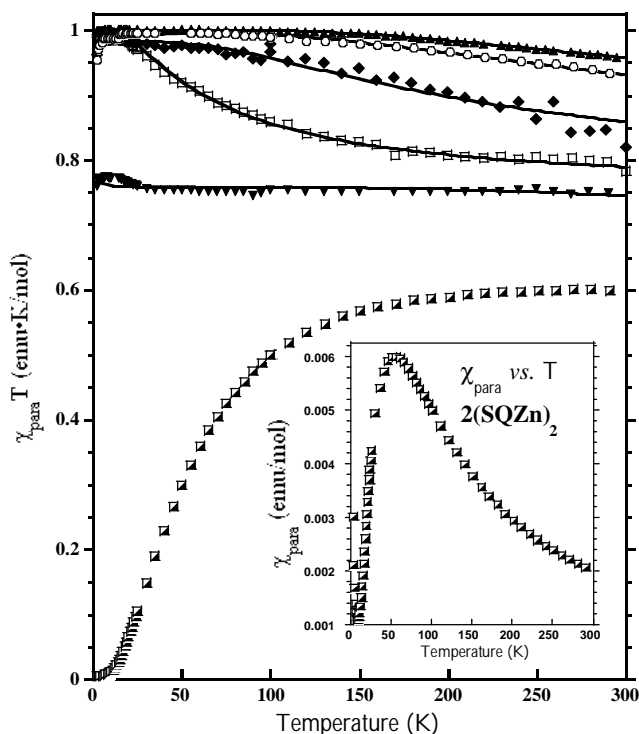
Figure 5.8. EPR Curie plots for biradical complexes **2(SQZnL)₂, 4(SQZnL)₂ — 7(SQZnL)₂**.

Table 5.3. Variable-Temperature Susceptibility Fit Parameters, and Results from Variable-Temperature EPR Experiments for **2(SQZnL)$_2$—7(SQZnL)$_2$.**[a]

Biradical	J (cm^{-1})[b]	$_zJ'$(cm^{-1})[c]	EPR Curie Plot, J(cm^{-1})
2(SQZnL)$_2$	-30.3 ± 0.8[d]	+0.011 ± 0.001	Curved, -35
3(SQZnL)$_2$	+24.4 ± 0.6	-0.032 ± 0.008	Curved, -3,-9,-38
4(SQZnL)$_2$	+87.0 ± 3.0	-0.024 ± 0.018	Linear, J • 0
5(SQZnL)$_2$[e]	+209.4 ± 1.4	-0.029 ± 0.002	Linear, J • 0
6(SQZnL)$_2$	+163.6 ± 1.6	-0.080 ± 0.004	Linear, J • 0
7(SQZnL)$_2$	+0.99 ± 0.06	-0.503 ± 0.021	Linear, J • 0

[a]Fits used g = 2.002. [b]J > 0 for triplet ground-state. [c]Intermolecular interaction. [d]J-value for average determined from χ_{para} vs T plot fit parameters and T$_{max}$. [e]Fit parameters from ref [24].

Discussion

The basic design principle for synthesizing high-spin molecules has worked well in our series. By connecting a spin containing group to coupler that promotes ferromagnetic coupling and stericly protecting the spin we have created a series high-spin biradicals that for the most part are air stable. **6(SQZnL)$_2$** was the only compound that had to be complexed and crystallized in an N$_2$ glove-box. Although **4(SQZnL)$_2$** was complexed in a N$_2$ glove box, X-ray quality crystals were grown in CH$_2$Cl$_2$/MeOH in the air.

Control over the semiquinone torsion angles was achieved by increasing or decreasing the size of the capping group, **Figure 5.9**. This can be seen in semiquinone ring torsion angles relative to the ethene couplers in our X-ray crystal structures, **Table 5.2**. Generally, the SQ ring torsion angles increase in going from **6(SQZnL)$_2$**, in which the conformation is held nearly planar by covalent bonds, to **2(SQZnL)$_2$**. The similarity in the conformations of **3(SQZnL)$_2$** and **4(SQZnL)$_2$** was unexpected, as molecular mechanics predicted a *ca.* 10° difference in SQ ring torsions.[20] Nevertheless, an

isostructural series of TMM-type biradicals with a range of semiquinone ring angles is
achieved.
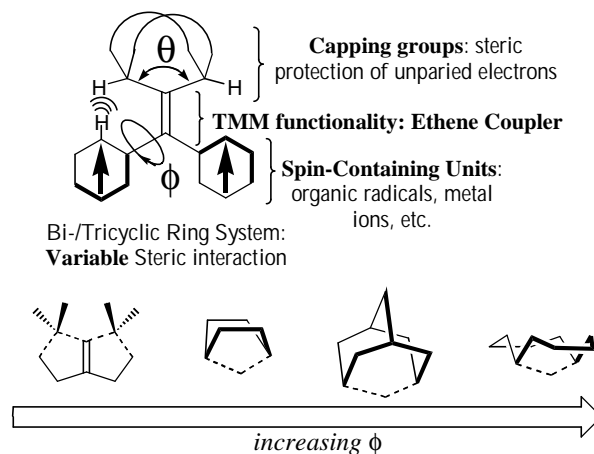
Figure 5.9. Design elements for creating conformational dependent exchange coupling in a generalized TMM-type biradical. The larger the capping group the larger θ and therefore φ.

The ZFS parameters in organic biradicals is the result of dipolar interactions and

therefore should correlate with molecular structure, **Figure 5.10**.[38-41]
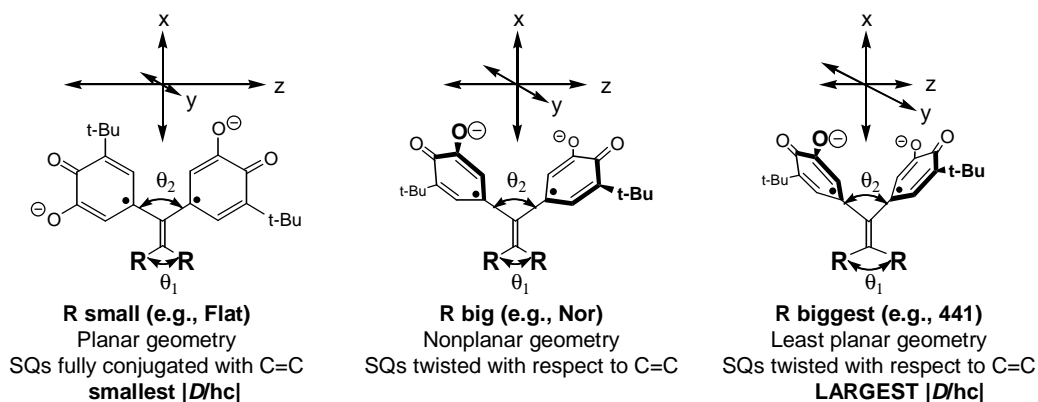
Figure 5.10. How conformation manifests itself in the zero-field splitting parameters. Axes are drawn for illustrative purposes only.

As can been seen in **Table 5.2**, D decreases within the series **2(SQZnL)₂—7(SQZnL)₂**

consistent with the corresponding decrease in semiquinone torsions as depicted in **Figure**

5.10. Thus, Increasing the delocalization decreases D. We also know that increasing the

delocalization of the spin into the coupler increases the ferromagnetic contribution to **J**.

This trend in experimental ZFS parameters, in frozen solution, is consistent with the

conformations determined by the crystal structures. We conclude that the conformations

found in the crystals are similar to the conformations found in frozen solution. This is

also supported by the similarity of the solution and solid state **J** parameters for

2(SQZnL)$_2$, **Table 5.2**. In addition, we conclude that severe torsions of the semiquinone

rings, such as in **2(SQZnL)$_2$**, cause the unpaired electrons of the semiquinone π-system

to be "stacked" in such a way to favor incipient σ-bond formation.[42,43] Thus, the same

structural features that give rise to large a large D, also result in an increase in the

antiferromagnetic coupling in TMM-type biradicals.

The Nature of Exchange Coupling. The exchange coupling parameters for our TMM-

type biradicals can be correlated to the average semiquinone ring torsion angles via a

"Karplus-type" relation,[44] **Figure 5.11**, **Eq. 3**.

$$J = A\cos^2\left(f_{ave}\right) + B \qquad\qquad \textbf{Eq. 3}$$

Eq. 3 contains a $\cos^2 f$ term because overlap of the 2p-π orbitals if the semiquinone with

those of the ethene coupler vary as the cosine of the torsion angles (f) between the

groups.[45] Due to the small number of data points and to use the simplest model, we are

considering only a single trigonometric function and use an average of the two torsion

angles.[46] The fit to **Eq. 5** gives A = 213 cm^{-1} and B = -44 cm^{-1}. Given the simplicity of

our model and only four data points the A and B terms should be considered

semiquantitative, at best as suggested by the thickness of the curve.
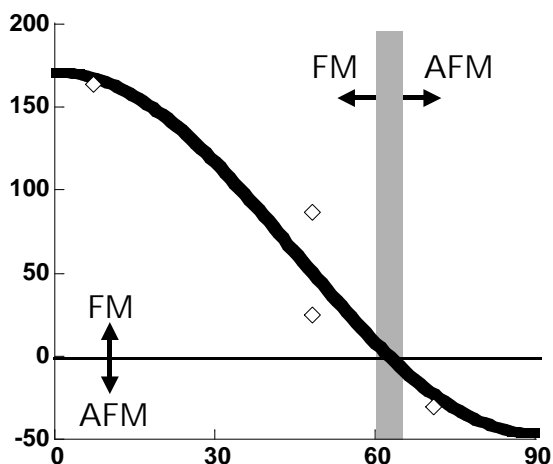
Figure 5.11. "Karplus-Conroy type" relationship for electron spin exchange coupling in **2(SQZnL)₂ - 4(SQZnL)₂, 6(SQZnL)₂**. The thickness in the lines is meant to represent the semiquantative fit to our data.

Generally speaking, the A term should be a function of both the coupler and the spin

density in the spin containing group. The B term is the only term that can account for J_{AF}

and in this case should be proportional to the through-space antiferromagnetic interaction

(incipient bond formation).

We can qualitatively extend this to other spin groups and couplers. Our ~200 cm⁻

¹ range in **J** values for **2(SQZnL)₂ - 4(SQZnL)₂, 6(SQZnL)₂** is most likely greater than a

corresponding range in related *m*-phenylene-type biradicals. This is in part due to the

inherently stronger ferromagnetic coupling provided in TMM-type biradicals (ΔE_{S-T}

TMM = 14.5 kcal/mol[47] ΔE_{S-T} MPH = 9.2 kcal/mol[48]). The TMM-type biradicals in our

studies exhibited a net ferromagnetic exchange coupling over a range of $\leq$ ~60°).

The correlation of semiquinone ring torsion and exchange parameter is not perfect

since the **J**-values for **3(SQZnL)₂** and **4(SQZnL)₂** differ by a factor of 3.6, yet the

semiquinone ring torsions are nearly identical. We note however that the geometries of

3(SQZnL)$_2$ and **4(SQZnL)$_2$** are different: the former is asymmetric, while the latter has (crystallographic) C$_2$ symmetry. Clearly, there is more to the exchange coupling in this series than semiquinone ring torsion, as is the case for Karplus-Conroy NMR correlation.[44] Nevertheless, our series of biradicals shows a clear variation from strong ferromagnetic exchange coupling to moderate antiferromagnetic coupling as semiquinone ring torsion increases.

Conclusion

Our experimental results demonstrate that conformational *J*-modulation is strong in TMM-type biradicals. The breadth in *J*-values for the TMM-type biradicals is most likely greater than the corresponding breadth in related meta-phenylene-type biradicals, although no magnetostructural study for a series of biradicals in the latter case has been reported.[11] The breadth in *J*-values for TMM-type biradicals studied herein is augmented by the larger contribution of through-space interaction to *J*$_{AF}$ brought about by the close spatial proximity of the semiquinone groups. In fact, spin density close to the coupler is critical, and the *J*-modulation in a similar isostructural series of bis(nitroxide) biradicals,[20,49] Chapter 6, is diminished compared to the present case. Nevertheless, TMM-type biradicals, as assessed by our bis(SQ) derivatives, can exhibit *net* ferromagnetic exchange coupling over a broad range of conformations (0 • torsions • *ca.* 60°). We also showed how energy matching of coupler and semiquinone orbitals can enhance exchange coupling, as demonstrated by the fact that the conformation of

5(SQZnL)$_2$ is similar to that of **3(SQZnL)$_2$**, but **J** is nearly one order of magnitude greater for the former.

Our results also indicate that for the molecules studied, there is a qualitative correlation between the molecular conformations observed in crystal structures, and those adopted in frozen solution, as judged by EPR zero-field splitting parameters. This relationship results in similar **J**-values for solution and solid-state species. However, we note that linear EPR Curie plots only indicate that **J** • 0. A notable exception to the correlation between solution and solid-state molecular conformation is the adamantyl-capped biradical, **3(SQZnL)$_2$**. The adamantyl group seems to impart interesting properties to TMM-type biradicals since we reported solvent-dependent conformational **J**-modulation for a bis(phenoxy) biradical analog of **3(SQZnL)$_2$**,[31] and hysteresis for a bis(nitroxide) derivative of **3(SQZnL)$_2$**.[50]

Experimental

General Methods. Unless noted otherwise, reactions were carried out in oven-dried glassware under a nitrogen atmosphere. THF and toluene were distilled under argon from sodium benzophenone ketyl, and acetonitrile and methylene chloride were distilled from CaH$_2$ under argon. *tert*-Butyl lithium (1.5M in pentane) was used as received from Aldrich Chemical Company. Other chemicals were purchased from Aldrich Chemical Company. X-Band EPR spectroscopy and electrochemistry were performed as described previously.[51] NMR spectra were recorded at 300 MHz for ^{1}H NMR (referenced to TMS) and 75 MHz for ^{13}C NMR. Elemental analyses were performed by Atlantic Microlab,

Inc, Norcross, GA. Mass spectrometry was carried out at the NC State University Mass Spectrometry Facility. Electronic absorption spectra were collected on a Shimadzu UV-3101PC scanning spectrophotometer.

Synthesis. Catechols $3(CatH_2)_2$ — $7(CatH_2)_2$[2,21] and their corresponding Zn^{II} complexes[22,24,52] were prepared as described previously, except for $4(SQZnL)_2$ and $6(SQZnL)_2$ which were prepared by a "comproportionation route" as described below. X-ray quality crystals for biradical complexes (except $6(SQZnL)_2$) were grown by layering methanol onto a methylene chloride solution of the biradical. Crystals of complex $6(SQZnL)_2$ were grown in a glovebox using an analogous procedure, but replacing methanol with *n*-heptane. Carbinol **8** was prepared as previously described.[2]

5,5´-di-*tert*-Butyl-3,3´,4,4´-tetramethoxybenzophenone (9). A 100 mL flask containing CrO_3 (1.1 g, 11.0 mmol) was pump/purged three times with nitrogen. Pyridine (1.7 mL, 21 mmol) was added and the mixture was dissolved in 20 mL dry CH_2Cl_2. The solution was stirred for 0.5 hr, and carbinol **8** (727.5 mg, 1.75 mmol) dissolved in 20 mL CH_2Cl_2 was cannulated into the reaction. After stirring for 6 h, the reaction was quenched with 1 mL 1M NaOH, washed with brine, and dried over Na_2SO_4. Methanol was added to the resulting yellow oil to give a white solid (638 mg, 88%). ^{1}H NMR ($CDCl_3$) δ 7.39 (d, 2H, J=2.1 Hz), 7.37 (d, 2H, J=1.8 Hz), 3.96 (s, 6H), 3.92 (s, 6H), 1.38 (s, 18H). ^{13}C NMR δ 195.6, 153.3, 152.5, 142.7, 132.4, 122.7, 112.1, 60.7, 56.1, 35.4, 30.6. IR (film from CH_2Cl_2) ν(cm^{-1}): 2955.0, 1649.9, 1573.0, 1453.5, 1410.0, 1359.7, 1323.9, 1292.6, 1250.3, 1222.4, 1153.6, 1066.8, 1003.7, 762.3. HRMS (FAB): (*m/z*) $C_{25}H_{34}O_5$ (M)$^+$ calcd 414.2406, found 414.2393.

5,5′-di-*tert*-Butyl-3,3′,4,4′-tetramethoxy-thiabenzophenone (10). An a 100 mL flask

benzophenone **9**, (81.3 mg, 0.20 mmol), phosphorous pentasulfide (131.0 mg, 0.29

mmol) and sodium bicarbonate (100.8 mg, 1.20 mmol) were taken up in 10 mL

acetonitrile. The mixture was refluxed for 4 hours during which time the color of the

mixture turned blue. The mixture was cooled to 0°C and quenched with saturated

aqueous $NaHCO_3$, washed twice with brine, and the blue solution was dried over

Na_2SO_4. The solvent was removed and the blue solid was taken up in hot methanol and

cooled to 0°C to induce precipitation (44.6 mg, 0.10 mmol) in 51% yield. ^{1}H NMR

($CDCl_3$) δ 7.41 (d, 2H, J=1.8 Hz), 7.25 (d, 2H, J=2.1 Hz), 3.96 (s, 6H), 3.91 (s, 6H), 1.35

(s, 18H). ^{13}C NMR δ 235.2, 153.0, 152.9, 142.3, 142.0, 122.2, 113.5, 60.7, 56.0, 35.4,

30.6. IR (film from CH_2Cl_2) ν(cm^{-1}): 2998.4, 2956.1, 2866.9, 2832.6, 2600.7, 1995.7,

1582.8, 1567.3, 1478.5, 1450.4, 1405.5, 1359.7, 1314.4, 1288.8, 1249.4, 1205.7, 1151.3,

1073.7, 1060.9, 1002.9, 882.7, 860.0, 790.0, 704.5, 669.5. HRMS (FAB): (*m/z*)

$C_{25}H_{34}O_4$ $(M+H)^+$ Calcd 414.2256. Found 414.2246. Anal. Calcd for $C_{25}H_{34}O_4$: C,

69.73; H, 7.96%. Found: C, 69.76; H, 7.88%.

11-[Bis-(3-*tert*-butyl-4,5-dimethoxyphenyl)-methylene]-bicyclo[4.4.1]undecane, (12).

In a 50 mL flask thione **10** (401.2 mg, 0.93 mmol) was dissolved in 15 mL THF. The

diazo **11**, (182.2 mg, 0.94 mmol) was dissolved in 5 mL THF and added drop wise to the

stirring benzothione **10** solution. Bubbling and a white precipitate that quickly

redissolved was observed. The blue solution was refluxed overnight. The solvent was

removed and the remaining solid was taken up in 15 mL of toluene. Triphenylphosphine

(502.3 mg, 1.92 mmol) was added and the solution was refluxed for 2 days. Solvent was

removed and the mixture purified by radial chromatography (gradient elution; petroleum ether to 10% ether/petroleum ether). The white solid was precipitated from petroleum ether producing **12** (396.2 mg, 0.72 mmol) in 77% yield. ^{1}H NMR (CDCl$_3$) δ 6.78 (d, 2H J=1.8 Hz), 6.62 (d, 2H J=1.5 Hz), 3.84 (s, 6H), 3.81 (s, 6H), 2.91 (pent., 2H, J=6.0 Hz), 1.68 (m, 4H), 1.55 (m, 12H), 1.36 (s, 18H). ^{13}C NMR δ 153.0, 146.6, 146.5, 142.7, 139.9, 139.4, 119.1, 111.0, 60.5, 56.0, 41.0, 35.2, 32.7, 30.9, 27.2. IR (film from CH$_2$Cl$_2$) ν(cm^{-1}): 2951.7, 2921.9, 2863.2, 1568.2, 1465.5, 1409.1, 1358.0, 1327.6, 1303.0, 1257.7, 1234.7, 1152.7, 1136.0, 1074.0, 1010.3, 937.1, 908.6, 878.7, 849.1, 780.0, 736.5, 704.4, 675.2. Anal. Calcd for C$_{36}$H$_{52}$O$_4$: C, 78.79; H, 955%. Found: C, 78.73; H, 9.76%.

11-[Bis-(3-*tert*-butyl-4,5-dihydroxyphenyl)-methylene]-bicyclo[4.4.1]undecane, (2(CatH$_2$)$_2$). A dry 50 mL flask containing tetramethoxyether **12** (153.6 mg, 0.28 mmol) and 30 mL dry CH$_2$Cl$_2$ was pumped/purged three times with nitrogen. The solution was cooled to –78 °C. Boron tribromide (1.0 M in CH$_2$Cl$_2$, 5.6 mL, 5.6 mmol) was added dropwise and the solution was stirred overnight (-78 °C to 25 °C). The solution was poured onto ice, washed with brine, and dried over Na$_2$SO$_4$. The crude catechol was used without further purification. ^{1}H NMR (CDCl$_3$) δ 6.72 (d, 2H, J=1.5 Hz), 6.49 (d, 2H, J=1.8 Hz), 5.43 (s, 2H), 4.75 (s, 2H), 2.97 (pent., 2H, J=6 Hz), 1.67 (m, 4H), 1.53 (m, 12H) 1.39 (s, 18H). ^{13}C NMR δ 146.7, 142.7, 141.4, 138.9, 136.3, 136.2, 119.7, 113.4, 41.0, 34.8, 32.6, 29.9, 27.2. IR (film from CH$_2$Cl$_2$) ν(cm^{-1}): 3519.7, 2921.2, 1590.2, 1483.7, 1415.4, 1362.6, 1289.6, 1237.6, 1049.9, 963.9, 862.7, 801.7, 737.7, 705.3, 663.9. HRMS (FAB): (*m/z*) C$_{32}$H$_{44}$O$_4$ (M)$^+$ Calcd 492.3240. Found 492.3238.

Di(5-*tert*-butyl-3,4-hydroxyphenyl)methylene-bicyclo[4.4.1]undecane (2(Q)$_2$). A 50 mL flask containing **2(CATH$_2$)$_2$** (73.9 mg, 0.15 mmol) and 522 mg Fetizon's reagent was stirred with 25 mL THF overnight. The mixture was filtered through SiO$_2$. Radial chromatography (CH$_2$Cl$_2$) yielded a yellow/green solid (65.9 mg, 90%). ^{1}H NMR (CDCl$_3$) δ 6.62 (d, 2H, J=1.8 Hz), 6.21 (d, 2H J=1.8 Hz), 3.07 (pent., 2H, J=5.4 Hz), 1.76 (m, 4H), 1.55 (m, 18H), 1.27 (s, 18H). ^{13}C NMR δ 180.1, 179.3, 155.6, 152.9, 152.5, 136.0, 133.2, 127.2, 44.0, 35.9, 32.3, 28.4, 26.8. IR (film from CH$_2$Cl$_2$) ν(cm^{-1}): 2923.6, 1660.4, 1613.5, 1469.4, 1367.6, 1266.0, 1238.6, 910.4, 834.1, 805.4, 731.0. HRMS (FAB): (*m/z*) C$_{32}$H$_{40}$O$_4$ (M+H)$^+$ Calcd 489.3005. Found 489.3034.

Magnetic Susceptibility Measurements. Magnetic susceptibilities were measured on a Quantum Design MPMS-XL7 SQUID magnetometer using an applied field of 1 Tesla for Curie plots. Microcrystalline samples were loaded into the sample space of a Delrin sample holder, and mounted to the sample rod. Data were corrected for sample holder and molecular diamagnetism. The decrease in the χT data at low temperatures was accounted for with a Weiss correction, using the expression $\chi_{eff} = \chi/(1-J\chi)$, where J = $2zJ\phi_{inter}/(Ng^2\beta^2)$.[36] The origin of $J\phi_{inter}$ may be zero-field splitting, intermolecular interaction, saturation effects, or some combination of all three.[37] The other terms have their usual meaning.[36] The data are plotted as χT *vs.* T **Figure 5.8**, except for **2(SQZnL)$_2$** which is also displayed as χ *vs.* T, **Figure 5.8** inset.

References

(1)   Shultz, D. A.; Fico, R. M., Jr.; Bodnar, S. H.; Kumar, R. K.; Vostrikova, K. E.; Kampf, J. W.; Boyle, P. D. *J. Am. Chem. Soc.* **2003**, *125*, 11761.

(2)   Shultz, D. A.; Lee, H.; Fico, R. M., Jr. *Tetrahedron* **1999**, *55*, 12079.

(3)   Borden, W. T.; Davidson, E. R. *J. Am. Chem. Soc.* **1977**, *99*, 4587.

(4)   Dougherty, D. A. *Acc. Chem. Res.* **1991**, *24*, 88.

(5)   Rajca, A. *Chem. Rev.* **1994**, *94*, 871.

(6)   Lahti, P. M., Ed. *Magnetic Properties of Organic Materials*; Marcel Dekker: New York, 1999.

(7)   For work on substiuent and conformation effects on biradicals using computational chemistry and EPR spectroscopy, see the following: West, A. P., Jr.; Silverman, S. K.; Dougherty, D. A. *J. Am. Chem. Soc.* **1996**, *118*, 1452; Silverman, S. K.; Dougherty, D. A. *J. Phys. Chem.* **1993**, *97*, 13273.

(8)   West, A. P., Jr.; Silverman, S. K.; Dougherty, D. A. *J. Am. Chem. Soc.* **1996**, *118*, 1452.

(9)   For electronic modulation of **J** for singlet ground-state biradicals, see: Berson, J. A. Structural Determinants of the Chemical and Magnetic Properties of Non-Kekule Molecules. In *Magnetic Properties of Organic Materials*; Lahti, P. M., Ed.; Marcel Dekker: New York, 1999, pp 7.

(10)   Shultz, D. A.; Bodnar, S. H.; Lee, H.; Kampf, J. W.; Incarvito, C. D.; Rheingold, A. L. *J. Am. Chem. Soc.* **2002**, *124*, 10054.

(11)   Shultz, D. A. *Conformational Exchange Modulation in Trimethylenemethane (TMM)-Type Biradicals*; In *Magnetic Properties of Organic Materials*; Lahti, P., Ed.; Marcel Dekker, Inc.: New York, 1999.

(12)   Dei, A.; Gatteschi, D.; Sangregorio, C.; Sorace, L.; Vaz, M. G. F. *Inorg. Chem.* **2003**, *42*, 1701.

(13)   Fujita, J.; Tanaka, M.; Suemune, H.; Koga, N.; Matsuda, K.; Iwamura, H. *J. Am. Chem. Soc.* **1996**, *118*, 9347.

(14)   Okada, K.; Imakura, T.; Oda, M.; Murai, H.; Baumgarten, M. *J. Am. Chem. Soc.* **1996**, *118*, 3047.

(15)   Adam, W.; van Barneveld, C.; Bottle, S. E.; Engert, H.; Hanson, G. R.; Harrer, H. M.; Heim, C.; Nau, W. M.; Wang, D. *J. Am. Chem. Soc.* **1996**, *118*, 3974.

(16)   Fang, S.; Lee, M.-S.; Hrovat, D. A.; Borden, W. T. *J. Am. Chem Soc.* **1995**, *117*, 6727.

(17)   Silverman, S. K.; Dougherty, D. A. *J. Phys. Chem.* **1993**, *97*, 13273.

(18)   Kanno, F.; Inoue, K.; Koga, N.; Iwamura, H. *J. Am. Chem. Soc.* **1993**, *115*, 847.

(19)   Dvolaitzky, M.; Chiarelli, R.; Rassat, A. *Angew. Chem., Int. Ed. Engl.* **1992**, *31*, 180.

(20)   Shultz, D. A.; Boal, A. K.; Lee, H.; Farmer, G. T. *J. Org. Chem.* **1999**, *64*, 4386.

(21)   Shultz, D. A.; Boal, A. K.; Lee, H.; Farmer, G. T. *J. Org. Chem.* **1998**, *63*, 9462.

(22)   Ruf, M.; Noll, B. C.; Groner, M. D.; Yee, G. T.; Pierpont, C. G. *Inorg. Chem.* **1997**, *36*, 4860.

(23)   Scheeren, J. W.; Ooms, P. H. J.; Nivard, R. J. F. *Synthesis* **1973**, 149.

(24)   Shultz, D. A.; Bodnar, S. H.; Kampf, J. W. *Chem. Commun.* **2001**, 93.

(25) Pierpont, C. G.; Lange, C. W. *Prog. Inorg. Chem.* **1994**, *41*, 331.

(26) Ruf, M.; Lawrence, A. M.; Noll, B. C.; Pierpont, C. G. *Inorg. Chem.* **1998**, *37*, 1992.

(27) Shultz, D. A.; Bodnar, S. H.; Kumar, R. K.; Lee, H.; Kampf, J. W. *Inorg. Chem.* **2001**, *40*, 546.

(28) Wasserman, E.; Snyder, L. C.; Yager, W. A. *J. Chem. Phys.* **1964**, *41*, 1763.

(29) Some of the g=2 signal is a double-quantum transition as shown by power dependence studies, see: deGroot, M. S.; van der Waals, J. H. *Physica* **1963**, *29*, 1128.

(30) Bruker; 1.25, Shareware Version ed.; Brüker Analytische Messtechnik GmbH, 1996.

(31) Shultz, D. A.; Boal, A. K.; Farmer, G. T. *J. Am. Chem. Soc.* **1997**, *119*, 3846.

(32) Berson, J. A., Ed. *The Chemistry of the Quinonoid Compounds, Vol. II*; John Wiley & Sons: New York, 1988.

(33) Shultz, D. A.; Boal, A. K.; Driscoll, D. J.; Farmer, G. T.; Hollomon, M. G.; Kitchin, J. R.; Miller, D. B.; Tew, G. N. *Mol. Cryst. Liq. Cryst.* **1997**, *305*, 303.

(34) Kahn, O. *Molecular Magnetism*; VCH: New York, 1993.

(35) Bleaney, B.; Bowers, K. D. *Proc. R. Soc. London* **1952**, *A214*, 451.

(36) O'Connor, C. J. *Prog. Inorg. Chem.* **1982**, *29*, 203.

(37) Caneschi, A.; Dei, A.; Mussari, C. P.; Shultz, D. A.; Sorace, L.; Vostrikova, K. E. *Inorg. Chem.* **2002**, *41*, 1086.

(38) Ullmann, E. F.; Boocock, D. G. B. *Chem. Comm.* **1969**, 1161.

(39) Mukai, K.; Tamaki, T. *Bull. Chem. Soc. Jpn.* **1977**, *50*, 1239.

(40) Sandberg, K. A.; Shultz, D. A. *J. Phys. Org. Chem.* **1998**, *11*, 819.

(41) We were unsuccessful at calculating the ZFS parameters for our biradicals using the methods described in Sandberg, K. A.; Shultz, D. A. *J. Phys. Org. Chem.* **1998**, *11*, 819., possibly due to the fact several of the biradicals are between the extremes of disjoint and nondisjoint.

(42) Hatfield, W. E. *Chapter 7. Properties of Condensed Compounds (Compounds with Spin Exchange)*; In *Theory and applications of molecular paramagnetism*; Boudreaux, E. A., Mulay, L. N., Eds.; Wiley Interscience: New York, 1976, pp 381.

(43) Anderson, P. W. *Phys. Rev.* **1959**, *115*, 2.

(44) Karplus, M. *J. Am. Chem. Soc.* **1963**, *85*, 2870.

(45) Streitwieser, A., Jr. *Molecular Orbital Theory for Organic Chemists*; In *Molecular Orbital Theory for Organic Chemists*; Wiley & Sons: New York, 1961, p 16.

(46) The same qualitative result is also obtained from a $\cos(f_1)\cos(f_2)$ function.

(47) Wenthold, P. G.; Hu, J.; Squires, R. R.; Lineberger, W. C. *J. Am. Chem. Soc.* **1996**, *118*, 475.

(48) Wenthold, P. G.; Kim, J. B.; Lineberger, W. C. *J. Am. Chem. Soc.* **1997**, *119*, 1354.

(49) Shultz, D. A.; Fico, R. M., Jr.; Lee, H.; Kampf, J. W.; Kirschbaum, K.; Pinkerton, A. A.; Boyle, P. D. *J. Am. Chem. Soc.* **2003**, *Accepted.*

(50)   Shultz, D. A.; Fico, R. M., Jr.; Boyle, P. D.; Kampf, J. W. *J. Am. Chem. Soc.* **2001**, *123*, 10403.

(51)   Shultz, D. A.; Farmer, G. T. *J. Org. Chem.* **1998**, *63*, 6254.

(52)   Shultz, D. A.; Bodnar, S. H. *Inorg. Chem.* **1999**, *38*, 591.

Chapter 6 Conformational Exchange Modulation in Trimethylenemethane-Type Biradicals: The Roles of Conformation and Spin Density.[1,2]

Introduction

As discussed in Chapter 5, large amplitude bond torsions between the spin containing group and the coupling unit can dramatically affect exchange coupling in organic biradicals.[3-11] In this Chapter, we discuss the role of the spin containing group, and the resulting spin density in the coupler, on the magnitude of the exchange coupling. The structural aspects of this series is similar to those in Chapter 5, see **Scheme 6.1**. In this series, the semiquinone ring is replaced by a *t*-butylphenyl nitroxide.

TMM-type biradicals having a 1,1-diarylethene moiety are an interesting class of molecules with which to study this behavior because the conformation and dynamics of diarylethene have been previously studied.[12] Substitution *para* to the 1,1-diphenylene with a spin containing group produces a biradical that is expected to be a ground state triplet based on the topology, **Figure 6.1**.[13,14]
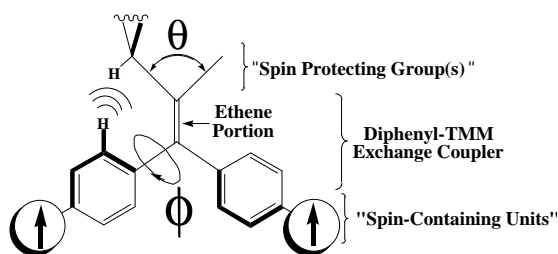
Figure 6.1. TMM-type 1,1-diarylethene.

This generalized TMM-type biradical will have a lower symmetry (C_2 or C_{2v}) than the parent trimethylenemethane, TMM (D_{3h}). The lower symmetry will decrease the energetic preference for the high-spin state.[15] This is in part due to the SOMOs no longer

being degenerate. If the spin containing units contain heteroatoms at active positions the energy gap between the SOMOs will widen according to the heteroatom electronegativities. Despite this symmetry lowering and SOMO energy difference, the triplet state of heteroatom substituted TMM-type biradicals is still predicted to be the ground state.[13,16-19]

One of the advantages of using TMM-type couplers instead of MPH-type couplers is that the parent biradical has a larger singlet-triplet gap (14.5 kcal/mol)[20] than MPH (9.2 kcal/mol)[21] In Chapter 5,we discussed the effects of bond torsions on a series of TMM type bis(semiquinones), **Scheme 6.1**.[15] Within that series of compounds we demonstrated that molecular conformation controls both ferromagnetic and antiferromagnetic exchange contributions to *J* using a simple torsion model given by **Eq. 6.1** where ϕ is the average torsion angle between semiquinone rings and the ethane coupler.

$$J = A\cos^2(\phi) + B \qquad\qquad \textbf{Eq. 6.1}$$

Generally speaking, the A term should be a function of both the coupler and the spin density in the spin containing group. The B term accounts for the antiferromagnetic coupling and for our series should be proportional to the through-space antiferromagnetic interaction. This model contains a $\cos^2\phi$ term because the overlap of 2p-π orbitals of the semiquinone groups with those of the coupler varies as the cosine-squared of the torsion angles (ϕ) between the two groups.[22] Due to the small number of data points and for comparison purposes between semiquinone, Chapter 5, and nitroxide spin groups, our primary concern was to keep **Eq. 6.1** simple.[23]

Scheme 6.1. Spin protecting groups used for the TMM-type bis(nitroxide) biradicals.
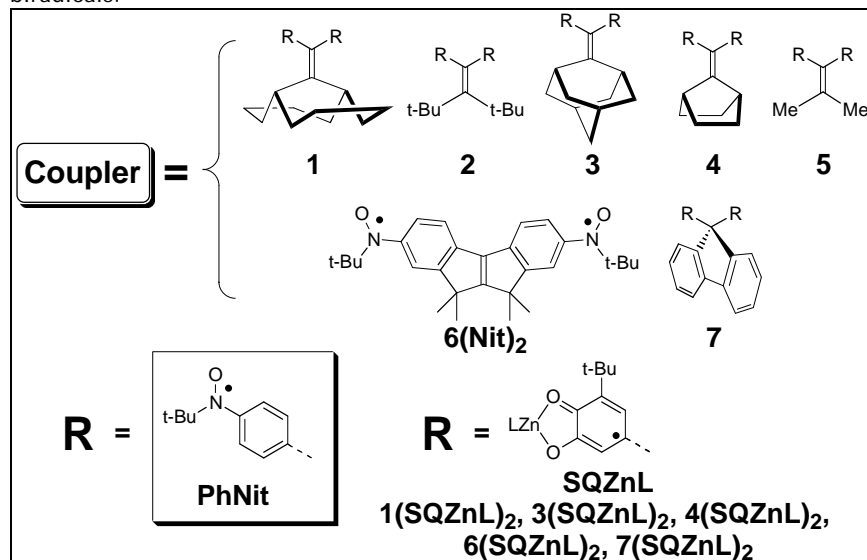
We showed that J for **1(SQZnL)₂**, **3(SQZnL)₂**, **4(SQZnL)₂**, and **6(SQZnL)₂** had a range of J-values from -30.3 cm^{-1} (antiferromagnetic) to +163.6 cm^{-1} (ferromagnetic) yielding a "fit" to **Eq. 6.1** with A = + 213 cm^{-1} and B = -44 cm^{-1}. These parameters gave net ferromagnetic coupling over a wide range of semiquinone ring torsion angles. At severe torsions, $\phi > ca.$ 60°, the net antiferromagnetic exchange is caused by a molecular conformation in which the semiquinone rings are "stacked." This stacking is equivalent to Anderson's incipient bonding,[24,25] and provides an effective antiferromagnetic pathway.

Here we present the molecular structures and magnetometry of a related series of dinitroxide biradicals, **1(PhNit)₂ — 4(PhNit)₂**, **6(Nit)₂**, and **7(PhNit)₂**, **Scheme 1**. The exchange parameters for this series also show cos$^2\phi$ dependence (ϕ = average *phenyl* ring torsion angle) despite the added C-N bond torsions of the nitroxide groups. Most

importantly, the new parameters A and B in **Eq. 1** reflect spin density differences between

the semiquinone discussed in Chapter 5, and phenyl-nitroxide radical fragments.

Results and discussion

    Molecular Structures. The syntheses and EPR spectra of **1(PhNit)$_2$** —

4(PhNit)$_2$, **6(Nit)$_2$**, and **7(PhNit)$_2$** were presented earlier.[19] Iwamura reported the

magnetic properties of **5(PhNit)$_2$**,[26,27] but in our hands this biradical was sufficiently

unstable so as to prevent formation of X-ray-quality crystals. Thermal ellipsoid plots for

1(PhNit)$_2$, — **4(PhNit)$_2$**, **6(Nit)$_2$** and **7(PhNit)$_2$** are shown in **Figure 6.2**.

1(PhNit)$_2$

2(PhNit)$_2$

3(PhNit)$_2$

4(PhNit)$_2$
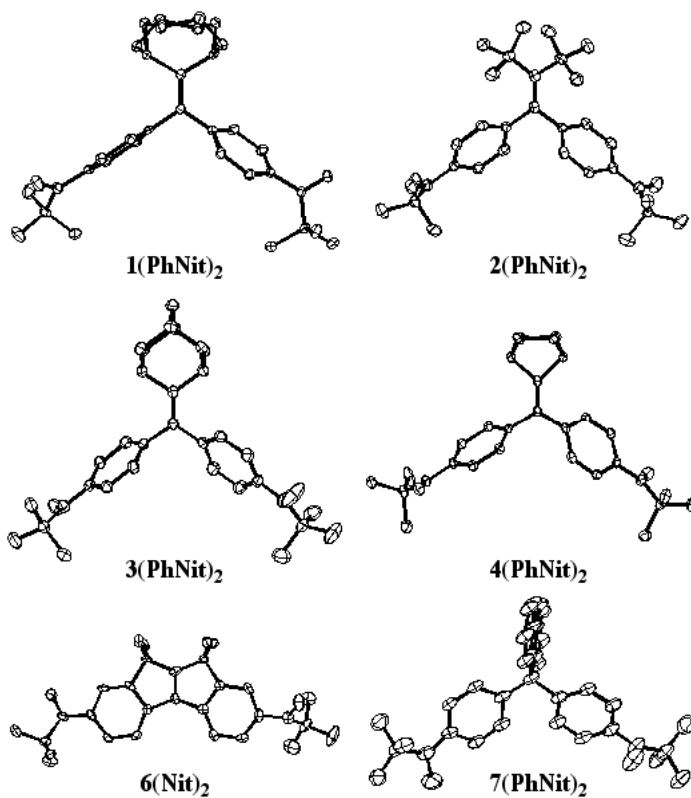
6(Nit)$_2$

7(PhNit)$_2$

Figure 6.2. Thermal ellipsoid plots for **1(PhNit)$_2$**, — **4(PhNit)$_2$**, **6(Nit)$_2$,** and **7(PhNit)$_2$**.
Hydrogens are omitted for clarity.

Important torsion angles are listed in **Table 6.1**. A complete record of bond lengths and

angles can be found in the **Appendix B**.

Table 6.1. Phenyl Ring and Nitroxide Group Torsion Angles in Dinitroxides **1(PhNit)$_2$**, — **4(PhNit)$_2$**, **6(Nit)$_2$** and **7(PhNit)$_2$**.[a]

Biradical	Phenyl Torsions[a]	Average Phenyl Torsion	Nitroxide Torsions[b]	Average Nitroxide Torsion
1(PhNit)$_2$	65.92 ± 0.05	**74.2 ± 8.2**	40.68 ± 0.1	**31.9 ± 8.7**
	82.37 ± 0.05		23.14 ± 0.1	
2(PhNit)$_2$	54.3 ± 0.1	**54.9 ± 0.6**	9.8 ± 0.2	**10.5 ± 0.7**
	55.5 ± 0.1		11.1 ± 0.2	
3(PhNit)$_2$	54.73 ± 0.08	**54.1 ± 0.6**	11.23 ± 0.07	**10.6 ± 0.7**
	53.47 ± 0.08		9.9 ± 0.1	
	@ 25K: 50.7 ± 0.08	**52.5 ± 1.8**	@ 25K: 36.8 ± 1.1	**28.5 ± 8.3**
	54.3 ± 0.08		20.2 ± 1.0	
4(PhNit)$_2$	43.19 ± 0.11	**47.0 ± 3.8**	31.4 ± 0.2	**31.4 ± 0.2**
	50.84 ± 0.11		31.3 ± 0.2	
6(PhNit)$_2$	1.9 ± 0.3	**1.9 ± 0.3**	30.1 ± 0.2	**29.3 ± 0.9**
	1.8 ± 0.3		28.4 ± 0.2	
7(PhNit)$_2$[c]	39.2 ± 0.5	**40.1 ± 0.9**	13.5 ± 0.4	**18.9 ± 5.4**
	41.0 ± 0.5		24.3 ± 0.5	

[a]Phenyl torsion angle defined as the angle between the plane of a phenyl ring and the plane containing the Ethene Coupler. [b]Nitroxide torsion angle defined as O-N-C$_{phenyl}$-C$_{phenyl}$. [c]**7(PhNit)$_2$** torsion angles defined as bond torsion between the phenyl rings through the sp^3 carbon of the fluorenyl group.

As predicted[19] and seen in Chapter 5, the phenyl ring torsions decrease in going from

1(PhNit)$_2$ to **6(Nit)$_2$**. By contrast, the nitroxide N-O bond torsions vary randomly with a

series average N-O torsion of 24.5 ± 12.8°. The phenyl ring torsions for the dinitroxides

1(PhNit)$_2$, **4(PhNit)$_2$**, and **6(Nit)$_2$** parallel the semiquinone ring torsions for the

corresponding bis(semiquinone)s **1(SQZnL)$_2$**, **4(SQZnL)$_2$**, and **6(SQZnL)$_2$**, again

demonstrating the role of the capping group in controlling the conformation of these

TMM-type biradicals. Finally, **2(PhNit)$_2$** has no bis(semiquinone) analog. This

dinitroxide is interesting because of the noteworthy torsion of the Ethene C=C, 27.5 ±

0.6° — a value quite similar to 24° for 1,1-diphenyl-2,2-di-*tert*-butylethene.[28]

Structural Phase Transition in Crystals of 3(PhNit)$_2$. During the course of our study of the magnetic properties of crystalline solids of this series of dinitroxides, we discovered that **3(PhNit)$_2$** undergoes a temperature-dependent hysteretic phase transition. This is the only dinitroxide that we have studied that exhibits this behavior. We also note that the bis(phenoxy) and bis(semiquinone) biradical adamantly capped analogs exit as multiple rotamers in frozen solution.[15,29]

The crystal structures of **3(PhNit)$_2$** and **4(PhNit)$_2$** are very similar as shown in **Figure 6.3**.[23]
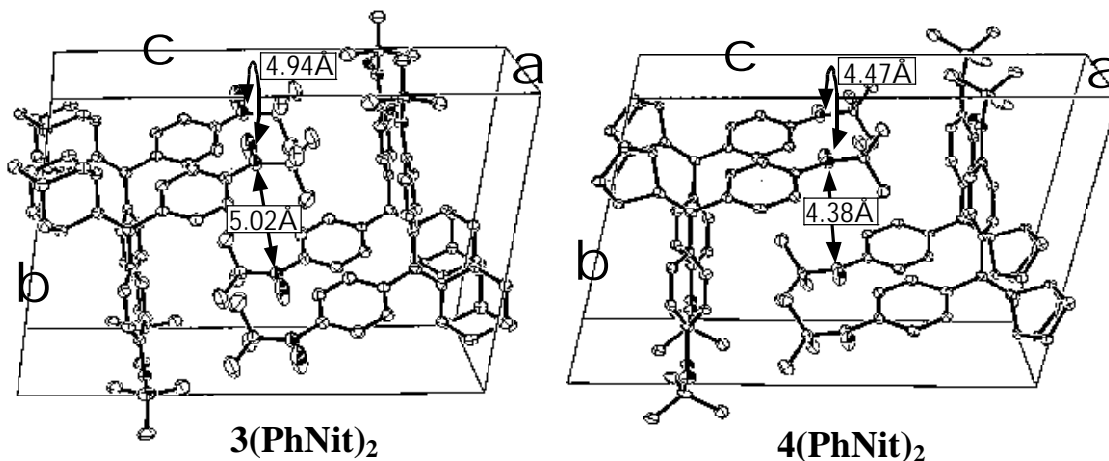
Figure 6.3. Packing diagrams for **3(PhNit)$_2$** and **4(PhNit)$_2$**.

For both of the biradicals, the unit cell contains two centrosymmetrically related dinitroxide molecules having phenyl ring torsions in accord with previous predictions[19] as given in **Table 6.2** and **Figure 6.3**.

Table 6.2. Unit Cell and Structural Parameters for $3(PhNit)_2$ and $4(PhNit)_2$.

Biradical	Unit Cell Parameters	Shortest Intermolecular Nitroxide Distances	Phenyl Torsions[a]	Nitroxide Torsions[b]
$3(PhNit)_2$	a = 6.2271 Å b = 12.170 Å c = 17.882 Å α = 99.872° β = 99.659° γ = 95.631°	5.02 Å (NN); 4.94 Å (NO); 6.23 Å (NN)	54.8°, 56.2° (55.5°)[c]	12.7°, 13.2° (12.9°)[c]
$4(PhNit)_2$	a = 6.1933 Å b = 11.4950 Å c = 17.478 Å α = 104.577° β = 99.635° γ = 94.942°	4.38 Å (NN); 4.47 Å (NO); 5.99 Å (NN)	42.8°, 53.8° (48.3°)[c]	29.0°, 28.8° (28.9°)[c]

[a]Torsion angles between planes of phenyl rings and C=C. [b]Torsions between N-O bond vectors and phenyl ring planes. [c]Average values.

For $3(PhNit)_2$ the shortest NO distance between two molecules is 4.94 Å. They are related by a unit translation along the a-axis, **Figure 6.3**. The next shortest distance is 5.02 Å between two centrosymmetrically related nitrogens in two different layers along the a-axis. For $4(PhNit)_2$ the corresponding intermolecular NN/NO distances are shorter as seen in **Table 6.2** and **Figure 6.3**.

These structural elements and molecular packing allow us to predict weak intramolecular exchange coupling (χT = $ca.$ 0.75 emu K/mol), and even weaker intermolecular coupling. The weak intramolecular coupling is consistent with moderate spin density in the phenyl rings of $tert$-butyl-phenyl nitroxides,[19,30] combined with the phenyl torsions (with respect to the C=C coupler fragment). In fact, weak intramolecular exchange was reported by Iwamura and coworkers for $5(PhNit)_2$ (J = +5.2 cm^{-1}).[27]

Regardless of the structural similarities, the overall magnetic behaviors of $3(PhNit)_2$ and $4(PhNit)_2$ are quite different as shown in **Figure 6.4**.[23] As predicted, χT per dinitroxide is $ca.$ 0.75 emu·K/mol at 300 K for both $3(PhNit)_2$ and $4(PhNit)_2$,

consistent with weakly-coupled biradicals.[31] As the temperature is lowered, χT for

4(PhNit)₂ continues to follow the trend expected for a weakly-coupled biradical, but for

3(PhNit)₂ a dramatic deviation from biradical behavior is observed. Near T = 60 K, χT

for **3(PhNit)₂** shows a precipitous decrease to 0.38 emu·K/mol. This behavior is

consistent with weak intramolecular exchange coupling until T = 60 K whereupon a

phase transition causes a strong antiferromagnetic alignment of individual nitroxide units

between two molecules. Moreover, this spin alignment must be characterized by an

antiferromagnetic exchange parameter significantly greater than the one characterizing

intramolecular exchange, $|J_{\text{intra}}|$. The most likely mechanism for this enhanced

antiferromagnetic coupling is a substantial decrease in intermolecular contacts.[23] In this

way, χT is consistent with *one spin* per molecule below 60 K.[23]
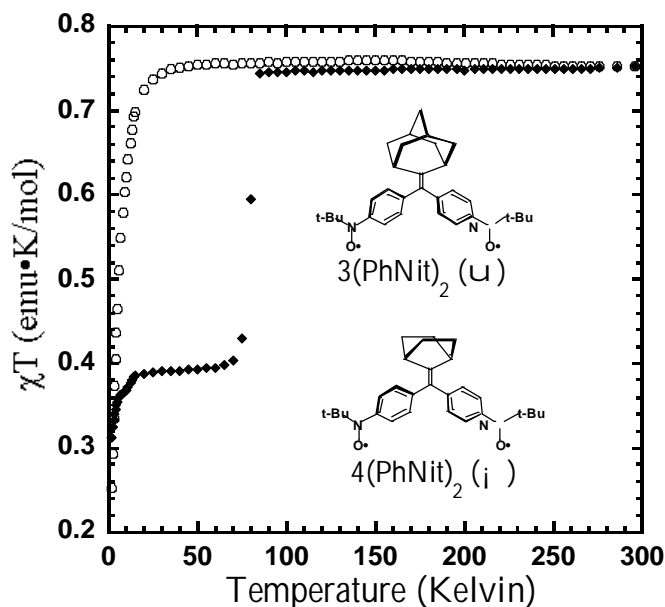
Figure 6.4. Plot of χT vs temperature for **3(PhNit)₂** (○) and **4(PhNit)₂** (◆).

Most importantly, the χT curve for **3(PhNit)$_2$** shown in **Figure 6.4** is not followed when the temperature is *increased* from 2 to 300 K, *i.e.*, hysteresis is observed.[23] An expanded view of the χT data between 50 K and 90 K is shown in **Figure 6.5**. As seen in **Figure 6.5**, the temperature at which χT decreases on lowering the temperature ($T_{1/2}\downarrow$ = 67 K) is 13 K lower than the temperature at which χT increases when increasing the temperature ($T_{1/2}\uparrow$ = 80 K). $T_{1/2}$ is the temperature at which 50% phase conversion occurs. Thus, crystals of **3(PhNit)$_2$** exhibit a 13 K-wide hysteresis loop giving rise to magnetic bistability.
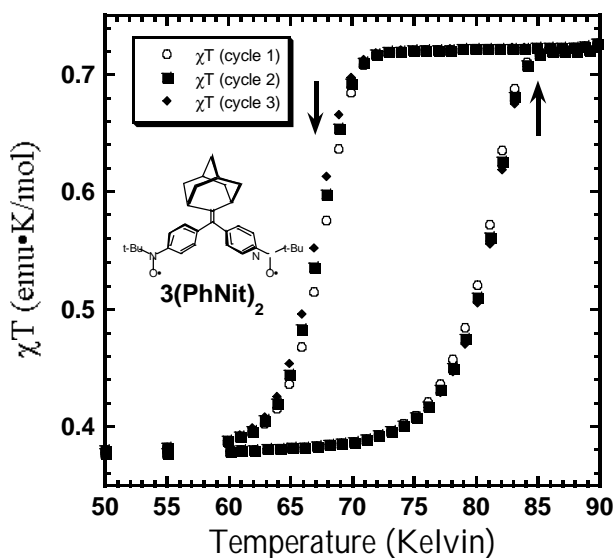
Figure 6.5. Hysteresis loop for **3(PhNit)$_2$**.

The molecular structure of **3(PhNit)$_2$** below and above the phase transition as well as pictures of the unit cell below and above the transition are shown in **Figure 6.6**. Torsion angles for both the 25 K and 158 K structures are listed in **Table 6.2**.
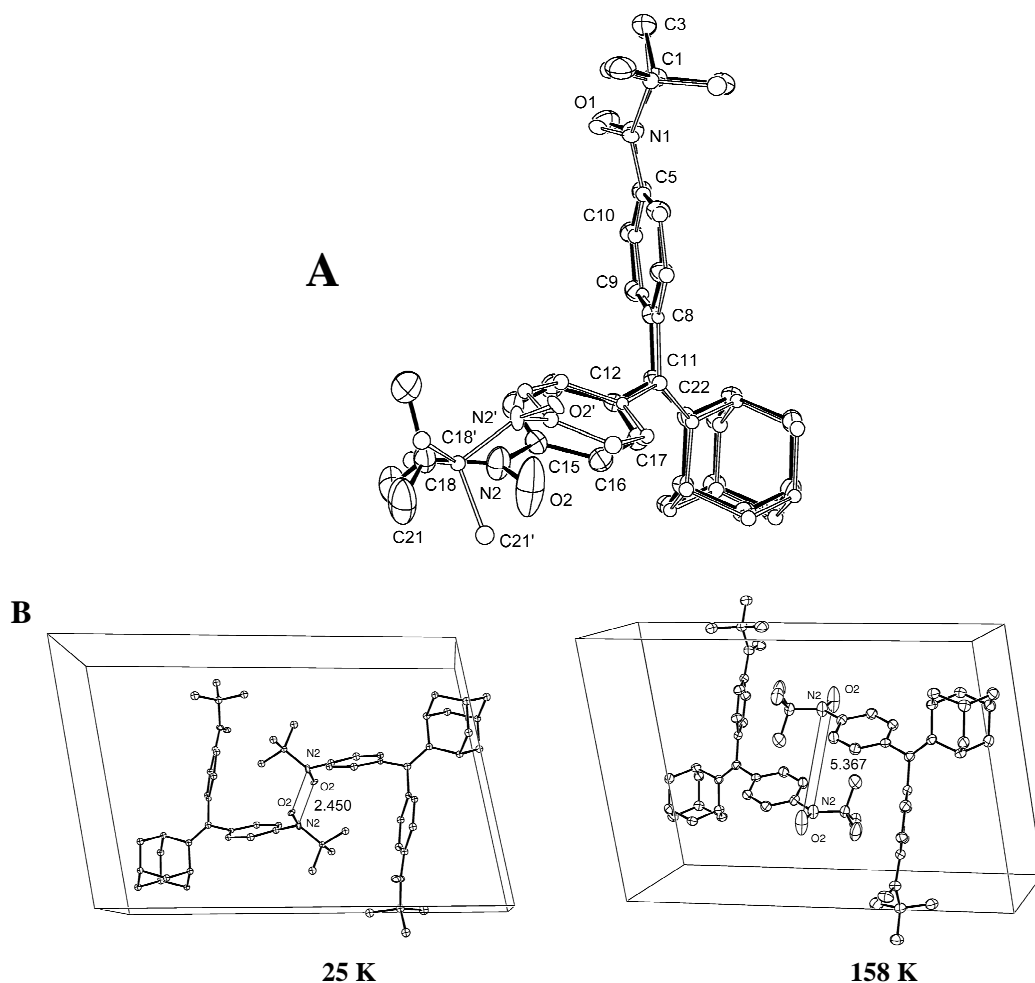
Figure 6.6. **A**: Overlay of thermal ellipsoid plots for **3(PhNit)₂** below (25 K; open ellipsoids) and above (158 K; hatched ellipsoids) the structural phase transition. **B**: Unit cell comparison. Intermolecular N•••O contacts are 2.450 Å at 25 Kelvin (left) and 5.367 Å at 158 Kelvin (right).

As seen in **Figure 6.6A**, the molecular structures of **3(PhNit)₂** at 158 K and 25 K

differ significantly. The differences in molecular structures can be explained by three

primary displacive components. The first two components are nitroxide and *tert*-butyl

torsions, and these differences are summarized in **Table 6.3**. The largest numeric change

(•Torsion = -57.9º) is the torsion of the *tert*-butyl group relative to the nitroxide group.

This brings the *tert*-butyl group from an eclipsed conformation to *gauche* relative to the

nitroxide group, and presumably lowers the steric repulsion between the methyl groups and the oxygen atom, O2. The second largest change (•Torsion = 24º) is the torsion of the nitroxide group around the N-C$_{phenyl}$ bond. At 25K, greater nitroxide torsion is observed.

Table 6.3. Structural differences for **3(PhNit)$_2$**, above and below the phase transition.

Bond Torsion	25 K (°)	158 K (°)	• Torsion (25 K – 158 K; °)
C22-C11-C12-C17	56.3	54.8	1.5
O2-N2-C15-C16	36.7	12.7	24.0
O2-N2-C18-C21	-73.1	-15.2	-57.9
C22-C11-C8-C9	55.5	56.2	-0.7
O1-N1-C5-C10	20.3	13.2	7.1
O1-N1-C1-C3	-20.7	-7.3	-13.4

The third component of displacement involves the C12 phenyl ring. The dihedral angle between the phenyl group at 25K and the same phenyl group 158K is 11.1º. Although the angular displacement seems modest, it results in large linear displacements on the periphery of the molecule. The displacement due to this "dihedral deformation" is 0.65 Å at C15, and would give even more pronounced displacements for atoms in the *tert*-butylnitroxide group. Taken together, the two torsions and the dihedral deformation result in overall atomic displacements for C18, N2 and O2 of 0.93 Å, 1.12 Å and 1.78 Å, respectively. It is the sum of these changes which brings the intermolecular nitroxide-nitroxide distance from ~5.4 Å to ~2.5 Å. In contrast, the corresponding atomic displacements for the other nitroxide group, C5, N1, O1, and C1 are 0.12 Å, 0.15 Å, 0.26 Å, 0.14 Å respectively.

Another point worth noting in **Figure 6.6B** is that the probability displacement ellipsoids of the *tert*-butylnitroxide group (N2-O2) involved in the quasi-dimerization suggests significantly higher amplitudes of internal motion at 158K than does the other

nitroxide group (N1-O1). This observation is chemically significant because it indicates that at nearly 90 K above the transition temperature the dynamic aspects of the crystal structure are already giving an indication of a possible pathway to the low temperature structure.

Solid-State Magnetic Susceptibility Measurements. Plots of the magnetic susceptibility data for all of the compounds are plotted in **Figure 6.7** (as films in poly[vinylchloride], see below) and **Figure 6.8** (as crystals). Modeling the temperature-dependent χT products of biradicals having monoradical impurity can be achieved by fitting to a field-independent van Vleck expression, **Eq. 6.2**,[31,32]

$$\chi T = (x)\frac{2Ng^2\beta^2}{k\left[3+e^{-2J/kT}\right]} + (1-x)\frac{Ng^2\beta^2}{2kT}$$ **Eq. 6.2**

where x is the mole fraction of biradical, g is the isotropic Landé constant (g = 2.0023), β is the Bohr magneton, T is temperature in Kelvin, k is Boltzmann's constant, and J is the intramolecular nitroxide-nitroxide exchange coupling parameter. When $J < 0$, χ exhibits a maximum at T_{max} = 1.285J/k.[31] Therefore in singlet ground-state biradicals, χ *vs.* T plots are preferred over χT *vs.* T plots, while the opposite is true for triplet ground-state biradicals. The singlet- and triplet-state energies were derived using the Hamiltonian, $H = -2J\hat{S}_1 \cdot \hat{S}_2$, where $\hat{S}_1$ and $\hat{S}_2$ are the spin operators for the nitroxides. The decrease (increase) in the χT (χ) data at low temperatures was accounted for with a Weiss mean-field correction, using the expression $\chi_{eff} = \chi/(1-J\chi)$, where $J = 2zJ'/(Ng^2\beta^2)$.[33] The origin of zJ' may be zero-field splitting, intermolecular interaction, saturation effects, or

some combination of all three.[34] The other terms have their usual meanings.[33] All curve

fit results are presented in **Table 6.4**.
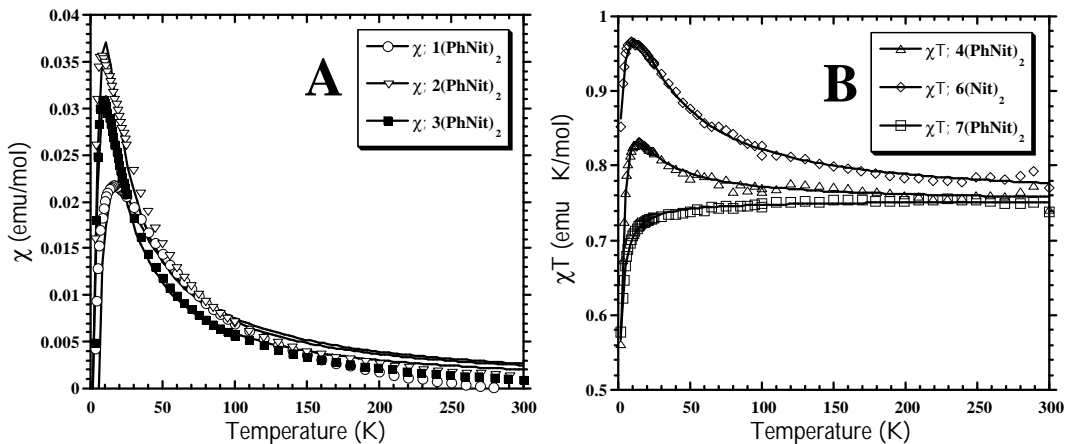
Figure 6.7. **A**: χ *vs.* T plots: **1(PhNit)₂** (○); **2(PhNit)₂** (▽); **3(PhNit)₂** (■). **B**: χT*vs.* T plots: **4(PhNit)₂** (△); **6(Nit)₂** (◇); **7(PhNit)₂** (□) as films in poly[vinylchloride] (see text for details).
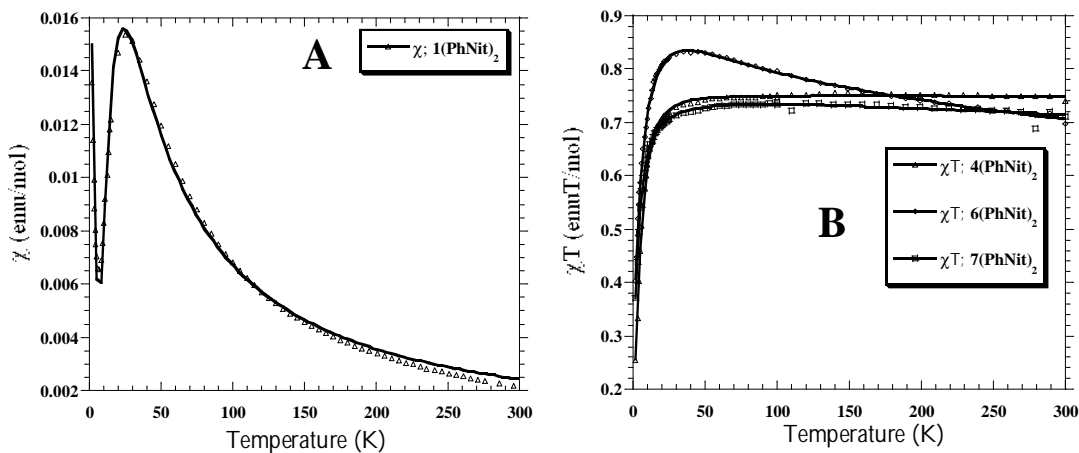
Figure 6.8. **A**: χ *vs.* T plots: **1(PhNit)₂** (△). **B**: χT*vs.* T plots: **4(PhNit)₂** (△); **6(Nit)₂** (◇); **7(PhNit)₂** (□) as crystals.

Table 6.4. Magnetic Data for Dinitroxides $1(PhNit)_2$, — $7(PhNit)_2$.[a]

Biradical	Purity[b]	Sample Form	zJ' (cm^{-1})	J (cm^{-1})	Reference
$1(PhNit)_2$	96%	Crystal	+0.25	-14.03 ± 0.12[a]	
	86%	PVC film	[e]	-11.8 ± 1.2[c]	This work
$2(PhNit)_2$	---	Crystal	---	---	
	74%	PVC film	[e]	-5.75 ± 0.31[c]	This work
$3(PhNit)_2$	---	Crystal		Hysteresis	
	79%	PVC film	[e]	-5.11 ± 0.24[c]	This work
$4(PhNit)_2$	100%	Crystal	-3.0	$+6.79 \pm 0.18$[c]	
	100%	PVC film	-0.79	$+6.07 \pm 0.15$[c]	This work
$5(PhNit)_2$	88%	Crystal	-3.82[d]	+5.24	26
	---	PVC film	[e]	---	
$6(Nit)_2$	80%	Crystal	-2.14	$+25.5 \pm 1.6$[a]	
	95%	PVC film	[e]	$+26.35 \pm 1.73$[c]	This work
$7(PhNit)_2$	55%	Crystal	-0.56	-2.61 ± 0.01[c]	
	24%	PVC film	[e]	-2.85 ± 0.13[c]	This work

[a]Magnetic susceptibility measured by SQUID magnetometry between 2 and 300 K with an applied field of 0.5 Tesla. [b]Magnetic susceptibility measured by SQUID magnetometry between 2 and 300 K with an applied field of 1 Tesla. [c]This is the reported Weiss constant, θ, converted to cm^{-1}.

The fit parameters for a crystalline sample of $4(PhNit)_2$ show that zJ' is within one order of magnitude of the exchange parameter J.[23] As such, the mean field correction is inappropriate,[33] and therefore the magnetic susceptibility for all biradicals were measured on solid solutions of the biradicals in poly[vinyl chloride] in an attempt to attenuate intermolecular exchange interactions. Measuring the temperature-dependent magnetic susceptibility in polymer films also affords us the opportunity to determine an exchange parameter for $3(PhNit)_2$ that undergoes a hysteretic phase transition in the crystal form (see above). Perusal of **Table 6.4** shows that for most of the compounds, nearly identical J-values are estimated from crystal and PVC film samples, suggesting similar molecular conformations in crystal and PVC films.

The exchange coupling for $1(PhNit)_2$ is antiferromagnetic (J • -12 cm^{-1}) and compares reasonably with the value calculated from the EPR Curie plot (-24 cm^{-1}).[19] The

net antiferromagnetic coupling is due to the molecular conformation: the large bond torsions compromise the coupler's ability to effect ferromagnetic coupling.

We were unable to obtain reasonable fits to the magnetic susceptibility data for crystals of **2(PhNit)₂** using either **Eq. 6.2** or an alternating 1-D chain model.[25,35] Therefore, the magnetic susceptibility data in a PVC film was used for subsequent analysis. We attribute the linear Curie plot we reported for a frozen 2-methyltetrahydrofuran solution of **2(PhNit)₂**[19] to an overall weaker J in frozen solution compared to both the solid and the PVC film.

As discussed above, crystals of **3(PhNit)₂** undergo a structural phase transition, so only a film was useful for estimating J. Like **1(PhNit)₂** and **2(PhNit)₂**, the exchange parameter is antiferromagnetic.

Dinitroxide **4(PhNit)₂** is the first biradical in the series to exhibit ferromagnetic intramolecular exchange coupling. J-values for the crystal and PVC film are comparable ($J \bullet +6.4 \pm 0.3$ cm^{-1}), and slightly more ferromagnetic than the value for **5(PhNit)₂** reported by Iwamura.[26,27]

The strongest net ferromagnetic coupling in the series is for **6(Nit)₂** in which the coupler is part of an essentially planar π-system. The weakest net intramolecular exchange coupling is for **7(PhNit)₂** that lacks a C=C coupler. This again shows that an ethene coupler is a more effective exchange coupler than an sp^3 carbon.[15]

The exchange coupling parameters for those dinitroxides having a simple C=C coupler (**1(PhNit)₂ — 4(PhNit)₂, 6(Nit)₂**) can be correlated to the average phenyl ring torsion angles (ϕ) via a Karplus-Conroy-type relation,[36] **Eq. 6.1**.[23] The data are displayed

in **Figure 6.9**, along with the corresponding data for bis(semiquinone)s. The J-values

used for **Figure 6.9** are those calculated for crystalline samples, except for that of

2(PhNit)$_2$ with comes from our fit of the film data. For three of the four dinitroxides, this

ensures that the J-values correspond to the same conformations measured by X-ray

crystallography, but necessarily omits data for **3(PhNit)$_2$**. For the dinitroxides, the "fit"

to **Eq. 6.1** gives $A = +44$ cm^{-1} and $B = -17$ cm^{-1}. Our omission of nitroxide torsions is

validated by the acceptable correlation of J with average phenyl torsion displayed in

Figure 6.9. Also, as seen in **Table 6.1**, the average nitroxide torsions range from 10 to

30. This portion of the cos^2 curve has relatively little slope, so changes in J for this range

of torsion angles are expected to be minimal.

Given the simplicity of our model, **Eq. 6.1**, the A- and B-terms should be

considered semiquantitative, as suggested by the thickness of the curves in **Figure 6.9**.[23]

Nevertheless, we stated previously that the A-term should be a function of both the

coupler and the spin density in the spin-containing group, and that the B-term should be

proportional to the through-space antiferromagnetic interaction. The ratio of the

bis(semiquinone) to dinitroxide A-term from **Eq. 6.1** is: 213/44 • 5. This ratio is nearly

equal to the ratio of the corresponding semiquinone ring to phenyl-nitroxide ring spin

densities: ρ_{SQ}/ρ_{PhNit} • 0.5/0.125 = 4.[30,37,38] Thus, the phenyl-*tert*-butyl-nitroxide group

presents less spin density to the coupler (which is measured by the magnitude of A) than

does the semiquinone group. Considering the overall weaker coupling of the

dinitroxides, the A-term in **Eq. 6.1** is smaller, and so is the antiferromagnetic B-term

compared to the bis(semiquinone)s. This spin-density relationship with J is suggested by

Eq. 6.3:

$$J = J_0\rho_i \cdot \rho_j \qquad\qquad \textbf{Eq. 6.3}$$

where ρ_i and ρ_j are the spin densities on the atoms that are attached to the coupler, and J_0

is the intrinsic exchange parameter for the parent biradical in which $\rho_i = \rho_j = 1$.[14,23,39,40]

Thus, the A-term in **Eq. 6.1** tracks the conformation-dependent change in spin density

"available" to the coupler to affect ferromagnetic exchange.[23]

As noted previously, TMM-type bis(semiquinone) biradicals exhibit net

ferromagnetic exchange coupling over a broad range of semiquinone ring torsions (•

~60°).[15] By comparison, TMM-type dinitroxides exhibit net ferromagnetic coupling over

a *smaller* range of phenyl ring torsions (• ~50°). This can be seen by comparing the

torsion angles for which the curves calculated by **Eq. 6.1** cross the horizontal dashed line

at $J = 0$ in **Figure 6.9**. Thus, the intrinsically weaker exchange coupling in the

dinitroxides is more sensitive to bond torsions compared to the bis(semiquinone)s. It is

important to note that the dinitroxides presented here also have a range of nitroxide

torsion angles with respect to the phenyl ring, nevertheless, our simple approach that

takes into account only phenyl ring torsion is effective at communicating the

conformational exchange modulation.
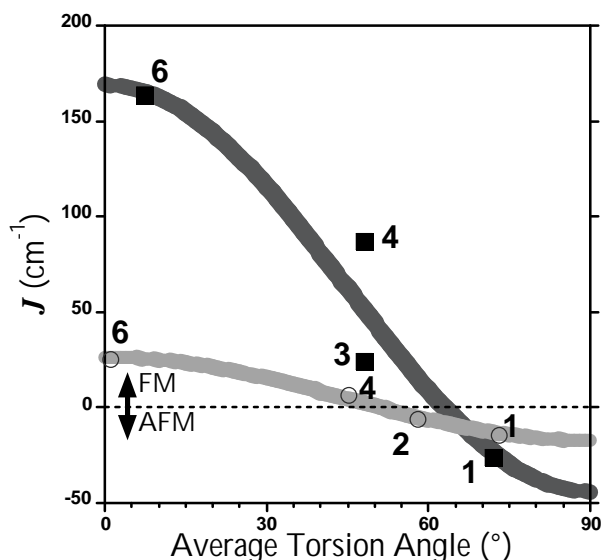
Figure 6.9. "Karplus-Conroy-type" relationship for electron spin exchange coupling in bis(semiquinone) biradicals **1(SQZnL)$_2$**, **3(SQZnL)$_2$**, **4(SQZnL)$_2$**, and **6(SQZnL)$_2$** (₵; dark curve), and dinitroxides **1(PhNit)$_2$** — **4(PhNit)$_2$**, and **6(Nit)$_2$** (¡; light curve). For clarity, data points are marked by the **coupler** (see **Scheme 1**), and not the molecule designations. Datum for **2(PhNit)$_2$** is from PVC film.

EXPERIMENTAL

Magnetometry. Magnetic susceptibilities were measured on a Quantum Design MPMS-XL7 SQUID magnetometer using an applied field of 0.5 or 1 Tesla for Curie plots. Data for crystalline samples were corrected for molecular diamagnetism using Pascal's constants, while PVC film data were corrected for both diamagnetism and for paramagnetic impurities (mononitroxides).

Microcrystalline samples were loaded into the sample space of a Delrin sample holder, and mounted directly to the sample rod. The sample holder was subtracted out using an empty Delrin sample holder as the background.

Poly[vinylchloride] (9002-86-2, PVC) was precipitated from cyclohexanone/methanol and dried over P_2O_5 under vacuum to remove any trace impurities. PVC films containing 3-5% w/w biradical were placed in a clear plastic straw and mounted directly to the sample rod. As a control, **3(PhNit)₂** was tested at various concentrations. At concentrations higher than 5% w/w, biradical **3(PhNit)₂** aggregates to form crystals that display hysteresis in the susceptibility plot. Therefore, 5% w/w was the maximum concentration used for magnetic susceptibility studies. Films were cast as solutions in methylene chloride into a glass trough and evaporated. The films were then rolled into a tight spiral for maximum sample density in the SQUID. Samples were evacuated overnight to remove any traces of solvent. A blank sample of PVC (166 mg, 6 mm length) was cast and served as the background. To obtain the best background subtraction, films were maintained at 6 mm length and ~170 mg total mass.

X-Ray Crystallography. The crystal structures of **3(PhNit)₂** (at 158 K, above the phase transition) and **4(PhNit)₂** were presented earlier.[2] Details for **1(PhNit)₂**, **2(PhNit)₂**, **6(Nit)₂**, and **7(PhNit)₂** are listed in **Appendix B**.

References
(1)   Shultz, D. A.; Fico, R. M., Jr.; Lee, H.; Kampf, J. W.; Kirschbaum, K.; Pinkerton, A. A.; Boyle, P. D. *J. Am. Chem. Soc.* **2003**, *Accepted*.
(2)   Shultz, D. A.; Fico, R. M., Jr.; Boyle, P. D.; Kampf, J. W. *J. Am. Chem. Soc.* **2001**, *123*, 10403.
(3)   Shultz, D. A. *Conformational Exchange Modulation in Trimethylenemethane (TMM)-Type Biradicals*; In *Magnetic Properties of Organic Materials*; Lahti, P., Ed.; Marcel Dekker, Inc.: New York, 1999.
(4)   Dei, A.; Gatteschi, D.; Sangregorio, C.; Sorace, L.; Vaz, M. G. F. *Inorg. Chem.* **2003**, *42*, 1701.
(5)   Fujita, J.; Tanaka, M.; Suemune, H.; Koga, N.; Matsuda, K.; Iwamura, H. *J. Am. Chem. Soc.* **1996**, *118*, 9347.

(6)   Okada, K.; Imakura, T.; Oda, M.; Murai, H.; Baumgarten, M. *J. Am. Chem. Soc.* **1996**, *118*, 3047.

(7)   Adam, W.; van Barneveld, C.; Bottle, S. E.; Engert, H.; Hanson, G. R.; Harrer, H. M.; Heim, C.; Nau, W. M.; Wang, D. *J. Am. Chem. Soc.* **1996**, *118*, 3974.

(8)   Fang, S.; Lee, M.-S.; Hrovat, D. A.; Borden, W. T. *J. Am. Chem Soc.* **1995**, *117*, 6727.

(9)   Silverman, S. K.; Dougherty, D. A. *J. Phys. Chem.* **1993**, *97*, 13273.

(10)   Kanno, F.; Inoue, K.; Koga, N.; Iwamura, H. *J. Am. Chem. Soc.* **1993**, *115*, 847.

(11)   Dvolaitzky, M.; Chiarelli, R.; Rassat, A. *Angew. Chem., Int. Ed. Engl.* **1992**, *31*, 180.

(12)   Kaftory, M.; Nugiel, D. A.; Biali, S. E.; Rappoport, Z. *J. Am. Chem. Soc.* **1989**, *111*, 8181.

(13)   Dougherty, D. A. *Acc. Chem. Res.* **1991**, *24*, 88.

(14)   Rajca, A. *Chem. Rev.* **1994**, *94*, 871.

(15)   Shultz, D. A.; Fico, R. M., Jr.; Bodnar, S. H.; Kumar, R. K.; Vostrikova, K. E.; Kampf, J. W.; Boyle, P. D. *J. Am. Chem. Soc.* **2003**, *125*, 11761.

(16)   Borden, W. T.; Davidson, E. R. *J. Am. Chem. Soc.* **1977**, *99*, 4587.

(17)   Borden, W. T., Ed. *Diradicals*; Wiley: New York, 1982.

(18)   Borden, W. T.; Iwamura, H.; Berson, J. A. *Acc. Chem. Res.* **1994**, *27*, 109.

(19)   Shultz, D. A.; Boal, A. K.; Lee, H.; Farmer, G. T. *J. Org. Chem.* **1999**, *64*, 4386.

(20)   Wenthold, P. G.; Hu, J.; Squires, R. R.; Lineberger, W. C. *J. Am. Chem. Soc.* **1996**, *118*, 475.

(21)   Wenthold, P. G.; Kim, J. B.; Lineberger, W. C. *J. Am. Chem. Soc.* **1997**, *119*, 1354.

(22)   Streitwieser, A., Jr. *Molecular Orbital Theory for Organic Chemists*; In *Molecular Orbital Theory for Organic Chemists*; Wiley & Sons: New York, 1961, p 16.

(23)   The same qualitative result is also obtained from a $\cos(f_1)\cos(f_2)$ function.

(24)   Anderson, P. W. *Phys. Rev.* **1959**, *115*, 2.

(25)   Hatfield, W. E. *Chapter 7. Properties of Condensed Compounds (Compounds with Spin Exchange)*; In *Theory and applications of molecular paramagnetism*; Mulay, L. N., Ed.; Wiley Interscience: New York, 1976, pp 381.

(26)   Matsumoto, T.; Koga, N.; Iwamura, H. *J. Am. Chem. Soc.* **1992**, *114*, 5448.

(27)   Matsumoto, T.; Ishida, T.; Koga, N.; Iwamura, H. *J. Am. Chem. Soc.* **1992**, *114*, 9952.

(28)   Mugnoli, A.; Simonetta, M. *J. Chem. Soc. Perkin Trans. 2* **1976**, 1831.

(29)   Shultz, D. A.; Boal, A. K.; Farmer, G. T. *J. Am. Chem. Soc.* **1997**, *119*, 3846.

(30)   Aurich, H. G.; Hahn, K.; Stork, K.; Weiss, W. *Tetrahedron* **1977**, *33*, 969.

(31)   Kahn, O. *Molecular Magnetism*; VCH: New York, 1993.

(32)   Bleaney, B.; Bowers, K. D. *Proc. R. Soc. London* **1952**, *A214*, 451.

(33)   O'Connor, C. J. *Prog. Inorg. Chem.* **1982**, *29*, 203.

(34)   Caneschi, A.; Dei, A.; Mussari, C. P.; Shultz, D. A.; Sorace, L.; Vostrikova, K. E. *Inorg. Chem.* **2002**, *41*, 1086.

(35)   Georges, R.; Borras-Almenar, J. J.; Coronado, E.; Curely, J.; Drillon, M. *One-dimensional Magnetism: An Overview of the Models*; In *Magnetism: Molecules to Materials, Models and Experiments*; Drillon, M., Ed.; Wiley-VCH: New York, 2001, pp 1.

(36)   Karplus, M. *J. Am. Chem. Soc.* **1963**, *85*, 2870.

(37)   Shultz, D. A.; Gwaltney, K. P.; Lee, H. *J. Org. Chem.* **1998**, *63*, 769.

(38)   Wheeler, D. E.; Rodriquez, J. H.; McCusker, J. K. *J. Phys. Chem. A* **1999**, *103*, 4101.

(39)   Jacobs, S. J.; Shultz, D. A.; Jain, R.; Novak, J.; Dougherty, D. A. *J. Am. Chem. Soc.* **1993**, *115*, 1744.

(40)   Rajca, A. *High-Spin Polyradicals*; In *Magnetic Properties of Organic Materials*; Lahti, P., Ed.; Marcel Dekker, Inc.: New York, 1999, pp 345.

Chapter 7 Conclusion[1-5]

A basic design and coupling theme to build ferromagnetically coupled organic polyradicals is to connect a spin containing fragment to a coupler that promotes ferromagnetic coupling.[6-16] In this Dissertation we have discussed three different spin containing groups: verdazyl,[17] semiquinone[18-20] and nitroxide.[21] We have probed the effects of various spacer groups in a biradical series where the biradicals are attached through a nodal position to the coupling units.[2] We also designed two different series of TMM-type biradicals to study both conformational effects and spin distribution effects on TMM-type couplers.[1,5]

A series of bis(verdazyl)s were studied with varying spacer groups. The bis(verdazyl)s studied were connected to various couplers through the nodal positions on the verdazyl. Although previous studies had indicated that bis(verdazyl)s linked either *para* or *meta* through benzene were ground state triplets,[6,13,16] we suspect that in fact the singlet/triplet states were either degenerate or the spacing was to small to be observed via EPR.[22] We found that adding any spacer between the bis(verdazyl)s decreased the amount of coupling as seen be EPR and by electrochemistry. UV-Vis spectroscopy did show extended conjugation in the HOMO, suggesting that in the HOMO there is spin density on the atoms connecting the verdazyl spin unit to the coupler.[2] Due to the verdazyls ability to bind to metal atoms, and the observed extended conjugation in the spaced biradicals, these biradicals might prove to be good candidates for making photoactive spin systems.[17]

Two series of TMM-type biradicals were studied.[1,5] Both series shared a common coupling unit, as well as the same spin protecting groups. The spin protecting groups sterically protected the spins in the TMM-coupler. These protecting groups also served as a mechanism for controlling the torsion angles between the spin protecting group and the TMM-coupler.

The spin containing group for the first series of compounds was semiquinone anion radical. Within this series we observed a range in average torsion angles from 7.3° to 71.1°, based on the spin protecting group, **Table 7.1**. The exchange coupling ranged from –14.03 cm^{-1} to +26.35 cm^{-1}, antiferromagnetic coupling to ferromagnetic coupling respectively.[1,5]

The second spin containing group was t-butyl nitroxide. Within this series we observed a range in torsion angles of 1.9° to 74.2°. The range in J was –14.03 to 25.5, **Table 7.1**. This range is smaller than the bis(semiquinone)s due to less spin density of the nitroxide delocalizing into the coupling group but also ranges from antiferromangetic coupling to ferromagnetic coupling between the radical containing groups.[5]

Table 7.1. Average spin protecting group torsions and exchange coupling parameters for the TMM-type bis(semiquinone)s and TMM-type bis(nitroxide)s.

Capping group	Biradical[a]	Ave. SQ Torsion°	J (cm^{-1})	Biradical[b]	Ave. Nit. Torsion°	J (cm^{-1}) crystal	J (cm^{-1}) PVC
441 t-bu	**2(SQZnL)₂**	71.1±3.5	-30.3±0.8	**1(PhNit)₂**	74.2±8.2	-14.03±0.12	-11.8±1.2
				2(PhNit)₂	54.9±0.6	---	-5.75±0.31
Ada	**3(SQZnL)₂**	48.23±0.4	+24.4±0.6	**3(PhNit)₂**	54.1±0.6	Hysteresis	---
				@25 K	52.5±1.8		5.11±0.24
Nor	**4(SQZnL)₂**	48.4±0.29	+87.0±3.0	**4(PhNit)₂**	47.0±3.8	+6.79±0.18	+6.07±0.15
Flat	**6(SQZnL)₂**	7.3±2.4	+163.6±1.6	**6(Nit)₂**	1.9±0.3	+25.5±1.6	+26.4±1.7
flu	**7(SQZnL)₂**	47.4±2.5	+0.99±0.06	**7(PhNit)₂**	40.1±0.9	-2.61±0.01	-2.85±0.13

[a]Biradical labels from Chapter 5.[1] [b]Biradical labels from Chapter 6.[5]

In both series the adamantyl capped biradical displayed different properties than the other capping groups. For **3(SQZnL)$_2$**, the biradical displayed multiple rotamers in frozen *m*-THF.[1] **3(PhNit)$_2$** on the other hand, underwent a temperature dependent hysterisis.[4]

Both the bis(semiquinone)s and the Bis(nitroxide)s were fit to a Karplus-Conroy-type relationship based on **Eq. 7.1**.[23]

$$J = A\cos^2(f_{ave}) + B \qquad\qquad \textbf{Eq. 7.1}$$

For the bis(semiquinone) series A = 213 cm^{-1} and B = -44 cm^{-1}.[1] For the bis(nitroxide) series A = 44 cm^{-1} and B = -17 cm^{-1}.[5] Since the A-term is should be a function of both the coupler and the spin density in the spin containing group the ratio of A$_{semiquinone}$/A$_{nitroxide}$ should be proportional to the spin density in each of the rings:

$$\frac{A_{semiquinone}}{A_{nitroxide}} = \frac{213}{44} \approx 5$$

$$\frac{r_{SQ}}{r_{PhNit}} \approx \frac{0.5}{0.125} = 4$$

All of the spin containing groups studied can bind to metal centers. This opens up the possibility of using these spin groups to make extended spin systems and polymers.

References
(1)   Shultz, D. A.; Fico, R. M., Jr.; Bodnar, S. H.; Kumar, R. K.; Vostrikova, K. E.; Kampf, J. W.; Boyle, P. D. *J. Am. Chem. Soc.* **2003**, *125*, 11761.
(2)   Fico, R. M., Jr.; Hay, M. F.; Reese, S.; Hammond, S.; Lambert, E.; Fox, M. A. *J. Org. Chem.* **1999**, *64*, 9386.
(3)   Shultz, D. A.; Lee, H.; Fico, R. M., Jr. *Tetrahedron* **1999**, *55*, 12079.
(4)   Shultz, D. A.; Fico, R. M., Jr.; Boyle, P. D.; Kampf, J. W. *J. Am. Chem. Soc.* **2001**, *123*, 10403.
(5)   Shultz, D. A.; Fico, R. M., Jr.; Lee, H.; Kampf, J. W.; Kirschbaum, K.; Pinkerton, A. A.; Boyle, P. D. *J. Am. Chem. Soc.* **2003**, *Accepted.*

(6)   Borden, W. T.; Iwamura, H.; Berson, J. A. *Acc. Chem. Res.* **1994**, *27*, 109.
(7)   Bush, L. C.; Heath, R. B.; Feng, X. W.; Wang, P. A.; Maksimovic, L.; Song, A. I.; Chung, W.-S.; Berinstain, A. B.; Scaiano, J. C.; Berson, J. A. *J. Am. Chem. Soc.* **1997**, *119*, 1406.
(8)   Caneschi, A.; Gatteschi, D.; Sessoli, R.; Rey, P. *Acc. Chem. Res.* **1989**, *22*, 392.
(9)   Carlin, R. L. *Magnetochemistry*; Springer-Verlag: New York, 1986.
(10)   Dougherty, D. A. *Acc. Chem. Res.* **1991**, *24*, 88.
(11)   Gatteschi, D., Ed. *Molecular Magnetic Materials*; Kluwer Academic Publishers: Amsterdam, 1991.
(12)   Gatteschi, D.; Sessoli, R. *J. Magn. Magn. Mat.* **1992**, *104*, 2092.
(13)   Iwamura, H.; Koga, N. *Acc. Chem. Res.* **1993**, *26*, 346.
(14)   Kahn, O. *Molecular Magnetism*; VCH: New York, 1993.
(15)   Lahti, P. M., Ed. *Magnetic Properties of Organic Materials*; Marcel Dekker: New York, 1999.
(16)   Rajca, A. *Chem. Rev.* **1994**, *94*, 871.
(17)   Hicks, R. G. *Aust. J. Chem.* **2001**, *54*, 597.
(18)   Pierpont, C. G.; Buchanan, R. M. *Coord. Chem. Rev.* **1981**, *38*, 45.
(19)   Pierpont, C. G.; Lange, C. W. *Prog. Inorg. Chem.* **1994**, *41*, 331.
(20)   Pierpont, C. G.; Attia, A. S. *Coll. Czech. Chem. Comm.* **2001**, *66*, 33.
(21)   Amabilino, D. B.; Veciana, J. *Nitroxide-based Organic Magnets*; In *Magnetism: Molecules to Materials II: Molecule-Based Materials*; Miller, J. S., Drillon, M., Eds.; Wiley-VCH: New York, 2001, pp 1.
(22)   Berson, J. A., Ed. *The Chemistry of the Quinonoid Compounds, Vol. II*; John Wiley & Sons: New York, 1988.
(23)   Karplus, M. *J. Am. Chem. Soc.* **1963**, *85*, 2870.

Appendix A Crystallographic Data for Chapter 5

Table A.1. Dioxolene bond lengths for **2(CatH₂)₂** − **4(CatH₂)₂**, **6(CatH₂)₂** and **7(CatH₂)₂**.

Biradical	*Bond*	Length (Å)	Bond	Length (Å)
2(SQZnL)₂	C1-O1	1.288(4)	C12-O4	1.286(4)
[semiquinone rings]	C1-C6	1.488(5)	C12-C11	1.469(5)
	C6-O2	1.273(4)	C11-O3	1.271(4)
	C6-C5	1.441(5)	C11-C16	1.446(5)
	C5-C4	1.367(5)	C16-C15	1.371(5)
	C4-C3	1.446(5)	C15-C14	1.440(5)
	C3-C2	1.372(5)	C14-C13	1.356(5)
	C2-C1	1.400(5)	C13-C12	1.414(5)
[SQ-ethene]	C3-C21	1.496(5)	C14-C21	1.503(5)
C=C	C21-C22	1.356(5)		
3(SQZnL)₂	C50-O3	1.290(7)	C1-O1	1.293(6)
[semiquinone rings]	C50-C55	1.474(8)	C1-C6	1.462(8)
	C55-O4	1.283(6)	C6-O2	1.278(7)
	C55-C54	1.441(8)	C6-C5	1.455(8)
	C54-C53	1.367(8)	C5-C4	1.374(8)
	C53-C52	1.437(8)	C4-C3	1.439(8)
	C52-C51	1.386(8)	C3-C2	1.376(8)
	C51-C50	1.397(8)	C2-C1	1.400(8)
[SQ-ethene]	C52-C99	1.497(8)	C3-C99	1.474(8)
C=C	C99-C100	1.355(8)		
4(SQZnL)₂	C1-O1	1.261(9)		
[semiquinone rings]	C1-C2	1.416(11)		
	C1-C6	1.461(12)		
	C2-C3	1.351(12)		
	C3-C4	1.409(13)		
	C4-C5	1.393(13)		
	C5-C6	1.466(13)		
	C6-O2	1.281(10)		
[SQ-ethene]	C3-C11	1.500(13)		
C=C	C11-C12	1.343(19)		
6(SQZnL)₂	O1-C1	1.282(9)	O3-C11	1.294(11)
[semiquinone rings]	O2-C2	1.323(10)	O4-C12	1.324(11)
	C1-C6	1.430(12)	C11-C12	1.441(15)
	C1-C2	1.469(12)	C11-C16	1.481(14)
	C2-C3	1.375(12)	C12-C13	1.384(13)
	C3-C4	1.422(13)	C13-C14	1.389(12)
	C4-C5	1.412(12)	C14-C15	1.416(14)
	C5-C6	1.361(12)	C15-C16	1.360(13)
[SQ-ethene]	C4-C21	1.421(12)	C14-C21	1.476(13)
C=C	C21-C22	1.362(13)		
7(SQZnL)₂	C10-O3	1.285(9)	C1-O1	1.304(10)
[semiquinone rings]	C10-C11	1.485(12)	C1-C2	1.437(12)
	C11-O4	1.277(10)	C2-O2	1.314(10)
	C11-C12	1.429(11)	C2-C3	1.442(12)
	C12-C13	1.371(11)	C3-C4	1.378(12)
	C13-C8	1.428(11)	C4-C5	1.420(13)
	C8-C9	1.368(12)	C5-C6	1.376(11)
	C9-C10	1.406(11)	C6-C1	1.420(12)

[SQ-fluorene]	C8-C7	1.521(11)	C5-C7	1.555(11)
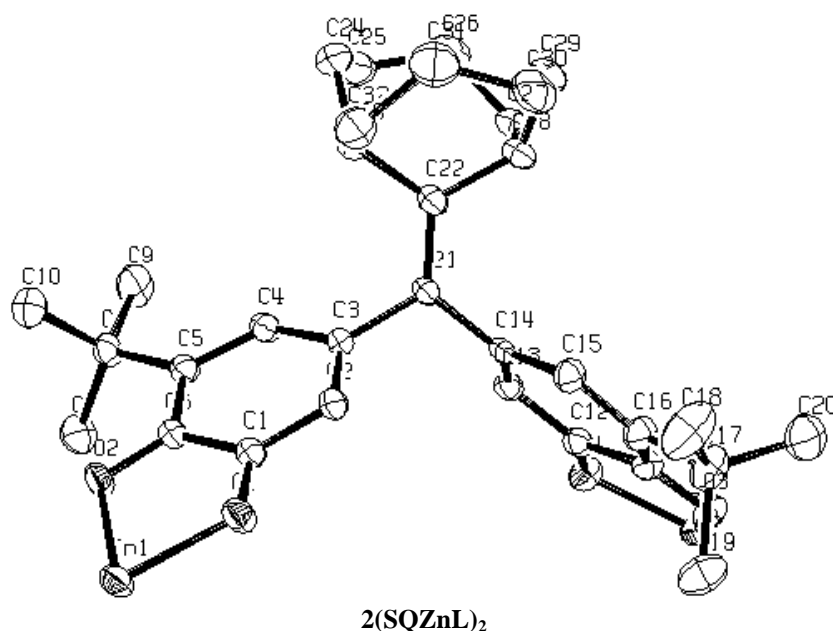
2(SQZnL)₂

Table A.2. Crystal data and structure refinement for rf441d (**2(SQZnL)₂**)

Identification code	rf441d
Empirical formula	C114.50 H142 B2 Cl9 N12 O4 Zn2
Formula weight	2221.81
Temperature	150(2) K
Wavelength	0.71073 A
Crystal system, space group	Triclinic, P-1
Unit cell dimensions	a = 15.8309(15) A alpha = 100.534(3) deg.
	b = 18.2583(18) A beta = 96.673(3) deg.
	c = 24.387(2) A gamma = 113.552(3) deg.
Volume	6211.1(10) A^3
Z, Calculated density	2, 1.188 Mg/m^3
Absorption coefficient	0.631 mm^-1
F(000)	2336
Crystal size	0.62 x 0.60 x 0.58 mm
Theta range for data collection	2.96 to 28.44 deg.
Limiting indices	21<=h<=20, -24<=k<=23, -32<=l<=32
Reflections collected / unique	73436 / 30348 [R(int) = 0.0719]
Completeness to theta =	28.44 96.9 %
Absorption correction	Semi-empirical from equivalents
Max. and min. transmission	0.7109 and 0.6956
Refinement method	Full-matrix least-squares on F^2
Data / restraints / parameters	30348 / 0 / 1305
Goodness-of-fit on F^2	1.599
Final R indices [I>2sigma(I)]	R1 = 0.0821, wR2 = 0.2337
R indices (all data)	R1 = 0.1136, wR2 = 0.2446
Extinction coefficient	0.0008(4)
Largest diff. peak and hole	0.928 and -0.959 e.A^-3

3(SQZnL)₂

Table A.3. Crystal data and structure refinement for kva (**3(SQZnL)₂**).

Identification code	kva
Empirical formula	C111 H133 B2 Cl4 N12 O4 Zn2
Formula weight	1993.45
Temperature	158(2) K
Wavelength	0.71073 A
Crystal system, space group	Triclinic, P-1
Unit cell dimensions	a = 13.3366(13) Aalpha = 106.665(2) deg.
	b = 18.8734(18) A beta = 96.630(2) deg.
	c = 27.555(3) Agamma = 104.208(2) deg.
Volume	6311.0(11) A^3
Z, Calculated density	2, 1.049 Mg/m^3
Absorption coefficient	0.512 mm^-1
F(000)	2106
Crystal size	0.32 x 0.34 x 0.34 mm
Theta range for data collection	0.79 to 24.71 deg.
Limiting indices	-15<=h<=15, -22<=k<=21, -32<=l<=32
Reflections collected / unique	81861 / 21510 [R(int) = 0.0442]
Completeness to theta =	24.71 99.9 %
Absorption correction	multi-scan
Refinement method	Full-matrix least-squares on F^2
Data / restraints / parameters	21510 / 0 / 1286
Goodness-of-fit on F^2	2.159
Final R indices [I>2sigma(I)]	R1 = 0.0941, wR2 = 0.2774
R indices (all data)	R1 = 0.1170, wR2 = 0.2850
Extinction coefficient	0.0019(4)

Largest diff. peak and hole   1.692 and -0.545 e.A^-3
The likely contribution of 3.5 CH2Cl2 lattice solvates per cell as suggested by
PLATON have not been included in the above derived quantities. The residiual
electron density is associated with one of the partial occupancy lattice solvates
located on the difference map. Further details are provided in the .cif file.

4(SQZnL)$_2$

Table A.4. Crystal data and structure refinement for rfnor (**4(SQZnL)$_2$**).

Identification code	rfnor
Empirical formula	C108 H128 B2 Cl4 N12 O4 Zn2
Formula weight	1952.38
Temperature	118(2) K
Wavelength	0.71073 A
Crystal system, space group	Monoclinic, C2/c
Unit cell dimensions	a = 32.376(2) A alpha = 90 deg.
	b = 18.9790(12) A beta = 116.337(3) deg.
	c = 18.4471(12) A gamma = 90 deg.
Volume	10158.4(11) A^3
Z, Calculated density	4, 1.277 Mg/m^3
Absorption coefficient	0.635 mm^-1
F(000)	4120
Crystal size	0.24 x 0.20 x 0.18 mm
Theta range for data collection	2.80 to 23.30 deg.
Limiting indices	-35<=h<=32, -21<=k<=21, -20<=l<=20
Reflections collected / unique	33091 / 7306 [R(int) = 0.0636]
Completeness to theta =	23.30 99.6 %
Absorption correction	Semi-empirical from equivalents
Max. and min. transmission	0.8942 and 0.8625

Refinement method   Full-matrix least-squares on F^2
Data / restraints / parameters 7306 / 0 / 608
Goodness-of-fit on F^2   1.025
Final R indices [I>2sigma(I)]   R1 = 0.0903, wR2 = 0.2638
R indices (all data)   R1 = 0.1366, wR2 = 0.3128
Largest diff. peak and hole   0.787 and -0.768 e.A^-3

6(SQZnL)₂

Table A.5. Crystal data and structure refinement for flat (**6(SQZnL)₂**).

Identification code	flat
Empirical formula	C113.50 H141 B2 Cl N12 O4 Zn2
Formula weight	1925.19
Temperature	123(2) K
Wavelength	0.71073 A
Crystal system, space group	Triclinic, P-1
Unit cell dimensions	a = 18.2397(13) A alpha = 81.610(4) deg.
	b = 18.3714(14) A beta = 67.429(3) deg.
	c = 18.3630(13) A gamma = 70.397(3) deg.
Volume	5351.6(7) A^3
Z, Calculated density	2, 1.195 Mg/m^3
Absorption coefficient	0.530 mm^-1
F(000)	2050
Crystal size	0.36 x 0.22 x 0.10 mm
Theta range for data collection	2.70 to 22.01 deg.
Limiting indices	-17<=h<=19, -18<=k<=19, -19<=l<=19
Reflections collected / unique	36621 / 13069 [R(int) = 0.0812]
Completeness to theta =	22.01 99.4 %
Absorption correction	Semi-empirical from equivalents
Max. and min. transmission	0.9489 and 0.8322
Refinement method	Full-matrix least-squares on F^2
Data / restraints / parameters	13069 / 91 / 1246

Goodness-of-fit on F^2   1.051
Final R indices [I>2sigma(I)]   R1 = 0.0814, wR2 = 0.2151
R indices (all data)   R1 = 0.1488, wR2 = 0.2440
Largest diff. peak and hole   0.708 and -0.666 e.A^-3

7(SQZnL)2

Table A.6. Crystal data and structure refinement for X98050 (**7(SQZnL)2**)

Identification code	X98050
Empirical formula	C113.37H126.74B2CI4.74N12O4Zn2
FW	2041.92
Temperature	-125°C
lambda	0.71073Å
Space Group	Monoclinic,P21/c
Cell Dimensions	a=19.2443(16)
	b=25.525(2)
	c=24.118(3)
	β =108.666(10)°
Volume	11223.9(19)Å3
Z, Dcalc	4,1.208Mg•m-3
F(000)	4301.50
Crystal dimensions	34X0.20X0.18mm
Mu	59mm-1
2Theta(max)	49.9
Hmin,max	-22, 21
Kmin,max	0, 30
Lmin,max	0, 28
No. of reflections measured	19865

138

No. of unique reflections	19583
No. of reflections1.0sigma(Inet)	10214
Merging R-value on intensities	0.141
Weights based on counting-statistics were used.	
The weight modifier K in Kfo2 is	0.001000
The residuals are as follows:	
For significant reflections,	
RF	0.091
Rw	0.090
GoF	1.55
For all reflections	
RF	0.092
Rw	0.091

The last least squares cycle was calculated with 268 atoms, 1261 parameters and10186 out of19583 reflections.

Cell dimensions were obtained from 24 reflections with 2Theta angle in the range 24.00 - 34.00°

The intensity data were collected on a Nonius diffractometer, The h,k,l ranges used during structure solution and refinement

No correction was made for absorption

CRYSTALLOGRAPHIC INFORMATION

2(SQZnL)$_2$. Green plates of **rf441d** were crystallized from a dichloromethane/methanol solution at 25 deg. C. A crystal of dimensions 0.62 x 0.60 x 0.58 mm was mounted on a standard Bruker SMART CCD-based X-ray diffractometer equipped with a LT-2 low temperature device and normal focus Mo-target X-ray tube (λ = 0.71073 A) operated at 2000 W power (50 kV, 40 mA). The X-ray intensities were measured at 150(2) K; the detector was placed at a distance 4.954 cm from the crystal. A total of 2821 frames were collected with a scan width of 0.3° in ω and phi with an exposure time of 45 s/frame. The frames were integrated with the Bruker SAINT software package with a narrow frame algorithm. The integration of the data yielded a total of 73436 reflections to a maximum 2θ value of 56.94° of which 30250 were independent and 19922 were greater than 2σ(I). The final cell constants (Table 1) were based on the xyz centroids of 6810 reflections above 10σ(I). Analysis of the data showed negligible decay during data collection; the data were processed with SADABS and corrected for absorption. The structure was solved and refined with the Bruker SHELXTL (version 5.10) software package, using the space group P1bar with Z = 2 for the formula $C_{110}H_{132}N_{12}B_2O_4Zn_2 \cdot (CH_2Cl_2)_{4.5}$.   All non-hydrogen atoms were refined anisotropically with the hydrogen atoms placed in idealized positions. Full matrix least-squares refinement based on F^2 converged at R1 = 0.0821 and wR2 = 0.2337 [based on I > 2sigma(I)], R1 = 0.1136 and wR2 = 0.2446 for all data. The molecule lies on a two-fold rotation site in the crystal lattice. Additional details are presented in Table 1 and are given as Supporting information as a CIF file.

Sheldrick, G.M. SHELXTL, v. 5.10; Bruker Analytical X-ray, Madison, WI, 1997.

139

Sheldrick, G.M. SADABS. Program for Empirical Absorption Correction of Area Detector Data,

University of Gottingen: Gottingen, Germany, 1996.
Saint Plus, v. 6.02, Bruker Analytical X-ray, Madison, WI, 1999.

Table 1. Crystal data and structure refinement for rf441d (**2(SQZnL)$_2$**)

Identification code	rf441d
Empirical formula	C114.50 H142 B2 Cl9 N12 O4 Zn2
Formula weight	2221.81
Temperature	150(2) K
Wavelength	0.71073 A
Crystal system, space group	Triclinic, P-1
Unit cell dimensions	a = 15.8309(15) A alpha = 100.534(3) deg.
	b = 18.2583(18) A beta = 96.673(3) deg.
	c = 24.387(2) A gamma = 113.552(3) deg.
Volume	6211.1(10) A^3
Z, Calculated density	2, 1.188 Mg/m^3
Absorption coefficient	0.631 mm^-1
F(000)	2336
Crystal size	0.62 x 0.60 x 0.58 mm
Theta range for data collection	2.96 to 28.44 deg.
Limiting indices	-21<=h<=20, -24<=k<=23, -32<=l<=32
Reflections collected / unique	73436 / 30348 [R(int) = 0.0719]
Completeness to theta =	28.44 96.9 %
Absorption correction	Semi-empirical from equivalents
Max. and min. transmission	0.7109 and 0.6956
Refinement method	Full-matrix least-squares on F^2
Data / restraints / parameters	30348 / 0 / 1305
Goodness-of-fit on F^2	1.599
Final R indices [I>2sigma(I)]	R1 = 0.0821, wR2 = 0.2337
R indices (all data)	R1 = 0.1136, wR2 = 0.2446
Extinction coefficient	0.0008(4)
Largest diff. peak and hole	0.928 and -0.959 e.A^-3

Table 2. Atomic coordinates (x 10^4) and equivalent isotropic displacement parameters (A^2 x 10^3) for rf441d.
U(eq) is defined as one third of the trace of the orthogonalized Uij tensor.

_____

	x	y	z	U(eq)
Zn(1)	5849(1)	2240(1)	2604(1)	24(1)
Zn(2)	-544(1)	-3022(1)	1030(1)	23(1)
O(1)	4501(2)	1873(2)	2623(1)	27(1)
O(2)	5732(2)	1484(2)	3183(1)	26(1)
O(3)	-497(2)	-1829(2)	1190(1)	28(1)
O(4)	496(2)	-2448(2)	1715(1)	26(1)
C(1)	4188(3)	1341(2)	2918(1)	22(1)
C(2)	3239(3)	970(2)	2953(2)	23(1)
C(3)	2942(2)	399(2)	3267(1)	21(1)
C(4)	3612(3)	171(2)	3559(2)	23(1)
C(5)	4553(3)	516(2)	3556(1)	22(1)
C(6)	4880(2)	1122(2)	3231(1)	21(1)

C(7)	5261(3)	296(2)	3888(2)	25(1)
C(8)	5785(3)	-19(3)	3481(2)	35(1)
C(9)	4775(3)	-377(3)	4187(2)	39(1)
C(10)	5964(3)	1070(3)	4352(2)	37(1)
C(11)	65(3)	-1369(2)	1658(1)	23(1)
C(12)	607(3)	-1720(2)	1960(2)	23(1)
C(13)	1203(3)	-1259(2)	2499(1)	23(1)
C(14)	1281(2)	-499(2)	2744(1)	22(1)
C(15)	774(3)	-147(2)	2436(2)	25(1)
C(16)	201(3)	-536(2)	1905(2)	26(1)
C(17)	-263(3)	-124(3)	1560(2)	35(1)
C(18)	9(4)	769(3)	1871(2)	54(1)
C(19)	88(4)	-118(3)	996(2)	44(1)
C(20)	-1326(4)	-589(3)	1448(2)	45(1)
C(21)	1929(2)	7(2)	3309(1)	20(1)
C(22)	1637(3)	129(2)	3805(2)	24(1)
C(23)	2337(3)	733(3)	4342(2)	30(1)
C(24)	2238(3)	421(3)	4887(2)	37(1)
C(25)	1929(3)	-499(3)	4801(2)	44(1)
C(26)	885(3)	-1032(3)	4619(2)	40(1)
C(27)	426(3))	-1117(3	4007(2)	34(1)
C(28)	609(3)	-309(3)	3821(2)	29(1)
C(29)	221(3)	217(3)	4176(2)	35(1)
C(30)	562(3)	1109(3)	4116(2)	43(1)
C(31)	1501(4)	1704(3)	4531(2)	47(1)
C(32)	2374(3)	1595(3)	4408(2)	40(1)
C(33)	8496(4)	2266(4)	1400(2)	57(1)
C(34)	7627(3)	1828(3)	1607(2)	40(1)
C(35)	7102(3)	1001(3)	1541(2)	45(1)
C(36)	6357(3)	929(3)	1818(2)	31(1)
C(37)	5598(3)	161(3)	1870(2)	32(1)
C(38)	4751(3)	130(3)	1983(2)	34(1)
C(39)	4058(3)	-593(3)	2052(2)	43(1)
C(40)	4159(4)	-1322(3)	1984(2)	46(1)
C(41)	4994(4)	-1294(3)	1846(2)	51(1)
C(42)	5714(3)	-568(3)	1800(2)	43(1)
C(43)	3406(4)	-2107(3)	2055(3)	67(2)
C(44)	3662(10)	-2384(7)	2517(4)	245(11)
C(45)	2887(6)	-2707(5)	1540(3)	105(3)
C(46)	9514(3)	4345(3)	2939(2)	44(1)
C(47)	8613(3)	3952(2)	3144(2)	34(1)
C(48)	8460(3)	4016(3)	3697(2)	37(1)
C(49)	7500(3)	3519(2)	3641(2)	29(1)
C(50)	6938(3)	3387(2)	4086(2)	31(1)
C(51)	7355(3)	3470(3)	4642(2)	41(1)
C(52)	6833(4)	3379(3)	5063(2)	48(1)
C(53)	5884(4)	3199(3)	4952(2)	39(1)
C(54)	5459(3)	3098(3)	4398(2)	40(1)
C(55)	5972(3)	3195(3)	3968(2)	35(1)
C(56)	5322(4)	3106(4)	5416(2)	56(1)
C(57)	5889(6)	3758(5)	5974(3)	84(2)
C(58)	4986(5)	2263(4)	5504(3)	77(2)
C(59)	7382(4)	4141(5)	1207(3)	76(2)

C(60)	6611(3)	3779(3)	1516(2)	48(1)
C(61)	5753(4)	3803(3)	1486(2)	50(1)
C(62)	5340(3)	3401(3)	1884(2)	32(1)
C(63)	4467(3)	3331(2)	2083(2)	32(1)
C(64)	4497(3)	3570(3)	2662(2)	36(1)
C(65)	3685(3)	3505(3)	2850(2)	43(1)
C(66)	2817(3)	3205(3)	2473(2)	41(1)
C(67)	2800(3)	2977(3)	1896(2)	41(1)
C(68)	3622(3)	3052(3)	1703(2)	37(1)
C(69)	1924(4)	3124(4)	2689(2)	55(1)
C(70)	1941(5)	3946(5)	2915(3)	81(2)
C(71)	1743(4)	2599(4)	3121(2)	55(1)
C(72)	-3977(3)	-5476(3)	-87(2)	44(1)
C(73)	-3347(3)	-4702(3)	361(2)	30(1)
C(74)	-3578(3)	-4252(3)	785(2)	34(1)
C(75)	-2724(3)	-3601(2)	1098(2)	28(1)
C(76)	-2570(3)	-2960(2)	1611(2)	29(1)
C(77)	-1794(3)	-2675(3)	2051(2)	33(1)
C(78)	-1671(3)	-2107(3)	2555(2)	36(1)
C(79)	-2340(3)	-1816(3)	2628(2)	39(1)
C(80)	-3118(4)	-2085(3)	2181(2)	49(1)
C(81)	-3234(3)	-2643(3)	1681(2)	42(1)
C(82)	-2236(4)	-1217(3)	3182(2)	52(1)
C(83)	-2052(5)	-367(4)	3100(3)	68(2)
C(84)	-3086(5)	-1554(4)	3457(2)	72(2)
C(85)	-2057(3)	-4385(3)	-1187(2)	37(1)
C(86)	-1281(3)	-3744(2)	-709(1)	26(1)
C(87)	-603(3)	-2981(2)	-704(2)	28(1)
C(88)	-96(3)	-2624(2)	-140(2)	26(1)
C(89)	731(3)	-1825(2)	93(2)	29(1)
C(90)	1392(3)	-1690(3)	574(2)	36(1)
C(91)	2195(4)	-941(3)	769(2)	47(1)
C(92)	2360(4)	-321(3)	479(2)	51(1)
C(93)	1704(4)	-456(3)	10(2)	48(1)
C(94)	901(3)	-1194(3)	-188(2)	37(1)
C(95)	3246(6)	488(5)	700(3)	99(3)
C(96)	3233(5)	943(4)	1287(3)	78(2)
C(97)	4000(8)	543(8)	571(7)	333(18)
C(98)	-1324(3)	-6139(2)	-107(2)	35(1)
C(99)	-907(3)	-5434(2)	415(2)	27(1)
C(100)	-339(3)	-5347(2)	921(2)	27(1)
C(101)	-176(3)	-4592(2)	1279(2)	24(1)
C(102)	269(3)	-4243(2)	1887(2)	25(1)
C(103)	1037(3)	-4358(3)	2122(2)	31(1)
C(104)	1444(3)	-4044(3)	2693(2)	34(1)
C(105)	1121(3)	-3583(2)	3059(2)	33(1)
C(106)	351(3)	-3471(3)	2830(2)	34(1)
C(107)	-81(3)	-3808(2)	2251(2)	30(1)
C(108)	1613(4)	-3206(3)	3682(2)	48(1)
C(109)	2282(4)	-2306(4)	3780(3)	66(2)
C(110)	949(5)	-3301(4)	4086(2)	62(2)
N(1)	6439(2)	1680(2)	2050(1)	26(1)
N(2)	7218(2)	2231(2)	1918(1)	31(1)

N(3)	7093(2)	3164(2)	3092(1)	29(1)
N(4)	7782(2)	3434(2)	2783(1)	28(1)
N(5)	5900(2)	3105(2)	2123(1)	27(1)
N(6)	6701(2)	3365(2)	1904(1)	33(1)
N(7)	-2012(2)	-3637(2)	868(1)	26(1)
N(8)	-2396(2)	-4327(2)	419(1)	26(1)
N(9)	-461(2)	-3143(2)	183(1)	25(1)
N(10)	-1174(2)	-3839(2)	-170(1)	24(1)
N(11)	-622(2)	-4223(2)	996(1)	23(1)
N(12)	1061(2)	-4750(2)	469(1)	24(1)
B(1)	7533(3)	3175(3)	2121(2)	30(1)
B(2)	-1748(3)	-4572(3)	72(2)	26(1)
Cl(1)	4197(2)	4754(2)	5840(1)	118(1)
Cl(2)	3367(2)	3987(2)	4637(1)	119(1)
Cl(3)	-1662(2)	-3240(2)	3685(1)	139(1)
Cl(4)	-2467(3)	-4696(2)	2764(2)	170(2)
Cl(5)	-656(3)	-3458(2)	5011(1)	157(1)
Cl(6)	-1258(2)	-4670(2)	5672(1)	147(1)
Cl(11)	8391(1)	1867(1)	3999(1)	70(1)
Cl(12)	9052(1)	2045(1)	2954(1)	73(1)
C(200)	3546(9)	4728(6)	5222(4)	130(4)
C(201)	-1974(9)	-4283(7)	3435(6)	142(4)
C(202)	-700(6)	-3672(5)	5666(3)	87(2)
C(205)	8070(4)	1769(4)	3267(3)	57(1)

_____

Table 3. Bond lengths [A] and angles [deg] for rf441d.

_____

Zn(1)-O(1)	1.974(3)	C(11)-C(16)	1.446(5)
Zn(1)-N(3)	2.051(3)	C(11)-C(12)	1.469(5)
Zn(1)-N(1)	2.073(3)	C(12)-C(13)	1.414(5)
Zn(1)-N(5)	2.114(3)	C(13)-C(14)	1.356(5)
Zn(1)-O(2)	2.123(2)	C(14)-C(15)	1.440(5)
Zn(2)-O(4)	1.986(3)	C(14)-C(21)	1.503(5)
Zn(2)-N(9)	2.061(3)	C(15)-C(16)	1.371(5)
Zn(2)-N(7)	2.088(3)	C(16)-C(17)	1.530(5)
Zn(2)-O(3)	2.111(3)	C(17)-C(20)	1.515(7)
Zn(2)-N(11)	2.132(3)	C(17)-C(18)	1.525(6)
O(1)-C(1)	1.288(4)	C(17)-C(19)	1.543(6)
O(2)-C(6)	1.273(4)	C(21)-C(22)	1.356(5)
O(3)-C(11)	1.271(4)	C(22)-C(28)	1.509(5)
O(4)-C(12)	1.286(4)	C(22)-C(23)	1.522(5)
C(1)-C(2)	1.400(5)	C(23)-C(32)	1.529(6)
C(1)-C(6)	1.488(5)	C(23)-C(24)	1.541(5)
C(2)-C(3)	1.372(5)	C(24)-C(25)	1.515(7)
C(3)-C(4)	1.446(5)	C(25)-C(26)	1.504(7)
C(3)-C(21)	1.496(5)	C(26)-C(27)	1.536(6)
C(4)-C(5)	1.367(5)	C(27)-C(28)	1.548(6)
C(5)-C(6)	1.441(5)	C(28)-C(29)	1.529(6)
C(5)-C(7)	1.530(5)	C(29)-C(30)	1.539(6)
C(7)-C(9)	1.529(5)	C(30)-C(31)	1.540(7)
C(7)-C(8)	1.539(5)	C(31)-C(32)	1.528(7)
C(7)-C(10)	1.544(6)	C(33)-C(34)	1.489(6)

C(34)-N(2)	1.350(5)	C(78)-C(79)	1.377(6)
C(34)-C(35)	1.370(7)	C(79)-C(80)	1.400(7)
C(35)-C(36)	1.399(6)	C(79)-C(82)	1.521(6)
C(36)-N(1)	1.330(5)	C(80)-C(81)	1.378(7)
C(36)-C(37)	1.477(6)	C(82)-C(83)	1.517(8)
C(37)-C(38)	1.381(6)	C(82)-C(84)	1.529(8)
C(37)-C(42)	1.398(6)	C(85)-C(86)	1.502(6)
C(38)-C(39)	1.392(6)	C(86)-N(10)	1.356(4)
C(39)-C(40)	1.386(7)	C(86)-C(87)	1.374(6)
C(40)-C(41)	1.384(8)	C(87)-C(88)	1.398(5)
C(40)-C(43)	1.510(7)	C(88)-N(9)	1.340(4)
C(41)-C(42)	1.395(7)	C(88)-C(89)	1.470(6)
C(43)-C(44)	1.397(13)	C(89)-C(90)	1.391(6)
C(43)-C(45)	1.410(9)	C(89)-C(94)	1.397(5)
C(46)-C(47)	1.510(6)	C(90)-C(91)	1.396(6)
C(47)-N(4)	1.354(5)	C(91)-C(92)	1.395(7)
C(47)-C(48)	1.390(6)	C(92)-C(93)	1.366(8)
C(48)-C(49)	1.398(6)	C(92)-C(95)	1.523(8)
C(49)-N(3)	1.333(5)	C(93)-C(94)	1.383(7)
C(49)-C(50)	1.477(5)	C(95)-C(97)	1.239(14)
C(50)-C(51)	1.389(6)	C(95)-C(96)	1.524(10)
C(50)-C(55)	1.406(6)	C(98)-C(99)	1.496(6)
C(51)-C(52)	1.385(6)	C(99)-N(12)	1.352(5)
C(52)-C(53)	1.384(7)	C(99)-C(100)	1.383(5)
C(53)-C(54)	1.382(6)	C(100)-C(101)	1.397(5)
C(53)-C(56)	1.510(6)	C(101)-N(11)	1.365(5)
C(54)-C(55)	1.394(6)	C(101)-C(102)	1.468(5)
C(56)-C(58)	1.481(8)	C(102)-C(107)	1.391(5)
C(56)-C(57)	1.532(9)	C(102)-C(103)	1.391(5)
C(59)-C(60)	1.498(6)	C(103)-C(104)	1.374(6)
C(60)-N(6)	1.344(5)	C(104)-C(105)	1.393(6)
C(60)-C(61)	1.370(7)	C(105)-C(106)	1.388(6)
C(61)-C(62)	1.391(6)	C(105)-C(108)	1.518(6)
C(62)-N(5)	1.340(5)	C(106)-C(107)	1.400(6)
C(62)-C(63)	1.484(5)	C(108)-C(110)	1.503(8)
C(63)-C(68)	1.380(6)	C(108)-C(109)	1.511(8)
C(63)-C(64)	1.387(6)	N(1)-N(2)	1.362(4)
C(64)-C(65)	1.383(6)	N(2)-B(1)	1.552(6)
C(65)-C(66)	1.399(7)	N(3)-N(4)	1.377(4)
C(66)-C(67)	1.386(7)	N(4)-B(1)	1.551(5)
C(66)-C(69)	1.526(6)	N(5)-N(6)	1.375(4)
C(67)-C(68)	1.400(6)	N(6)-B(1)	1.552(6)
C(69)-C(70)	1.490(8)	N(7)-N(8)	1.373(4)
C(69)-C(71)	1.526(8)	N(8)-B(2)	1.549(5)
C(72)-C(73)	1.497(6)	N(9)-N(10)	1.363(4)
C(73)-N(8)	1.359(5)	N(10)-B(2)	1.553(5)
C(73)-C(74)	1.377(6)	N(11)-N(12)	1.366(4)
C(74)-C(75)	1.403(6)	N(12)-B(2)	1.542(5)
C(75)-N(7)	1.334(5)	CI(1)-C(200)	1.706(9)
C(75)-C(76)	1.470(5)	CI(2)-C(200)	1.687(8)
C(76)-C(77)	1.382(6)	CI(3)-C(201)	1.729(12)
C(76)-C(81)	1.400(6)	CI(4)-C(201)	1.623(13)
C(77)-C(78)	1.393(6)	CI(5)-C(202)	1.713(7)

CI(6)-C(202)	1.682(8)	C(14)-C(13)-C(12)	121.2(3)
CI(11)-C(205)	1.756(6)	C(13)-C(14)-C(15)	119.0(3)
CI(12)-C(205)	1.743(6)	C(13)-C(14)-C(21)	121.8(3)
O(1)-Zn(1)-N(3)	135.65(13)	C(15)-C(14)-C(21)	119.0(3)
O(1)-Zn(1)-N(1)	127.50(12)	C(16)-C(15)-C(14)	124.0(3)
N(3)-Zn(1)-N(1)	96.74(13)	C(15)-C(16)-C(11)	117.3(3)
O(1)-Zn(1)-N(5)	95.02(11)	C(15)-C(16)-C(17)	123.3(3)
N(3)-Zn(1)-N(5)	84.62(13)	C(11)-C(16)-C(17)	119.4(3)
N(1)-Zn(1)-N(5)	92.65(12)	C(20)-C(17)-C(18)	108.0(4)
O(1)-Zn(1)-O(2)	80.43(10)	C(20)-C(17)-C(16)	110.2(4)
N(3)-Zn(1)-O(2)	93.11(11)	C(18)-C(17)-C(16)	112.0(3)
N(1)-Zn(1)-O(2)	96.38(11)	C(20)-C(17)-C(19)	111.0(4)
N(5)-Zn(1)-O(2)	170.90(12)	C(18)-C(17)-C(19)	107.9(4)
O(4)-Zn(2)-N(9)	128.46(12)	C(16)-C(17)-C(19)	107.7(4)
O(4)-Zn(2)-N(7)	136.43(12)	C(22)-C(21)-C(3)	122.9(3)
N(9)-Zn(2)-N(7)	95.06(12)	C(22)-C(21)-C(14)	124.2(3)
O(4)-Zn(2)-O(3)	79.49(10)	C(3)-C(21)-C(14)	112.8(3)
N(9)-Zn(2)-O(3)	97.13(11)	C(21)-C(22)-C(28)	120.2(3)
N(7)-Zn(2)-O(3)	94.79(12)	C(21)-C(22)-C(23)	120.2(3)
O(4)-Zn(2)-N(11)	95.69(11)	C(28)-C(22)-C(23)	119.6(3)
N(9)-Zn(2)-N(11)	91.49(11)	C(22)-C(23)-C(32)	111.5(3)
N(7)-Zn(2)-N(11)	83.73(12)	C(22)-C(23)-C(24)	114.8(3)
O(3)-Zn(2)-N(11)	171.35(10)	C(32)-C(23)-C(24)	113.8(3)
C(1)-O(1)-Zn(1)	114.6(2)	C(25)-C(24)-C(23)	115.2(3)
C(6)-O(2)-Zn(1)	110.8(2)	C(26)-C(25)-C(24)	116.0(4)
C(11)-O(3)-Zn(2)	111.4(2)	C(25)-C(26)-C(27)	116.4(3)
C(12)-O(4)-Zn(2)	114.6(2)	C(26)-C(27)-C(28)	117.1(4)
O(1)-C(1)-C(2)	123.0(3)	C(22)-C(28)-C(29)	115.2(3)
O(1)-C(1)-C(6)	117.4(3)	C(22)-C(28)-C(27)	109.5(3)
C(2)-C(1)-C(6)	119.7(3)	C(29)-C(28)-C(27)	111.9(3)
C(3)-C(2)-C(1)	120.5(3)	C(28)-C(29)-C(30)	115.1(3)
C(2)-C(3)-C(4)	119.7(3)	C(31)-C(30)-C(29)	112.6(4)
C(2)-C(3)-C(21)	120.6(3)	C(32)-C(31)-C(30)	116.1(4)
C(4)-C(3)-C(21)	119.7(3)	C(31)-C(32)-C(23)	117.4(4)
C(5)-C(4)-C(3)	123.4(3)	N(2)-C(34)-C(35)	107.2(4)
C(4)-C(5)-C(6)	117.7(3)	N(2)-C(34)-C(33)	122.7(4)
C(4)-C(5)-C(7)	122.8(3)	C(35)-C(34)-C(33)	130.1(4)
C(6)-C(5)-C(7)	119.5(3)	C(34)-C(35)-C(36)	106.4(4)
O(2)-C(6)-C(5)	124.5(3)	N(1)-C(36)-C(35)	109.2(4)
O(2)-C(6)-C(1)	116.5(3)	N(1)-C(36)-C(37)	123.6(4)
C(5)-C(6)-C(1)	119.0(3)	C(35)-C(36)-C(37)	127.2(4)
C(9)-C(7)-C(5)	111.7(3)	C(38)-C(37)-C(42)	117.6(4)
C(9)-C(7)-C(8)	108.0(3)	C(38)-C(37)-C(36)	121.9(4)
C(5)-C(7)-C(8)	110.2(3)	C(42)-C(37)-C(36)	120.5(4)
C(9)-C(7)-C(10)	107.6(3)	C(37)-C(38)-C(39)	121.0(4)
C(5)-C(7)-C(10)	108.9(3)	C(40)-C(39)-C(38)	122.2(5)
C(8)-C(7)-C(10)	110.4(3)	C(41)-C(40)-C(39)	116.3(4)
O(3)-C(11)-C(16)	124.5(3)	C(41)-C(40)-C(43)	121.4(5)
O(3)-C(11)-C(12)	116.6(3)	C(39)-C(40)-C(43)	122.3(5)
C(16)-C(11)-C(12)	118.9(3)	C(40)-C(41)-C(42)	122.3(5)
O(4)-C(12)-C(13)	123.6(3)	C(41)-C(42)-C(37)	120.4(5)
O(4)-C(12)-C(11)	117.0(3)	C(44)-C(43)-C(45)	117.4(7)
C(13)-C(12)-C(11)	119.5(3)	C(44)-C(43)-C(40)	114.9(6)

C(45)-C(43)-C(40)	114.6(6)	C(78)-C(79)-C(80)	118.4(4)
N(4)-C(47)-C(48)	107.9(4)	C(78)-C(79)-C(82)	120.8(4)
N(4)-C(47)-C(46)	122.5(4)	C(80)-C(79)-C(82)	120.8(4)
C(48)-C(47)-C(46)	129.6(4)	C(81)-C(80)-C(79)	121.5(4)
C(47)-C(48)-C(49)	105.5(4)	C(80)-C(81)-C(76)	120.4(4)
N(3)-C(49)-C(48)	110.1(3)	C(83)-C(82)-C(79)	111.9(4)
N(3)-C(49)-C(50)	120.7(4)	C(83)-C(82)-C(84)	111.4(5)
C(48)-C(49)-C(50)	129.2(4)	C(79)-C(82)-C(84)	111.6(5)
C(51)-C(50)-C(55)	117.8(4)	N(10)-C(86)-C(87)	107.5(3)
C(51)-C(50)-C(49)	120.8(4)	N(10)-C(86)-C(85)	122.3(3)
C(55)-C(50)-C(49)	121.3(4)	C(87)-C(86)-C(85)	130.1(3)
C(52)-C(51)-C(50)	120.6(4)	C(86)-C(87)-C(88)	106.2(3)
C(51)-C(52)-C(53)	122.0(4)	N(9)-C(88)-C(87)	109.3(3)
C(54)-C(53)-C(52)	117.7(4)	N(9)-C(88)-C(89)	122.3(3)
C(54)-C(53)-C(56)	120.6(5)	C(87)-C(88)-C(89)	128.4(3)
C(52)-C(53)-C(56)	121.6(4)	C(90)-C(89)-C(94)	118.1(4)
C(53)-C(54)-C(55)	121.3(4)	C(90)-C(89)-C(88)	121.6(3)
C(54)-C(55)-C(50)	120.5(4)	C(94)-C(89)-C(88)	120.2(4)
C(58)-C(56)-C(53)	111.3(5)	C(91)-C(90)-C(89)	120.4(4)
C(58)-C(56)-C(57)	110.9(5)	C(90)-C(91)-C(92)	120.7(4)
C(53)-C(56)-C(57)	111.3(5)	C(93)-C(92)-C(91)	118.5(4)
N(6)-C(60)-C(61)	108.2(4)	C(93)-C(92)-C(95)	122.0(5)
N(6)-C(60)-C(59)	121.4(4)	C(91)-C(92)-C(95)	119.5(6)
C(61)-C(60)-C(59)	130.4(4)	C(92)-C(93)-C(94)	121.5(4)
C(60)-C(61)-C(62)	106.1(4)	C(93)-C(94)-C(89)	120.8(4)
N(5)-C(62)-C(61)	109.5(4)	C(97)-C(95)-C(92)	120.0(9)
N(5)-C(62)-C(63)	120.9(3)	C(97)-C(95)-C(96)	120.7(9)
C(61)-C(62)-C(63)	129.4(4)	C(92)-C(95)-C(96)	110.5(6)
C(68)-C(63)-C(64)	118.8(4)	N(12)-C(99)-C(100)	107.3(3)
C(68)-C(63)-C(62)	121.3(4)	N(12)-C(99)-C(98)	123.4(4)
C(64)-C(63)-C(62)	119.9(4)	C(100)-C(99)-C(98)	129.3(3)
C(65)-C(64)-C(63)	120.2(4)	C(99)-C(100)-C(101)	106.6(3)
C(64)-C(65)-C(66)	122.0(4)	N(11)-C(101)-C(100)	109.1(3)
C(67)-C(66)-C(65)	117.2(4)	N(11)-C(101)-C(102)	120.8(3)
C(67)-C(66)-C(69)	121.5(4)	C(100)-C(101)-C(102)	129.6(3)
C(65)-C(66)-C(69)	121.3(4)	C(107)-C(102)-C(103)	117.8(4)
C(66)-C(67)-C(68)	121.1(4)	C(107)-C(102)-C(101)	121.1(3)
C(63)-C(68)-C(67)	120.8(4)	C(103)-C(102)-C(101)	121.1(3)
C(70)-C(69)-C(71)	112.3(5)	C(104)-C(103)-C(102)	121.2(4)
C(70)-C(69)-C(66)	111.7(5)	C(103)-C(104)-C(105)	121.7(4)
C(71)-C(69)-C(66)	111.5(4)	C(106)-C(105)-C(104)	117.6(4)
N(8)-C(73)-C(74)	107.4(4)	C(106)-C(105)-C(108)	121.7(4)
N(8)-C(73)-C(72)	123.4(4)	C(104)-C(105)-C(108)	120.7(4)
C(74)-C(73)-C(72)	129.1(4)	C(105)-C(106)-C(107)	120.9(4)
C(73)-C(74)-C(75)	106.0(4)	C(102)-C(107)-C(106)	120.8(4)
N(7)-C(75)-C(74)	109.9(3)	C(110)-C(108)-C(109)	110.1(5)
N(7)-C(75)-C(76)	122.0(4)	C(110)-C(108)-C(105)	113.8(4)
C(74)-C(75)-C(76)	128.1(4)	C(109)-C(108)-C(105)	111.0(4)
C(77)-C(76)-C(81)	117.5(4)	C(36)-N(1)-N(2)	107.0(3)
C(77)-C(76)-C(75)	121.7(3)	C(36)-N(1)-Zn(1)	139.5(3)
C(81)-C(76)-C(75)	120.7(4)	N(2)-N(1)-Zn(1)	113.0(2)
C(76)-C(77)-C(78)	122.3(4)	C(34)-N(2)-N(1)	110.1(3)
C(79)-C(78)-C(77)	119.8(4)	C(34)-N(2)-B(1)	128.6(3)

N(1)-N(2)-B(1)	121.3(3)	N(10)-N(9)-Zn(2)	113.2(2)
C(49)-N(3)-N(4)	107.1(3)	C(86)-N(10)-N(9)	109.9(3)
C(49)-N(3)-Zn(1)	139.0(3)	C(86)-N(10)-B(2)	129.9(3)
N(4)-N(3)-Zn(1)	113.1(2)	N(9)-N(10)-B(2)	120.2(3)
C(47)-N(4)-N(3)	109.4(3)	N(12)-N(11)-C(101)	106.2(3)
C(47)-N(4)-B(1)	129.9(3)	N(12)-N(11)-Zn(2)	112.0(2)
N(3)-N(4)-B(1)	120.6(3)	C(101)-N(11)-Zn(2)	139.1(3)
C(62)-N(5)-N(6)	106.6(3)	C(99)-N(12)-N(11)	110.8(3)
C(62)-N(5)-Zn(1)	140.2(3)	C(99)-N(12)-B(2)	129.3(3)
N(6)-N(5)-Zn(1)	112.2(2)	N(11)-N(12)-B(2)	119.1(3)
C(60)-N(6)-N(5)	109.5(3)	N(4)-B(1)-N(2)	108.9(3)
C(60)-N(6)-B(1)	130.3(3)	N(4)-B(1)-N(6)	109.4(3)
N(5)-N(6)-B(1)	120.2(3)	N(2)-B(1)-N(6)	108.3(3)
C(75)-N(7)-N(8)	106.7(3)	N(12)-B(2)-N(8)	109.4(3)
C(75)-N(7)-Zn(2)	138.9(3)	N(12)-B(2)-N(10)	109.1(3)
N(8)-N(7)-Zn(2)	114.2(2)	N(8)-B(2)-N(10)	108.5(3)
C(73)-N(8)-N(7)	110.0(3)	CI(2)-C(200)-CI(1)	117.7(5)
C(73)-N(8)-B(2)	130.1(3)	CI(4)-C(201)-CI(3)	116.9(6)
N(7)-N(8)-B(2)	120.0(3)	CI(6)-C(202)-CI(5)	117.0(4)
C(88)-N(9)-N(10)	107.0(3)	CI(12)-C(205)-CI(11)	111.3(3)
C(88)-N(9)-Zn(2)	135.6(3)		

Table 4. Anisotropic displacement parameters (A^2 x 10^3) for rf441d.
The anisotropic displacement factor exponent takes the form: -2 pi^2 [h^2 a*^2 U11 + 2 h k a* b* U12]

U11 U22 U33 U23 U13 U12

	U11	U22	U33	U23	U13	U12
Zn(1)	21(1)	28(1)	27(1)	11(1)	10(1)	10(1)
Zn(2)	26(1)	24(1)	21(1)	7(1)	6(1)	12(1)
O(1)	22(1)	36(1)	31(1)	18(1)	11(1)	16(1)
O(2)	16(1)	34(1)	32(1)	15(1)	8(1)	12(1)
O(3)	33(2)	30(1)	22(1)	7(1)	1(1)	16(1)
O(4)	32(2)	25(1)	26(1)	7(1)	3(1)	16(1)
C(1)	19(2)	26(2)	22(2)	7(1)	6(1)	11(2)
C(2)	19(2)	30(2)	23(2)	7(2)	5(1)	14(2)
C(3)	16(2)	29(2)	18(2)	4(1)	4(1)	10(2)
C(4)	22(2)	27(2)	23(2)	9(1)	8(1)	12(2)
C(5)	21(2)	26(2)	21(2)	8(1)	6(1)	12(2)
C(6)	17(2)	26(2)	22(2)	7(1)	5(1)	9(2)
C(7)	21(2)	33(2)	29(2)	13(2)	6(2)	15(2)
C(8)	32(2)	44(2)	39(2)	11(2)	10(2)	26(2)
C(9)	34(2)	52(3)	44(2)	30(2)	6(2)	23(2)
C(10)	29(2)	44(2)	35(2)	10(2)	3(2)	15(2)
C(11)	24(2)	26(2)	19(2)	7(1)	5(1)	10(2)
C(12)	22(2)	27(2)	24(2)	12(2)	9(1)	12(2)
C(13)	21(2)	33(2)	22(2)	12(2)	8(1)	16(2)
C(14)	16(2)	31(2)	21(2)	11(1)	10(1)	10(2)
C(15)	25(2)	26(2)	25(2)	7(2)	4(2)	13(2)
C(16)	29(2)	30(2)	25(2)	7(2)	4(2)	18(2)
C(17)	41(2)	31(2)	34(2)	4(2)	-3(2)	22(2)
C(18)	82(4)	42(3)	45(3)	4(2)	-8(3)	43(3)
C(19)	60(3)	44(2)	33(2)	19(2)	8(2)	26(2)
C(20)	46(3)	60(3)	45(3)	14(2)	8(2)	38(3)

C(21)	16(2)	27(2)	20(2)	8(1)	7(1)	10(1)
C(22)	20(2)	33(2)	24(2)	9(2)	8(1)	14(2)
C(23)	22(2)	47(2)	22(2)	6(2)	6(2)	16(2)
C(24)	35(2)	55(3)	23(2)	9(2)	6(2)	22(2)
C(25)	44(3)	69(3)	33(2)	21(2)	17(2)	32(3)
C(26)	44(3)	52(3)	39(2)	21(2)	19(2)	28(2)
C(27)	31(2)	43(2)	33(2)	12(2)	17(2)	16(2)
C(28)	23(2)	40(2)	28(2)	12(2)	12(2)	14(2)
C(29)	28(2)	52(3)	33(2)	11(2)	14(2)	23(2)
C(30)	42(3)	55(3)	49(3)	16(2)	16(2)	33(2)
C(31)	53(3)	45(3)	45(3)	4(2)	13(2)	25(2)
C(32)	36(2)	40(2)	36(2)	2(2)	7(2)	13(2)
C(33)	49(3)	63(3)	65(3)	12(3)	38(3)	26(3)
C(34)	34(2)	54(3)	42(2)	12(2)	21(2)	27(2)
C(35)	39(3)	49(3)	48(3)	5(2)	21(2)	20(2)
C(36)	29(2)	39(2)	30(2)	8(2)	6(2)	19(2)
C(37)	27(2)	34(2)	30(2)	2(2)	4(2)	11(2)
C(38)	28(2)	35(2)	34(2)	3(2)	1(2)	13(2)
C(39)	29(2)	49(3)	37(2)	6(2)	2(2)	6(2)
C(40)	45(3)	34(2)	45(3)	5(2)	3(2)	6(2)
C(41)	53(3)	29(2)	62(3)	5(2)	0(3)	16(2)
C(42)	38(3)	40(2)	52(3)	10(2)	8(2)	20(2)
C(43)	51(4)	39(3)	88(4)	7(3)	10(3)	1(3)
C(44)	252(16)	170(11)	82(6)	57(7)	-20(8)	-137(11)
C(45)	91(6)	83(5)	75(5)	34(4)	-13(4)	-26(4)
C(46)	25(2)	46(3)	57(3)	22(2)	12(2)	8(2)
C(47)	26(2)	29(2)	47(2)	14(2)	10(2)	8(2)
C(48)	28(2)	31(2)	41(2)	10(2)	-1(2)	4(2)
C(49)	28(2)	30(2)	31(2)	8(2)	6(2)	14(2)
C(50)	30(2)	30(2)	31(2)	9(2)	5(2)	12(2)
C(51)	37(3)	55(3)	32(2)	13(2)	6(2)	20(2)
C(52)	50(3)	65(3)	24(2)	11(2)	4(2)	23(3)
C(53)	47(3)	47(2)	28(2)	9(2)	11(2)	24(2)
C(54)	40(3)	50(3)	33(2)	8(2)	10(2)	24(2)
C(55)	36(2)	46(2)	26(2)	9(2)	5(2)	21(2)
C(56)	61(3)	86(4)	42(3)	27(3)	27(2)	45(3)
C(57)	92(5)	116(6)	52(3)	13(4)	27(3)	53(5)
C(58)	86(5)	90(5)	90(5)	45(4)	60(4)	52(4)
C(59)	56(4)	125(5)	98(5)	91(4)	50(3)	55(4)
C(60)	37(3)	66(3)	64(3)	48(3)	26(2)	29(2)
C(61)	46(3)	67(3)	64(3)	46(3)	24(2)	33(3)
C(62)	26(2)	38(2)	38(2)	18(2)	9(2)	16(2)
C(63)	26(2)	34(2)	46(2)	20(2)	15(2)	17(2)
C(64)	27(2)	42(2)	46(2)	13(2)	6(2)	21(2)
C(65)	41(3)	54(3)	44(2)	12(2)	14(2)	30(2)
C(66)	31(2)	43(2)	57(3)	13(2)	12(2)	23(2)
C(67)	32(2)	52(3)	48(3)	16(2)	8(2)	26(2)
C(68)	33(2)	42(2)	42(2)	16(2)	10(2)	20(2)
C(69)	37(3)	69(3)	65(3)	12(3)	15(2)	30(3)
C(70)	80(5)	111(6)	90(5)	25(4)	33(4)	77(5)
C(71)	37(3)	70(4)	57(3)	10(3)	19(2)	22(3)
C(72)	24(2)	51(3)	48(3)	8(2)	5(2)	12(2)
C(73)	24(2)	38(2)	31(2)	11(2)	4(2)	14(2)

C(74)	28(2)	47(2)	35(2)	15(2)	12(2)	21(2)
C(75)	30(2)	35(2)	27(2)	10(2)	9(2)	20(2)
C(76)	30(2)	35(2)	30(2)	10(2)	12(2)	20(2)
C(77)	35(2)	41(2)	34(2)	10(2)	14(2)	26(2)
C(78)	33(2)	44(2)	33(2)	5(2)	6(2)	23(2)
C(79)	43(3)	52(3)	31(2)	5(2)	10(2)	31(2)
C(80)	45(3)	67(3)	49(3)	5(2)	16(2)	41(3)
C(81)	33(2)	58(3)	44(2)	8(2)	5(2)	30(2)
C(82)	57(3)	64(3)	42(3)	-2(2)	8(2)	40(3)
C(83)	82(5)	60(3)	57(3)	-8(3)	3(3)	39(3)
C(84)	97(5)	88(5)	44(3)	7(3)	26(3)	55(4)
C(85)	43(3)	43(2)	21(2)	3(2)	4(2)	16(2)
C(86)	32(2)	35(2)	19(2)	5(2)	7(2)	22(2)
C(87)	36(2)	34(2)	21(2)	9(2)	6(2)	21(2)
C(88)	31(2)	31(2)	21(2)	9(2)	10(2)	18(2)
C(89)	35(2)	33(2)	25(2)	11(2)	11(2)	18(2)
C(90)	37(2)	41(2)	27(2)	10(2)	7(2)	15(2)
C(91)	39(3)	55(3)	36(2)	9(2)	3(2)	10(2)
C(92)	47(3)	42(3)	50(3)	4(2)	13(2)	7(2)
C(93)	58(3)	36(2)	41(2)	11(2)	20(2)	11(2)
C(94)	47(3)	38(2)	29(2)	11(2)	10(2)	19(2)
C(95)	80(6)	79(5)	79(5)	5(4)	12(4)	-18(4)
C(96)	79(5)	48(3)	86(5)	-8(3)	-37(4)	30(3)
C(97)	149(12)	227(16)	330(20)	189(17)	166(15)	-131(12)
C(98)	36(2)	31(2)	39(2)	3(2)	6(2)	19(2)
C(99)	27(2)	22(2)	34(2)	8(2)	14(2)	9(2)
C(100)	29(2)	31(2)	31(2)	12(2)	13(2)	20(2)
C(101)	22(2)	26(2)	28(2)	12(2)	9(1)	13(2)
C(102)	26(2)	26(2)	29(2)	12(2)	12(2)	13(2)
C(103)	26(2)	37(2)	39(2)	14(2)	12(2)	18(2)
C(104)	26(2)	41(2)	39(2)	15(2)	5(2)	18(2)
C(105)	36(2)	31(2)	31(2)	12(2)	3(2)	14(2)
C(106)	41(2)	38(2)	31(2)	11(2)	9(2)	25(2)
C(107)	34(2)	39(2)	30(2)	16(2)	11(2)	24(2)
C(108)	51(3)	57(3)	32(2)	5(2)	-9(2)	29(3)
C(109)	57(4)	62(4)	56(3)	-6(3)	-12(3)	19(3)
C(110)	79(4)	78(4)	32(2)	14(3)	6(3)	38(3)
N(1)	20(2)	34(2)	28(2	12(1)	9(1)	12(1)
N(2)	22(2)	42(2)	33(2)	14(2)	14(1)	15(2)
N(3)	24(2)	31(2)	32(2)	13(1)	11(1)	7(1)
N(4)	23(2)	30(2)	35(2)	14(1)	13(1)	12(1)
N(5)	22(2)	35(2)	32(2)	17(1)	13(1)	16(1)
N(6)	27(2)	45(2)	38(2)	26(2)	16(1)	18(2)
N(7)	27(2)	30(2)	27(2)	7(1)	7(1)	16(1)
N(8)	27(2)	28(2)	21(1)	6(1)	5(1)	12(1)
N(9)	28(2)	26(2)	23(1)	6(1)	6(1)	12(1)
N(10)	26(2)	27(2)	21(1)	6(1)	7(1)	14(1)
N(11)	27(2)	24(2)	22(1)	6(1)	6(1)	14(1)
N(12)	27(2)	25(2)	25(2)	5(1)	7(1)	16(1)
B(1)	22(2)	40(2)	34(2)	17(2)	12(2)	15(2)
B(2)	26(2)	27(2)	25(2)	7(2)	6(2)	12(2)
CI(1)	156(2)	140(2)	85(1)	28(1)	10(1)	94(2)
CI(2)	129(2)	93(2)	104(2)	-6(1)	5(1)	37(1)

Cl(3)	159(3)	93(2)	131(2)	16(1)	-7(2)	37(2)
Cl(4)	141(3)	112(2)	223(4)	-34(2)	3(3)	63(2)
Cl(5)	178(3)	177(3)	96(2)	39(2)	62(2)	46(2)
Cl(6)	141(2)	89(2)	156(2)	32(2)	-36(2)	13(2)
Cl(11)	61(1)	76(1)	82(1)	30(1)	29(1)	31(1)
Cl(12)	62(1)	94(1)	74(1)	27(1)	23(1)	39(1)
C(200)	179(11)	104(6)	99(6)	-23(5)	-44(7)	95(7)
C(201)	139(9)	145(9)	188(12)	81(9)	16(8)	94(8)
C(202)	100(6)	90(5)	64(4)	11(4)	20(4)	36(4)
C(205)	35(3)	64(3)	81(4)	22(3)	12(3)	28(3)

Table 5. Hydrogen coordinates (x 10^4) and isotropic displacement parameters (A^2 x 10^3) for rf441d.

x y z   U(eq)

	x	y	z	U(eq)		x	y	z	U(eq)
H(2)	2797	1114	2757	58(1)	H(31A)	1607	2276	4531	58(1)
H(4)	3387	-241	3763	58(1)	H(31B)	1437	1638	4921	58(1)
H(8A)	5329	-502	3184	58(1)	H(32A)	2915	1981	4720	58(1)
H(8B)	6222	-174	3697	58(1)	H(32B)	2507	1766	4053	58(1)
H(8C)	6139	418	3305	58(1)	H(33A)	8366	2571	1135	58(1)
H(9A)	4425	-194	4443	58(1)	H(33B)	8693	1863	1203	58(1)
H(9B)	5251	-484	4409	58(1)	H(33C)	8999	2653	1725	58(1)
H(9C)	4340	-884	3902	58(1)	H(35)	7219	563	1346	58(1)
H(10A)	6303	1508	4172	58(1)	H(38)	4639	608	2014	58(1)
H(10B)	6416	933	4570	58(1)	H(39)	3497	-585	2149	58(1)
H(10C)	5621	1261	4609	58(1)	H(41)	5079	-1786	1781	58(1)
H(13)	1556	-1486	2693	58(1)	H(42)	6286	-569	1720	58(1)
H(15)	840	389	2611	58(1)	H(43)	2930	-1920	2181	58(1)
H(18A)	-261	1023	1625	58(1)	H(44A)	3139	-2898	2528	58(1)
H(18B)	697	1076	1966	58(1)	H(44B)	3808	-1964	2872	58(1)
H(18C)	-236	780	2222	58(1)	H(44C)	4218	-2483	2474	58(1)
H(19A)	-45	-683	798	58(1)	H(45A)	2471	-2523	1334	58(1)
H(19B)	769	229	1078	58(1)	H(45B)	2507	-3231	1624	58(1)
H(19C)	-236	104	753	58(1)	H(45C)	3321	-2783	1305	58(1)
H(20A)	-1513	-1178	1288	58(1)	H(46A)	9691	3915	2761	58(1)
H(20B)	-1613	-376	1177	58(1)	H(46B)	10018	4732	3264	58(1)
H(20C)	-1540	-516	1807	58(1)	H(46C)	9419	4642	2659	58(1)
H(23)	2969	793	4274	58(1)	H(48)	8913	4331	4041	58(1)
H(24A)	2852	717	5161	58(1)	H(51)	8004	3590	4733	58(1)
H(24B)	1775	569	5063	58(1)	H(52)	7135	3442	5440	58(1)
H(25A)	2240	-679	4510	58(1)	H(54)	4805	2961	4309	58(1)
H(25B)	2161	-597	5163	58(1)	H(55)	5666	3130	3591	58(1)
H(26A)	569	-806	4884	58(1)	H(56)	4755	3196	5288	58(1)
H(26B)	763	-1591	4665	58(1)	H(57A)	6337	3593	6167	58(1)
H(27A)	-264	-1435	3956	58(1)	H(57B)	5459	3806	6222	58(1)
H(27B)	645	-1449	3743	58(1)	H(57C)	6233	4291	5891	58(1)
H(28)	248	-476	3420	58(1)	H(58A)	4682	1856	5136	58(1)
H(29A)	398	234	4583	58(1)	H(58B)	4532	2189	5754	58(1)
H(29B)	-476	-58	4065	58(1)	H(58C)	5523	2186	5682	58(1)
H(30A)	642	1116	3720	58(1)	H(59A)	7897	4635	1466	58(1)
H(30B)	76	1304	4187	58(1)	H(59B)	7135	4291	879	58(1)

H(59C)	7618	3734	1074	58(1)	H(94)	460	-1272	-517	58(1)
H(61)	5492	4044	1242	58(1)	H(95)	3092	827	461	58(1)
H(64)	5076	3779	2929	58(1)	H(96A)	3217	603	1557	58(1)
H(65)	3718	3668	3248	58(1)	H(96B)	2672	1051	1262	58(1)
H(67)	2221	2767	1628	58(1)	H(96C)	3800	1468	1418	58(1)
H(68)	3599	2910	1305	58(1)	H(97A)	4517	865	903	58(1)
H(69)	1384	2826	2353	58(1)	H(97B)	4109	818	259	58(1)
H(70A)	1334	3871	3014	58(1)	H(97C)	3968	-11	448	58(1)
H(70B)	2053	4259	2623	58(1)	H(98A)	-2013	-6372	-172	58(1)
H(70C)	2446	4250	3255	58(1)	H(98B)	-1117	-6565	-53	58(1)
H(71A)	2249	2880	3462	58(1)	H(98C)	-1114	-5941	-437	58(1)
H(71B)	1723	2061	2952	58(1)	H(100)	-106	-5726	1009	58(1)
H(71C)	1138	2519	3225	58(1)	H(103)	1284	-4659	1883	58(1)
H(72A)	-3948	-5368	-466	58(1)	H(104)	1958	-4144	2842	58(1)
H(72B)	-4627	-5658	-33	58(1)	H(106)	113	-3160	3069	58(1)
H(72C)	-3769	-5908	-57	58(1)	H(107)	-621	-3739	2105	58(1)
H(74)	-4191	-4359	851	58(1)	H(108)	2001	-3501	3777	58(1)
H(77)	-1328	-2873	2008	58(1)	H(10D)	1935	-2007	3652	58(1)
H(78)	-1126	-1921	2848	58(1)	H(10E)	2779	-2259	3565	58(1)
H(80)	-3577	-1878	2222	58(1)	H(10F)	2566	-2070	4188	58(1)
H(81)	-3767	-2814	1383	58(1)	H(11A)	1311	-3090	4480	58(1)
H(82)	-1672	-1156	3453	58(1)	H(11B)	521	-3886	4020	58(1)
H(83A)	-2568	-411	2812	58(1)	H(11C)	583	-2990	4020	58(1)
H(83B)	-1457	-136	2971	58(1)	H(1)	8094	3480	1967	58(1)
H(83C)	-2011	-4	3462	58(1)	H(2A)	-2137	-5073	-248	58(1)
H(84A)	-2967	-1182	3831	58(1)	H(20N)	2922	4669	5293	155
H(84B)	-3188	-2103	3504	58(1)	H(20O)	3857	5270	5134	155
H(84C)	-3647	-1594	3212	58(1)	H(20L)	-1399	-4372	3510	171
H(85A)	-2085	-4931	-1187	58(1)	H(20M)	-2411	-4584	3661	171
H(85B)	-1932	-4261	-1552	58(1)	H(20J)	-45	-3451	5884	105
H(85C)	-2660	-4381	-1135	58(1)	H(20K)	-1011	-3366	5871	105
H(87)	-500	-2743	-1019	58(1)	H(20F)	7620	1191	3077	69
H(90)	1296	-2111	770	58(1)	H(20G)	7752	2127	3211	69
H(91)	2635	-851	1103	58(1)					
H(93)	1801	-34	-186	58(1)					

_____

3(SQZnL)$_2$. Green, rectangular blocks of **kva** were grown from a dichloromethane/methanol solution at room temperature. A crystal of dimensions 0.34 x 0.34 x 0.32 mm was mounted on a standard Bruker SMART CCD-based X-ray diffractometer equipped with a LT-2 low temperature device and normal focus Mo-target X-ray tube (λ = 0.71073 A) operated at 2000 W power (50 kV, 40 mA). The X-ray intensities were measured at 158(2) K; the detector was placed at a distance 5.058 cm from the crystal. A total of 3332 frames were collected with a scan width of 0.3° in ω and phi with an exposure time of 30 s/frame. The frames were integrated with the Bruker SAINT software package with a narrow frame algorithm. The integration of the data yielded a total of 81861 reflections to a maximum 2θ value of 49.92° of which 25810 were independent and 14823 were greater than 2σ(I). The final cell constants (Table 1) were based

on the xyz centroids of 7006 reflections above $10\sigma(I)$. Analysis of the data showed negligible decay during data collection; the data were processed with SADABS and corrected for absorption. The structure was solved and refined with the Bruker SHELXTL (version 5.10) software package, using the space group P1bar with Z = 2 for the formula $C_{111}H_{133}B_2N_{12}O_4Cl_4Zn_2$ which includes the contribution of disordered lattice solvate.   All non-hydrogen atoms were allowed to refine anisotropically with hydrogen atoms placed in idealized positions. Full matrix least-squares refinement based on F^2 converged at R1 = 0.0941 and wR2 = 0.2774 [based on I > 2sigma(I)], R1 = 0.1170 and wR2 = 0.2850 for all data. Additional details are presented in Table 1 and are given as Supporting Information as a CIF file.

Sheldrick, G.M. SHELXTL, v. 5.10; Bruker Analytical X-ray, Madison, WI, 1997.

Sheldrick, G. M. SADABS.   Program for Empirical Absorption Correction of Area Detector Data, University of Gottingen: Gottingen, Germany, 1996.
Saint Plus, v. 6.02, Bruker Analytical X-ray, Madison, WI, 1999

Table 1. Crystal data and structure refinement for kva (**3(SQZnL)$_2$**).

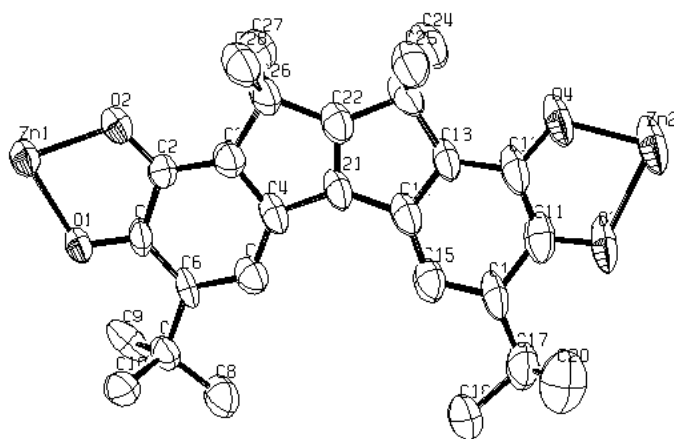|	
Identification code	kva
Empirical formula	C111 H133 B2 Cl4 N12 O4 Zn2
Formula weight	1993.45
Temperature	158(2) K
Wavelength	0.71073 A
Crystal system, space group	Triclinic, P-1
Unit cell dimensions	a = 13.3366(13) Aalpha = 106.665(2) deg.
	b = 18.8734(18) A beta = 96.630(2) deg.
	c = 27.555(3) Agamma = 104.208(2) deg.
Volume	6311.0(11) A^3
Z, Calculated density	2, 1.049 Mg/m^3
Absorption coefficient	0.512 mm^-1
F(000)	2106
Crystal size	0.32 x 0.34 x 0.34 mm
Theta range for data collection	0.79 to 24.71 deg.
Limiting indices	-15<=h<=15, -22<=k<=21, -32<=l<=32
Reflections collected / unique	81861 / 21510 [R(int) = 0.0442]
Completeness to theta =	24.71 99.9 %
Absorption correction	multi-scan
Refinement method	Full-matrix least-squares on F^2
Data / restraints / parameters	21510 / 0 / 1286
Goodness-of-fit on F^2	2.159
Final R indices [I>2sigma(I)]	R1 = 0.0941, wR2 = 0.2774
R indices (all data)	R1 = 0.1170, wR2 = 0.2850
Extinction coefficient	0.0019(4)
Largest diff. peak and hole	1.692 and -0.545 e.A^-3

The likely contribution of 3.5 CH2Cl2 lattice solvates per cell as suggested by PLATON have not been included in the above derived quantities. The residiual electron density is associated with one of the partial occupancy lattice solvates located on the difference map. Further details are provided in the .cif file.

Table 2. Atomic coordinates (x 10^4) and equivalent isotropic displacement parameters (A^2 x 10^3) for kva.
U(eq) is defined as one third of the trace of the orthogonalized Uij tensor.

_____

	x	y	z	U(eq)		x	y	z	U(eq)
Zn(1)	1197(1)	285(1)	2447(1)	38(1)	C(31)	4997(6)	628(4)	1466(3)	53(2)
Zn(2)	3662(1)	6382(1)	3380(1)	36(1)	C(32)	3874(6)	421(4)	1334(3)	51(2)
O(1)	2004(3)	964(2)	2120(2)	40(1)	C(33)	3258(5)	27(3)	1585(3)	44(2)
O(2)	265(3)	1062(2)	2468(2)	38(1)	C(34)	5706(6)	1065(4)	1185(3)	60(2)
O(3)	3304(3)	5251(2)	3082(1)	38(1)	C(35)	5891(6)	1943(4)	1415(3)	68(2)
O(4)	2882(3)	6227(2)	2629(2)	39(1)	C(36)	5290(8)	805(6)	612(3)	89(3)
N(1)	-70(4)	-679(3)	2147(2)	44(1)	C(37)	568(8)	-858(5)	4003(3)	84(3)
N(2)	-127(4)	-1195(3)	2404(2)	45(1)	C(38)	848(6)	-217(4)	3787(3)	59(2)
N(3)	2155(4)	-520(3)	2387(2)	42(1)	C(39)	1087(6)	577(4)	4026(3)	59(2)
N(4)	1809(4)	-1050(3)	2635(2)	42(1)	C(40)	1323(5)	914(4)	3657(2)	46(2)
N(5)	1235(4)	378(3)	3208(2)	41(1)	C(41)	1638(5)	1762(4)	3718(2)	42(2)
N(6)	935(4)	-325(3)	3289(2)	49(1)	C(42)	2227(5)	2078(4)	3425(2)	44(2)
N(7)	2750(4)	6927(3)	3807(2)	36(1)	C(43)	2485(5)	2876(4)	3499(2)	49(2)
N(8)	3328(4)	7555(3)	4222(2)	37(1)	C(44)	2149(5)	3365(4)	3887(3)	49(2)
N(9)	4793(4)	7374(3)	3419(2)	39(1)	C(45)	1566(6)	3046(4)	4189(3)	54(2)
N(10)	5000(4)	7942(3)	3889(2)	39(1)	C(46)	1282(5)	2251(4)	4113(2)	48(2)
N(11)	4725(4)	6401(3)	4049(2)	36(1)	C(47)	2394(6)	4226(4)	3959(3)	59(2)
N(12)	4914(4)	7094(3)	4443(2)	36(1)	C(48)	2900(8)	4713(5)	4503(3)	88(3)
C(1)	1595(4)	1487(3)	2044(2)	33(1)	C(49)	1429(8)	4405(5)	3771(4)	107(4)
C(2)	2030(5)	1988(3)	1784(2)	36(1)	C(50)	2902(4)	4977(3)	2594(2)	33(1)
C(3)	1574(5)	2542(3)	1717(2)	33(1)	C(51)	2677(5)	4195(3)	2307(2)	34(1)
C(4)	668(5)	2625(3)	1939(2)	40(2)	C(52)	2243(5)	3931(3)	1783(2)	38(2)
C(5)	180(4)	2152(3)	2193(2)	34(1)	C(53)	1970(5)	4464(3)	1547(2)	42(2)
C(6)	643(5)	1549(3)	2247(2)	36(1)	C(54)	2145(5)	5234(3)	1802(2)	38(1)
C(7)	-798(5)	2228(3)	2418(2)	41(2)	C(55)	2642(5)	5518(3)	2341(2)	35(1)
C(8)	-1162(6)	2904(4)	2328(3)	60(2)	C(56)	1802(5)	5781(4)	1545(2)	46(2)
C(9)	-572(5)	2373(4)	3000(3)	51(2)	C(57)	991(6)	6082(4)	1817(3)	60(2)
C(10)	-1716(5)	1490(4)	2148(3)	52(2)	C(58)	1343(6)	5368(4)	962(3)	64(2)
C(11)	-1343(7)	-2457(5)	2386(4)	87(3)	C(59)	2744(6)	6468(4)	1595(3)	54(2)
C(12)	-1040(6)	-1781(4)	2194(3)	59(2)	C(60)	3063(6)	8624(4)	4932(3)	55(2)
C(13)	-1573(6)	-1629(4)	1789(3)	66(2)	C(61)	2686(5)	7927(4)	4460(2)	42(2)
C(14)	-963(5)	-935(4)	1773(3)	46(2)	C(62)	1656(5)	7527(4)	4191(2)	45(2)
C(15)	-1149(6)	-526(4)	1415(2)	48(2)	C(63)	1741(5)	6918(3)	3786(2)	35(1)
C(16)	-320(6)	-111(4)	1244(3)	53(2)	C(64)	863(5)	6343(3)	3374(2)	38(1)
C(17)	-510(6)	270(4)	903(3)	56(2)	C(65)	-66(5)	6529(4)	3244(3)	49(2)
C(18)	-1581(7)	228(4)	709(3)	57(2)	C(66)	-879(5)	6020(4)	2851(3)	46(2)
C(19)	-2376(6)	-175(4)	873(3)	58(2)	C(67)	-819(5)	5311(3)	2574(2)	41(2)
C(20)	-2170(6)	-549(4)	1228(3)	56(2)	C(68)	98(5)	5126(4)	2691(3)	46(2)
C(21)	-1787(7)	659(4)	333(3)	67(2)	C(69)	927(5)	5628(3)	3086(2)	42(2)
C(22)	-1363(8)	1542(4)	592(3)	79(3)	C(70)	-1738(5)	4741(4)	2148(3)	52(2)
C(23)	-1343(8)	421(5)	-152(3)	87(3)	C(71)	-2079(7)	5110(5)	1760(3)	77(2)
C(24)	2408(6)	-2017(4)	2963(3)	61(2)	C(72)	-2636(6)	4409(5)	2360(3)	74(2)
C(25)	2513(6)	-1444(4)	2680(3)	45(2)	C(73)	6060(6)	9327(4)	4309(3)	60(2)
C(26)	3327(6)	-1174(4)	2449(3)	50(2)	C(74)	5662(5)	8599(4)	3865(3)	47(2)
C(27)	3076(5)	-604(4)	2269(2)	41(2)	C(75)	5889(6)	8436(4)	3369(3)	52(2)
C(28)	3691(5)	-169(4)	1994(3)	46(2)	C(76)	5349(5)	7672(3)	3116(2)	42(2)
C(29)	4806(6)	38(5)	2121(3)	63(2)	C(77)	5411(5)	7179(4)	2601(3)	50(2)
C(30)	5417(6)	423(5)	1856(3)	67(2)	C(78)	5275(5)	6381(4)	2487(3)	48(2)

C(79)	5344(6)	5935(4)	2007(3)	58(2)	C(102)	4126(6)	3243(4)	785(3)	59(2)
C(80)	5552(6)	6236(4)	1622(3)	56(2)	C(103)	3095(5)	3485(4)	821(2)	46(2)
C(81)	5691(6)	7003(5)	1724(3)	60(2)	C(104)	2577(7)	3448(4)	282(3)	59(2)
C(82)	5606(5)	7500(4)	2205(3)	52(2)	C(105)	2344(7)	2621(4)	-93(3)	66(2)
C(83)	5602(6)	5719(6)	1084(3)	72(2)	C(106)	1612(6)	2065(4)	108(3)	53(2)
C(84)	4637(8)	5585(6)	705(3)	108(4)	C(107)	2110(5)	2086(3)	635(2)	45(2)
C(85)	6611(6)	6013(5)	924(3)	68(2)	C(108)	3173(6)	1889(4)	597(3)	50(2)
C(86)	5834(6)	7749(4)	5380(2)	54(2)	C(109)	3415(7)	2413(4)	-119(3)	63(2)
C(87)	5492(5)	7081(4)	4880(2)	42(2)	C(111)	3838(8)	436(6)	3651(4)	24(2)
C(88)	5687(5)	6374(4)	4768(3)	48(2)	C(112)	8509(8)	10238(6)	3107(4)	31(3)
C(89)	5220(5)	5972(4)	4241(2)	42(2)	C(113)	8431(8)	3524(6)	4883(4)	27(2)
C(90)	5277(5)	5211(4)	3932(3)	46(2)	C(114)	8158(9)	5229(6)	3891(4)	32(3)
C(91)	5354(6)	4648(4)	4187(3)	65(2)	B(1)	773(6)	-1089(5)	2842(3)	49(2)
C(92)	5420(7)	3939(4)	3905(4)	80(3)	B(2)	4557(6)	7772(4)	4343(3)	40(2)
C(93)	5388(6)	3726(4)	3376(4)	81(3)	Cl(1)	3639(2)	11(2)	4125(1)	44(1)
C(94)	5340(6)	4276(4)	3143(3)	65(2)	Cl(2)	5185(2)	768(2)	3636(1)	43(1)
C(95)	5286(5)	5005(4)	3417(3)	46(2)	Cl(3)	7351(2)	9756(2)	2645(1)	46(1)
C(96)	5414(9)	2929(6)	3066(5)	126(4)	Cl(4)	8261(3)	10756(3)	3690(2)	91(2)
C(97)	6306(9)	2710(7)	3214(4)	121(4)	Cl(5)	8896(3)	2848(2)	4468(1)	57(1)
C(98)	4589(7)	2498(5)	2631(4)	97(3)	Cl(6)	7062(2)	3240(2)	4776(1)	38(1)
C(99)	2049(5)	3102(3)	1468(2)	37(1)	Cl(7)	8771(4)	6024(3)	4428(1)	78(1)
C(100)	2395(5)	2919(3)	1018(2)	40(2)	Cl(8)	8730(4)	4475(3)	3823(2)	80(1)
C(101)	3903(6)	2449(4)	414(3)	54(2)					

_____

Table 3. Bond lengths [A] and angles [deg] for kva.

_____

Zn(1)-O(1)	1.955(4)	N(7)-C(63)	1.336(7)
Zn(1)-N(1)	2.038(5)	N(7)-N(8)	1.369(6)
Zn(1)-N(5)	2.047(5)	N(8)-C(61)	1.348(7)
Zn(1)-O(2)	2.136(4)	N(8)-B(2)	1.560(9)
Zn(1)-N(3)	2.198(5)	N(9)-C(76)	1.331(8)
Zn(2)-O(3)	1.965(4)	N(9)-N(10)	1.370(6)
Zn(2)-N(7)	2.042(5)	N(10)-C(74)	1.357(8)
Zn(2)-N(9)	2.062(5)	N(10)-B(2)	1.526(9)
Zn(2)-O(4)	2.112(4)	N(11)-C(89)	1.342(7)
Zn(2)-N(11)	2.177(5)	N(11)-N(12)	1.383(6)
O(1)-C(1)	1.293(6)	N(12)-C(87)	1.362(8)
O(2)-C(6)	1.278(7)	N(12)-B(2)	1.552(8)
O(3)-C(50)	1.290(7)	C(1)-C(2)	1.400(8)
O(4)-C(55)	1.283(6)	C(1)-C(6)	1.462(8)
N(1)-N(2)	1.353(7)	C(2)-C(3)	1.376(8)
N(1)-C(14)	1.364(8)	C(3)-C(4)	1.439(8)
N(2)-C(12)	1.359(8)	C(3)-C(99)	1.474(8)
N(2)-B(1)	1.534(9)	C(4)-C(5)	1.374(8)
N(3)-C(27)	1.341(8)	C(5)-C(6)	1.455(8)
N(3)-N(4)	1.385(7)	C(5)-C(7)	1.528(8)
N(4)-C(25)	1.347(8)	C(7)-C(9)	1.529(9)
N(4)-B(1)	1.548(9)	C(7)-C(10)	1.534(8)
N(5)-C(40)	1.326(8)	C(7)-C(8)	1.544(9)
N(5)-N(6)	1.379(7)	C(11)-C(12)	1.502(10)
N(6)-C(38)	1.352(8)	C(12)-C(13)	1.390(10)
N(6)-B(1)	1.552(9)	C(13)-C(14)	1.378(9)

C(14)-C(15)	1.450(9)	C(65)-C(66)	1.375(9)
C(15)-C(20)	1.385(9)	C(66)-C(67)	1.364(8)
C(15)-C(16)	1.401(10)	C(67)-C(68)	1.380(9)
C(16)-C(17)	1.372(9)	C(67)-C(70)	1.528(9)
C(17)-C(18)	1.441(10)	C(68)-C(69)	1.386(9)
C(18)-C(19)	1.349(10)	C(70)-C(72)	1.474(10)
C(18)-C(21)	1.529(10)	C(70)-C(71)	1.518(10)
C(19)-C(20)	1.401(10)	C(73)-C(74)	1.483(9)
C(21)-C(23)	1.518(11)	C(74)-C(75)	1.398(9)
C(21)-C(22)	1.539(10)	C(75)-C(76)	1.372(9)
C(24)-C(25)	1.494(9)	C(76)-C(77)	1.482(9)
C(25)-C(26)	1.385(10)	C(77)-C(78)	1.407(9)
C(26)-C(27)	1.401(9)	C(77)-C(82)	1.412(9)
C(27)-C(28)	1.447(9)	C(78)-C(79)	1.377(9)
C(28)-C(33)	1.389(9)	C(79)-C(80)	1.365(10)
C(28)-C(29)	1.415(10)	C(80)-C(81)	1.354(10)
C(29)-C(30)	1.371(10)	C(80)-C(83)	1.542(10)
C(30)-C(31)	1.348(10)	C(81)-C(82)	1.421(10)
C(31)-C(32)	1.426(10)	C(83)-C(84)	1.481(12)
C(31)-C(34)	1.527(10)	C(83)-C(85)	1.492(11)
C(32)-C(33)	1.354(9)	C(86)-C(87)	1.507(9)
C(34)-C(36)	1.503(11)	C(87)-C(88)	1.377(9)
C(34)-C(35)	1.540(10)	C(88)-C(89)	1.413(9)
C(37)-C(38)	1.484(10)	C(89)-C(90)	1.470(9)
C(38)-C(39)	1.389(10)	C(90)-C(95)	1.363(9)
C(39)-C(40)	1.375(9)	C(90)-C(91)	1.449(9)
C(40)-C(41)	1.505(9)	C(91)-C(92)	1.370(11)
C(41)-C(42)	1.349(9)	C(92)-C(93)	1.390(13)
C(41)-C(46)	1.420(9)	C(93)-C(94)	1.378(12)
C(42)-C(43)	1.408(9)	C(93)-C(96)	1.513(12)
C(43)-C(44)	1.394(9)	C(94)-C(95)	1.389(9)
C(44)-C(45)	1.365(10)	C(96)-C(97)	1.406(12)
C(44)-C(47)	1.526(9)	C(96)-C(98)	1.416(13)
C(45)-C(46)	1.401(9)	C(99)-C(100)	1.355(8)
C(47)-C(49)	1.483(11)	C(100)-C(103)	1.508(9)
C(47)-C(48)	1.491(11)	C(100)-C(107)	1.546(8)
C(50)-C(51)	1.397(8)	C(101)-C(102)	1.487(9)
C(50)-C(55)	1.474(8)	C(101)-C(108)	1.495(9)
C(51)-C(52)	1.386(8)	C(101)-C(109)	1.512(10)
C(52)-C(53)	1.437(8)	C(102)-C(103)	1.557(10)
C(52)-C(99)	1.497(8)	C(103)-C(104)	1.537(10)
C(53)-C(54)	1.367(8)	C(104)-C(105)	1.537(9)
C(54)-C(55)	1.441(8)	C(105)-C(106)	1.522(10)
C(54)-C(56)	1.533(8)	C(105)-C(109)	1.575(11)
C(56)-C(57)	1.516(9)	C(106)-C(107)	1.512(9)
C(56)-C(59)	1.528(9)	C(107)-C(108)	1.559(9)
C(56)-C(58)	1.544(9)	C(111)-Cl(1)	1.733(11)
C(60)-C(61)	1.488(8)	C(111)-Cl(2)	1.760(10)
C(61)-C(62)	1.394(9)	C(112)-Cl(4)	1.738(12)
C(62)-C(63)	1.391(8)	C(112)-Cl(3)	1.740(11)
C(63)-C(64)	1.482(8)	C(113)-Cl(6)	1.735(10)
C(64)-C(69)	1.384(8)	C(113)-Cl(5)	1.742(10)
C(64)-C(65)	1.404(9)	C(114)-Cl(7)	1.719(11)

C(114)-CI(8)	1.748(11)	C(74)-N(10)-B(2)	130.2(5)
O(1)-Zn(1)-N(1)	131.32(19)	N(9)-N(10)-B(2)	120.9(5)
O(1)-Zn(1)-N(5)	131.52(19)	C(89)-N(11)-N(12)	106.3(5)
N(1)-Zn(1)-N(5)	96.8(2)	C(89)-N(11)-Zn(2)	143.7(4)
O(1)-Zn(1)-O(2)	80.17(16)	N(12)-N(11)-Zn(2)	109.7(3)
N(1)-Zn(1)-O(2)	93.82(18)	C(87)-N(12)-N(11)	110.2(5)
N(5)-Zn(1)-O(2)	93.06(18)	C(87)-N(12)-B(2)	128.8(5)
O(1)-Zn(1)-N(3)	98.07(18)	N(11)-N(12)-B(2)	120.8(5)
N(1)-Zn(1)-N(3)	85.8(2)	O(1)-C(1)-C(2)	122.7(5)
N(5)-Zn(1)-N(3)	89.60(19)	O(1)-C(1)-C(6)	117.4(5)
O(2)-Zn(1)-N(3)	177.34(17)	C(2)-C(1)-C(6)	119.9(5)
O(3)-Zn(2)-N(7)	123.00(18)	C(3)-C(2)-C(1)	120.8(6)
O(3)-Zn(2)-N(9)	140.72(19)	C(2)-C(3)-C(4)	119.0(5)
N(7)-Zn(2)-N(9)	96.27(19)	C(2)-C(3)-C(99)	121.8(5)
O(3)-Zn(2)-O(4)	80.38(15)	C(4)-C(3)-C(99)	118.9(5)
N(7)-Zn(2)-O(4)	99.84(17)	C(5)-C(4)-C(3)	123.9(5)
N(9)-Zn(2)-O(4)	93.40(18)	C(4)-C(5)-C(6)	116.8(5)
O(3)-Zn(2)-N(11)	91.95(16)	C(4)-C(5)-C(7)	123.9(5)
N(7)-Zn(2)-N(11)	94.64(18)	C(6)-C(5)-C(7)	119.3(5)
N(9)-Zn(2)-N(11)	84.75(19)	O(2)-C(6)-C(5)	123.5(5)
O(4)-Zn(2)-N(11)	165.51(17)	O(2)-C(6)-C(1)	117.0(5)
C(1)-O(1)-Zn(1)	115.2(4)	C(5)-C(6)-C(1)	119.4(5)
C(6)-O(2)-Zn(1)	110.0(4)	C(5)-C(7)-C(9)	110.6(5)
C(50)-O(3)-Zn(2)	114.6(3)	C(5)-C(7)-C(10)	109.6(5)
C(55)-O(4)-Zn(2)	110.9(3)	C(9)-C(7)-C(10)	110.1(5)
N(2)-N(1)-C(14)	107.7(5)	C(5)-C(7)-C(8)	111.7(5)
N(2)-N(1)-Zn(1)	114.6(4)	C(9)-C(7)-C(8)	107.9(5)
C(14)-N(1)-Zn(1)	137.4(4)	C(10)-C(7)-C(8)	106.8(5)
N(1)-N(2)-C(12)	109.3(5)	N(2)-C(12)-C(13)	107.7(6)
N(1)-N(2)-B(1)	121.1(5)	N(2)-C(12)-C(11)	123.0(7)
C(12)-N(2)-B(1)	129.6(6)	C(13)-C(12)-C(11)	129.3(7)
C(27)-N(3)-N(4)	106.4(5)	C(14)-C(13)-C(12)	106.4(7)
C(27)-N(3)-Zn(1)	141.1(4)	N(1)-C(14)-C(13)	108.8(6)
N(4)-N(3)-Zn(1)	111.2(4)	N(1)-C(14)-C(15)	122.4(6)
C(25)-N(4)-N(3)	110.5(5)	C(13)-C(14)-C(15)	128.7(6)
C(25)-N(4)-B(1)	129.4(6)	C(20)-C(15)-C(16)	118.3(6)
N(3)-N(4)-B(1)	119.9(5)	C(20)-C(15)-C(14)	119.8(6)
C(40)-N(5)-N(6)	106.4(5)	C(16)-C(15)-C(14)	121.8(6)
C(40)-N(5)-Zn(1)	139.2(4)	C(17)-C(16)-C(15)	121.1(7)
N(6)-N(5)-Zn(1)	113.6(4)	C(16)-C(17)-C(18)	119.5(7)
C(38)-N(6)-N(5)	110.1(5)	C(19)-C(18)-C(17)	119.2(7)
C(38)-N(6)-B(1)	129.4(6)	C(19)-C(18)-C(21)	121.5(7)
N(5)-N(6)-B(1)	120.5(5)	C(17)-C(18)-C(21)	119.3(7)
C(63)-N(7)-N(8)	106.6(4)	C(18)-C(19)-C(20)	120.7(7)
C(63)-N(7)-Zn(2)	139.7(4)	C(15)-C(20)-C(19)	121.2(7)
N(8)-N(7)-Zn(2)	113.2(4)	C(23)-C(21)-C(18)	113.2(7)
C(61)-N(8)-N(7)	110.3(5)	C(23)-C(21)-C(22)	109.5(7)
C(61)-N(8)-B(2)	129.1(5)	C(18)-C(21)-C(22)	111.9(6)
N(7)-N(8)-B(2)	120.5(5)	N(4)-C(25)-C(26)	106.9(6)
C(76)-N(9)-N(10)	107.3(5)	N(4)-C(25)-C(24)	123.6(6)
C(76)-N(9)-Zn(2)	139.9(4)	C(26)-C(25)-C(24)	129.3(6)
N(10)-N(9)-Zn(2)	112.5(4)	C(25)-C(26)-C(27)	106.8(6)
C(74)-N(10)-N(9)	108.9(5)	N(3)-C(27)-C(26)	109.3(6)

N(3)-C(27)-C(28)	124.2(6)	C(59)-C(56)-C(58)	107.2(6)
C(26)-C(27)-C(28)	126.5(6)	C(54)-C(56)-C(58)	111.4(5)
C(33)-C(28)-C(29)	116.7(7)	N(8)-C(61)-C(62)	107.3(5)
C(33)-C(28)-C(27)	124.1(6)	N(8)-C(61)-C(60)	123.9(6)
C(29)-C(28)-C(27)	119.1(6)	C(62)-C(61)-C(60)	128.8(6)
C(30)-C(29)-C(28)	120.9(7)	C(63)-C(62)-C(61)	105.6(6)
C(31)-C(30)-C(29)	122.4(8)	N(7)-C(63)-C(62)	110.2(5)
C(30)-C(31)-C(32)	117.2(7)	N(7)-C(63)-C(64)	123.4(5)
C(30)-C(31)-C(34)	120.7(7)	C(62)-C(63)-C(64)	126.4(6)
C(32)-C(31)-C(34)	122.1(7)	C(69)-C(64)-C(65)	116.9(6)
C(33)-C(32)-C(31)	121.3(7)	C(69)-C(64)-C(63)	123.0(6)
C(32)-C(33)-C(28)	121.5(7)	C(65)-C(64)-C(63)	119.9(5)
C(36)-C(34)-C(31)	113.4(7)	C(66)-C(65)-C(64)	121.4(6)
C(36)-C(34)-C(35)	109.5(7)	C(67)-C(66)-C(65)	121.4(6)
C(31)-C(34)-C(35)	111.0(6)	C(66)-C(67)-C(68)	117.8(6)
N(6)-C(38)-C(39)	106.4(6)	C(66)-C(67)-C(70)	121.0(6)
N(6)-C(38)-C(37)	123.4(7)	C(68)-C(67)-C(70)	121.2(6)
C(39)-C(38)-C(37)	130.2(7)	C(67)-C(68)-C(69)	121.8(6)
C(40)-C(39)-C(38)	106.7(6)	C(64)-C(69)-C(68)	120.6(6)
N(5)-C(40)-C(39)	110.4(6)	C(72)-C(70)-C(71)	111.2(7)
N(5)-C(40)-C(41)	121.7(6)	C(72)-C(70)-C(67)	111.9(6)
C(39)-C(40)-C(41)	127.9(6)	C(71)-C(70)-C(67)	111.4(6)
C(42)-C(41)-C(46)	119.0(6)	N(10)-C(74)-C(75)	107.6(5)
C(42)-C(41)-C(40)	124.2(6)	N(10)-C(74)-C(73)	123.3(6)
C(46)-C(41)-C(40)	116.8(6)	C(75)-C(74)-C(73)	129.1(6)
C(41)-C(42)-C(43)	121.3(6)	C(76)-C(75)-C(74)	105.6(6)
C(44)-C(43)-C(42)	120.4(6)	N(9)-C(76)-C(75)	110.6(6)
C(45)-C(44)-C(43)	118.1(6)	N(9)-C(76)-C(77)	121.0(5)
C(45)-C(44)-C(47)	121.1(7)	C(75)-C(76)-C(77)	128.1(6)
C(43)-C(44)-C(47)	120.7(7)	C(78)-C(77)-C(82)	117.8(6)
C(44)-C(45)-C(46)	122.2(7)	C(78)-C(77)-C(76)	121.7(6)
C(45)-C(46)-C(41)	118.9(7)	C(82)-C(77)-C(76)	120.5(6)
C(49)-C(47)-C(48)	112.4(8)	C(79)-C(78)-C(77)	120.8(7)
C(49)-C(47)-C(44)	110.3(6)	C(80)-C(79)-C(78)	122.4(7)
C(48)-C(47)-C(44)	111.8(6)	C(81)-C(80)-C(79)	117.8(7)
O(3)-C(50)-C(51)	122.7(5)	C(81)-C(80)-C(83)	120.9(7)
O(3)-C(50)-C(55)	117.5(5)	C(79)-C(80)-C(83)	121.3(7)
C(51)-C(50)-C(55)	119.7(5)	C(80)-C(81)-C(82)	123.2(7)
C(52)-C(51)-C(50)	120.3(5)	C(77)-C(82)-C(81)	118.0(7)
C(51)-C(52)-C(53)	119.0(5)	C(84)-C(83)-C(85)	114.7(7)
C(51)-C(52)-C(99)	120.5(5)	C(84)-C(83)-C(80)	110.3(7)
C(53)-C(52)-C(99)	120.5(5)	C(85)-C(83)-C(80)	112.0(7)
C(54)-C(53)-C(52)	124.3(6)	N(12)-C(87)-C(88)	107.5(5)
C(53)-C(54)-C(55)	116.8(5)	N(12)-C(87)-C(86)	123.5(5)
C(53)-C(54)-C(56)	123.0(5)	C(88)-C(87)-C(86)	129.0(6)
C(55)-C(54)-C(56)	120.1(5)	C(87)-C(88)-C(89)	106.2(6)
O(4)-C(55)-C(54)	124.2(5)	N(11)-C(89)-C(88)	109.7(5)
O(4)-C(55)-C(50)	116.0(5)	N(11)-C(89)-C(90)	123.5(6)
C(54)-C(55)-C(50)	119.7(5)	C(88)-C(89)-C(90)	126.8(6)
C(57)-C(56)-C(59)	108.7(6)	C(95)-C(90)-C(91)	117.4(6)
C(57)-C(56)-C(54)	108.3(5)	C(95)-C(90)-C(89)	123.8(6)
C(59)-C(56)-C(54)	110.6(5)	C(91)-C(90)-C(89)	118.8(6)
C(57)-C(56)-C(58)	110.6(6)	C(92)-C(91)-C(90)	119.5(8)

C(91)-C(92)-C(93)	122.5(8)		C(104)-C(103)-C(102)	109.4(6)
C(94)-C(93)-C(92)	117.1(7)		C(105)-C(104)-C(103)	109.0(6)
C(94)-C(93)-C(96)	121.1(10)		C(106)-C(105)-C(104)	108.8(6)
C(92)-C(93)-C(96)	121.8(9)		C(106)-C(105)-C(109)	109.7(6)
C(93)-C(94)-C(95)	122.1(8)		C(104)-C(105)-C(109)	108.9(7)
C(90)-C(95)-C(94)	121.4(7)		C(107)-C(106)-C(105)	111.6(6)
C(97)-C(96)-C(98)	125.8(9)		C(106)-C(107)-C(100)	109.4(5)
C(97)-C(96)-C(93)	116.5(9)		C(106)-C(107)-C(108)	108.5(5)
C(98)-C(96)-C(93)	117.5(8)		C(100)-C(107)-C(108)	106.3(5)
C(100)-C(99)-C(3)	125.0(5)		C(101)-C(108)-C(107)	111.0(5)
C(100)-C(99)-C(52)	120.1(5)		C(101)-C(109)-C(105)	108.7(6)
C(3)-C(99)-C(52)	114.6(5)		CI(1)-C(111)-CI(2)	112.2(5)
C(99)-C(100)-C(103)	125.5(5)		CI(4)-C(112)-CI(3)	111.6(6)
C(99)-C(100)-C(107)	123.6(6)		CI(6)-C(113)-CI(5)	111.5(6)
C(103)-C(100)-C(107)	110.9(5)		CI(7)-C(114)-CI(8)	113.8(6)
C(102)-C(101)-C(108)	109.1(6)		N(2)-B(1)-N(4)	109.4(6)
C(102)-C(101)-C(109)	110.3(6)		N(2)-B(1)-N(6)	110.4(6)
C(108)-C(101)-C(109)	110.2(6)		N(4)-B(1)-N(6)	108.5(6)
C(101)-C(102)-C(103)	111.0(6)		N(10)-B(2)-N(12)	108.8(5)
C(100)-C(103)-C(104)	111.3(6)		N(10)-B(2)-N(8)	110.2(5)
C(100)-C(103)-C(102)	106.0(5)		N(12)-B(2)-N(8)	110.2(5)

Symmetry transformations used to generate equivalent atoms:

Table 4. Anisotropic displacement parameters (A^2 x 10^3) for kva.
The anisotropic displacement factor exponent takes the form: -2 pi^2 [h^2 a*^2 U11 + ... + 2 h k a* b* U12]

	U11	U22	U33	U23	U13	U12
Zn(1)	42(1)	33(1)	41(1)	16(1)	7(1)	11(1)
Zn(2)	42(1)	29(1)	32(1)	6(1)	6(1)	10(1)
O(1)	44(3)	35(2)	47(3)	18(2)	15(2)	16(2)
O(2)	40(2)	36(2)	42(2)	19(2)	10(2)	10(2)
O(3)	46(3)	35(2)	27(2)	6(2)	-2(2)	12(2)
O(4)	51(3)	27(2)	36(2)	7(2)	6(2)	12(2)
N(1)	49(3)	36(3)	46(3)	16(3)	9(3)	8(2)
N(2)	47(3)	37(3)	60(4)	28(3)	14(3)	13(3)
N(3)	48(3)	34(3)	46(3)	16(2)	8(3)	12(2)
N(4)	48(3)	35(3)	45(3)	16(2)	9(3)	14(2)
N(5)	49(3)	41(3)	40(3)	18(3)	11(2)	17(3)
N(6)	63(4)	47(3)	49(3)	28(3)	18(3)	22(3)
N(7)	44(3)	29(3)	33(3)	6(2)	2(2)	11(2)
N(8)	44(3)	36(3)	28(3)	7(2)	4(2)	13(2)
N(9)	50(3)	31(3)	31(3)	4(2)	8(2)	8(2)
N(10)	48(3)	26(3)	34(3)	3(2)	5(2)	6(2)
N(11)	39(3)	33(3)	35(3)	9(2)	8(2)	8(2)
N(12)	41(3)	36(3)	27(3)	3(2)	3(2)	13(2)
C(1)	36(3)	32(3)	30(3)	9(3)	4(3)	12(3)
C(2)	42(4)	31(3)	33(3)	9(3)	7(3)	9(3)
C(3)	36(3)	26(3)	33(3)	7(3)	8(3)	5(3)
C(4)	46(4)	30(3)	38(3)	9(3)	-2(3)	10(3)
C(5)	32(3)	31(3)	34(3)	7(3)	-1(3)	6(3)

C(6)	39(4)	28(3)	35(3)	6(3)	-1(3)	9(3)
C(7)	38(4)	37(3)	47(4)	13(3)	5(3)	11(3)
C(8)	51(4)	56(5)	87(6)	33(4)	20(4)	28(4)
C(9)	39(4)	57(4)	52(4)	7(3)	11(3)	17(3)
C(10)	39(4)	48(4)	66(5)	16(4)	6(3)	11(3)
C(11)	72(6)	74(6)	126(8)	69(6)	11(5)	0(5)
C(12)	53(5)	44(4)	76(5)	24(4)	3(4)	5(4)
C(13)	59(5)	48(4)	84(6)	31(4)	-2(4)	1(4)
C(14)	36(4)	41(4)	57(4)	17(3)	0(3)	8(3)
C(15)	56(4)	32(3)	43(4)	8(3)	-3(3)	4(3)
C(16)	56(4)	41(4)	48(4)	8(3)	-4(3)	8(3)
C(17)	67(5)	46(4)	45(4)	13(3)	1(4)	9(4)
C(18)	75(5)	42(4)	41(4)	-2(3)	-9(4)	20(4)
C(19)	63(5)	52(4)	54(5)	12(4)	3(4)	14(4)
C(20)	55(5)	45(4)	58(5)	14(3)	-6(4)	11(3)
C(21)	86(6)	64(5)	49(5)	19(4)	5(4)	24(4)
C(22)	130(8)	57(5)	62(5)	22(4)	17(5)	43(5)
C(23)	109(8)	88(7)	65(6)	31(5)	11(5)	27(6)
C(24)	82(6)	45(4)	73(5)	28(4)	22(4)	35(4)
C(25)	56(4)	40(4)	44(4)	13(3)	8(3)	22(3)
C(26)	54(4)	52(4)	49(4)	13(3)	6(3)	29(4)
C(27)	40(4)	40(4)	41(4)	9(3)	9(3)	13(3)
C(28)	46(4)	38(4)	50(4)	6(3)	7(3)	15(3)
C(29)	52(5)	72(5)	55(5)	16(4)	6(4)	9(4)
C(30)	54(5)	73(5)	49(5)	7(4)	3(4)	-3(4)
C(31)	49(4)	41(4)	61(5)	5(3)	18(4)	12(3)
C(32)	61(5)	48(4)	49(4)	12(3)	20(4)	23(4)
C(33)	46(4)	36(4)	56(4)	14(3)	22(3)	18(3)
C(34)	57(5)	58(5)	56(5)	11(4)	15(4)	6(4)
C(35)	52(5)	74(6)	75(5)	29(4)	19(4)	6(4)
C(36)	93(7)	104(7)	68(6)	15(5)	28(5)	36(6)
C(37)	126(8)	78(6)	76(6)	48(5)	56(6)	39(6)
C(38)	89(6)	61(5)	51(4)	33(4)	31(4)	36(4)
C(39)	87(6)	63(5)	45(4)	28(4)	30(4)	33(4)
C(40)	51(4)	46(4)	42(4)	14(3)	3(3)	22(3)
C(41)	44(4)	48(4)	36(4)	15(3)	4(3)	13(3)
C(42)	36(4)	56(4)	36(4)	14(3)	2(3)	11(3)
C(43)	45(4)	58(5)	39(4)	16(3)	5(3)	9(3)
C(44)	45(4)	50(4)	48(4)	20(3)	0(3)	8(3)
C(45)	61(5)	51(4)	49(4)	13(4)	6(4)	19(4)
C(46)	59(4)	52(4)	36(4)	12(3)	8(3)	21(3)
C(47)	63(5)	45(4)	62(5)	16(4)	6(4)	7(4)
C(48)	140(9)	49(5)	77(6)	21(5)	21(6)	32(5)
C(49)	91(7)	79(7)	149(10)	67(7)	-28(7)	8(5)
C(50)	37(3)	30(3)	32(3)	10(3)	9(3)	10(3)
C(51)	45(4)	30(3)	29(3)	11(3)	5(3)	14(3)
C(52)	49(4)	27(3)	36(3)	7(3)	6(3)	10(3)
C(53)	50(4)	37(4)	38(4)	13(3)	-3(3)	12(3)
C(54)	48(4)	31(3)	35(3)	10(3)	5(3)	14(3)
C(55)	42(4)	29(3)	34(3)	9(3)	7(3)	10(3)
C(56)	59(4)	39(4)	40(4)	14(3)	4(3)	18(3)
C(57)	60(5)	64(5)	74(5)	39(4)	13(4)	31(4)
C(58)	80(5)	61(5)	52(4)	30(4)	-11(4)	18(4)

C(59)	69(5)	42(4)	59(5)	25(3)	12(4)	20(4)
C(60)	63(5)	47(4)	45(4)	-1(3)	10(3)	18(4)
C(61)	50(4)	41(4)	40(4)	12(3)	12(3)	20(3)
C(62)	55(4)	41(4)	40(4)	9(3)	10(3)	20(3)
C(63)	40(4)	32(3)	34(3)	12(3)	4(3)	12(3)
C(64)	48(4)	29(3)	40(4)	14(3)	10(3)	13(3)
C(65)	50(4)	40(4)	60(4)	15(3)	13(4)	17(3)
C(66)	40(4)	41(4)	53(4)	11(3)	1(3)	14(3)
C(67)	46(4)	36(4)	42(4)	18(3)	10(3)	10(3)
C(68)	48(4)	36(4)	50(4)	11(3)	5(3)	9(3)
C(69)	45(4)	35(4)	48(4)	16(3)	9(3)	12(3)
C(70)	42(4)	45(4)	58(4)	11(3)	-1(3)	7(3)
C(71)	71(6)	81(6)	61(5)	17(5)	-12(4)	11(5)
C(72)	53(5)	71(6)	83(6)	14(5)	2(4)	10(4)
C(73)	80(5)	34(4)	53(4)	8(3)	12(4)	5(4)
C(74)	49(4)	34(4)	47(4)	10(3)	5(3)	1(3)
C(75)	58(5)	39(4)	51(4)	13(3)	12(3)	2(3)
C(76)	48(4)	37(4)	34(3)	7(3)	9(3)	4(3)
C(77)	39(4)	60(5)	44(4)	13(3)	16(3)	2(3)
C(78)	58(4)	42(4)	44(4)	9(3)	21(3)	17(3)
C(79)	59(5)	55(4)	56(5)	7(4)	18(4)	15(4)
C(80)	54(5)	52(5)	54(5)	9(4)	16(4)	8(4)
C(81)	58(5)	76(6)	37(4)	21(4)	13(3)	-1(4)
C(82)	47(4)	57(4)	48(4)	15(4)	18(3)	4(3)
C(83)	66(5)	105(7)	40(4)	10(4)	21(4)	29(5)
C(84)	86(7)	127(9)	54(5)	-31(6)	15(5)	3(6)
C(85)	79(6)	85(6)	49(5)	26(4)	24(4)	26(5)
C(86)	59(5)	62(5)	35(4)	9(3)	1(3)	18(4)
C(87)	39(4)	44(4)	40(4)	14(3)	5(3)	11(3)
C(88)	49(4)	45(4)	45(4)	14(3)	-4(3)	11(3)
C(89)	41(4)	39(4)	47(4)	16(3)	6(3)	11(3)
C(90)	41(4)	36(4)	55(4)	14(3)	-1(3)	10(3)
C(91)	67(5)	39(4)	77(5)	20(4)	-17(4)	8(4)
C(92)	95(7)	38(4)	90(7)	15(4)	-30(5)	17(4)
C(93)	64(5)	35(4)	119(8)	5(5)	-32(5)	20(4)
C(94)	47(4)	61(5)	69(5)	-4(4)	-6(4)	19(4)
C(95)	42(4)	42(4)	53(4)	10(3)	7(3)	17(3)
C(96)	117(7)	93(6)	153(8)	5(6)	-23(6)	71(6)
C(97)	125(9)	123(9)	109(9)	0(7)	12(7)	79(8)
C(98)	78(6)	72(5)	104(6)	-21(5)	-1(5)	24(5)
C(99)	53(4)	25(3)	30(3)	8(3)	4(3)	10(3)
C(100)	51(4)	34(3)	33(3)	10(3)	4(3)	12(3)
C(101)	66(5)	43(4)	59(5)	19(3)	25(4)	19(3)
C(102)	61(5)	56(5)	62(5)	24(4)	24(4)	10(4)
C(103)	67(5)	30(3)	38(4)	10(3)	17(3)	6(3)
C(104)	97(6)	37(4)	46(4)	15(3)	25(4)	18(4)
C(105)	104(7)	51(4)	38(4)	15(3)	14(4)	16(4)
C(106)	68(5)	46(4)	41(4)	10(3)	10(3)	11(4)
C(107)	63(4)	32(3)	35(4)	7(3)	9(3)	11(3)
C(108)	65(5)	41(4)	49(4)	14(3)	21(3)	21(3)
C(109)	90(6)	46(4)	53(5)	11(4)	32(4)	17(4)
C(111)	18(4)	27(4)	19(4)	-3(3)	-4(3)	7(3)
C(112)	13(5)	41(6)	50(6)	31(5)	14(4)	6(4)

C(113)	23(6)	23(6)	32(6)	1(5)	13(5)	7(4)
C(114)	30(5)	40(6)	22(5)	5(4)	-12(4)	15(5)
Cl(1)	41(2)	51(2)	47(2)	18(2)	13(1)	19(2)
Cl(2)	34(2)	65(2)	21(1)	6(1)	1(1)	7(1)
Cl(3)	40(2)	41(2)	56(2)	26(2)	21(2)	-6(1)
Cl(4)	58(3)	117(4)	61(3)	-2(3)	24(2)	-10(2)
Cl(5)	42(2)	78(2)	50(2)	0(2)	29(2)	33(2)
Cl(6)	32(2)	44(2)	59(2)	33(2)	20(1)	27(1)
Cl(7)	94(3)	93(3)	17(2)	-5(2)	-5(2)	11(2)
Cl(8)	83(3)	112(4)	96(3)	60(3)	40(2)	78(3)

_____

Table 5. Hydrogen coordinates (x 10^4) and isotropic displacement parameters (A^2 x 10^3) for kva.
_____

 x y z U(eq)
_____

	x	y	z	U(eq)		x	y	z	U(eq)
H(2)	2636	1946	1656	88(2)	H(35B)	6313	2203	1223	88(2)
H(4)	396	3023	1909	88(2)	H(35C)	6250	2121	1770	88(2)
H(8A)	-1820	2900	2438	88(2)	H(36A)	5198	261	466	88(2)
H(8B)	-1253	2849	1967	88(2)	H(36B)	5784	1083	455	88(2)
H(8C)	-640	3385	2523	88(2)	H(36C)	4624	906	549	88(2)
H(9A)	-1214	2361	3128	88(2)	H(37A)	-158	-1151	3864	88(2)
H(9B)	-64	2869	3171	88(2)	H(37B)	674	-650	4373	88(2)
H(9C)	-297	1978	3067	88(2)	H(37C)	1009	-1189	3912	88(2)
H(10A)	-1531	1056	2206	88(2)	H(39)	1087	830	4370	88(2)
H(10B)	-1860	1408	1784	88(2)	H(42)	2469	1762	3168	88(2)
H(10C)	-2333	1542	2286	88(2)	H(43)	2882	3079	3288	88(2)
H(11A)	-834	-2740	2337	88(2)	H(45)	1349	3368	4454	88(2)
H(11B)	-2028	-2790	2195	88(2)	H(46)	868	2046	4318	88(2)
H(11C)	-1362	-2274	2746	88(2)	H(47)	2902	4342	3741	88(2)
H(13)	-2215	-1935	1572	88(2)	H(48A)	2381	4690	4717	88(2)
H(16)	369	-94	1363	88(2)	H(48B)	3192	5239	4518	88(2)
H(17)	49	553	799	88(2)	H(48C)	3452	4525	4625	88(2)
H(19)	-3069	-204	748	88(2)	H(49A)	1349	4317	3406	88(2)
H(20)	-2728	-817	1341	88(2)	H(49B)	1488	4937	3948	88(2)
H(21)	-2554	530	224	88(2)	H(49C)	824	4077	3838	88(2)
H(22A)	-639	1679	761	88(2)	H(51)	2819	3850	2468	88(2)
H(22B)	-1774	1708	842	88(2)	H(53)	1653	4273	1198	88(2)
H(22C)	-1411	1790	335	88(2)	H(57A)	412	5654	1804	88(2)
H(23A)	-593	659	-74	88(2)	H(57B)	737	6402	1648	88(2)
H(23B)	-1664	585	-414	88(2)	H(57C)	1311	6380	2171	88(2)
H(23C)	-1490	-131	-276	88(2)	H(58A)	779	4911	915	88(2)
H(24A)	2540	-1750	3328	88(2)	H(58B)	1886	5227	791	88(2)
H(24B)	2910	-2300	2889	88(2)	H(58C)	1077	5709	819	88(2)
H(24C)	1707	-2369	2854	88(2)	H(59A)	2515	6803	1433	88(2)
H(26)	3925	-1341	2419	88(2)	H(59B)	3270	6284	1430	88(2)
H(29)	5129	-90	2388	88(2)	H(59C)	3039	6748	1954	88(2)
H(30)	6147	549	1948	88(2)	H(60A)	3477	8516	5195	88(2)
H(32)	3559	560	1071	88(2)	H(60B)	2467	8758	5054	88(2)
H(33)	2528	-117	1481	88(2)	H(60C)	3487	9048	4850	88(2)
H(34)	6393	967	1236	88(2)	H(62)	1041	7642	4266	88(2)
H(35A)	5224	2052	1397	88(2)	H(65)	-134	7006	3428	88(2)

H(66)	-1481	6163	2772	88(2)	H(96)	5028	2694	3290	88(2)
H(68)	161	4651	2500	88(2)	H(97A)	6148	2157	3078	88(2)
H(69)	1531	5483	3158	88(2)	H(97B)	6493	2876	3584	88(2)
H(70)	-1487	4313	1962	88(2)	H(97C)	6884	2947	3080	88(2)
H(71A)	-2552	4717	1463	88(2)	H(98A)	4510	2813	2419	88(2)
H(71B)	-1469	5369	1656	88(2)	H(98B)	3942	2342	2745	88(2)
H(71C)	-2431	5477	1916	88(2)	H(98C)	4756	2048	2434	88(2)
H(72A)	-2414	4141	2581	88(2)	H(100)	3020	2843	1197	88(2)
H(72B)	-3196	4054	2082	88(2)	H(101)	4566	2315	399	88(2)
H(72C)	-2884	4817	2557	88(2)	H(10D)	4622	3606	675	88(2)
H(73A)	5491	9422	4477	88(2)	H(10E)	4449	3260	1124	88(2)
H(73B)	6346	9749	4188	88(2)	H(103)	3257	4011	1064	88(2)
H(73C)	6602	9284	4551	88(2)	H(10F)	1926	3587	300	88(2)
H(75)	6316	8775	3238	88(2)	H(10G)	3046	3810	161	88(2)
H(78)	5136	6153	2739	88(2)	H(105)	2008	2588	-437	88(2)
H(79)	5246	5408	1943	88(2)	H(10H)	959	2201	129	88(2)
H(81)	5851	7216	1467	88(2)	H(10I)	1442	1544	-133	88(2)
H(82)	5676	8020	2257	88(2)	H(107)	1636	1721	759	88(2)
H(83)	5596	5214	1117	88(2)	H(10J)	3506	1905	934	88(2)
H(84A)	4647	6054	632	88(2)	H(10K)	3035	1370	359	88(2)
H(84B)	4026	5430	846	88(2)	H(10L)	3285	1897	-362	88(2)
H(84C)	4611	5186	392	88(2)	H(10M)	3892	2776	-237	88(2)
H(85A)	6675	6524	909	88(2)	H(11D)	3543	868	3713	88(2)
H(85B)	6614	5675	590	88(2)	H(11E)	346762		3316	88(2)
H(85C)	7195	6030	1171	88(2)	H(11H)	8856	9865	3164	88(2)
H(86A)	6267	7627	5629	88(2)	H(11I)	898210590		2980	88(2)
H(86B)	5223	7841	5508	88(2)	H(11F)	8713	3586	5238	88(2)
H(86C)	6231	8204	5320	88(2)	H(11G)	8676	4020	4832	88(2)
H(88)	6053	6197	4993	88(2)	H(11J)	8176	5387	3586	88(2)
H(91)	5360	4766	4539	88(2)	H(11K)	7423	5039	3909	88(2)
H(92)	5489	3587	4074	88(2)	H(1)	605	-1527	2973	88(2)
H(94)	5344	4156	2791	88(2)	H(2A)	4835	8232	4652	88(2)
H(95)	5256	5359	3244	88(2)					

_____

4(SQZnL)₂. Brown blocks of **rfnor** were crystallized from a methanol/dichloromethane solution at 22 deg. C. A crystal of dimensions 0.24 x 0.20 x 0.18 mm was mounted on a standard Bruker SMART CCD-based X-ray diffractometer equipped with a LT-2 low temperature device and normal focus Mo-target X-ray tube (λ = 0.71073 A) operated at 2000 W power (50 kV, 40 mA). The X-ray intensities were measured at 118(2) K; the detector was placed at a distance 4.950 cm from the crystal. A total of 2927 frames were collected with a scan width of 0.2° in ω with an exposure time of 60 s/frame. The frames were integrated with the Bruker SAINT software package with a narrow frame algorithm. The integration of the data yielded a total of 33091 reflections to a maximum 2θ value of 46.77° of which 7306 were independent and 4627 were greater than $2\sigma(I)$. The final cell constants (Table 1) were based on the xyz centroids of 7402 reflections above $10\sigma(I)$. Analysis of the data showed negligible decay during data collection; the data were processed with SADABS and corrected for absorption. The structure was solved and refined with the

Bruker SHELXTL (version 5.10) software package, using the space group C2/c with Z = 4 for the formula $C_{106}H_{124}B_2N_{12}O_4Zn_2 \cdot (CH_2Cl)_2$. The complex lies on a two-fold rotation axis in the crystal lattice with the dichloromethane lattice solvate molecules on general positions. All non-hydrogen atoms were refined anisotropically with the hydrogen atoms placed in idealized positions. Full matrix least-squares refinement based on F^2 converged at R1 = 0.0903 and wR2 = 0.2638 [based on I > 2sigma(I)], R1 = 0.1366 and wR2 = 0.3128 for all data. Additional details are presented in Table 1 and are given as Supporting Information in a CIF file.

Sheldrick, G.M. SHELXTL, v. 5.10; Bruker Analytical X-ray, Madison, WI, 1997.

Sheldrick, G.M. SADABS. Program for Empirical Absorption Correction of Area Detector Data, University of Gottingen: Gottingen, Germany, 1996.
Saint Plus, v. 6.29, Bruker Analytical X-ray, Madison, WI, 2001.

Table 1. Crystal data and structure refinement for rfnor (**4(SQZnL)₂**).

Identification code	rfnor
Empirical formula	C108 H128 B2 Cl4 N12 O4 Zn2
Formula weight	1952.38
Temperature	118(2) K
Wavelength	0.71073 A
Crystal system, space group	Monoclinic, C2/c
Unit cell dimensions	a = 32.376(2) A alpha = 90 deg.
	b = 18.9790(12) A beta = 116.337(3) deg.
	c = 18.4471(12) A gamma = 90 deg.
Volume	10158.4(11) A^3
Z, Calculated density	4, 1.277 Mg/m^3
Absorption coefficient	0.635 mm^-1
F(000)	4120
Crystal size	0.24 x 0.20 x 0.18 mm
Theta range for data collection	2.80 to 23.30 deg.
Limiting indices	-35<=h<=32, -21<=k<=21, -20<=l<=20
Reflections collected / unique	33091 / 7306 [R(int) = 0.0636]
Completeness to theta =	23.30 99.6 %
Absorption correction	Semi-empirical from equivalents
Max. and min. transmission	0.8942 and 0.8625
Refinement method	Full-matrix least-squares on F^2
Data / restraints / parameters	7306 / 0 / 608
Goodness-of-fit on F^2	1.025
Final R indices [I>2sigma(I)]	R1 = 0.0903, wR2 = 0.2638
R indices (all data)	R1 = 0.1366, wR2 = 0.3128
Largest diff. peak and hole	0.787 and -0.768 e.A^-3

Table 2. Atomic coordinates (x 10^4) and equivalent isotropic displacement parameters (A^2 x 10^3) for rfnor.
U(eq) is defined as one third of the trace of the orthogonalized Uij tensor.
_____

x y z   U(eq)

_____

	x	y	z	U(eq)		x	y	z	U(eq)
Zn(1)	3543(1)	-2572(1)	3862(1)	54(1)	C(32)	2655(3)	-1446(4)	3372(4)	53(2)
Cl(1)	2659(1)	1951(2)	1210(2)	121(1)	C(33)	2801(3)	-1047(3)	4126(5)	52(2)
Cl(2)	3555(1)	2600(2)	1752(3)	130(1)	C(34)	2481(3)	-875(4)	4407(5)	60(2)
C(1)	4126(3)	-2280(4)	5450(5)	54(2)	C(35)	2591(3)	-455(4)	5074(5)	64(2)
C(2)	4330(3)	-1894(5)	6182(5)	74(2)	C(36)	3032(3)	-179(4)	5494(4)	58(2)
C(3)	4766(3)	-2030(5)	6735(6)	82(3)	C(37)	3358(3)	-346(4)	5217(5)	61(2)
C(4)	5016(3)	-2588(5)	6615(6)	81(3)	C(38)	3243(3)	-776(4)	4546(5)	58(2)
C(5)	4854(3)	-3002(5)	5920(7)	82(3)	C(39)	3165(3)	294(5)	6235(5)	76(2)
C(6)	4394(3)	-2822(4)	5288(5)	64(2)	C(40)	2782(4)	792(6)	6139(7)	108(4)
C(7)	5115(4)	-3627(5)	5802(8)	96(3)	C(41)	3309(4)	-158(6)	6986(6)	97(3)
C(8)	5590(4)	-3727(7)	6527(9)	141(5)	C(42)	2369(4)	-4119(5)	1333(5)	88(3)
C(9)	5188(5)	-3536(6)	5041(9)	125(4)	C(43)	2700(3)	-4023(4)	2212(5)	66(2)
C(10)	4832(4)	-4310(5)	5697(8)	110(4)	C(44)	2843(3)	-4486(4)	2835(5)	68(2)
C(11)	5000	-1611(8)	7500	85(4)	C(45)	3154(3)	-4134(4)	3535(5)	54(2)
C(12)	5000	-903(7)	7500	81(4)	C(46)	3395(3)	-4412(4)	4351(5)	58(2)
C(13)	4822(4)	-367(5)	6808(6)	87(3)	C(47)	3506(3)	-5129(4)	4461(6)	72(2)
C(14)	4515(4)	82(7)	7049(7)	110(4)	C(48)	3717(3)	-5412(5)	5217(7)	80(3)
C(15)	4736(4)	71(7)	7967(7)	110(4)	C(49)	3833(3)	-5024(5)	5908(6)	74(2)
C(16)	3243(5)	-2529(7)	757(6)	111(4)	C(50)	3720(3)	-4297(5)	5807(6)	73(2)
C(17)	3517(4)	-2376(5)	1630(6)	88(3)	C(51)	3505(3)	-4005(4)	5053(5)	62(2)
C(18)	3967(4)	-2144(6)	2038(6)	98(3)	C(52)	4068(4)	-5317(6)	6768(7)	98(3)
C(19)	4074(3)	-2114(5)	2841(5)	78(3)	C(53)	4343(5)	-6001(9)	6807(10)	173(7)
C(20)	4512(3)	-1898(5)	3537(6)	78(3)	C(54)	3724(4)	-5459(8)	7089(8)	130(5)
C(21)	4515(3)	-1516(4)	4173(5)	74(2)	N(1)	3705(3)	-2308(3)	2941(4)	64(2)
C(22)	4931(4)	-1302(5)	4788(6)	85(3)	N(2)	3358(3)	-2466(3)	2189(4)	66(2)
C(23)	5340(4)	-1432(6)	4816(6)	88(3)	N(3)	2931(2)	-1905(3)	3229(3)	52(2)
C(24)	5337(4)	-1836(7)	4197(7)	109(4)	N(4)	2673(2)	-2134(3)	2449(4)	55(2)
C(25)	4926(4)	-2064(6)	3559(6)	101(4)	N(5)	3187(2)	-3465(3)	3338(4)	52(2)
C(26)	5812(5)	-1205(7)	5506(7)	132(5)	N(6)	2910(2)	-3399(3)	2517(4)	58(2)
C(27)	5951(5)	-1556(8)	6262(9)	154(6)	O(1)	3723(2)	-2152(3)	4917(3)	61(1)
C(28)	5816(4)	-397(6)	5527(7)	124(5)	O(2)	4202(2)	-3107(3)	4586(4)	71(2)
C(29)	1886(3)	-1996(4)	1285(5)	73(2)	B(1)	2877(4)	-2697(5)	2084(6)	63(2)
C(30)	2247(3)	-1842(4)	2131(5)	59(2)	C(55)	3103(4)	2175(6)	990(8)	111(4)
C(31)	2230(3)	-1404(4)	2700(4)	58(2)					

_____

Table 3. Bond lengths [A] and angles [deg] for rfnor.

_____

Zn(1)-O(1)	1.938(5)		C(3)-C(11)	1.500(13)
Zn(1)-N(5)	2.038(6)		C(4)-C(5)	1.393(13)
Zn(1)-N(1)	2.048(6)		C(5)-C(6)	1.466(13)
Zn(1)-O(2)	2.199(6)		C(5)-C(7)	1.525(13)
Zn(1)-N(3)	2.201(6)		C(6)-O(2)	1.281(10)
Cl(1)-C(55)	1.709(11)		C(7)-C(9)	1.535(16)
Cl(2)-C(55)	1.716(12)		C(7)-C(8)	1.538(15)
C(1)-O(1)	1.261(9)		C(7)-C(10)	1.549(14)
C(1)-C(2)	1.416(11)		C(11)-C(12)	1.343(19)
C(1)-C(6)	1.461(12)		C(11)-C(3)	#11.500(13)
C(2)-C(3)	1.351(12)		C(12)-C(13)	#11.530(13)
C(3)-C(4)	1.409(13)		C(12)-C(13)	1.530(12)

C(13)-C(14)	1.520(14)	N(5)-N(6)	1.381(8)
C(13)-C(15)	#11.544(15)	N(6)-B(1)	1.534(11)
C(14)-C(15)	1.518(15)	O(1)-Zn(1)-N(5)	132.2(2)
C(15)-C(13)	#11.544(15)	O(1)-Zn(1)-N(1)	131.2(2)
C(16)-C(17)	1.482(14)	N(5)-Zn(1)-N(1)	96.3(2)
C(17)-N(2)	1.352(11)	O(1)-Zn(1)-O(2)	78.6(2)
C(17)-C(18)	1.382(14)	N(5)-Zn(1)-O(2)	95.6(2)
C(18)-C(19)	1.364(13)	N(1)-Zn(1)-O(2)	94.7(3)
C(19)-N(1)	1.339(11)	O(1)-Zn(1)-N(3)	95.4(2)
C(19)-C(20)	1.488(13)	N(5)-Zn(1)-N(3)	92.2(2)
C(20)-C(25)	1.358(14)	N(1)-Zn(1)-N(3)	85.5(3)
C(20)-C(21)	1.376(12)	O(2)-Zn(1)-N(3)	172.1(2)
C(21)-C(22)	1.384(13)	O(1)-C(1)-C(2)	121.8(7)
C(22)-C(23)	1.324(14)	O(1)-C(1)-C(6)	118.7(7)
C(23)-C(24)	1.371(15)	C(2)-C(1)-C(6)	119.4(8)
C(23)-C(26)	1.554(15)	C(3)-C(2)-C(1)	120.7(9)
C(24)-C(25)	1.397(14)	C(2)-C(3)-C(4)	120.5(9)
C(26)-C(27)	1.427(16)	C(2)-C(3)-C(11)	122.0(9)
C(26)-C(28)	1.534(18)	C(4)-C(3)-C(11)	117.5(9)
C(29)-C(30)	1.507(11)	C(5)-C(4)-C(3)	124.0(9)
C(30)-N(4)	1.353(10)	C(4)-C(5)-C(6)	115.9(8)
C(30)-C(31)	1.360(11)	C(4)-C(5)-C(7)	124.2(10)
C(31)-C(32)	1.386(10)	C(6)-C(5)-C(7)	119.9(9)
C(32)-N(3)	1.354(9)	O(2)-C(6)-C(1)	115.9(7)
C(32)-C(33)	1.466(10)	O(2)-C(6)-C(5)	124.9(8)
C(33)-C(34)	1.388(10)	C(1)-C(6)-C(5)	119.2(8)
C(33)-C(38)	1.389(11)	C(5)-C(7)-C(9)	111.3(9)
C(34)-C(35)	1.374(11)	C(5)-C(7)-C(8)	112.0(10)
C(35)-C(36)	1.391(11)	C(9)-C(7)-C(8)	108.0(10)
C(36)-C(37)	1.398(11)	C(5)-C(7)-C(10)	109.6(8)
C(36)-C(39)	1.529(11)	C(9)-C(7)-C(10)	107.6(10)
C(37)-C(38)	1.389(10)	C(8)-C(7)-C(10)	108.2(10)
C(39)-C(40)	1.506(13)	C(12)-C(11)-C(3)	122.0(7)
C(39)-C(41)	1.516(13)	C(12)-C(11)-C(3)	122.0(7)
C(42)-C(43)	1.507(12)	C(3)-C(11)-C(3)	115.9(13)
C(43)-C(44)	1.354(12)	C(11)-C(12)-C(13)	131.6(5)
C(43)-N(6)	1.357(9)	C(11)-C(12)-C(13)	131.6(5)
C(44)-C(45)	1.404(11)	C(13)-C(12)-C(13)	96.7(10)
C(45)-N(5)	1.338(9)	C(14)-C(13)-C(12)	100.5(8)
C(45)-C(46)	1.452(11)	C(14)-C(13)-C(15)	105.5(9)
C(46)-C(47)	1.401(11)	C(12)-C(13)-C(15)	100.0(7)
C(46)-C(51)	1.410(11)	C(13)-C(14)-C(15)	105.8(9)
C(47)-C(48)	1.361(13)	C(14)-C(15)-C(13)	#1103.3(9)
C(48)-C(49)	1.373(13)	N(2)-C(17)-C(18)	106.9(9)
C(49)-C(50)	1.419(13)	N(2)-C(17)-C(16)	123.8(10)
C(49)-C(52)	1.528(13)	C(18)-C(17)-C(16)	129.3(9)
C(50)-C(51)	1.366(12)	C(19)-C(18)-C(17)	107.6(8)
C(52)-C(54)	1.502(15)	N(1)-C(19)-C(18)	109.1(9)
C(52)-C(53)	1.558(18)	N(1)-C(19)-C(20)	121.6(7)
N(1)-N(2)	1.375(9)	C(18)-C(19)-C(20)	129.2(8)
N(2)-B(1)	1.547(12)	C(25)-C(20)-C(21)	117.6(9)
N(3)-N(4)	1.375(8)	C(25)-C(20)-C(19)	120.8(9)
N(4)-B(1)	1.558(11)	C(21)-C(20)-C(19)	121.5(9)

C(20)-C(21)-C(22)	119.3(10)		C(47)-C(46)-C(51)	117.0(8)
C(23)-C(22)-C(21)	124.7(10)		C(47)-C(46)-C(45)	119.3(8)
C(22)-C(23)-C(24)	115.7(10)		C(51)-C(46)-C(45)	123.6(7)
C(22)-C(23)-C(26)	125.6(11)		C(48)-C(47)-C(46)	120.8(9)
C(24)-C(23)-C(26)	118.6(11)		C(47)-C(48)-C(49)	123.1(9)
C(23)-C(24)-C(25)	121.8(11)		C(48)-C(49)-C(50)	116.9(9)
C(20)-C(25)-C(24)	120.7(10)		C(48)-C(49)-C(52)	125.0(9)
C(27)-C(26)-C(28)	116.5(11)		C(50)-C(49)-C(52)	118.1(10)
C(27)-C(26)-C(23)	116.1(10)		C(51)-C(50)-C(49)	120.8(9)
C(28)-C(26)-C(23)	107.0(11)		C(50)-C(51)-C(46)	121.4(8)
N(4)-C(30)-C(31)	107.4(7)		C(54)-C(52)-C(49)	111.1(9)
N(4)-C(30)-C(29)	122.9(7)		C(54)-C(52)-C(53)	109.9(10)
C(31)-C(30)-C(29)	129.7(8)		C(49)-C(52)-C(53)	111.2(11)
C(30)-C(31)-C(32)	106.8(7)		C(19)-N(1)-N(2)	107.4(6)
N(3)-C(32)-C(31)	110.0(6)		C(19)-N(1)-Zn(1)	138.9(6)
N(3)-C(32)-C(33)	123.5(6)		N(2)-N(1)-Zn(1)	112.9(5)
C(31)-C(32)-C(33)	126.4(7)		C(17)-N(2)-N(1)	109.0(8)
C(34)-C(33)-C(38)	117.3(7)		C(17)-N(2)-B(1)	130.0(8)
C(34)-C(33)-C(32)	119.7(7)		N(1)-N(2)-B(1)	120.9(6)
C(38)-C(33)-C(32)	122.7(7)		C(32)-N(3)-N(4)	105.0(6)
C(35)-C(34)-C(33)	122.2(7)		C(32)-N(3)-Zn(1)	141.6(5)
C(34)-C(35)-C(36)	120.7(8)		N(4)-N(3)-Zn(1)	111.1(4)
C(35)-C(36)-C(37)	117.8(7)		C(30)-N(4)-N(3)	110.7(6)
C(35)-C(36)-C(39)	122.1(8)		C(30)-N(4)-B(1)	129.6(7)
C(37)-C(36)-C(39)	120.1(7)		N(3)-N(4)-B(1)	119.5(6)
C(38)-C(37)-C(36)	120.8(8)		C(45)-N(5)-N(6)	107.0(6)
C(37)-C(38)-C(33)	121.1(8)		C(45)-N(5)-Zn(1)	139.3(5)
C(40)-C(39)-C(41)	111.5(9)		N(6)-N(5)-Zn(1)	113.6(4)
C(40)-C(39)-C(36)	111.9(8)		C(43)-N(6)-N(5)	109.7(6)
C(41)-C(39)-C(36)	109.6(7)		C(43)-N(6)-B(1)	129.5(7)
C(44)-C(43)-N(6)	107.1(7)		N(5)-N(6)-B(1)	120.8(6)
C(44)-C(43)-C(42)	130.3(8)		C(1)-O(1)-Zn(1)	116.7(5)
N(6)-C(43)-C(42)	122.6(8)		C(6)-O(2)-Zn(1)	109.0(5)
C(43)-C(44)-C(45)	108.0(7)		N(6)-B(1)-N(2)	110.2(7)
N(5)-C(45)-C(44)	108.2(7)		N(6)-B(1)-N(4)	108.4(6)
N(5)-C(45)-C(46)	123.7(6)		N(2)-B(1)-N(4)	110.4(6)
C(44)-C(45)-C(46)	128.1(7)		CI(1)-C(55)-CI(2)	115.1(7)

Symmetry transformations used to generate equivalent atoms:
#1 -x+1,y,-z+3/2

Table 4. Anisotropic displacement parameters (A^2 x 10^3) for rfnor.
The anisotropic displacement factor exponent takes the form:-2 pi^2[h^2 a*^2 U11 + 2 h k a* b* U12]

	U11	U22	U33	U23	U13	U12
Zn(1)	72(1)	40(1)	52(1)	-8(1)	29(1)	-12(1)
CI(1)	142(3)	88(2)	168(3)	-37(2)	100(2)	-24(2)
CI(2)	100(2)	126(3)	159(3)	-42(2)	53(2)	-4(2)
C(1)	61(5)	41(4)	66(5)	4(4)	31(4)	0(4)
C(2)	67(6)	81(6)	67(6)	-3(5)	24(5)	-3(5)
C(3)	81(7)	84(7)	89(7)	-5(5)	47(6)	7(5)

166

C(4)	73(6)	73(6)	81(7)	-3(5)	18(5)	-3(5)
C(5)	75(6)	59(6)	118(8)	3(5)	47(6)	-2(5)
C(6)	69(5)	48(4)	75(6)	5(4)	32(5)	-10(4)
C(7)	92(7)	61(6)	152(10)	-8(6)	71(8)	-3(5)
C(8)	73(7)	110(10)	200(15)	-18(10)	25(8)	21(7)
C(9)	135(10)	89(8)	188(13)	-4(9)	106(10)	17(8)
C(10)	105(8)	59(6)	174(12)	-1(7)	71(8)	9(6)
C(11)	77(9)	104(11)	53(7)	011(6)	0	
C(12)	90(9)	60(8)	70(8)	015(7)	0	
C(13)	103(7)	82(7)	60(5)	-3(5)	22(5)	14(6)
C(14)	107(8)	104(9)	103(9)	0(7)	34(7)	14(7)
C(15)	136(10)	106(9)	97(8)	1(7)	60(8)	26(8)
C(16)	140(10)	150(11)	56(6)	-26(6)	55(7)	-41(8)
C(17)	125(9)	92(7)	67(6)	-17(5)	60(6)	-21(6)
C(18)	111(8)	122(9)	89(7)	-27(7)	69(7)	-48(7)
C(19)	107(7)	79(6)	69(6)	-13(5)	59(6)	-26(6)
C(20)	95(7)	76(6)	86(6)	-14(5)	60(6)	-42(5)
C(21)	106(7)	59(5)	67(5)	-12(4)	49(5)	-29(5)
C(22)	120(9)	72(6)	73(6)	-13(5)	52(6)	-32(6)
C(23)	106(8)	89(7)	81(7)	-6(6)	53(6)	-32(6)
C(24)	99(8)	144(11)	97(8)	-18(8)	57(7)	-50(8)
C(25)	119(9)	120(9)	87(7)	-31(7)	68(7)	-46(8)
C(26)	184(13)	119(10)	70(7)	-5(7)	36(8)	-78(10)
C(27)	142(12)	109(11)	148(13)	7(10)	9(10)	-20(9)
C(28)	136(10)	112(10)	95(8)	11(7)	25(7)	-57(8)
C(29)	93(6)	58(5)	56(5)	-2(4)	21(5)	-12(5)
C(30)	76(6)	40(4)	55(5)	3(4)	24(4)	-3(4)
C(31)	68(5)	43(4)	59(5)	4(4)	25(4)	0(4)
C(32)	70(5)	35(4)	49(4)	3(3)	21(4)	1(3)
C(33)	68(5)	24(3)	64(5)	1(3)	28(4)	0(3)
C(34)	67(5)	47(4)	65(5)	-8(4)	29(4)	-10(4)
C(35)	75(6)	51(5)	68(5)	-5(4)	34(5)	-6(4)
C(36)	75(5)	44(4)	55(5)	-5(3)	27(4)	-1(4)
C(37)	66(5)	47(4)	59(5)	-10(4)	18(4)	0(4)
C(38)	70(5)	41(4)	63(5)	-7(4)	30(4)	7(4)
C(39)	88(6)	67(6)	74(6)	-22(5)	38(5)	-2(5)
C(40)	110(8)	87(8)	126(9)	-49(7)	51(7)	-1(6)
C(41)	102(8)	112(9)	76(7)	-24(6)	39(6)	-4(6)
C(42)	109(7)	60(5)	72(6)	-21(5)	19(5)	-12(5)
C(43)	80(6)	47(5)	75(6)	-16(4)	38(5)	-5(4)
C(44)	81(6)	43(4)	87(6)	-15(4)	43(5)	-11(4)
C(45)	61(5)	37(4)	66(5)	-8(4)	30(4)	-3(3)
C(46)	64(5)	35(4)	84(6)	-6(4)	39(4)	-10(3)
C(47)	76(6)	51(5)	90(7)	1(5)	37(5)	-2(4)
C(48)	77(6)	50(5)	111(8)	3(6)	39(6)	-5(4)
C(49)	64(5)	66(6)	94(7)	20(5)	34(5)	-1(4)
C(50)	66(5)	78(6)	81(6)	-2(5)	38(5)	-12(5)
C(51)	74(5)	44(4)	74(6)	5(4)	37(5)	-8(4)
C(52)	89(7)	92(8)	106(8)	30(6)	37(6)	-5(6)
C(53)	143(12)	205(17)	177(15)	112(13)	77(11)	86(12)
C(54)	122(10)	156(12)	123(10)	49(9)	66(8)	17(9)
N(1)	85(5)	57(4)	54(4)	-16(3)	35(4)	-20(4)
N(2)	89(5)	62(4)	60(4)	-13(3)	45(4)	-18(4)

N(3)	72(4)	38(3)	45(3)	-6(3)	25(3)	-9(3)
N(4)	76(4)	38(3)	48(4)	-7(3)	24(3)	-7(3)
N(5)	66(4)	38(3)	55(4)	-11(3)	29(3)	-5(3)
N(6)	74(4)	39(3)	61(4)	-17(3)	29(3)	-10(3)
O(1)	75(4)	47(3)	57(3)	-7(2)	26(3)	-2(3)
O(2)	81(4)	49(3)	90(4)	-12(3)	45(3)	-10(3)
B(1)	90(7)	51(5)	50(5)	-13(4)	33(5)	-8(5)
C(55)	132(10)	91(8)	133(10)	-38(7)	80(9)	-33(7)

_____

Table 5. Hydrogen coordinates (x 10^4) and isotropic displacement parameters (A^2 x 10^3) for rfnor.

_____

x y z   U(eq)

_____

	x	y	z	U(eq)		x	y	z	U(eq)
H(2A)	4158	-1535	6285	89	H(29C)	1990	-1823	894	110
H(4A)	5314	-2689	7035	98	H(31A)	1975	-1123	2647	69
H(8A)	5755	-3277	6658	211	H(34A)	2176	-1053	4129	72
H(8B)	5767	-4076	6391	211	H(35A)	2363	-353	5250	77
H(8C)	5550	-3892	6996	211	H(37A)	3662	-163	5492	73
H(9A)	4889	-3469	4570	188	H(38A)	3471	-886	4371	70
H(9B)	5338	-3957	4961	188	H(39A)	3437	582	6297	91
H(9C)	5384	-3123	5105	188	H(40A)	2507	521	6055	162
H(10A)	4745	-4350	6140	165	H(40B)	2712	1098	5671	162
H(10B)	5019	-4718	5704	165	H(40C)	2878	1081	6627	162
H(10C)	4554	-4294	5180	165	H(41A)	3416	145	7465	145
H(13)	4675	-566	6248	104	H(41B)	3560	-473	7033	145
H(14A)	4199	-117	6824	131	H(41C)	3046	-439	6946	145
H(14B)	4497	570	6847	131	H(42A)	2116	-3781	1180	132
H(15A)	4531	-155	8168	132	H(42B)	2245	-4600	1246	132
H(15B)	4811	554	8191	132	H(42C)	2531	-4041	1001	132
H(16A)	3141	-3021	688	167	H(44A)	2751	-4964	2804	81
H(16B)	3432	-2448	474	167	H(47A)	3433	-5422	4003	87
H(16C)	2973	-2218	533	167	H(48A)	3787	-5901	5269	96
H(18A)	4167	-2027	1803	118	H(50A)	3793	-4009	6270	87
H(21A)	4233	-1400	4188	88	H(51A)	3429	-3518	5000	75
H(22A)	4924	-1043	5223	102	H(52A)	4291	-4955	7123	118
H(24A)	5621	-1964	4202	130	H(53A)	4468	-6199	7354	260
H(25A)	4936	-2338	3136	121	H(53B)	4597	-5889	6674	260
H(26A)	6046	-1339	5315	158	H(53C)	4138	-6345	6418	260
H(27A)	6283	-1493	6593	231	H(54A)	3572	-5018	7110	194
H(27B)	5881	-2060	6168	231	H(54B)	3881	-5660	7634	194
H(27C)	5784	-1357	6546	231	H(54C)	3492	-5794	6733	194
H(28A)	5564	-229	5640	186	H(1)	2666	-2754	1494	76
H(28B)	5775	-214	5003	186	H(55A)	2980	2483	506	133
H(28C)	6111	-232	5952	186	H(55B)	3221	1741	848	133
H(29A)	1597	-1760	1193	110					
H(29B)	1834	-2505	1218	110					

_____

6(SQZnL)₂. Red-brown plates of **flat** were crystallized from a dichloromethane/heptane solution at 22 deg. C. A crystal of dimensions 0.36 x 0.22 x 0.10 mm was mounted on a standard Bruker SMART CCD-

based X-ray diffractometer equipped with a LT-2 low temperature device and normal focus Mo-target X-ray tube (λ = 0.71073 A) operated at 2000 W power (50 kV, 40 mA). The X-ray intensities were measured at 123(2) K; the detector was placed at a distance 4.950 cm from the crystal. A total of 3863 frames were collected with a scan width of 0.2° in ω with an exposure time of 75 s/frame. The frames were integrated with the Bruker SAINT software package with a narrow frame algorithm. The integration of the data yielded a total of 36621 reflections to a maximum 2θ value of 44.31° of which 13069 were independent and 6997 were greater than 2σ(I). The final cell constants (Table 1) were based on the xyz centroids of 5636 reflections above 10σ(I). Analysis of the data showed negligible decay during data collection; the data were processed with SADABS and corrected for absorption. The structure was solved and refined with the Bruker SHELXTL (version 5.10) software package, using the space group P1bar with Z = 2 for the formula $C_{106}H_{124}B_2N_{12}O_4Zn_2(C7H16)(CH2Cl2)_{0.5}$. All non-hydrogen atoms were refined anisotropically with the hydrogen atoms placed in idealized positions. Full matrix least-squares refinement based on F^2 converged at R1 = 0.0814 and wR2 = 0.2151 [based on I > 2sigma(I)], R1 = 0.1488 and wR2 = 0.2440 for all data. Additional details are presented in Table 1 and are given as Supporting Information in a CIF file.

Sheldrick, G.M. SHELXTL, v. 5.10; Bruker Analytical X-ray, Madison, WI, 1997.

Sheldrick, G.M. SADABS. Program for Empirical Absorption Correction of Area Detector Data, University of Gottingen: Gottingen, Germany, 1996.

Saint Plus, v. 6.29, Bruker Analytical X-ray, Madison, WI, 2001.

6(SQZnL)₂. Red-brown plates of **flat** were crystallized from a dichloromethane/heptane solution at 22 deg. C. A crystal of dimensions 0.36 x 0.22 x 0.10 mm was mounted on a standard Bruker SMART CCD-based X-ray diffractometer equipped with a LT-2 low temperature device and normal focus Mo-target X-ray tube (λ = 0.71073 A) operated at 2000 W power (50 kV, 40 mA). The X-ray intensities were measured at 123(2) K; the detector was placed at a distance 4.950 cm from the crystal. A total of 3863 frames were collected with a scan width of 0.2° in ω with an exposure time of 75 s/frame. The frames were integrated with the Bruker SAINT software package with a narrow frame algorithm. The integration of the data yielded a total of 36621 reflections to a maximum 2θ value of 44.31° of which 13069 were independent and 6997 were greater than 2σ(I). The final cell constants (Table 1) were based on the xyz centroids of 5636 reflections above 10σ(I). Analysis of the data showed negligible decay during data collection; the data were processed with SADABS and corrected for absorption. The structure was solved and refined with the Bruker SHELXTL (version 5.10) software package, using the space group P1bar with Z = 2 for the formula $C_{106}H_{124}B_2N_{12}O_4Zn_2(C7H16)(CH2Cl2)_{0.5}$. All non-hydrogen atoms were refined anisotropically with the hydrogen atoms placed in idealized positions. Full matrix least-squares refinement

based on F^2 converged at R1 = 0.0814 and wR2 = 0.2151 [based on I > 2sigma(I)], R1 = 0.1488 and wR2 = 0.2440 for all data. Additional details are presented in Table 1 and are given as Supporting Information in a CIF file.

Sheldrick, G.M. SHELXTL, v. 5.10; Bruker Analytical X-ray, Madison, WI, 1997.

Sheldrick, G.M. SADABS.   Program for Empirical Absorption Correction of Area Detector Data, University of Gottingen: Gottingen, Germany, 1996.
Saint Plus, v. 6.29, Bruker Analytical X-ray, Madison, WI, 2001.

Table 1. Crystal data and structure refinement for flat (**6(SQZnL)₂**).

Identification code	flat
Empirical formula	C113.50 H141 B2 Cl N12 O4 Zn2
Formula weight	1925.19
Temperature	123(2) K
Wavelength	0.71073 A
Crystal system, space group	Triclinic, P-1
Unit cell dimensions	a = 18.2397(13) A alpha = 81.610(4) deg.
	b = 18.3714(14) A beta = 67.429(3) deg.
	c = 18.3630(13) A gamma = 70.397(3) deg.
Volume	5351.6(7) A^3
Z, Calculated density	2, 1.195 Mg/m^3
Absorption coefficient	0.530 mm^-1
F(000)	2050
Crystal size	0.36 x 0.22 x 0.10 mm
Theta range for data collection	2.70 to 22.01 deg.
Limiting indices	-17<=h<=19, -18<=k<=19, -19<=l<=19
Reflections collected / unique	36621 / 13069 [R(int) = 0.0812]
Completeness to theta =	22.01 99.4 %
Absorption correction	Semi-empirical from equivalents
Max. and min. transmission	0.9489 and 0.8322
Refinement method	Full-matrix least-squares on F^2
Data / restraints / parameters	13069 / 91 / 1246
Goodness-of-fit on F^2	1.051
Final R indices [I>2sigma(I)]	R1 = 0.0814, wR2 = 0.2151
R indices (all data)	R1 = 0.1488, wR2 = 0.2440
Largest diff. peak and hole	0.708 and -0.666 e.A^-3

Table 2. Atomic coordinates (x 10^4) and equivalent isotropic displacement parameters (A^2 x 10^3) for flat.
U(eq) is defined as one third of the trace of the orthogonalized Uij tensor.

_____

	x	y	z	U(eq)
_____

Zn(1)	6287(1)	1533(1)	135(1)	59(1)
Zn(2)	9669(1)	2992(1)	4328(1)	90(1)
O(1)	5643(4)	2630(3)	734(4)	58(2)
O(2)	6828(4)	1384(4)	907(4)	58(2)

O(3)	8807(4)	3982(5)	3946(4)	78(2)
O(4)	9328(4)	2476(5)	3730(4)	79(2)
N(1)	5221(6)	1359(4)	247(5)	64(2)
N(2)	5180(7)	1178(4)	-444(5)	70(3)
N(3)	6948(6)	460(5)	-496(5)	71(3)
N(4)	6718(6)	462(5)	-1126(5)	73(3)
N(5)	6478(5)	2097(5)	-935(5)	60(2)
N(6)	6184(6)	1853(5)	-1417(5)	74(3)
N(7)	10559(5)	3525(7)	3962(6)	89(3)
N(8)	10689(6)	3749(7)	4573(6)	89(4)
N(9)	9016(5)	3383(6)	5446(5)	91(3)
N(10)	9498(6)	3505(7)	5814(5)	104(4)
N(11)	10588(6)	2066(8)	4783(5)	98(4)
N(12)	10832(6)	2429(7)	5223(6)	104(4)
B(1)	5968(10)	1101(8)	-1218(8)	74(4)
B(2)	10468(9)	3323(12)	5369(10)	114(7)
C(1)	5979(6)	2695(5)	1209(5)	49(2)
C(2)	6649(6)	2011(5)	1296(5)	50(2)
C(3)	7054(6)	2050(6)	1779(5)	54(3)
C(4)	6871(6)	2771(6)	2110(5)	55(3)
C(5)	6208(6)	3414(6)	2039(5)	56(3)
C(6)	5737(6)	3387(6)	1626(5)	51(3)
C(7)	4997(6)	4081(5)	1588(5)	51(3)
C(8)	4812(7)	4726(6)	2117(6)	76(3)
C(9)	4220(6)	3822(6)	1854(6)	80(3)
C(10)	5194(6)	4392(5)	736(5)	62(3)
C(11)	8455(6)	3738(7)	3580(6)	69(3)
C(12)	8743(6)	2918(7)	3458(6)	71(3)
C(13)	8376(6)	2626(6)	3082(5)	57(3)
C(14)	7735(6)	3130(7)	2856(5)	61(3)
C(15)	7473(6)	3941(6)	2938(5)	62(3)
C(16)	7826(6)	4277(7)	3271(5)	65(3)
C(17)	7605(8)	5141(7)	3342(6)	77(3)
C(18)	6987(8)	5579(7)	2923(7)	88(4)
C(19)	7167(7)	5334(7)	4233(6)	88(4)
C(20)	8392(9)	5410(9)	2975(8)	113(5)
C(21)	7460(6)	2671(6)	2475(5)	57(3)
C(22)	7954(6)	1923(6)	2444(5)	60(3)
C(23)	8578(6)	1802(6)	2841(6)	65(3)
C(24)	8456(7)	1237(7)	3548(6)	85(4)
C(25)	9480(6)	1540(7)	2249(6)	77(3)
C(26)	7736(6)	1431(6)	1992(5)	60(3)
C(27)	7377(7)	819(6)	2510(6)	80(3)
C(28)	8482(6)	1097(6)	1253(6)	74(3)
C(29)	4242(9)	862(8)	-942(8)	106(5)
C(30)	4436(9)	1103(7)	-306(8)	80(4)
C(31)	3961(8)	1242(6)	468(7)	74(3)
C(32)	4461(8)	1407(6)	801(7)	68(3)
C(33)	4244(7)	1608(6)	1632(6)	61(3)
C(34)	3436(8)	1978(7)	2089(8)	81(3)
C(35)	3224(8)	2167(7)	2849(8)	84(3)
C(36)	3816(8)	1997(7)	3194(7)	77(3)
C(37)	4623(7)	1618(6)	2738(7)	70(3)

C(38)	4853(7)	1400(6)	1977(6)	60(3)
C(39)	3564(8)	2252(8)	4047(7)	92(4)
C(40)	3607(11)	3028(10)	4040(8)	135(6)
C(41)	4049(12)	1679(11)	4493(8)	187(10)
C(42)	7171(10)	-231(8)	-2372(7)	115(5)
C(43)	7250(11)	-100(8)	-1638(7)	93(4)
C(44)	7859(10)	-490(8)	-1339(8)	111(5)
C(45)	7656(9)	-137(7)	-629(7)	90(4)
C(46)	8111(5)	-380(5)	-64(4)	97(4)
C(47)	8976(6)	-677(7)	-381(4)	185(8)
C(48)	9423(4)	-1013(8)	112(6)	222(10)
C(49)	9006(6)	-1052(7)	922(6)	162(7)
C(50)	8142(6)	-755(5)	1239(4)	97(4)
C(51)	7695(4)	-419(4)	746(4)	81(3)
C(52)	9473(13)	-1439(12)	1508(11)	210(7)
C(53)	9442(16)	-2270(12)	1622(13)	195(8)
C(54)	10342(16)	-1330(20)	1092(18)	245(10)
C(55)	5996(11)	2203(8)	-2718(8)	129(5)
C(56)	6226(9)	2329(7)	-2051(7)	91(4)
C(57)	6543(9)	2890(7)	-1993(7)	97(4)
C(58)	6699(7)	2730(6)	-1280(6)	64(3)
C(59)	7075(6)	3115(6)	-954(5)	53(3)
C(60)	7533(7)	2733(6)	-489(6)	65(3)
C(61)	7897(6)	3123(7)	-188(6)	64(3)
C(62)	7826(6)	3899(6)	-369(6)	57(3)
C(63)	7388(6)	4270(6)	-842(5)	54(3)
C(64)	7009(6)	3907(6)	-1132(5)	58(3)
C(65)	8217(7)	4327(7)	-47(7)	78(3)
C(66)	9145(9)	4138(12)	-534(13)	203(11)
C(67)	8046(14)	4208(11)	802(8)	184(9)
C(68)	11448(10)	4535(10)	4830(9)	145(6)
C(69)	11202(10)	4162(9)	4299(11)	109(5)
C(70)	11398(9)	4252(8)	3499(9)	105(5)
C(71)	11003(8)	3814(8)	3312(8)	86(4)
C(72)	11073(8)	3674(9)	2504(5)	87(9)
C(73)	10392(7)	3584(11)	2402(6)	120(9)
C(74)	10447(7)	3442(12)	1657(7)	121(9)
C(75)	11182(8)	3389(9)	1015(6)	82(9)
C(76)	11863(7)	3478(8)	1117(5)	74(6)
C(77)	11809(7)	3621(9)	1862(6)	82(6)
C(78)	11250(10)	3128(7)	202(7)	102(4)
C(72')	11022(9)	3669(10)	2508(5)	69(10)
C(73')	10968(10)	2960(8)	2391(7)	74(7)
C(74')	11022(11)	2789(8)	1656(9)	81(7)
C(75')	11128(8)	3326(10)	1038(6)	101(11)
C(76')	11182(13)	4035(10)	1155(6)	137(11)
C(77')	11129(14)	4206(9)	1890(7)	130(11)
C(78')	11250(10)	3128(7)	202(7)	102(4)
C(79)	12054(10)	2476(9)	-146(8)	133(5)
C(80)	11326(13)	3795(9)	-385(9)	162(7)
C(81)	9382(8)	3903(9)	7112(7)	123(6)
C(82)	9018(8)	3755(8)	6553(7)	101(5)
C(83)	8227(7)	3839(8)	6651(6)	92(4)

C(84)	8229(7)	3580(7)	5965(6)	81(4)
C(85)	7515(6)	3582(7)	5784(6)	73(3)
C(86)	6750(6)	4146(6)	6074(5)	63(3)
C(87)	6074(6)	4153(7)	5918(6)	68(3)
C(88)	6111(6)	3599(6)	5448(6)	63(3)
C(89)	6877(7)	3038(7)	5162(6)	78(3)
C(90)	7568(7)	3016(7)	5321(6)	79(4)
C(91)	5363(7)	3634(7)	5256(7)	77(3)
C(92)	5525(7)	3730(8)	4384(6)	90(4)
C(93)	5052(9)	2947(8)	5606(8)	110(5)
C(94)	11786(8)	2128(9)	5980(7)	124(6)
C(95)	11401(8)	1913(12)	5491(7)	114(6)
C(96)	11540(8)	1228(11)	5205(8)	120(6)
C(97)	11028(7)	1321(10)	4775(6)	90(4)
C(98)	10968(7)	710(9)	4372(7)	94(4)
C(99)	10694(7)	846(8)	3764(8)	93(4)
C(100)	10697(8)	232(9)	3392(8)	104(4)
C(101)	10917(8)	-489(9)	3656(9)	101(4)
C(102)	11218(12)	-629(11)	4263(11)	150(7)
C(103)	11218(11)	-21(12)	4628(10)	139(6)
C(104)	10917(12)	-1158(10)	3237(10)	140(5)
C(105)	11334(16)	-1083(14)	2332(12)	135(8)
C(106)	10950(30)	-1919(14)	3670(20)	190(30)
C(200)	13556(14)	-437(16)	5232(14)	264(16)
C(201)	13711(12)	-541(14)	4353(14)	208(12)
C(202)	14620(20)	-594(14)	4028(18)	245(13)
C(203)	15050(18)	-638(17)	3219(10)	227(14)
C(204)	15894(14)	-526(13)	2915(11)	171(8)
C(205)	16492(13)	-1301(18)	3047(13)	240(16)
C(206)	16826(18)	-2125(12)	2783(13)	214(12)

Table 3. Bond lengths [A] and angles [deg] for flat.

Zn(1)-O(2)	1.959(6)		N(3)-N(4)	1.373(11)
Zn(1)-N(1)	2.004(10)		N(4)-C(43)	1.343(14)
Zn(1)-N(5)	2.044(8)		N(4)-B(1)	1.522(16)
Zn(1)-N(3)	2.165(9)		N(5)-C(58)	1.350(12)
Zn(1)-O(1)	2.172(6)		N(5)-N(6)	1.383(10)
Zn(2)-O(4)	1.930(7)		N(6)-C(56)	1.342(12)
Zn(2)-N(7)	2.021(12)		N(6)-B(1)	1.519(14)
Zn(2)-N(9)	2.031(8)		N(7)-C(71)	1.314(15)
Zn(2)-O(3)	2.198(7)		N(7)-N(8)	1.375(11)
Zn(2)-N(11)	2.269(11)		N(8)-C(69)	1.306(18)
O(1)-C(1)	1.282(9)		N(8)-B(2)	1.53(2)
O(2)-C(2)	1.323(10)		N(9)-C(84)	1.342(13)
O(3)-C(11)	1.294(11)		N(9)-N(10)	1.384(11)
O(4)-C(12)	1.324(11)		N(10)-C(82)	1.350(13)
N(1)-C(32)	1.352(13)		N(10)-B(2)	1.575(17)
N(1)-N(2)	1.393(10)		N(11)-C(97)	1.332(16)
N(2)-C(30)	1.331(14)		N(11)-N(12)	1.389(13)
N(2)-B(1)	1.568(16)		N(12)-C(95)	1.347(15)
N(3)-C(45)	1.347(14)		N(12)-B(2)	1.57(2)

C(1)-C(6)	1.430(12)	C(49)-C(52)	1.570(11)
C(1)-C(2)	1.469(12)	C(50)-C(51)	1.3900
C(2)-C(3)	1.375(12)	C(52)-C(53)	1.530(13)
C(3)-C(4)	1.422(13)	C(52)-C(54)	1.539(14)
C(3)-C(26)	1.513(13)	C(55)-C(56)	1.508(14)
C(4)-C(5)	1.412(12)	C(56)-C(57)	1.375(14)
C(4)-C(21)	1.421(12)	C(57)-C(58)	1.413(13)
C(5)-C(6)	1.361(12)	C(58)-C(59)	1.447(13)
C(6)-C(7)	1.531(12)	C(59)-C(60)	1.378(12)
C(7)-C(8)	1.511(12)	C(59)-C(64)	1.418(13)
C(7)-C(9)	1.526(14)	C(60)-C(61)	1.406(13)
C(7)-C(10)	1.533(12)	C(61)-C(62)	1.389(13)
C(11)-C(12)	1.441(15)	C(62)-C(63)	1.360(13)
C(11)-C(16)	1.481(14)	C(62)-C(65)	1.522(13)
C(12)-C(13)	1.384(13)	C(63)-C(64)	1.379(12)
C(13)-C(14)	1.389(12)	C(65)-C(67)	1.467(16)
C(13)-C(23)	1.524(14)	C(65)-C(66)	1.522(17)
C(14)-C(15)	1.416(14)	C(68)-C(69)	1.537(17)
C(14)-C(21)	1.476(13)	C(69)-C(70)	1.370(19)
C(15)-C(16)	1.360(13)	C(70)-C(71)	1.394(16)
C(16)-C(17)	1.513(15)	C(71)-C(72)	1.491(14)
C(17)-C(18)	1.544(14)	C(71)-C(72')	1.523(15)
C(17)-C(20)	1.548(16)	C(72)-C(73)	1.3900
C(17)-C(19)	1.554(14)	C(72)-C(77)	1.3900
C(21)-C(22)	1.362(13)	C(73)-C(74)	1.3900
C(22)-C(23)	1.513(13)	C(74)-C(75)	1.3900
C(22)-C(26)	1.543(13)	C(75)-C(76)	1.3900
C(23)-C(24)	1.534(14)	C(75)-C(78)	1.580(14)
C(23)-C(25)	1.538(13)	C(76)-C(77)	1.3900
C(26)-C(27)	1.516(14)	C(78)-C(80)	1.517(18)
C(26)-C(28)	1.529(13)	C(78)-C(79)	1.523(18)
C(29)-C(30)	1.502(14)	C(72')-C(73')	1.3900
C(30)-C(31)	1.360(15)	C(72')-C(77')	1.3900
C(31)-C(32)	1.399(14)	C(73')-C(74')	1.3900
C(32)-C(33)	1.491(15)	C(74')-C(75')	1.3900
C(33)-C(34)	1.372(15)	C(75')-C(76')	1.3900
C(33)-C(38)	1.404(13)	C(76')-C(77')	1.3900
C(34)-C(35)	1.362(15)	C(81)-C(82)	1.514(15)
C(35)-C(36)	1.381(15)	C(82)-C(83)	1.340(15)
C(36)-C(37)	1.375(15)	C(83)-C(84)	1.410(14)
C(36)-C(39)	1.549(16)	C(84)-C(85)	1.460(14)
C(37)-C(38)	1.374(13)	C(85)-C(86)	1.388(13)
C(39)-C(40)	1.452(17)	C(85)-C(90)	1.394(14)
C(39)-C(41)	1.497(17)	C(86)-C(87)	1.365(13)
C(42)-C(43)	1.470(16)	C(87)-C(88)	1.397(14)
C(43)-C(44)	1.369(18)	C(88)-C(89)	1.386(13)
C(44)-C(45)	1.404(17)	C(88)-C(91)	1.514(14)
C(45)-C(46)	1.497(15)	C(89)-C(90)	1.384(14)
C(46)-C(47)	1.3900	C(91)-C(92)	1.507(14)
C(46)-C(51)	1.3900	C(91)-C(93)	1.514(15)
C(47)-C(48)	1.3900	C(94)-C(95)	1.494(17)
C(48)-C(49)	1.3900	C(95)-C(96)	1.34(2)
C(49)-C(50)	1.3900	C(96)-C(97)	1.393(17)

C(97)-C(98)	1.487(18)	C(58)-N(5)-Zn(1)	138.0(6)
C(98)-C(103)	1.34(2)	N(6)-N(5)-Zn(1)	113.6(6)
C(98)-C(99)	1.350(16)	C(56)-N(6)-N(5)	109.1(8)
C(99)-C(100)	1.398(17)	C(56)-N(6)-B(1)	131.3(9)
C(100)-C(101)	1.324(17)	N(5)-N(6)-B(1)	119.2(8)
C(101)-C(102)	1.379(19)	C(71)-N(7)-N(8)	106.7(11)
C(101)-C(104)	1.54(2)	C(71)-N(7)-Zn(2)	139.5(8)
C(102)-C(103)	1.38(2)	N(8)-N(7)-Zn(2)	113.2(10)
C(104)-C(106)	1.502(14)	C(69)-N(8)-N(7)	109.9(12)
C(104)-C(105)	1.547(13)	C(69)-N(8)-B(2)	128.2(12)
C(200)-C(201)	1.56(3)	N(7)-N(8)-B(2)	119.1(13)
C(201)-C(202)	1.51(3)	C(84)-N(9)-N(10)	106.3(8)
C(202)-C(203)	1.39(3)	C(84)-N(9)-Zn(2)	139.7(7)
C(203)-C(204)	1.50(2)	N(10)-N(9)-Zn(2)	114.0(7)
C(204)-C(205)	1.53(3)	C(82)-N(10)-N(9)	110.1(9)
C(205)-C(206)	1.51(3)	C(82)-N(10)-B(2)	129.9(10)
O(2)-Zn(1)-N(1)	130.0(3)	N(9)-N(10)-B(2)	120.0(9)
O(2)-Zn(1)-N(5)	131.9(3)	C(97)-N(11)-N(12)	105.9(10)
N(1)-Zn(1)-N(5)	97.1(3)	C(97)-N(11)-Zn(2)	146.5(9)
O(2)-Zn(1)-N(3)	101.2(3)	N(12)-N(11)-Zn(2)	107.5(9)
N(1)-Zn(1)-N(3)	87.9(4)	C(95)-N(12)-N(11)	110.7(13)
N(5)-Zn(1)-N(3)	87.8(3)	C(95)-N(12)-B(2)	126.8(13)
O(2)-Zn(1)-O(1)	79.5(2)	N(11)-N(12)-B(2)	122.5(10)
N(1)-Zn(1)-O(1)	93.0(3)	N(6)-B(1)-N(4)	108.6(10)
N(5)-Zn(1)-O(1)	90.4(3)	N(6)-B(1)-N(2)	110.7(10)
N(3)-Zn(1)-O(1)	178.1(3)	N(4)-B(1)-N(2)	110.8(9)
O(4)-Zn(2)-N(7)	130.1(4)	N(8)-B(2)-N(12)	108.6(10)
O(4)-Zn(2)-N(9)	126.9(4)	N(8)-B(2)-N(10)	112.6(12)
N(7)-Zn(2)-N(9)	101.3(4)	N(12)-B(2)-N(10)	106.7(13)
O(4)-Zn(2)-O(3)	79.4(3)	O(1)-C(1)-C(6)	123.1(8)
N(7)-Zn(2)-O(3)	91.8(3)	O(1)-C(1)-C(2)	115.7(8)
N(9)-Zn(2)-O(3)	87.6(3)	C(6)-C(1)-C(2)	121.1(8)
O(4)-Zn(2)-N(11)	106.9(4)	O(2)-C(2)-C(3)	123.2(8)
N(7)-Zn(2)-N(11)	83.9(4)	O(2)-C(2)-C(1)	118.0(8)
N(9)-Zn(2)-N(11)	88.8(3)	C(3)-C(2)-C(1)	118.8(8)
O(3)-Zn(2)-N(11)	173.7(4)	C(2)-C(3)-C(4)	118.8(8)
C(1)-O(1)-Zn(1)	110.8(6)	C(2)-C(3)-C(26)	129.6(9)
C(2)-O(2)-Zn(1)	114.8(5)	C(4)-C(3)-C(26)	111.5(8)
C(11)-O(3)-Zn(2)	109.6(7)	C(5)-C(4)-C(21)	132.3(10)
C(12)-O(4)-Zn(2)	116.0(7)	C(5)-C(4)-C(3)	121.0(8)
C(32)-N(1)-N(2)	104.8(9)	C(21)-C(4)-C(3)	106.7(8)
C(32)-N(1)-Zn(1)	139.4(7)	C(6)-C(5)-C(4)	122.2(9)
N(2)-N(1)-Zn(1)	115.6(8)	C(5)-C(6)-C(1)	117.3(8)
C(30)-N(2)-N(1)	110.4(10)	C(5)-C(6)-C(7)	121.2(9)
C(30)-N(2)-B(1)	131.7(10)	C(1)-C(6)-C(7)	121.4(8)
N(1)-N(2)-B(1)	117.8(9)	C(8)-C(7)-C(9)	107.6(8)
C(45)-N(3)-N(4)	104.4(9)	C(8)-C(7)-C(6)	112.7(8)
C(45)-N(3)-Zn(1)	141.2(9)	C(9)-C(7)-C(6)	109.1(8)
N(4)-N(3)-Zn(1)	111.5(7)	C(8)-C(7)-C(10)	108.6(8)
C(43)-N(4)-N(3)	112.9(11)	C(9)-C(7)-C(10)	110.2(8)
C(43)-N(4)-B(1)	126.9(11)	C(6)-C(7)-C(10)	108.7(7)
N(3)-N(4)-B(1)	120.0(9)	O(3)-C(11)-C(12)	116.0(10)
C(58)-N(5)-N(6)	107.4(7)	O(3)-C(11)-C(16)	121.8(11)

C(12)-C(11)-C(16)	122.2(10)	C(38)-C(37)-C(36)	123.3(11)
O(4)-C(12)-C(13)	123.1(11)	C(37)-C(38)-C(33)	118.6(10)
O(4)-C(12)-C(11)	118.7(9)	C(40)-C(39)-C(41)	113.1(14)
C(13)-C(12)-C(11)	118.2(10)	C(40)-C(39)-C(36)	110.3(11)
C(12)-C(13)-C(14)	119.0(10)	C(41)-C(39)-C(36)	112.5(11)
C(12)-C(13)-C(23)	129.7(9)	N(4)-C(43)-C(44)	105.8(12)
C(14)-C(13)-C(23)	111.2(9)	N(4)-C(43)-C(42)	125.1(15)
C(13)-C(14)-C(15)	123.3(10)	C(44)-C(43)-C(42)	129.1(15)
C(13)-C(14)-C(21)	107.7(9)	C(43)-C(44)-C(45)	107.1(13)
C(15)-C(14)-C(21)	128.8(9)	N(3)-C(45)-C(44)	109.8(13)
C(16)-C(15)-C(14)	121.2(10)	N(3)-C(45)-C(46)	122.9(10)
C(15)-C(16)-C(11)	115.6(11)	C(44)-C(45)-C(46)	127.2(13)
C(15)-C(16)-C(17)	123.9(10)	C(47)-C(46)-C(51)	120.0
C(11)-C(16)-C(17)	120.4(9)	C(47)-C(46)-C(45)	117.4(7)
C(16)-C(17)-C(18)	110.6(9)	C(51)-C(46)-C(45)	122.0(8)
C(16)-C(17)-C(20)	111.1(10)	C(46)-C(47)-C(48)	120.0
C(18)-C(17)-C(20)	108.8(10)	C(49)-C(48)-C(47)	120.0
C(16)-C(17)-C(19)	107.8(10)	C(48)-C(49)-C(50)	120.0
C(18)-C(17)-C(19)	108.0(9)	C(48)-C(49)-C(52)	122.5(10)
C(20)-C(17)-C(19)	110.5(9)	C(50)-C(49)-C(52)	117.5(10)
C(22)-C(21)-C(4)	111.5(9)	C(49)-C(50)-C(51)	120.0
C(22)-C(21)-C(14)	108.4(9)	C(50)-C(51)-C(46)	120.0
C(4)-C(21)-C(14)	140.0(10)	C(53)-C(52)-C(54)	116(2)
C(21)-C(22)-C(23)	112.3(9)	C(53)-C(52)-C(49)	105.0(15)
C(21)-C(22)-C(26)	110.4(8)	C(54)-C(52)-C(49)	103.9(17)
C(23)-C(22)-C(26)	137.2(9)	N(6)-C(56)-C(57)	109.0(9)
C(22)-C(23)-C(13)	100.2(8)	N(6)-C(56)-C(55)	122.8(10)
C(22)-C(23)-C(24)	112.7(9)	C(57)-C(56)-C(55)	128.1(10)
C(13)-C(23)-C(24)	112.7(8)	C(56)-C(57)-C(58)	106.0(10)
C(22)-C(23)-C(25)	111.4(8)	N(5)-C(58)-C(57)	108.5(9)
C(13)-C(23)-C(25)	108.9(9)	N(5)-C(58)-C(59)	122.3(8)
C(24)-C(23)-C(25)	110.5(8)	C(57)-C(58)-C(59)	129.1(10)
C(3)-C(26)-C(27)	109.1(9)	C(60)-C(59)-C(64)	117.2(9)
C(3)-C(26)-C(28)	111.0(8)	C(60)-C(59)-C(58)	122.4(9)
C(27)-C(26)-C(28)	112.7(9)	C(64)-C(59)-C(58)	120.3(9)
C(3)-C(26)-C(22)	99.6(8)	C(59)-C(60)-C(61)	120.9(10)
C(27)-C(26)-C(22)	112.9(8)	C(62)-C(61)-C(60)	120.9(9)
C(28)-C(26)-C(22)	110.8(9)	C(63)-C(62)-C(61)	118.0(9)
N(2)-C(30)-C(31)	108.7(10)	C(63)-C(62)-C(65)	120.6(10)
N(2)-C(30)-C(29)	121.4(13)	C(61)-C(62)-C(65)	121.4(10)
C(31)-C(30)-C(29)	129.8(13)	C(62)-C(63)-C(64)	122.3(9)
C(30)-C(31)-C(32)	106.0(11)	C(63)-C(64)-C(59)	120.5(9)
N(1)-C(32)-C(31)	110.0(10)	C(67)-C(65)-C(62)	114.0(11)
N(1)-C(32)-C(33)	121.6(10)	C(67)-C(65)-C(66)	112.8(14)
C(31)-C(32)-C(33)	128.4(12)	C(62)-C(65)-C(66)	109.6(9)
C(34)-C(33)-C(38)	118.1(10)	N(8)-C(69)-C(70)	108.6(12)
C(34)-C(33)-C(32)	120.9(11)	N(8)-C(69)-C(68)	123.2(16)
C(38)-C(33)-C(32)	121.1(11)	C(70)-C(69)-C(68)	128.0(18)
C(35)-C(34)-C(33)	121.8(12)	C(69)-C(70)-C(71)	105.2(15)
C(34)-C(35)-C(36)	121.3(12)	N(7)-C(71)-C(70)	109.4(12)
C(37)-C(36)-C(35)	116.8(11)	N(7)-C(71)-C(72)	124.2(12)
C(37)-C(36)-C(39)	122.9(11)	C(70)-C(71)-C(72)	126.4(15)
C(35)-C(36)-C(39)	120.3(12)	N(7)-C(71)-C(72')	121.3(12)

C(70)-C(71)-C(72')	129.2(15)	C(86)-C(87)-C(88)	122.2(10)
C(72)-C(71)-C(72')	3.4(7)	C(89)-C(88)-C(87)	115.3(10)
C(73)-C(72)-C(77)	120.0	C(89)-C(88)-C(91)	123.3(10)
C(73)-C(72)-C(71)	118.9(9)	C(87)-C(88)-C(91)	121.4(9)
C(77)-C(72)-C(71)	121.1(9)	C(90)-C(89)-C(88)	123.4(11)
C(72)-C(73)-C(74)	120.0	C(89)-C(90)-C(85)	120.1(10)
C(75)-C(74)-C(73)	120.0	C(92)-C(91)-C(93)	111.8(11)
C(74)-C(75)-C(76)	120.0	C(92)-C(91)-C(88)	112.4(9)
C(74)-C(75)-C(78)	118.0(9)	C(93)-C(91)-C(88)	111.6(9)
C(76)-C(75)-C(78)	121.6(9)	C(96)-C(95)-N(12)	106.0(12)
C(77)-C(76)-C(75)	120.0	C(96)-C(95)-C(94)	130.6(14)
C(76)-C(77)-C(72)	120.0	N(12)-C(95)-C(94)	123.3(17)
C(80)-C(78)-C(79)	104.9(13)	C(95)-C(96)-C(97)	109.2(14)
C(80)-C(78)-C(75)	108.1(11)	N(11)-C(97)-C(96)	108.2(14)
C(79)-C(78)-C(75)	111.0(11)	N(11)-C(97)-C(98)	124.7(11)
C(73')-C(72')-C(77')	120.0	C(96)-C(97)-C(98)	127.0(15)
C(73')-C(72')-C(71)	118.1(11)	C(103)-C(98)-C(99)	118.8(16)
C(77')-C(72')-C(71)	121.9(11)	C(103)-C(98)-C(97)	117.1(14)
C(72')-C(73')-C(74')	120.0	C(99)-C(98)-C(97)	124.1(13)
C(75')-C(74')-C(73')	120.0	C(98)-C(99)-C(100)	120.4(13)
C(74')-C(75')-C(76')	120.0	C(101)-C(100)-C(99)	121.1(14)
C(75')-C(76')-C(77')	120.0	C(100)-C(101)-C(102)	118.2(16)
C(76')-C(77')-C(72')	120.0	C(100)-C(101)-C(104)	120.3(14)
C(83)-C(82)-N(10)	107.4(10)	C(102)-C(101)-C(104)	121.2(14)
C(83)-C(82)-C(81)	130.6(11)	C(101)-C(102)-C(103)	120.3(16)
N(10)-C(82)-C(81)	122.0(11)	C(98)-C(103)-C(102)	120.8(16)
C(82)-C(83)-C(84)	108.0(10)	C(106)-C(104)-C(101)	118(2)
N(9)-C(84)-C(83)	108.0(10)	C(106)-C(104)-C(105)	124(2)
N(9)-C(84)-C(85)	123.5(9)	C(101)-C(104)-C(105)	110.9(15)
C(83)-C(84)-C(85)	128.2(10)	C(202)-C(201)-C(200)	97(2)
C(86)-C(85)-C(90)	117.0(10)	C(203)-C(202)-C(201)	119(3)
C(86)-C(85)-C(84)	121.2(10)	C(202)-C(203)-C(204)	117(2)
C(90)-C(85)-C(84)	121.8(9)	C(203)-C(204)-C(205)	106(2)
C(87)-C(86)-C(85)	122.0(10)	C(206)-C(205)-C(204)	140(3)

_____

 Symmetry transformations used to generate equivalent atoms:

 Table 4. Anisotropic displacement parameters (A^2 x 10^3) for flat.
 The anisotropic displacement factor exponent takes the form:-2 pi^2[h^2 a*^2 U11+2 h k a* b* U12]

_____

	U11	U22	U33	U23	U13	U12
Zn(1)	84(1)	58(1)	51(1)	9(1)	-42(1)	-26(1)
Zn(2)	51(1)	156(1)	60(1)	-49(1)	-30(1)	1(1)
O(1)	81(5)	58(4)	55(4)	9(3)	-48(4)	-24(3)
O(2)	73(5)	60(4)	51(4)	8(3)	-38(4)	-18(4)
O(3)	55(4)	139(7)	53(4)	-32(4)	-27(4)	-24(4)
O(4)	53(4)	131(6)	52(4)	-40(4)	-32(4)	7(4)
N(1)	100(7)	58(5)	57(6)	7(4)	-51(6)	-29(5)
N(2)	115(8)	56(5)	73(7)	7(5)	-64(7)	-36(5)
N(3)	104(7)	58(6)	59(6)	9(5)	-41(6)	-26(6)
N(4)	118(8)	65(6)	50(6)	7(5)	-32(6)	-47(6)

N(5)	91(6)	53(5)	55(5)	3(4)	-49(5)	-24(5)
N(6)	128(8)	74(6)	59(6)	29(5)	-65(6)	-55(6)
N(7)	40(6)	154(10)	73(7)	-58(7)	-32(5)	6(6)
N(8)	62(7)	146(10)	64(7)	-56(7)	-42(6)	5(6)
N(9)	52(6)	165(10)	56(6)	-40(6)	-40(5)	8(6)
N(10)	62(6)	179(11)	67(6)	-60(7)	-41(6)	12(6)
N(11)	49(6)	169(11)	62(6)	-42(7)	-27(5)	7(7)
N(12)	54(6)	180(11)	69(7)	-59(7)	-34(5)	14(7)
B(1)	131(13)	66(9)	62(9)	7(7)	-56(10)	-52(9)
B(2)	58(10)	190(19)	94(13)	-90(13)	-32(9)	5(11)
C(1)	64(6)	63(7)	39(5)	3(5)	-33(5)	-27(5)
C(2)	70(7)	50(6)	38(5)	-1(5)	-28(5)	-16(5)
C(3)	57(6)	58(7)	47(6)	-5(5)	-25(5)	-10(5)
C(4)	50(6)	80(8)	38(5)	-1(5)	-24(5)	-14(6)
C(5)	56(6)	65(7)	44(6)	-2(5)	-21(5)	-11(5)
C(6)	57(6)	75(7)	34(5)	5(5)	-32(5)	-22(5)
C(7)	59(7)	56(6)	39(6)	2(5)	-27(5)	-12(5)
C(8)	73(7)	84(8)	62(7)	-24(6)	-35(6)	7(6)
C(9)	64(7)	96(9)	77(8)	27(7)	-42(6)	-15(6)
C(10)	82(7)	53(6)	51(6)	0(5)	-30(6)	-12(5)
C(11)	58(7)	113(10)	38(6)	-23(6)	-14(6)	-25(7)
C(12)	53(7)	110(10)	50(6)	-33(6)	-29(6)	1(7)
C(13)	50(6)	83(8)	44(6)	-14(5)	-28(5)	-8(6)
C(14)	56(7)	87(8)	43(6)	-8(6)	-27(5)	-11(6)
C(15)	60(7)	84(8)	43(6)	-16(6)	-22(5)	-11(6)
C(16)	52(6)	109(9)	38(6)	-21(6)	-24(5)	-12(6)
C(17)	93(9)	94(9)	64(8)	-14(7)	-42(7)	-30(7)
C(18)	118(10)	88(8)	82(8)	-3(7)	-68(8)	-22(7)
C(19)	97(9)	112(10)	69(8)	-28(7)	-50(7)	-16(7)
C(20)	116(11)	151(13)	87(10)	-3(9)	-27(9)	-73(10)
C(21)	55(6)	80(8)	39(6)	-7(5)	-27(5)	-12(6)
C(22)	56(6)	79(8)	45(6)	-9(5)	-23(5)	-9(6)
C(23)	57(7)	85(8)	48(6)	-2(6)	-31(6)	0(6)
C(24)	78(8)	107(9)	68(8)	-6(7)	-42(7)	-8(7)
C(25)	58(7)	100(9)	65(7)	-28(6)	-26(6)	2(6)
C(26)	71(7)	69(7)	43(6)	-4(6)	-33(6)	-10(6)
C(27)	103(9)	76(8)	67(7)	7(6)	-47(7)	-21(7)
C(28)	69(7)	91(8)	54(7)	-8(6)	-30(6)	-3(6)
C(29)	161(13)	113(10)	114(10)	5(8)	-90(10)	-81(10)
C(30)	122(11)	81(8)	89(10)	23(7)	-78(9)	-59(8)
C(31)	91(9)	86(8)	77(9)	14(7)	-54(8)	-47(7)
C(32)	93(9)	63(7)	74(8)	15(6)	-56(8)	-31(7)
C(33)	83(8)	54(7)	62(7)	13(6)	-35(7)	-34(6)
C(34)	81(9)	92(9)	88(9)	5(7)	-47(8)	-30(7)
C(35)	88(9)	88(9)	85(10)	-2(7)	-37(8)	-34(7)
C(36)	89(9)	76(8)	73(8)	3(7)	-39(8)	-25(7)
C(37)	77(8)	81(8)	63(8)	4(6)	-42(7)	-22(7)
C(38)	68(7)	68(7)	55(7)	16(5)	-37(6)	-25(5)
C(39)	103(10)	110(11)	68(8)	1(8)	-27(7)	-44(8)
C(40)	197(17)	150(15)	75(10)	-28(9)	-44(10)	-69(13)
C(41)	240(20)	190(17)	75(10)	-17(11)	-88(13)	51(15)
C(42)	176(14)	116(11)	61(8)	-14(7)	-18(9)	-77(10)
C(43)	142(13)	86(10)	49(8)	1(8)	-16(9)	-56(9)

C(44)	134(13)	92(10)	59(9)	-12(8)	3(9)	-16(9)
C(45)	117(11)	77(9)	51(8)	10(7)	-16(7)	-20(8)
C(46)	99(7)	86(8)	74(6)	13(7)	-21(6)	-7(7)
C(47)	108(8)	227(17)	106(8)	34(11)	-10(6)	43(11)
C(48)	103(9)	300(20)	133(8)	48(14)	-19(6)	50(12)
C(49)	130(7)	155(12)	121(8)	25(10)	-41(7)	38(10)
C(50)	121(7)	73(8)	78(7)	-1(6)	-34(6)	-7(7)
C(51)	111(7)	64(7)	61(6)	-8(6)	-26(5)	-22(6)
C(52)	182(10)	208(12)	167(10)	16(12)	-90(10)	56(11)
C(53)	230(16)	166(12)	95(13)	-14(11)	-89(13)	96(11)
C(54)	181(13)	314(19)	189(18)	-1(16)	-111(14)	36(14)
C(55)	247(15)	134(11)	105(10)	47(8)	-135(11)	-115(11)
C(56)	155(11)	95(8)	75(8)	35(7)	-83(8)	-71(8)
C(57)	177(13)	103(9)	76(8)	41(7)	-91(9)	-89(9)
C(58)	109(9)	61(7)	47(6)	17(5)	-47(6)	-40(6)
C(59)	78(7)	66(7)	35(5)	9(5)	-29(5)	-39(6)
C(60)	99(8)	70(7)	51(6)	14(5)	-48(6)	-40(6)
C(61)	73(7)	78(8)	50(6)	0(6)	-35(6)	-20(6)
C(62)	54(6)	66(8)	57(7)	-13(6)	-18(5)	-21(5)
C(63)	67(7)	52(6)	54(6)	-10(5)	-26(6)	-21(5)
C(64)	67(7)	64(7)	43(6)	-1(5)	-21(5)	-20(6)
C(65)	81(8)	85(8)	86(9)	-27(7)	-42(7)	-23(7)
C(66)	72(11)	240(20)	300(30)	-200(20)	-27(13)	-26(12)
C(67)	360(30)	228(19)	85(11)	23(11)	-116(15)	-210(20)
C(68)	148(13)	187(16)	140(13)	-60(12)	-106(12)	-16(12)
C(69)	101(11)	131(12)	126(14)	-48(10)	-82(11)	-8(10)
C(70)	125(12)	123(11)	108(12)	-21(9)	-78(10)	-38(9)
C(71)	57(8)	119(10)	88(10)	-45(9)	-42(8)	4(7)
C(72)	85(14)	102(16)	89(12)	-31(11)	-43(9)	-22(12)
C(73)	93(13)	200(20)	96(12)	-74(15)	-44(11)	-39(15)
C(74)	102(13)	200(20)	86(11)	-44(15)	-43(10)	-45(16)
C(75)	121(17)	70(20)	79(9)	-5(11)	-53(10)	-44(17)
C(76)	86(12)	72(13)	69(10)	13(10)	-40(10)	-23(11)
C(77)	102(12)	93(14)	82(12)	25(11)	-65(10)	-42(12)
C(78)	156(11)	99(9)	65(7)	-7(6)	-65(8)	-24(8)
C(72')	42(18)	85(16)	69(14)	-49(11)	-15(14)	7(14)
C(73')	85(15)	80(13)	48(10)	-20(10)	-16(11)	-16(12)
C(74')	100(16)	86(14)	58(12)	-31(10)	-33(12)	-11(13)
C(75')	140(20)	105(19)	85(14)	6(12)	-81(17)	-26(19)
C(76')	210(30)	118(17)	101(15)	-11(14)	-67(18)	-52(19)
C(77')	190(30)	117(17)	100(16)	-13(12)	-42(17)	-71(18)
C(78')	156(11)	99(9)	65(7)	-7(6)	-65(8)	-24(8)
C(79)	140(13)	164(12)	76(9)	-19(9)	-37(9)	-19(9)
C(80)	280(20)	134(11)	110(11)	12(9)	-120(15)	-66(13)
C(81)	103(10)	196(15)	73(8)	-58(9)	-63(8)	11(10)
C(82)	69(9)	159(12)	67(8)	-53(8)	-39(7)	15(8)
C(83)	55(8)	153(12)	58(7)	-37(7)	-30(6)	7(7)
C(84)	57(8)	131(10)	43(6)	-31(6)	-28(6)	9(7)
C(85)	57(7)	105(9)	45(6)	-27(6)	-22(6)	4(7)
C(86)	58(7)	82(8)	40(6)	-7(5)	-16(5)	-8(6)
C(87)	44(7)	97(9)	47(6)	2(6)	-16(5)	-3(6)
C(88)	54(7)	87(8)	43(6)	-7(6)	-21(5)	-9(6)
C(89)	72(8)	103(9)	44(6)	-17(6)	-21(6)	-3(7)

C(90)	48(7)	115(10)	60(7)	-16(7)	-28(6)	7(6)
C(91)	60(7)	98(9)	75(8)	-1(7)	-32(6)	-16(7)
C(92)	76(8)	146(11)	69(8)	17(8)	-53(7)	-36(8)
C(93)	129(12)	119(11)	122(11)	46(9)	-83(10)	-61(10)
C(94)	77(9)	208(16)	84(9)	-47(10)	-55(8)	8(9)
C(95)	51(8)	219(18)	54(8)	-32(10)	-35(7)	13(10)
C(96)	75(10)	187(17)	73(10)	4(10)	-42(8)	9(10)
C(97)	49(7)	156(13)	48(7)	-7(8)	-25(6)	2(8)
C(98)	69(8)	131(10)	66(8)	-1(8)	-32(7)	-3(8)
C(99)	76(8)	105(9)	107(10)	4(8)	-63(8)	-7(7)
C(100)	101(10)	113(9)	113(11)	13(8)	-76(9)	-12(9)
C(101)	76(8)	111(9)	115(10)	22(8)	-49(8)	-18(8)
C(102)	195(17)	132(12)	154(16)	67(11)	-118(14)	-54(14)
C(103)	150(14)	167(14)	110(12)	36(11)	-93(11)	-26(13)
C(104)	146(15)	130(11)	159(12)	25(11)	-77(12)	-45(13)
C(105)	145(14)	117(12)	151(11)	-16(10)	-44(10)	-55(11)
C(106)	270(70)	50(30)	120(40)	-20(20)	90(40)	-90(30)
C(04)	146(15)	130(11)	159(12)	25(11)	-77(12)	-45(13)
C(05)	145(14)	117(12)	151(11)	-16(10)	-44(10)	-55(11)
C(107)	100(20)	190(30)	190(30)	-80(30)	-30(20)	-60(20)
C(200)	152(19)	350(40)	139(19)	20(20)	-30(16)	70(20)
C(201)	82(13)	250(30)	170(20)	18(18)	-10(14)	39(14)
C(202)	290(40)	160(20)	250(30)	-60(20)	-120(30)	30(20)
C(203)	310(30)	430(40)	55(10)	35(16)	-63(15)	-260(30)
C(204)	190(20)	240(20)	136(16)	60(15)	-90(16)	-113(19)
C(205)	132(16)	340(40)	180(20)	180(30)	-46(15)	-70(20)
C(206)	350(30)	128(16)	250(30)	43(17)	-130(30)	-160(20)

_____

Table 5. Hydrogen coordinates (x 10^4) and isotropic displacement parameters (A^2 x 10^3) for flat.

_____

x y z	U(eq)							
H(1)	5847	973	-1662	89	H(20R)	8233	5969	3036	169
H(2)	10716	3463	5708	137	H(20S)	8656	5289	2413	169
H(5A)	6086	3881	2287	68	H(24A)	7861	1359	3871	127
H(8A)	4308	5137	2104	114	H(24B)	8763	1283	3866	127
H(8B)	5283	4935	1933	114	H(24C)	8665	707	3358	127
H(8C)	4723	4526	2659	114	H(25A)	9623	1002	2109	116
H(9A)	4109	3609	2393	120	H(25B)	9860	1581	2489	116
H(9B)	4309	3424	1500	120	H(25C)	9530	1870	1773	116
H(9C)	3742	4265	1839	120	H(27A)	6930	1056	2993	119
H(10A)	5316	3978	385	94	H(27B)	7817	414	2646	119
H(10B)	5680	4577	579	94	H(27C)	7151	593	2225	119
H(10C)	4713	4819	698	94	H(28A)	8311	842	940	111
H(15A)	7042	4257	2757	75	H(28B)	8927	719	1406	111
H(18A)	7216	5405	2378	133	H(28C)	8687	1515	938	111
H(18B)	6899	6135	2923	133	H(29A)	4356	1209	-1402	160
H(18C)	6454	5474	3203	133	H(29B)	3652	889	-744	160
H(19A)	6640	5211	4443	132	H(29C)	4590	331	-1093	160
H(19B)	7055	5886	4299	132	H(31A)	3404	1230	730	88
H(19C)	7530	5028	4518	132	H(34A)	3013	2105	1870	98
H(20Q)	8785	5142	3242	169	H(35A)	2657	2422	3148	100

Atom	x	y	z	U
H(37A)	5043	1500	2960	83
H(38A)	5413	1115	1691	72
H(39A)	2966	2276	4328	111
H(40A)	3243	3264	4552	202
H(40B)	3425	3339	3624	202
H(40C)	4183	3004	3939	202
H(41A)	4640	1645	4242	281
H(41B)	3984	1171	4492	281
H(41C)	3841	1847	5038	281
H(42A)	6633	-315	-2250	173
H(42B)	7624	-687	-2632	173
H(42C)	7205	222	-2724	173
H(44A)	8331	-919	-1568	133
H(47A)	9260	-650	-934	223
H(48A)	10014	-1216	-105	266
H(50A)	7858	-782	1792	117
H(51A)	7104	-216	963	97
H(52A)	9181	-1166	2023	252
H(53A)	9747	-2535	1117	293
H(53B)	8860	-2267	1815	293
H(53C)	9698	-2541	2006	293
H(54A)	10771	-1824	1098	367
H(54B)	10394	-943	1367	367
H(54C)	10415	-1160	544	367
H(55A)	6354	1701	-2954	194
H(55B)	6073	2614	-3118	194
H(55C)	5411	2212	-2515	194
H(57A)	6639	3302	-2358	116
H(60A)	7604	2198	-370	78
H(61A)	8196	2852	145	77
H(63A)	7342	4799	-978	65
H(64A)	6700	4189	-1452	69
H(65A)	7961	4891	-133	94
H(66A)	9407	4370	-294	305
H(66B)	9221	4346	-1072	305
H(66C)	9403	3576	-551	305
H(67A)	8224	3654	923	276
H(67B)	7447	4426	1093	276
H(67C)	8353	4465	959	276
H(68A)	11015	5023	5030	217
H(68B)	11979	4636	4525	217
H(68C)	11508	4184	5274	217
H(70A)	11733	4548	3148	126
H(73A)	9889	3621	2841	145
H(74A)	9981	3380	1587	145
H(76A)	12366	3442	678	88
H(77A)	12274	3682	1932	98
H(78)	10753	2972	266	122
H(73B)	10896	2593	2813	89
H(74B)	10985	2305	1576	97
H(76B)	11255	4402	733	165
H(77B)	11165	4690	1970	156
H(78')	11438	2988	663	122
H(79A)	12533	2652	-235	199
H(79B)	12083	2324	-649	199
H(79C)	12064	2031	221	199
H(80A)	10790	4207	-247	242
H(80B)	11480	3615	-916	242
H(80C)	11756	3995	-373	242
H(81A)	9738	3414	7248	185
H(81B)	8929	4138	7593	185
H(81C)	9714	4255	6857	185
H(83A)	7750	4039	7103	110
H(86A)	6695	4541	6391	76
H(87A)	5561	4547	6137	81
H(89A)	6932	2648	4840	93
H(90A)	8077	2615	5113	94
H(91A)	4905	4104	5514	93
H(92A)	5672	4207	4189	135
H(92B)	5022	3758	4291	135
H(92C)	5986	3288	4107	135
H(93A)	5464	2476	5337	165
H(93B)	4522	3025	5540	165
H(93C)	4967	2894	6169	165
H(94A)	12162	1661	6128	186
H(94B)	11347	2385	6458	186
H(94C)	12102	2481	5676	186
H(96A)	11926	755	5283	144
H(99A)	10497	1361	3588	112
H(10D)	10538	333	2942	125
H(10E)	11427	-1145	4431	180
H(10F)	11396	-122	5066	166
H(10G)	10319	-979	3283	168
H(10H)	10987	-1165	2075	203
H(10I)	11885	-1471	2153	203
H(10J)	11395	-565	2193	203
H(10K)	10933	-2289	3347	278
H(10L)	10464	-1848	4168	278
H(10M)	11461	-2117	3789	278
H(20A)	13852	-919	5440	396
H(20B)	12957	-306	5541	396
H(20C)	13763	-20	5268	396
H(20D)	13618	-1020	4272	249
H(20E)	13371	-90	4135	249
H(20F)	14672	-137	4210	294
H(20G)	14917	-1055	4275	294
H(20H)	14698	-245	2961	273
H(20I)	15114	-1151	3051	273
H(20J)	15895	-113	3205	206
H(20K)	16057	-383	2346	206
H(20L)	17010	-1167	2926	288
H(20M)	16271	-1363	3628	288
H(20N)	16399	-2257	2678	321
H(20O)	16976	-2470	3198	321
H(20P)	17321	-2184	2301	321

7(SQZnL)$_2$.
Data Collection. x98050 was mounted on the end of a glass fiber using a small amount of silicon grease and transferred to the diffractometer. The sample was maintained at a temperature of -125 deg C using a nitrogen cold stream. All X-ray measurements were made on an Enraf-Nonius CAD4-MACH diffractometer. The unit cell dimensions were determined by a fit of 24 well centered reflections and their Friedel pairs with theta 24 deg < 2(theta) < 34 deg. A quadrant of unique data was collected using the omega scan mode in a non-bisecting geometry. The adoption of a non-bisecting scan mode was accomplished by offsetting psi by 20.00 deg for each data point collected. This was done to minimize the interaction of the goniometer head with the cold stream. Three standard reflections were measured every 4800 seconds of X-ray exposure time. Scaling the data was accomplished using a 5 point smoothed curved routine fit to the intensity check reflections. The intensity data was corrected for Lorentz and polarization effects. Data was not corrected for absorption. During the data collection the crystal moved several times, which made reorientation of the crystal necessary. As a consequence, a total of 282 reflections were recollected throughout the data collection. The Rmerge for these reflections was 0.14.

Structure Solution and Refinement. The data were reduced using routines from the NRCVAX set of programs. The structure was solved using SIR92. Most non-H atom positions were recovered from the initial E-map. The remaining nonhydrogen atoms were obtained from subsequent difference Fourier maps. Hydrogen atoms were included in the model at calculated positions. The hydrogen atom positions and isotropic displacement parameters were allowed to ride on the parent atom. The structure contained 3 methylene chloride molecules, two of which were fractionally occupied. The first of the fractionally occupied solvent molecules had it's occupancy fixed at 0.5. The second fractionally occupied solvent molecule had it's occupancy factor refined to 0.87, and was then subsequently fixed. Refinement of the structure was performed using full matrix least-squares based on F. All non-H atoms were allowed to refine with anisotropic displacement parameters (ADP's). The calculated structure factors included corrections for anomalous dispersion from the usual tabulation (International Tables for X-ray Crystallography, Vol. IV, (1974), Table 2.3.1, Kynoch Press, Birmingham, England). A secondary extinction correction attempted, but disregarded during the final cycles of refinement because it refined to a physically meaningless value. Additional information and relevant literature references can be found in the REPORT.OUT file and the reference section of the Facility's Web page (see http://www.xray.ncsu.edu/ref.html).

Table S22. Atomic Parameters x,y,z and Biso. E.S.Ds. refer to the last digit printed.

	x	y	z	Biso
Zn1	.52907(5)	.25399(4)	.21002(4)	1.78(5)
Zn2	.00784(5)	.11708(4)	.25627(4)	1.21(4)
O1	.4357(3)	.2250(2)	.1579(3)	2.0(3)
O2	.4528(3)	.2989(2)	.2380(3)	1.9(3)
O3	.0938(3)	.1420(2)	.2362(2)	1.4(3)
O4	-.0439(3)	.1743(2)	.1929(2)	1.4(3)
C1	.3771(4)	.2459(3)	.1646(4)	1.6(4)
C2	.3851(5)	.2856(3)	.2084(4)	1.5(4)
C3	.3220(4)	.3082(3)	.2193(3)	1.3(4)
C4	.2546(5)	.2913(3)	.1832(4)	1.6(4)
C5	.2456(4)	.2550(3)	.1368(3)	1.4(4)
C6	.3058(4)	.2322(3)	.1276(4)	1.5(4)
C7	.1667(4)	.2453(4)	.0944(3)	1.5(4)
C8	.1122(4)	.2314(3)	.1259(4)	1.3(4)
C9	.1315(4)	.1973(3)	.1721(4)	1.4(4)

C10	.0790(4)	.1763(3)	.1951(3)	1.1(4)
C11	.0017(5)	.1940(3)	.1701(3)	1.2(4)
C12	-.0166(4)	.2323(3)	.1245(3)	1.3(4)
C13	.0380(4)	.2490(3)	.1036(3)	1.3(4)
C14	.1457(4)	.2941(3)	.0538(4)	1.3(4)
C15	.1391(4)	.2799(4)	-.0038(4)	1.7(4)
C16	.1223(5)	.3187(4)	-.0472(4)	2.3(5)
C17	.1108(5)	.3701(4)	-.0332(4)	2.7(5)
C18	.1158(5)	.3830(4)	.0235(4)	2.6(5)
C19	.1345(5)	.3452(4)	.0684(4)	2.1(4)
C20	.1635(4)	.2024(4)	.0501(4)	1.7(4)
C21	.1486(5)	.2236(4)	-.0057(4)	1.8(5)
C22	.1415(5)	.1921(4)	-.0543(4)	2.5(5)
C23	.1479(5)	.1377(5)	-.0453(4)	3.0(5)
C24	.1612(5)	.1162(4)	.0094(4)	2.9(5)
C25	.1684(5)	.1494(4)	.0580(4)	2.5(5)
C26	.3320(5)	.3495(3)	.2675(4)	1.8(4)
C27	.3783(5)	.3265(4)	.3276(4)	2.6(5)
C28	.2579(5)	.3662(4)	.2729(4)	2.3(4)
C29	.3697(5)	.3979(4)	.2527(4)	2.2(5)
C30	-.0950(4)	.2544(3)	.1006(3)	1.2(4)
C31	-.1040(5)	.2937(4)	.0512(4)	2.3(5)
C32	-.1501(5)	.2089(4)	.0756(4)	2.0(4)
C33	-.1151(5)	.2811(3)	.1507(4)	1.8(4)
B	.6940(5)	.2615(4)	.2600(5)	2.0(5)
N1	.5889(4)	.3180(3)	.2009(3)	2.0(4)
N2	.6635(4)	.3129(3)	.2274(3)	1.8(4)
N3	.5886(4)	.2365(3)	.2962(3)	1.9(3)
N4	.6613(4)	.2520(3)	.3092(3)	2.0(3)
N5	.6035(4)	.2066(3)	.1812(3)	1.8(3)
N6	.6746(4)	.2148(3)	.2158(3)	1.6(3)
C34	.6976(5)	.3571(4)	.2223(5)	2.6(5)
C35	.6453(5)	.3924(4)	.1915(5)	3.0(5)
C36	.5773(5)	.3655(4)	.1784(4)	2.3(5)
C37	.7794(5)	.3647(4)	.2460(5)	3.4(6)
C38	.6910(5)	.2552(4)	.3676(4)	2.7(5)
C39	.6397(5)	.2416(4)	.3932(4)	2.9(5)
C40	.5769(5)	.2295(4)	.3470(4)	2.4(5)
C41	.7690(5)	.2715(5)	.3962(4)	4.3(6)
C42	.7195(5)	.1779(3)	.2055(4)	1.8(4)
C43	.6775(5)	.1453(4)	.1635(4)	2.2(4)
C44	.6045(5)	.1648(4)	.1493(4)	2.0(5)
C45	.8008(5)	.1752(4)	.2365(4)	2.1(4)
C46	.5036(5)	.3863(4)	.1453(4)	2.3(5)
C47	.4470(5)	.3536(4)	.1127(4)	2.2(5)
C48	.3787(5)	.3748(4)	.0819(4)	2.5(5)
C49	.3662(5)	.4276(4)	.0823(4)	2.3(4)
C50	.4229(5)	.4599(4)	.1142(5)	3.0(5)
C51	.4903(5)	.4398(4)	.1459(5)	3.0(5)
C52	.2908(6)	.4503(4)	.0483(5)	3.4(5)
C53	.2531(6)	.4696(5)	.0914(5)	4.9(6)
C54	.2965(7)	.4939(5)	.0082(5)	5.6(7)
C55	.5050(5)	.2116(4)	.3510(4)	2.3(5)

C56	.4893(5)	.2173(4)	.4040(5)	3.2(5)
C57	.4226(6)	.2015(4)	.4084(4)	3.2(5)
C58	.3688(5)	.1795(4)	.3611(5)	2.6(5)
C59	.3844(5)	.1733(4)	.3091(4)	2.7(5)
C60	.4513(5)	.1887(4)	.3030(4)	2.3(5)
C61	.2933(6)	.1658(4)	.3627(5)	3.6(6)
C62	.2947(6)	.1411(5)	.4201(5)	4.3(6)
C63	.2438(6)	.2141(5)	.3487(5)	4.5(6)
C64	.5396(5)	.1427(4)	.1046(4)	2.3(5)
C65	.5309(6)	.0906(4)	.0955(5)	4.2(6)
C66	.4716(6)	.0679(4)	.0523(6)	4.9(6)
C67	.4205(6)	.0987(5)	.0162(5)	4.2(6)
C68	.4279(6)	.1529(4)	.0214(5)	3.9(6)
C69	.4872(5)	.1756(4)	.0651(5)	3.1(5)
C70	.3557(6)	.0746(5)	-.0329(6)	4.8(7)
C71	.3102(7)	.0425(6)	-.0076(7)	7.0(8)
C72	.3815(7)	.0430(5)	-.0751(6)	5.4(7)
B'	-.0533(6)	.0536(4)	.3362(4)	1.3(4)
N1'	-.0245(4)	.1478(3)	.3231(3)	1.3(3)
N2'	-.0514(4)	.1119(3)	.3533(3)	1.4(3)
N3'	-.0794(4)	.0665(3)	.2276(3)	1.4(3)
N4'	-.1027(4)	.0476(3)	.2715(3)	1.5(3)
N5'	.0629(4)	.0515(3)	.3078(3)	1.5(3)
N6'	.0244(4)	.0334(3)	.3434(3)	1.5(3)
C34'	-.0764(5)	.1372(3)	.3920(4)	1.5(4)
C35'	-.0663(4)	.1899(3)	.3865(4)	1.6(4)
C36'	-.0342(4)	.1951(3)	.3427(3)	1.0(4)
C37'	-.1080(5)	.1079(3)	.4331(4)	2.4(5)
C38'	-.1693(5)	.0245(3)	.2482(4)	1.7(4)
C39'	-.1872(5)	.0269(4)	.1888(4)	2.3(5)
C40'	-.1295(5)	.0527(3)	.1772(4)	1.7(4)
C41'	-.2112(5)	.0024(4)	.2857(4)	2.7(5)
C42'	.0656(5)	-.0030(3)	.3806(4)	1.8(4)
C43'	.1303(5)	-.0089(4)	.3683(4)	2.1(4)
C44'	.1260(5)	.0246(3)	.3226(4)	1.9(4)
C45'	.0414(6)	-.0291(4)	.4275(4)	2.5(5)
C46'	-.0125(4)	.2439(3)	.3200(3)	1.0(3)
C47'	.0482(4)	.2459(3)	.3002(3)	1.4(4)
C48'	.0687(4)	.2932(3)	.2815(4)	1.4(4)
C49'	.0310(5)	.3398(3)	.2829(3)	1.4(4)
C50'	-.0300(5)	.3367(3)	.3028(4)	1.5(4)
C51'	-.0512(5)	.2893(3)	.3201(3)	1.3(4)
C52'	.0571(4)	.3909(3)	.2645(4)	1.6(4)
C53'	.0501(5)	.3896(4)	.1988(4)	2.4(5)
C54'	.0193(6)	.4392(4)	.2778(4)	2.8(5)
C55'	-.1180(5)	.0632(3)	.1202(4)	2.1(4)
C56'	-.1783(6)	.0670(4)	.0680(4)	3.2(5)
C57'	-.1670(7)	.0760(5)	.0151(4)	4.0(6)
C58'	-.0981(7)	.0818(5)	.0116(4)	3.9(7)
C59'	-.0382(6)	.0779(4)	.0630(5)	3.6(6)
C60'	-.0488(5)	.0678(4)	.1165(4)	2.2(5)
C61'	-.0830(9)	.0942(6)	-.0458(5)	6.6(9)
C62'	-.0617(16)	.0532(7)	-.0711(9)	15.(2)

C63'	-.0475(6)	.1468(5)	-.0434(4)	4.1(6)
C64'	.1807(6)	.0305(4)	.2915(5)	2.7(5)
C65'	.1610(7)	.0347(4)	.2310(5)	4.2(6)
C66'	.2146(8)	.0387(5)	.2041(5)	5.3(8)
C67'	.2891(8)	.0392(5)	.2378(7)	5.9(9)
C68'	.3070(7)	.0332(5)	.2959(7)	4.8(7)
C69'	.2560(6)	.0294(4)	.3246(5)	3.3(5)
C70'	.3485(11)	.0427(7)	.2056(9)	11.5(15)
C71'	.3664(11)	-.0051(7)	.1857(9)	11.2(15)
C72'	.3445(8)	.0884(6)	.1683(6)	6.5(9)
C1s	.6099(8)	.1077(5)	.2863(6)	6.1(8)
Cl1s	.6855(3)	.11201(16)	.3456(2)	9.9(3)
Cl2s	.5848(2)	.04313(14)	.26136(18)	6.6(2)
C2s	.6245(13)	.3447(13)	.0405(14)	7.2(18)
Cl3s	.6358(4)	.2800(3)	.0648(3)	6.7(4)
Cl4s	.7071(6)	.3732(4)	.0475(5)	10.9(7)
C3s	.5745(8)	.1400(7)	.9493(7)	6.4(10)
Cl5s	.6588(3)	.1498(3)	1.0010(3)	12.0(4)
Cl6s	.5732(5)	.0901(4)	.9042(4)	17.7(7)

H4	.212	.305	.190	2.5		H37c	.791	.394	.272	4.2
H6	.299	.207	.097	2.3		H39	.645	.240	.434	3.7
H9	.182	.188	.189	2.1		H41a	.791	.278	.366	4.9
H13	.026	.274	.072	2.1		H41b	.771	.303	.419	4.9
H16	.119	.310	-.087	3.1		H41c	.796	.244	.421	4.9
H17	.099	.397	-.063	3.4		H43	.693	.115	.147	2.9
H18	.107	.419	.032	3.3		H45a	.815	.204	.264	2.8
H19	.139	.354	.108	2.8		H45b	.812	.143	.258	2.8
H22	.132	.207	-.093	3.3		H45c	.827	.177	.209	2.8
H23	.144	.115	-.078	3.7		H47	.455	.317	.112	3.1
H24	.165	.079	.015	3.6		H48	.340	.352	.060	3.2
H25	.178	.135	.097	3.4		H50	.415	.497	.114	3.6
H27a	.425	.316	.326	3.4		H51	.529	.462	.169	3.5
H27b	.385	.352	.358	3.4		H52	.261	.423	.025	3.9
H27c	.353	.297	.336	3.4		H53a	.249	.441	.116	5.5
H28a	.234	.336	.283	3.1		H53b	.283	.497	.115	5.5
H28b	.265	.392	.303	3.1		H53c	.205	.483	.071	5.5
H28c	.228	.380	.236	3.1		H54a	.319	.482	-.020	5.8
H29a	.377	.424	.283	3.0		H54b	.249	.508	-.012	5.8
H29b	.416	.388	.249	3.0		H54c	.326	.521	.032	5.8
H29c	.339	.412	.216	3.0		H56	.525	.234	.437	4.2
H31a	-.092	.277	.019	3.1		H57	.413	.204	.445	4.1
H31b	-.154	.306	.038	3.1		H59	.348	.158	.276	3.4
H31c	-.071	.323	.066	3.1		H60	.461	.184	.266	3.3
H32a	-.146	.183	.106	2.8		H61	.272	.141	.332	4.7
H32b	-.199	.222	.062	2.8		H62a	.325	.110	.427	5.4
H32c	-.139	.193	.044	2.8		H62b	.315	.166	.451	5.4
H33a	-.164	.295	.136	2.5		H62c	.246	.132	.420	5.4
H33b	-.112	.256	.181	2.5		H63a	.243	.228	.312	5.5
H33c	-.081	.309	.166	2.5		H63b	.195	.206	.347	5.5
H35	.653	.427	.180	3.7		H63c	.264	.240	.379	5.5
H37a	.801	.334	.266	4.2		H65	.567	.068	.121	4.4
H37b	.798	.371	.214	4.2		H66	.467	.031	.048	4.8

H68	.392	.175	-.005	4.2		H54'b	.040	.470	.268	3.7
H69	.493	.213	.068	3.8		H54'c	-.032	.437	.255	3.7
H70	.326	.103	-.054	5.3		H56'	-.227	.064	.070	3.8
H71a	.292	.063	.018	7.4		H57'	-.208	.077	-.020	4.6
H71b	.270	.027	-.037	7.4		H59'	.011	.083	.062	4.7
H71c	.341	.015	.014	7.4		H60'	-.008	.063	.152	3.1
H72a	.409	.065	-.093	5.6		H61'	-.131	.099	-.073	7.5
H72b	.413	.016	-.053	5.6		H62'a	-.091	.022	-.073	18.4
H72c	.341	.028	-.105	5.6		H62'b	-.058	.060	-.109	18.4
H	.746	.264	.276	2.9		H62'c	-.013	.048	-.044	18.4
H35'	-.078	.218	.409	2.3		H63'a	-.074	.173	-.030	5.0
H37'a	-.108	.071	.425	3.6		H63'b	.001	.144	-.016	5.0
H37'b	-.079	.115	.473	3.6		H63'c	-.044	.156	-.081	5.0
H37'c	-.157	.119	.427	3.6		H65'	.110	.034	.208	5.2
H39'	-.231	.014	.160	3.0		H66'	.203	.042	.162	6.6
H41'a	-.184	.007	.326	3.6		H68'	.358	.032	.318	5.8
H41'b	-.257	.020	.277	3.6		H69'	.271	.026	.366	4.3
H41'c	-.220	-.034	.278	3.6		H70'	.392	.050	.238	14.5
H43'	.170	-.032	.387	2.7		H71'a	.373	-.032	.215	14.2
H45'a	-.006	-.016	.425	3.3		H71'b	.323	-.013	.154	14.2
H45'b	.039	-.066	.421	3.3		H71'c	.408	-.005	.172	14.2
H45'c	.076	-.021	.465	3.3		H72'a	.340	.120	.188	7.9
H47'	.075	.214	.299	2.2		H72'b	.386	.091	.154	7.9
H48'	.110	.294	.268	2.2		H72'c	.301	.083	.136	7.9
H50'	-.057	.368	.304	2.3		H'	-.074	.034	.361	2.3
H51'	-.094	.288	.333	2.1		H1sa	.570	.123	.297	7.1
H52'	.108	.394	.286	2.4		H1sb	.617	.127	.255	7.1
H53'a	.075	.359	.192	3.3		H2sa	.597	.363	.062	9.8
H53'b	-.001	.388	.176	3.3		H2sb	.592	.345	-.001	10.2
H53'c	.071	.421	.188	3.3		H3sa	.560	.173	.924	12.3
H54'a	.025	.440	.319	3.7		H3sb	.538	.135	.968	12.1

Biso is the Mean of the Principal Axes of the Thermal Ellipsoid

Table S23. u(i,j) or U values *100.
E.S.Ds. refer to the last digit printed

	u11(U)	u22	u33	u12	u13	u23
Zn1	1.15(5)	2.83(6)	2.51(6)	-.01(5)	.21(4)	-.12(5)
Zn2	1.97(6)	1.48(5)	1.25(5)	-.26(5)	.68(4)	.10(5)
O1	1.1(3)	3.2(4)	3.1(4)	-.2(3)	.5(3)	-.8(3)
O2	1.5(3)	2.6(4)	3.0(4)	.2(3)	.6(3)	-.4(3)
O3	1.9(3)	1.6(3)	1.7(3)	.3(3)	.5(3)	.9(3)
O4	1.4(3)	2.4(3)	1.7(3)	-.2(3)	.7(3)	.5(3)
C1	1.9(5)	2.2(5)	1.8(5)	.3(4)	.4(4)	.4(4)
C2	1.4(5)	2.1(5)	2.5(5)	.0(4)	1.0(4)	.1(4)
C3	1.6(5)	2.0(5)	1.0(5)	.2(4)	-.1(4)	.0(4)
C4	2.5(5)	2.3(5)	1.7(5)	.5(4)	1.4(4)	1.3(4)
C5	.9(4)	3.0(5)	1.6(5)	.2(4)	.6(4)	1.4(4)
C6	1.6(5)	2.6(5)	1.5(5)	-.1(4)	.4(4)	.3(4)
C7	1.2(4)	3.7(6)	.7(4)	.2(4)	.2(3)	.2(4)
C8	1.0(4)	2.6(5)	1.6(5)	-.5(4)	.5(4)	-.1(4)
C9	.6(4)	2.6(5)	1.9(5)	-.4(4)	.2(4)	-.1(4)
C10	1.8(5)	1.6(5)	.7(4)	-.4(4)	.1(4)	.1(4)

C11	2.3(5)	1.5(5)	.9(4)	-.4(4)	.7(4)	-.1(4)
C12	1.6(5)	2.2(5)	1.0(4)	-.5(4)	.3(4)	-.5(4)
C13	1.3(4)	1.9(5)	1.8(5)	-.4(4)	.4(4)	.0(4)
C14	.2(4)	2.4(5)	2.3(5)	-.1(4)	.3(4)	.7(4)
C15	.6(5)	4.1(6)	1.6(5)	-.4(4)	.4(4)	.9(5)
C16	.9(5)	6.1(8)	1.7(5)	-.9(5)	.3(4)	1.4(5)
C17	1.4(5)	4.8(7)	3.9(7)	.7(5)	.4(5)	2.8(6)
C18	1.8(5)	3.9(6)	4.0(6)	-.5(5)	.8(5)	1.1(5)
C19	2.4(5)	3.6(6)	1.6(5)	-.4(5)	.0(4)	1.4(5)
C20	.9(5)	3.4(6)	2.1(5)	-.3(4)	.5(4)	.4(4)
C21	.9(5)	4.5(6)	1.6(5)	-.3(4)	.4(4)	.0(5)
C22	1.7(5)	5.6(8)	2.2(6)	.5(5)	.3(4)	1.1(5)
C23	2.6(6)	6.1(8)	2.5(6)	-.1(5)	.4(5)	-.9(6)
C24	3.7(6)	3.4(6)	3.7(6)	-.4(5)	1.0(5)	-.7(5)
C25	2.0(6)	5.0(7)	2.8(6)	.2(5)	.9(5)	.1(5)
C26	1.6(5)	2.2(5)	3.1(6)	.5(4)	1.0(4)	.3(4)
C27	3.9(6)	3.4(6)	2.4(6)	.4(5)	1.1(5)	-.7(5)
C28	3.2(6)	2.5(6)	3.0(6)	.5(5)	.9(5)	-.5(5)
C29	2.2(5)	3.1(6)	2.9(6)	-.4(4)	.8(4)	-.1(4)
C30	1.2(4)	1.7(5)	1.8(5)	-.3(4)	.5(4)	.3(4)
C31	1.5(5)	4.9(7)	2.5(6)	.9(5)	.9(4)	1.7(5)
C32	2.1(5)	3.3(6)	2.2(5)	.1(4)	.8(4)	-.1(4)
C33	1.4(5)	2.5(5)	2.6(5)	.3(4)	.4(4)	.3(4)
B	1.5(6)	2.7(7)	3.6(7)	.3(5)	1.0(5)	-1.3(5)
N1	1.1(4)	3.1(5)	3.2(5)	-.1(4)	.3(3)	-.4(4)
N2	.8(4)	2.4(5)	3.3(5)	-.1(3)	.2(3)	-.3(4)
N3	.8(4)	3.4(5)	2.7(5)	.3(3)	.1(3)	-.4(4)
N4	1.2(4)	4.0(5)	2.0(4)	.4(4)	.2(3)	-.9(4)
N5	1.2(4)	2.9(5)	2.2(4)	.1(3)	.0(3)	-.7(4)
N6	.7(4)	2.2(4)	2.7(4)	-.2(3)	-.1(3)	-.4(4)
C34	1.4(5)	3.5(6)	5.0(7)	-.6(5)	1.1(5)	-.4(5)
C35	2.6(6)	2.5(6)	5.9(7)	.1(5)	.7(5)	-.3(5)
C36	2.4(6)	2.2(5)	4.4(6)	-.1(4)	1.3(5)	.0(5)
C37	2.4(6)	3.3(6)	7.2(8)	-.6(5)	1.2(6)	-.3(6)
C38	2.6(5)	4.9(7)	2.3(5)	.3(5)	.1(4)	-.8(5)
C39	1.9(5)	6.2(8)	2.9(6)	.6(5)	.9(5)	.4(6)
C40	2.5(6)	4.4(7)	2.3(6)	.3(5)	.6(5)	-.1(5)
C41	2.5(6)	11.3(11)	2.0(6)	.0(6)	.2(5)	-2.1(6)
C42	1.9(5)	2.2(5)	2.2(5)	-.2(4)	.1(4)	.2(4)
C43	2.1(5)	2.7(6)	3.4(6)	.4(4)	.5(5)	-.9(5)
C44	2.1(5)	2.3(6)	3.7(6)	-.4(4)	1.4(5)	-.8(5)
C45	1.4(5)	3.2(6)	3.1(6)	.1(4)	.2(4)	-.4(5)
C46	1.8(5)	3.0(6)	3.9(6)	.2(5)	1.0(4)	.6(5)
C47	2.7(6)	2.5(6)	3.6(6)	.0(5)	1.5(5)	.6(5)
C48	3.2(6)	3.8(7)	2.3(5)	-.2(5)	.7(5)	-.3(5)
C49	2.6(6)	3.6(6)	2.1(5)	1.1(5)	.4(4)	-.2(5)
C50	3.0(6)	1.8(6)	5.9(8)	.7(5)	.5(5)	.2(5)
C51	2.1(6)	2.6(6)	5.6(7)	.6(5)	-.2(5)	.2(5)
C52	3.5(7)	3.8(7)	4.4(7)	.7(5)	-.3(5)	-.6(6)
C53	3.0(7)	8.0(10)	6.9(9)	1.9(6)	.6(6)	-3.4(7)
C54	5.5(9)	8.7(11)	4.9(8)	2.8(8)	-1.2(7)	1.5(7)
C55	2.4(6)	3.8(6)	2.2(5)	.9(5)	.3(5)	1.1(5)
C56	3.1(6)	4.9(7)	4.8(7)	1.8(5)	1.9(5)	1.7(6)

C57	2.8(6)	6.7(8)	3.2(6)	1.2(6)	1.7(5)	1.6(6)
C58	2.9(6)	3.8(6)	4.1(7)	1.3(5)	2.2(5)	2.1(5)
C59	2.7(6)	3.2(6)	4.2(7)	.5(5)	.9(5)	.7(5)
C60	1.7(5)	4.3(7)	3.5(6)	1.2(5)	1.7(5)	1.6(5)
C61	4.0(7)	4.8(8)	5.9(8)	1.0(6)	2.8(6)	2.9(6)
C62	2.6(6)	7.8(9)	7.1(9)	.8(6)	3.0(6)	3.9(7)
C63	2.1(6)	8.8(10)	7.1(9)	1.6(6)	2.4(6)	3.0(8)
C64	1.9(5)	2.8(6)	3.6(6)	.0(4)	.1(5)	-2.2(5)
C65	2.6(6)	4.7(8)	6.5(8)	.5(6)	-1.9(6)	-1.4(6)
C66	5.0(8)	1.5(6)	8.9(10)	1.0(5)	-2.3(7)	-1.2(6)
C67	3.1(7)	4.4(8)	7.2(9)	.0(6)	.1(6)	-2.8(7)
C68	3.0(7)	4.8(8)	5.1(8)	1.0(6)	-1.4(6)	-.3(6)
C69	3.0(6)	3.8(7)	4.7(7)	.3(5)	.7(5)	-.4(6)
C70	2.6(7)	4.5(8)	10.2(11)	.6(6)	.6(7)	-2.4(8)
C71	4.2(8)	9.5(12)	11.5(13)	-2.2(8)	.5(8)	-6.5(10)
C72	5.8(9)	5.9(9)	6.4(9)	-.6(7)	-1.3(7)	-2.2(7)
B'	3.4(6)	1.2(5)	.9(5)	-.8(5)	1.4(5)	.0(4)
N1'	2.2(4)	1.8(4)	1.1(4)	-.9(3)	1.0(3)	-.2(3)
N2'	2.9(4)	1.9(4)	.8(4)	-.4(3)	1.1(3)	-.1(3)
N3'	2.8(4)	1.2(4)	1.5(4)	-.3(3)	1.2(3)	.6(3)
N4'	3.1(5)	1.0(4)	1.9(4)	-.5(3)	1.4(4)	-.3(3)
N5'	2.4(4)	1.9(4)	1.2(4)	-.4(3)	.5(3)	.0(3)
N6'	3.4(5)	1.0(4)	1.1(4)	-.3(3)	.3(3)	.6(3)
C34'	2.6(5)	2.0(5)	1.2(5)	-.4(4)	.7(4)	-.2(4)
C35'	1.5(5)	2.0(5)	2.3(5)	.2(4)	.1(4)	.1(4)
C36'	1.2(5)	2.1(5)	.5(4)	.2(4)	.1(4)	-.7(4)
C37'	5.9(7)	1.6(5)	3.0(6)	-.5(5)	3.7(5)	.2(4)
C38'	3.1(6)	1.1(5)	2.9(6)	-.9(4)	1.9(5)	-.5(4)
C39'	1.9(5)	2.3(6)	4.4(7)	-.8(4)	.5(5)	-1.2(5)
C40'	2.9(6)	1.3(5)	1.9(5)	-.2(4)	.5(4)	-.2(4)
C41'	3.9(6)	3.5(6)	3.4(6)	-1.6(5)	2.2(5)	-1.0(5)
C42'	4.3(6)	1.0(5)	.9(5)	-.2(4)	.0(4)	-.5(4)
C43'	2.5(6)	2.3(5)	2.6(6)	.9(4)	-.4(5)	.6(4)
C44'	2.3(6)	2.0(5)	2.5(6)	.1(4)	-.1(4)	.3(4)
C45'	5.0(7)	3.0(6)	1.7(5)	.4(5)	1.1(5)	1.1(4)
C46'	1.5(4)	1.1(4)	.9(4)	-.7(4)	.1(3)	-.3(4)
C47'	1.9(5)	2.0(5)	1.3(5)	-.2(4)	.2(4)	-.3(4)
C48'	1.9(5)	2.1(5)	1.4(5)	.1(4)	.6(4)	-.4(4)
C49'	2.2(5)	1.7(5)	1.0(5)	-.8(4)	-.1(4)	-.5(4)
C50'	1.7(5)	1.7(5)	2.2(5)	.6(4)	.6(4)	-.4(4)
C51'	2.2(5)	2.0(5)	.8(4)	-.4(4)	.7(4)	.3(4)
C52'	1.8(5)	2.1(5)	2.1(5)	.4(4)	.3(4)	.3(4)
C53'	3.8(6)	2.2(6)	3.5(6)	-.4(5)	1.5(5)	1.2(5)
C54'	5.1(7)	1.8(5)	4.2(7)	-.3(5)	2.3(6)	.5(5)
C55'	3.6(6)	1.8(5)	2.4(6)	-.9(4)	.9(5)	-.6(4)
C56'	4.6(7)	3.9(7)	2.9(6)	-1.5(5)	.0(5)	.0(5)
C57'	6.2(9)	6.4(9)	1.9(6)	-2.5(7)	.3(6)	-.3(6)
C58'	7.8(10)	5.3(8)	1.5(6)	-.8(7)	1.2(6)	.1(5)
C59'	6.1(8)	5.5(8)	3.0(6)	.0(6)	2.8(6)	.3(6)
C60'	3.3(6)	3.0(6)	2.3(6)	-.3(5)	1.0(5)	-.1(4)
C61'	13.5(14)	10.6(13)	1.2(6)	-2.7(11)	2.6(8)	-.3(7)
C62'	43.(4)	8.2(13)	15.3(18)	3.3(18)	25.(2)	.6(12)
C63'	5.1(8)	8.1(10)	2.9(6)	3.0(7)	2.1(6)	3.2(6)

C64'	5.2(7)	1.6(5)	4.2(7)	1.9(5)	2.6(6)	1.2(5)
C65'	7.0(9)	4.6(8)	5.1(8)	3.4(7)	3.2(7)	1.6(6)
C66'	10.4(12)	6.5(9)	5.3(9)	4.1(9)	5.3(9)	2.8(7)
C67'	7.1(10)	5.6(9)	11.7(13)	4.7(8)	6.1(10)	3.6(9)
C68'	4.6(8)	5.5(9)	8.8(11)	2.0(6)	3.1(8)	2.1(8)
C69'	3.6(7)	3.7(7)	5.9(8)	1.8(5)	2.4(6)	1.2(6)
C70'	19.4(20)	12.7(16)	20.(2)	10.7(15)	18.3(18)	10.4(15)
C71'	20.(2)	9.4(13)	21.(2)	8.7(14)	18.2(19)	6.4(13)
C72'	10.8(13)	8.9(11)	7.5(10)	.8(9)	6.5(10)	.2(9)
C1s	9.8(11)	6.1(10)	8.1(10)	.4(8)	4.3(9)	1.4(8)
Cl1s	14.6(4)	6.7(3)	12.0(4)	4.2(3)	-1.5(3)	-1.4(3)
Cl2s	9.2(3)	5.9(2)	10.0(3)	-.1(2)	3.2(2)	1.8(2)
C2s	3.3(16)	12.(3)	11.(3)	-1.3(17)	1.9(16)	-5.(2)
Cl3s	10.7(6)	9.5(6)	4.5(4)	-4.2(5)	1.3(4)	1.4(4)
Cl4s	12.4(8)	8.4(7)	22.6(12)	1.1(6)	8.1(8)	6.3(7)
C3s	4.4(10)	9.5(14)	8.8(13)	.4(9)	.0(9)	-.1(11)
Cl5s	10.4(4)	21.2(7)	11.7(5)	-3.5(5)	.2(4)	4.1(5)
Cl6s	17.9(8)	23.2(9)	25.3(10)	.5(7)	5.5(7)	-13.5(8)

H4	3.2	H37b	5.3	H65	5.6	H54'a	4.7
H6	2.9	H37c	5.3	H66	6.1	H54'b	4.7
H9	2.7	H39	4.7	H68	5.3	H54'c	4.7
H13	2.7	H41a	6.3	H69	4.8	H56'	4.8
H16	3.9	H41b	6.3	H70	6.8	H57'	5.8
H17	4.3	H41c	6.3	H71a	9.4	H59'	5.9
H18	4.2	H43	3.7	H71b	9.4	H60'	3.9
H19	3.5	H45a	3.6	H71c	9.4	H61'	9.4
H22	4.2	H45b	3.6	H72a	7.0	H62'a	23.3
H23	4.7	H45c	3.6	H72b	7.0	H62'b	23.3
H24	4.6	H47	3.9	H72c	7.0	H62'c	23.3
H25	4.3	H48	4.1	H	3.6	H63'a	6.4
H27a	4.3	H50	4.6	H35'	2.9	H63'b	6.4
H27b	4.3	H51	4.4	H37'a	4.5	H63'c	6.4
H27c	4.3	H52	4.9	H37'b	4.5	H65'	6.6
H28a	3.9	H53a	7.0	H37'c	4.5	H66'	8.4
H28b	3.9	H53b	7.0	H39'	3.8	H68'	7.3
H28c	3.9	H53c	7.0	H41'a	4.6	H69'	5.4
H29a	3.8	H54a	7.4	H41'b	4.6	H70'	18.4
H29b	3.8	H54b	7.4	H41'c	4.6	H71'a	17.9
H29c	3.8	H54c	7.4	H43'	3.4	H71'b	17.9
H31a	4.0	H56	5.3	H45'a	4.2	H71'c	17.9
H31b	4.0	H57	5.2	H45'b	4.2	H72'a	10.0
H31c	4.0	H59	4.4	H45'c	4.2	H72'b	10.0
H32a	3.5	H60	4.2	H47'	2.7	H72'c	10.0
H32b	3.5	H61	5.9	H48'	2.8	H'	2.9
H32c	3.5	H62a	6.8	H50'	2.9	H1sa	9.0
H33a	3.2	H62b	6.8	H51'	2.7	H1sb	9.0
H33b	3.2	H62c	6.8	H52'	3.0	H2sa	12.5
H33c	3.2	H63a	7.0	H53'a	4.2	H2sb	13.0
H35	4.7	H63b	7.0	H53'b	4.2	H3sa	15.6
H37a	5.3	H63c	7.0	H53'c	4.2	H3sb	15.3

Anisotropic Temperature Factors are of the form Temp=-2*Pi*Pi*(h*h*u11*astar*astar+---
+2*h*k*u12*astar*bstar+---)

Table S24. The following Atoms are from the CD File
* Indicates that there are Symmetry Equivalents of an atom.
Name x y z

Name	x	y	z
Zn1	.52907(5)	.25399(4)	.21002(4)
Zn2	.00784(5)	.11708(3)	.25627(4)
O1	.43569(29)	.22496(23)	.15790(25)
O2	.45281(30)	.29890(22)	.23803(25)
O3	.09376(29)	.14201(20)	.23621(23)
O4	-.04393(28)	.17431(21)	.19286(23)
C1	.37707(44)	.24589(34)	.16456(35)
C2	.38512(45)	.28562(33)	.20839(37)
C3	.32196(44)	.30817(32)	.21925(34)
C4	.25461(46)	.29131(33)	.18322(36)
C5	.24562(40)	.25501(34)	.13685(34)
C6	.30576(44)	.23216(32)	.12762(35)
C7	.16674(41)	.24532(36)	.09439(32)
C8	.11224(43)	.23136(33)	.12587(35)
C9	.13152(41)	.19734(33)	.17211(36)
C10	.07897(43)	.17629(31)	.19506(33)
C11	.00167(45)	.19398(31)	.17014(34)
C12	-.01657(43)	.23229(32)	.12454(34)
C13	.03800(41)	.24896(33)	.10357(34)
C14	.14574(41)	.29411(33)	.05376(37)
C15	.13908(43)	.27994(37)	-.00379(37)
C16	.12229(46)	.31870(43)	-.04723(38)
C17	.11081(47)	.37011(42)	-.03317(44)
C18	.11577(47)	.38300(39)	.02352(43)
C19	.13445(48)	.34517(37)	.06844(37)
C20	.16351(44)	.20240(36)	.05005(38)
C21	.14859(45)	.22364(39)	-.00574(38)
C22	.14151(48)	.19207(42)	-.05427(40)
C23	.14793(52)	.13772(45)	-.04529(42)
C24	.16116(53)	.11620(40)	.00942(43)
C25	.16843(49)	.14938(41)	.05805(41)
C26	.33196(45)	.34954(33)	.26754(39)
C27	.37829(53)	.32652(38)	.32759(40)
C28	.25794(51)	.36618(36)	.27292(40)
C29	.36968(47)	.39794(36)	.25272(39)
C30	-.09498(41)	.25443(32)	.10062(33)
C31	-.10404(46)	.29375(38)	.05122(39)
C32	-.15014(47)	.20888(35)	.07562(38)
C33	-.11506(45)	.28113(34)	.15065(38)
B	.69401(54)	.26153(41)	.26001(48)
N1	.58887(37)	.31799(29)	.20085(32)
N2	.66354(36)	.31286(28)	.22744(31)
N3	.58862(35)	.23653(28)	.29619(31)
N4	.66128(35)	.25203(30)	.30921(29)
N5	.60345(36)	.20657(28)	.18125(30)
N6	.67465(35)	.21480(27)	.21580(30)

C34	.69755(49)	.35714(38)	.22229(45)
C35	.64530(52)	.39237(37)	.19150(46)
C36	.57726(50)	.36545(37)	.17840(43)
C37	.77935(53)	.36470(40)	.24598(49)
C38	.69101(50)	.25518(41)	.36763(39)
C39	.63965(48)	.24158(43)	.39316(41)
C40	.57689(50)	.22952(38)	.34701(40)
C41	.76896(54)	.27146(52)	.39621(42)
C42	.71951(47)	.17793(34)	.20550(38)
C43	.67745(48)	.14527(35)	.16349(40)
C44	.60454(48)	.16477(35)	.14926(41)
C45	.80081(46)	.17517(36)	.23654(39)
C46	.50358(47)	.38629(38)	.14532(41)
C47	.44700(51)	.35361(35)	.11271(41)
C48	.37874(51)	.37477(38)	.08187(39)
C49	.36617(50)	.42763(38)	.08226(39)
C50	.42293(53)	.45991(35)	.11423(46)
C51	.49025(50)	.43976(38)	.14592(46)
C52	.29077(56)	.45031(42)	.04833(47)
C53	.25312(58)	.46961(50)	.09138(54)
C54	.29650(67)	.49388(54)	.00819(54)
C55	.50503(50)	.21159(38)	.35105(40)
C56	.48926(54)	.21733(42)	.40396(47)
C57	.42258(55)	.20150(44)	.40842(44)
C58	.36878(52)	.17951(39)	.36106(45)
C59	.38442(51)	.17329(38)	.30911(44)
C60	.45134(48)	.18873(38)	.30300(41)
C61	.29326(57)	.16577(43)	.36265(48)
C62	.29472(56)	.14114(47)	.42014(51)
C63	.24384(55)	.21411(51)	.34867(52)
C64	.53959(49)	.14273(36)	.10458(41)
C65	.53092(56)	.09056(44)	.09550(52)
C66	.47160(64)	.06791(38)	.05228(56)
C67	.42051(58)	.09871(45)	.01624(53)
C68	.42786(56)	.15291(44)	.02141(48)
C69	.48722(54)	.17557(40)	.06510(46)
C70	.35570(61)	.07463(46)	-.03287(61)
C71	.31020(71)	.04252(59)	-.00757(68)
C72	.38152(67)	.04299(49)	-.07507(56)
B'	-.05330(57)	.05357(37)	.33624(40)
N1'	-.02446(36)	.14777(25)	.32308(27)
N2'	-.05137(36)	.11192(26)	.35329(26)
N3'	-.07938(37)	.06649(25)	.22755(28)
N4'	-.10269(38)	.04757(25)	.27145(29)
N5'	.06288(37)	.05153(27)	.30781(28)
N6'	.02440(39)	.03344(25)	.34337(28)
C34'	-.07643(46)	.13724(33)	.39204(35)
C35'	-.06631(44)	.18985(33)	.38646(37)
C36'	-.03418(42)	.19509(32)	.34271(33)
C37'	-.10800(54)	.10785(33)	.43310(39)
C38'	-.16928(49)	.02453(32)	.24823(39)
C39'	-.18717(48)	.02695(35)	.18882(43)
C40'	-.12950(48)	.05267(32)	.17717(37)

C41'	-.21125(53)	.00244(37)	.28569(43)
C42'	.06563(52)	-.00302(31)	.38064(35)
C43'	.13025(50)	-.00886(35)	.36827(39)
C44'	.12598(48)	.02455(34)	.32258(38)
C45'	.04138(55)	-.02913(36)	.42749(38)
C46'	-.01247(41)	.24393(30)	.31999(31)
C47'	.04822(43)	.24587(33)	.30025(33)
C48'	.06865(44)	.29317(33)	.28155(35)
C49'	.03099(46)	.33978(32)	.28291(34)
C50'	-.03003(45)	.33665(32)	.30280(36)
C51'	-.05124(45)	.28933(32)	.32012(34)
C52'	.05713(44)	.39092(33)	.26454(36)
C53'	.05007(50)	.38963(35)	.19879(40)
C54'	.01930(57)	.43917(35)	.27783(44)
C55'	-.11801(52)	.06323(34)	.12023(39)
C56'	-.17833(58)	.06700(40)	.06798(44)
C57'	-.16702(67)	.07599(46)	.01513(44)
C58'	-.09806(71)	.08185(45)	.01161(43)
C59'	-.03815(62)	.07791(44)	.06296(45)
C60'	-.04884(52)	.06776(36)	.11651(39)
C61'	-.08298(89)	.09424(63)	-.04583(48)
C62'	-.06175(155)	.05317(68)	-.07113(87)
C63'	-.04749(61)	.14684(50)	-.04342(44)
C64'	.18067(58)	.03050(35)	.29147(45)
C65'	.16105(67)	.03466(43)	.23096(51)
C66'	.21459(84)	.03867(49)	.20408(54)
C67'	.28907(79)	.03918(50)	.23779(74)
C68'	.30700(65)	.03317(48)	.29588(65)
C69'	.25602(58)	.02939(40)	.32464(49)
C70'	.34850(110)	.04271(72)	.20557(89)
C71'	.36643(111)	-.00506(67)	.18570(91)
C72'	.34446(81)	.08843(59)	.16828(61)
C1s	.60989(80)	.10767(52)	.28628(61)
Cl1s	.68546(27)	.11201(16)	.34565(20)
Cl2s	.58485(21)	.04313(13)	.26136(17)
C2s	.62453(133)	.34469(130)	.04054(136)
Cl3s	.63578(43)	.27998(31)	.06484(28)
Cl4s	.70710(56)	.37319(35)	.04747(53)
C3s	.57448(78)	.14001(67)	.94929(73)
Cl5s	.65879(31)	.14977(29)	1.00103(26)
Cl6s	.57324(45)	.09010(36)	.90425(41)
H4	.21156(0)	.30482(0)	.19015(0)
H6	.29943(0)	.20730(0)	.09652(0)
H9	.18225(0)	.18813(0)	.18940(0)
H13	.02565(0)	.27377(0)	.07199(0)
H16	.11913(0)	.30974(0)	-.08662(0)
H17	.09881(0)	.39653(0)	-.06308(0)
H18	.10694(0)	.41857(0)	.03235(0)
H19	.13864(0)	.35438(0)	.10797(0)
H22	.13195(0)	.20687(0)	-.09258(0)
H23	.14382(0)	.11514(0)	-.07802(0)
H24	.16483(0)	.07890(0)	.01462(0)
H25	.17754(0)	.13519(0)	.09659(0)

H27a	.42542(0)	.31598(0)	.32580(0)
H27b	.38464(0)	.35246(0)	.35762(0)
H27c	.35336(0)	.29664(0)	.33637(0)
H28a	.23420(0)	.33613(0)	.28268(0)
H28b	.26509(0)	.39224(0)	.30294(0)
H28c	.22787(0)	.38034(0)	.23621(0)
H29a	.37723(0)	.42387(0)	.28291(0)
H29b	.41615(0)	.38774(0)	.24930(0)
H29c	.33940(0)	.41229(0)	.21618(0)
H31a	-.09235(0)	.27739(0)	.01947(0)
H31b	-.15363(0)	.30636(0)	.03757(0)
H31c	-.07126(0)	.32257(0)	.06590(0)
H32a	-.14572(0)	.18341(0)	.10585(0)
H32b	-.19933(0)	.22227(0)	.06231(0)
H32c	-.13904(0)	.19273(0)	.04350(0)
H33a	-.16404(0)	.29484(0)	.13638(0)
H33b	-.11178(0)	.25612(0)	.18111(0)
H33c	-.08119(0)	.30924(0)	.16592(0)
H35	.65302(0)	.42734(0)	.18002(0)
H37a	.80137(0)	.33356(0)	.26648(0)
H37b	.79800(0)	.37095(0)	.21411(0)
H37c	.79094(0)	.39399(0)	.27232(0)
H39	.64533(0)	.24049(0)	.43416(0)
H41a	.79060(0)	.27844(0)	.36621(0)
H41b	.77052(0)	.30261(0)	.41887(0)
H41c	.79581(0)	.24404(0)	.42124(0)
H43	.69346(0)	.11518(0)	.14699(0)
H45a	.81481(0)	.20391(0)	.26350(0)
H45b	.81235(0)	.14272(0)	.25763(0)
H45c	.82703(0)	.17726(0)	.20879(0)
H47	.45530(0)	.31658(0)	.11182(0)
H48	.34000(0)	.35209(0)	.05970(0)
H50	.41477(0)	.49704(0)	.11368(0)
H51	.52859(0)	.46232(0)	.16891(0)
H52	.26115(0)	.42316(0)	.02474(0)
H53a	.24855(0)	.44101(0)	.11583(0)
H53b	.28280(0)	.49664(0)	.11516(0)
H53c	.20535(0)	.48337(0)	.07090(0)
H54a	.31914(0)	.48177(0)	-.01961(0)
H54b	.24871(0)	.50763(0)	-.01225(0)
H54c	.32616(0)	.52089(0)	.03201(0)
H56	.52517(0)	.23351(0)	.43667(0)
H57	.41304(0)	.20428(0)	.44501(0)
H59	.34759(0)	.15791(0)	.27638(0)
H60	.46069(0)	.18440(0)	.26648(0)
H61	.27247(0)	.14051(0)	.33239(0)
H62a	.32492(0)	.11034(0)	.42688(0)
H62b	.31526(0)	.16601(0)	.45089(0)
H62c	.24616(0)	.13182(0)	.41956(0)
H63a	.24308(0)	.22810(0)	.31153(0)
H63b	.19477(0)	.20553(0)	.34737(0)
H63c	.26387(0)	.23971(0)	.37870(0)
H65	.56744(0)	.06799(0)	.12067(0)

H66	.46679(0)	.03057(0)	.04791(0)
H68	.39157(0)	.17479(0)	-.00506(0)
H69	.49336(0)	.21290(0)	.06793(0)
H70	.32585(0)	.10273(0)	-.05430(0)
H71a	.29208(0)	.06320(0)	.01809(0)
H71b	.26968(0)	.02721(0)	-.03750(0)
H71c	.34131(0)	.01524(0)	.01444(0)
H72a	.40907(0)	.06489(0)	-.09282(0)
H72b	.41263(0)	.01571(0)	-.05306(0)
H72c	.34100(0)	.02768(0)	-.10500(0)
H	.74637(0)	.26429(0)	.27644(0)
H35'	-.07848(0)	.21752(0)	.40870(0)
H37'a	-.10773(0)	.07099(0)	.42530(0)
H37'b	-.07916(0)	.11455(0)	.47301(0)
H37'c	-.15748(0)	.11928(0)	.42666(0)
H39'	-.23094(0)	.01372(0)	.16050(0)
H41'a	-.18354(0)	.00717(0)	.32625(0)
H41'b	-.25748(0)	.02018(0)	.27716(0)
H41'c	-.21961(0)	-.03426(0)	.27755(0)
H43'	.17002(0)	-.03199(0)	.38746(0)
H45'a	-.00628(0)	-.01633(0)	.42544(0)
H45'b	.03912(0)	-.06634(0)	.42134(0)
H45'c	.07566(0)	-.02141(0)	.46534(0)
H47'	.07516(0)	.21437(0)	.29948(0)
H48'	.11004(0)	.29397(0)	.26753(0)
H50'	-.05700(0)	.36795(0)	.30435(0)
H51'	-.09381(0)	.28794(0)	.33263(0)
H52'	.10838(0)	.39435(0)	.28599(0)
H53'a	.07516(0)	.35919(0)	.19152(0)
H53'b	-.00089(0)	.38761(0)	.17599(0)
H53'c	.07123(0)	.42050(0)	.18804(0)
H54'a	.02471(0)	.43996(0)	.31880(0)
H54'b	.04029(0)	.47032(0)	.26751(0)
H54'c	-.03183(0)	.43742(0)	.25546(0)
H56'	-.22730(0)	.06404(0)	.06977(0)
H57'	-.20772(0)	.07743(0)	-.02047(0)
H59'	.01074(0)	.08272(0)	.06156(0)
H60'	-.00789(0)	.06312(0)	.15151(0)
H61'	-.13124(0)	.09899(0)	-.07326(0)
H62'a	-.09107(0)	.02243(0)	-.07270(0)
H62'b	-.05849(0)	.06022(0)	-.10932(0)
H62'c	-.01345(0)	.04753(0)	-.04410(0)
H63'a	-.07426(0)	.17326(0)	-.03044(0)
H63'b	.00092(0)	.14376(0)	-.01574(0)
H63'c	-.04412(0)	.15644(0)	-.08096(0)
H65'	.11024(0)	.03397(0)	.20755(0)
H66'	.20295(0)	.04164(0)	.16242(0)
H68'	.35826(0)	.03192(0)	.31797(0)
H69'	.27090(0)	.02615(0)	.36646(0)
H70'	.39231(0)	.04950(0)	.23764(0)
H71'a	.37323(0)	-.03157(0)	.21520(0)
H71'b	.32303(0)	-.01265(0)	.15356(0)
H71'c	.40815(0)	-.00452(0)	.17207(0)

H72'a	.33984(0)	.12043(0)	.18773(0)
H72'b	.38582(0)	.09085(0)	.15434(0)
H72'c	.30070(0)	.08272(0)	.13582(0)
H'	-.07400(0)	.03365(0)	.36087(0)
H1sa	.56985(0)	.12263(0)	.29695(0)
H1sb	.61705(0)	.12735(0)	.25536(0)
H2sa	.59686(0)	.36299(0)	.06199(0)
H2sb	.59171(0)	.34478(0)	-.00089(0)
H3sa	.56028(0)	.17307(0)	.92439(0)
H3sb	.53823(0)	.13512(0)	.96763(0)

Table S25. Bond lengths [Å] and angles [°] for **7(SQZnL)2**.

Zn1-O1	1.978(6)	C62-H62a	.960(11)
Zn1-O2	2.135(6)	C62-H62b	.960(13)
Zn1-N1	2.050(7)	C62-H62c	.960(10)
Zn1-N3	2.075(7)	C63-H63a	.960(11)
Zn1-N5	2.152(7)	C63-H63b	.960(10)
Zn2-O3	1.971(5)	C63-H63c	.960(14)
Zn2-O4	2.119(5)	C64-C65	1.351(15)
Zn2-N1'	2.058(7)	C64-C69	1.418(14)
Zn2-N3'	2.054(7)	C65-C66	1.401(15)
Zn2-N5'	2.150(7)	C65-H65	.960(11)
O1-C1	1.304(10)	C66-C67	1.339(16)
O2-C2	1.314(10)	C66-H66	.960(10)
O3-C10	1.285(9)	C67-C68	1.392(16)
O4-C11	1.277(10)	C67-C70	1.546(16)
C1-C2	1.437(12)	C68-C69	1.407(15)
C1-C6	1.420(12)	C68-H68	.960(10)
C2-C3	1.442(12)	C69-H69	.960(10)
C3-C4	1.378(12)	C70-C71	1.47(2)
C3-C26	1.538(12)	C70-C72	1.503(19)
C4-C5	1.420(13)	C70-H70	.960(12)
C4-H4	.960(8)	C71-H71a	.960(14)
C5-C6	1.376(11)	C71-H71b	.960(12)
C5-C7	1.555(11)	C71-H71c	.960(16)
C6-H6	.960(8)	C72-H72a	.960(14)
C7-C8	1.521(11)	C72-H72b	.960(13)
C7-C14	1.556(12)	C72-H72c	.960(11)
C7-C20	1.518(13)	B'-N2'	1.543(12)
C8-C9	1.368(12)	B'-N4'	1.555(12)
C8-C13	1.428(11)	B'-N6'	1.538(13)
C9-C10	1.406(11)	B'-H'	.960(9)
C9-H9	.960(8)	N1'-N2'	1.370(9)
C10-C11	1.485(12)	N1'-C36'	1.332(10)
C11-C12	1.429(11)	N2'-C34'	1.346(10)
C12-C13	1.371(11)	N3'-N4'	1.364(9)
C12-C30	1.540(11)	N3'-C40'	1.335(11)
C13-H13	.960(8)	N4'-C38'	1.357(11)
C14-C15	1.400(12)	N5'-N6'	1.380(10)
C14-C19	1.386(13)	N5'-C44'	1.341(11)
C15-C16	1.402(13)	N6'-C42'	1.359(11)
C15-C21	1.451(14)	C34'-C35'	1.370(12)

C16-C17	1.391(16)	C34'-C37'	1.516(12)
C16-H16	.960(9)	C35'-C36'	1.390(12)
C17-C18	1.380(15)	C35'-H35'	.960(9)
C17-H17	.960(9)	C36'-C46'	1.475(11)
C18-C19	1.409(13)	C37'-H37'a	.960(9)
C18-H18	.960(10)	C37'-H37'b	.960(10)
C19-H19	.960(9)	C37'-H37'c	.960(10)
C20-C21	1.393(13)	C38'-C39'	1.364(14)
C20-C25	1.366(14)	C38'-C41'	1.501(13)
C21-C22	1.391(14)	C39'-C40'	1.393(13)
C22-C23	1.403(16)	C39'-H39'	.960(9)
C22-H22	.960(9)	C40'-C55'	1.484(13)
C23-C24	1.376(15)	C41'-H41'a	.960(10)
C23-H23	.960(10)	C41'-H41'b	.960(10)
C24-C25	1.417(14)	C41'-H41'c	.960(9)
C24-H24	.960(10)	C42'-C43'	1.377(14)
C25-H25	.960(10)	C42'-C45'	1.509(13)
C26-C27	1.553(13)	C43'-C44'	1.375(13)
C26-C28	1.531(12)	C43'-H43'	.960(9)
C26-C29	1.532(13)	C44'-C64'	1.483(14)
C27-H27a	.960(10)	C45'-H45'a	.960(10)
C27-H27b	.960(9)	C45'-H45'b	.960(10)
C27-H27c	.960(10)	C45'-H45'c	.960(9)
C28-H28a	.960(10)	C46'-C47'	1.396(11)
C28-H28b	.960(9)	C46'-C51'	1.379(12)
C28-H28c	.960(9)	C47'-C48'	1.389(12)
C29-H29a	.960(9)	C47'-H47'	.960(8)
C29-H29b	.960(9)	C48'-C49'	1.399(12)
C29-H29c	.960(9)	C48'-H48'	.960(8)
C30-C31	1.525(12)	C49'-C50'	1.406(12)
C30-C32	1.560(12)	C49'-C52'	1.515(12)
C30-C33	1.539(12)	C50'-C51'	1.382(12)
C31-H31a	.960(9)	C50'-H50'	.960(8)
C31-H31b	.960(9)	C51'-H51'	.960(8)
C31-H31c	.960(10)	C52'-C53'	1.548(13)
C32-H32a	.960(9)	C52'-C54'	1.516(13)
C32-H32b	.960(9)	C52'-H52'	.960(8)
C32-H32c	.960(9)	C53'-H53'a	.960(10)
C33-H33a	.960(8)	C53'-H53'b	.960(9)
C33-H33b	.960(9)	C53'-H53'c	.960(9)
C33-H33c	.960(9)	C54'-H54'a	.960(10)
B-N2	1.544(13)	C54'-H54'b	.960(9)
B-N4	1.530(13)	C54'-H54'c	.960(10)
B-N6	1.563(12)	C55'-C56'	1.417(14)
B-H	.960(10)	C55'-C60'	1.367(14)
N1-N2	1.380(10)	C56'-C57'	1.379(15)
N1-C36	1.317(12)	C56'-H56'	.960(11)
N2-C34	1.332(12)	C57'-C58'	1.365(18)
N3-N4	1.389(9)	C57'-H57'	.960(11)
N3-C40	1.327(12)	C58'-C59'	1.400(16)
N4-C38	1.343(11)	C58'-C61'	1.536(16)
N5-N6	1.373(9)	C59'-C60'	1.396(13)
N5-C44	1.321(11)	C59'-H59'	.960(11)

N6-C42	1.353(11)	C60'-H60'	.960(9)
C34-C35	1.376(14)	C61'-C62'	1.34(2)
C34-C37	1.505(13)	C61'-C63'	1.50(2)
C35-C36	1.422(13)	C61'-H61'	.960(15)
C35-H35	.960(10)	C62'-H62'a	.96(2)
C36-C46	1.485(13)	C62'-H62'b	.960(14)
C37-H37a	.960(11)	C62'-H62'c	.96(3)
C37-H37b	.960(11)	C63'-H63'a	.960(11)
C37-H37c	.960(11)	C63'-H63'b	.960(11)
C38-C39	1.366(14)	C63'-H63'c	.960(10)
C38-C41	1.495(14)	C64'-C65'	1.389(16)
C39-C40	1.390(13)	C64'-C69'	1.414(15)
C39-H39	.960(9)	C65'-C66'	1.386(18)
C40-C55	1.489(13)	C65'-H65'	.960(12)
C41-H41a	.960(11)	C66'-C67'	1.40(2)
C41-H41b	.960(12)	C66'-H66'	.960(12)
C41-H41c	.960(12)	C67'-C68'	1.34(2)
C42-C43	1.361(12)	C67'-C70'	1.578(19)
C42-C45	1.504(12)	C68'-C69'	1.374(17)
C43-C44	1.423(12)	C68'-H68'	.960(12)
C43-H43	.960(9)	C69'-H69'	.960(11)
C44-C64	1.476(12)	C70'-C71'	1.39(2)
C45-H45a	.960(9)	C70'-C72'	1.46(2)
C45-H45b	.960(9)	C70'-H70'	.96(2)
C45-H45c	.960(9)	C71'-H71'a	.960(16)
C46-C47	1.397(13)	C71'-H71'b	.96(2)
C46-C51	1.390(14)	C71'-H71'c	.960(15)
C47-C48	1.395(13)	C72'-H72'a	.960(14)
C47-H47	.960(9)	C72'-H72'b	.960(13)
C48-C49	1.371(14)	C72'-H72'c	.960(15)
C48-H48	.960(9)	C1s-Cl1s	1.687(16)
C49-C50	1.388(14)	C1s-Cl2s	1.767(14)
C49-C52	1.533(13)	C1s-H1sa	.966(14)
C50-C51	1.376(13)	C1s-H1sb	.945(13)
C50-H50	.960(9)	Cl1s-Cl2s	2.908(6)
C51-H51	.960(10)	Cl1s-H1sa	2.175(5)
C52-C53	1.525(16)	Cl1s-H1sb	2.189(4)
C52-C54	1.502(18)	Cl2s-H1sa	2.258(4)
C52-H52	.960(10)	Cl2s-H1sb	2.255(3)
C53-H53a	.960(14)	C2s-Cl3s	1.74(4)
C53-H53b	.960(12)	C2s-Cl4s	1.71(3)
C53-H53c	.960(11)	C2s-H2sa	.97(3)
C54-H54a	.960(14)	C2s-H2sb	1.00(3)
C54-H54b	.960(11)	Cl3s-Cl4s	2.844(11)
C54-H54c	.960(14)	Cl3s-H2sa	2.241(9)
C55-C56	1.411(14)	Cl3s-H2sb	2.260(7)
C55-C60	1.409(14)	Cl4s-H2sa	2.273(10)
C56-C57	1.382(14)	Cl4s-H2sb	2.271(11)
C56-H56	.960(11)	C3s-Cl5s	1.719(16)
C57-C58	1.391(16)	C3s-Cl6s	1.669(19)
C57-H57	.960(10)	C3s-H3sa	1.021(17)
C58-C59	1.388(15)	C3s-H3sb	.946(17)
C58-C61	1.507(14)	Cl5s-Cl6s	2.832(10)

C59-C60	1.399(13)	Cl5s-H3sa	2.263(6)
C59-H59	.960(10)	Cl5s-H3sb	2.230(6)
C60-H60	.960(9)	Cl6s-H3sa	2.205(8)
C61-C62	1.514(15)	Cl6s-H3sb	2.184(8)
C61-C63	1.528(16)	H1sa-H1sb	1.55858(15)
C61-H61	.960(12)	H2sa-H2sb	1.55869(18)
O1-Zn1-O2	80.0(2)	C64-C65-C66	123.8(10)
O1-Zn1-N1	131.1(3)	C64-C65-H65	117.5(10)
O1-Zn1-N3	130.8(3)	C66-C65-H65	118.7(11)
O1-Zn1-N5	98.5(2)	C65-C66-C67	119.7(10)
O2-Zn1-N1	94.2(3)	C65-C66-H66	121.2(11)
O2-Zn1-N3	90.8(2)	C67-C66-H66	119.1(11)
O2-Zn1-N5	178.1(2)	C66-C67-C68	119.5(10)
N1-Zn1-N3	97.5(3)	C66-C67-C70	120.6(10)
N1-Zn1-N5	87.7(3)	C68-C67-C70	119.8(10)
N3-Zn1-N5	89.5(3)	C67-C68-C69	120.7(10)
O3-Zn2-O4	80.7(2)	C67-C68-H68	119.1(10)
O3-Zn2-N1'	123.8(2)	C69-C68-H68	120.2(11)
O3-Zn2-N3'	141.2(2)	C64-C69-C68	119.5(9)
O3-Zn2-N5'	95.5(2)	C64-C69-H69	119.6(10)
O4-Zn2-N1'	96.5(2)	C68-C69-H69	120.9(10)
O4-Zn2-N3'	92.6(2)	C67-C70-C71	110.2(12)
O4-Zn2-N5'	169.9(2)	C67-C70-C72	111.8(9)
N1'-Zn2-N3'	94.8(3)	C67-C70-H70	108.2(10)
N1'-Zn2-N5'	93.4(3)	C71-C70-C72	110.6(10)
N3'-Zn2-N5'	84.5(3)	C71-C70-H70	107.9(11)
Zn1-O1-C1	114.5(5)	C72-C70-H70	107.9(13)
Zn1-O2-C2	110.6(5)	C70-C71-H71a	110.4(13)
Zn2-O3-C10	114.4(5)	C70-C71-H71b	111.3(15)
Zn2-O4-C11	110.6(5)	C70-C71-H71c	106.6(12)
O1-C1-C2	119.1(7)	H71a-C71-H71b	109.5(13)
O1-C1-C6	121.5(8)	H71a-C71-H71c	109.5(16)
C2-C1-C6	119.4(8)	H71b-C71-H71c	109.5(14)
O2-C2-C1	115.9(7)	C70-C72-H72a	109.8(11)
O2-C2-C3	123.0(7)	C70-C72-H72b	107.3(12)
C1-C2-C3	121.1(7)	C70-C72-H72c	111.3(12)
C2-C3-C4	116.0(7)	H72a-C72-H72b	109.5(13)
C2-C3-C26	120.2(7)	H72a-C72-H72c	109.5(13)
C4-C3-C26	123.8(7)	H72b-C72-H72c	109.5(12)
C3-C4-C5	123.6(8)	N2'-B'-N4'	108.5(7)
C3-C4-H4	117.9(8)	N2'-B'-N6'	110.7(7)
C5-C4-H4	118.5(8)	N2'-B'-H'	109.0(8)
C4-C5-C6	120.5(7)	N4'-B'-N6'	109.8(7)
C4-C5-C7	118.0(7)	N4'-B'-H'	109.2(8)
C6-C5-C7	121.3(8)	N6'-B'-H'	109.6(8)
C1-C6-C5	119.2(8)	Zn2-N1'-N2'	115.0(5)
C1-C6-H6	120.6(8)	Zn2-N1'-C36'	137.3(6)
C5-C6-H6	120.2(8)	N2'-N1'-C36'	107.2(6)
C5-C7-C8	113.1(6)	B'-N2'-N1'	118.9(6)
C5-C7-C14	106.8(7)	B'-N2'-C34'	131.7(7)
C5-C7-C20	112.9(7)	N1'-N2'-C34'	109.2(7)
C8-C7-C14	114.9(7)	Zn2-N3'-N4'	113.4(5)
C8-C7-C20	107.7(7)	Zn2-N3'-C40'	138.4(6)

C14-C7-C20	101.0(6)	N4'-N3'-C40'	107.0(7)
C7-C8-C9	120.4(7)	B'-N4'-N3'	119.9(7)
C7-C8-C13	120.3(7)	B'-N4'-C38'	130.5(7)
C9-C8-C13	119.0(7)	N3'-N4'-C38'	109.6(7)
C8-C9-C10	121.5(7)	Zn2-N5'-N6'	110.9(5)
C8-C9-H9	118.8(8)	Zn2-N5'-C44'	142.2(6)
C10-C9-H9	119.7(8)	N6'-N5'-C44'	106.5(7)
O3-C10-C9	123.7(7)	B'-N6'-N5'	121.0(6)
O3-C10-C11	117.7(7)	B'-N6'-C42'	130.1(7)
C9-C10-C11	118.6(7)	N5'-N6'-C42'	108.9(7)
O4-C11-C10	116.4(7)	N2'-C34'-C35'	108.0(7)
O4-C11-C12	124.5(7)	N2'-C34'-C37'	121.6(7)
C10-C11-C12	119.1(7)	C35'-C34'-C37'	130.4(8)
C11-C12-C13	117.9(7)	C34'-C35'-C36'	106.3(7)
C11-C12-C30	120.6(7)	C34'-C35'-H35'	126.8(9)
C13-C12-C30	121.5(7)	C36'-C35'-H35'	126.9(8)
C8-C13-C12	123.7(8)	N1'-C36'-C35'	109.3(7)
C8-C13-H13	118.0(7)	N1'-C36'-C46'	123.1(7)
C12-C13-H13	118.2(8)	C35'-C36'-C46'	127.7(7)
C7-C14-C15	109.9(7)	C34'-C37'-H37'a	109.2(8)
C7-C14-C19	128.5(8)	C34'-C37'-H37'b	110.1(8)
C15-C14-C19	121.6(8)	C34'-C37'-H37'c	109.2(8)
C14-C15-C16	119.0(9)	H37'a-C37'-H37'b	109.5(9)
C14-C15-C21	108.4(7)	H37'a-C37'-H37'c	109.5(9)
C16-C15-C21	132.5(9)	H37'b-C37'-H37'c	109.5(8)
C15-C16-C17	120.0(9)	N4'-C38'-C39'	107.6(7)
C15-C16-H16	119.9(11)	N4'-C38'-C41'	122.2(8)
C17-C16-H16	120.1(9)	C39'-C38'-C41'	130.2(8)
C16-C17-C18	120.0(8)	C38'-C39'-C40'	106.5(8)
C16-C17-H17	119.9(10)	C38'-C39'-H39'	126.9(10)
C18-C17-H17	120.1(11)	C40'-C39'-H39'	126.6(10)
C17-C18-C19	121.2(9)	N3'-C40'-C39'	109.3(8)
C17-C18-H18	119.0(9)	N3'-C40'-C55'	121.1(8)
C19-C18-H18	119.8(10)	C39'-C40'-C55'	129.5(8)
C14-C19-C18	118.1(8)	C38'-C41'-H41'a	109.6(8)
C14-C19-H19	120.9(8)	C38'-C41'-H41'b	109.5(9)
C18-C19-H19	121.0(10)	C38'-C41'-H41'c	109.3(8)
C7-C20-C21	110.4(8)	H41'a-C41'-H41'b	109.5(9)
C7-C20-C25	129.1(8)	H41'a-C41'-H41'c	109.5(10)
C21-C20-C25	120.4(9)	H41'b-C41'-H41'c	109.5(9)
C15-C21-C20	110.1(8)	N6'-C42'-C43'	107.9(8)
C15-C21-C22	128.4(8)	N6'-C42'-C45'	122.9(8)
C20-C21-C22	121.4(9)	C43'-C42'-C45'	129.2(8)
C21-C22-C23	117.6(9)	C42'-C43'-C44'	106.3(8)
C21-C22-H22	121.2(10)	C42'-C43'-H43'	126.7(9)
C23-C22-H22	121.2(10)	C44'-C43'-H43'	127.0(10)
C22-C23-C24	121.5(9)	N5'-C44'-C43'	110.4(8)
C22-C23-H23	119.1(10)	N5'-C44'-C64'	122.8(8)
C24-C23-H23	119.3(11)	C43'-C44'-C64'	126.8(8)
C23-C24-C25	119.6(9)	C42'-C45'-H45'a	109.3(8)
C23-C24-H24	120.3(10)	C42'-C45'-H45'b	109.3(8)
C25-C24-H24	120.1(10)	C42'-C45'-H45'c	109.8(9)
C20-C25-C24	119.4(9)	H45'a-C45'-H45'b	109.5(10)

C20-C25-H25	119.6(10)	H45'a-C45'-H45'c	109.5(9)
C24-C25-H25	121.0(10)	H45'b-C45'-H45'c	109.5(9)
C3-C26-C27	110.0(7)	C36'-C46'-C47'	121.6(7)
C3-C26-C28	111.1(7)	C36'-C46'-C51'	119.4(7)
C3-C26-C29	109.3(7)	C47'-C46'-C51'	118.9(7)
C27-C26-C28	107.3(7)	C46'-C47'-C48'	119.7(8)
C27-C26-C29	110.4(7)	C46'-C47'-H47'	119.5(8)
C28-C26-C29	108.6(7)	C48'-C47'-H47'	120.7(8)
C26-C27-H27a	109.4(8)	C47'-C48'-C49'	121.9(8)
C26-C27-H27b	109.8(8)	C47'-C48'-H48'	119.1(8)
C26-C27-H27c	109.1(8)	C49'-C48'-H48'	119.0(8)
H27a-C27-H27b	109.5(9)	C48'-C49'-C50'	117.1(8)
H27a-C27-H27c	109.5(9)	C48'-C49'-C52'	120.2(8)
H27b-C27-H27c	109.5(9)	C50'-C49'-C52'	122.7(8)
C26-C28-H28a	109.1(8)	C49'-C50'-C51'	120.8(7)
C26-C28-H28b	110.1(8)	C49'-C50'-H50'	119.2(8)
C26-C28-H28c	109.2(8)	C51'-C50'-H50'	120.0(8)
H28a-C28-H28b	109.5(9)	C46'-C51'-C50'	121.4(7)
H28a-C28-H28c	109.5(9)	C46'-C51'-H51'	119.1(8)
H28b-C28-H28c	109.5(9)	C50'-C51'-H51'	119.4(8)
C26-C29-H29a	110.3(8)	C49'-C52'-C53'	110.7(7)
C26-C29-H29b	109.0(8)	C49'-C52'-C54'	114.3(7)
C26-C29-H29c	109.1(8)	C49'-C52'-H52'	107.5(7)
H29a-C29-H29b	109.5(8)	C53'-C52'-C54'	110.1(7)
H29a-C29-H29c	109.5(9)	C53'-C52'-H52'	107.0(8)
H29b-C29-H29c	109.5(9)	C54'-C52'-H52'	107.0(8)
C12-C30-C31	112.8(6)	C52'-C53'-H53'a	108.7(8)
C12-C30-C32	109.6(7)	C52'-C53'-H53'b	109.1(8)
C12-C30-C33	109.3(6)	C52'-C53'-H53'c	110.7(8)
C31-C30-C32	107.2(7)	H53'a-C53'-H53'b	109.5(9)
C31-C30-C33	109.1(7)	H53'a-C53'-H53'c	109.5(9)
C32-C30-C33	108.8(6)	H53'b-C53'-H53'c	109.5(9)
C30-C31-H31a	109.9(8)	C52'-C54'-H54'a	109.5(8)
C30-C31-H31b	110.0(8)	C52'-C54'-H54'b	110.3(9)
C30-C31-H31c	108.6(8)	C52'-C54'-H54'c	108.6(8)
H31a-C31-H31b	109.5(9)	H54'a-C54'-H54'b	109.5(10)
H31a-C31-H31c	109.5(8)	H54'a-C54'-H54'c	109.5(10)
H31b-C31-H31c	109.5(10)	H54'b-C54'-H54'c	109.5(9)
C30-C32-H32a	109.1(7)	C40'-C55'-C56'	120.9(9)
C30-C32-H32b	109.9(8)	C40'-C55'-C60'	120.8(8)
C30-C32-H32c	109.4(8)	C56'-C55'-C60'	118.3(9)
H32a-C32-H32b	109.5(8)	C55'-C56'-C57'	120.4(10)
H32a-C32-H32c	109.5(9)	C55'-C56'-H56'	119.4(10)
H32b-C32-H32c	109.5(8)	C57'-C56'-H56'	120.1(10)
C30-C33-H33a	110.1(8)	C56'-C57'-C58'	121.3(10)
C30-C33-H33b	109.5(8)	C56'-C57'-H57'	120.5(12)
C30-C33-H33c	108.8(7)	C58'-C57'-H57'	118.1(11)
H33a-C33-H33b	109.5(8)	C57'-C58'-C59'	118.6(9)
H33a-C33-H33c	109.5(9)	C57'-C58'-C61'	123.1(11)
H33b-C33-H33c	109.5(8)	C59'-C58'-C61'	118.2(11)
N2-B-N4	110.2(7)	C58'-C59'-C60'	120.6(10)
N2-B-N6	109.4(8)	C58'-C59'-H59'	119.9(10)
N2-B-H	109.0(9)	C60'-C59'-H59'	119.5(10)

N4-B-N6	109.9(8)	C55'-C60'-C59'	120.7(9)
N4-B-H	109.3(9)	C55'-C60'-H60'	118.3(9)
N6-B-H	109.1(8)	C59'-C60'-H60'	120.9(10)
Zn1-N1-N2	114.3(5)	C58'-C61'-C62'	115.0(13)
Zn1-N1-C36	138.6(6)	C58'-C61'-C63'	111.4(10)
N2-N1-C36	107.0(7)	C58'-C61'-H61'	103.1(13)
B-N2-N1	119.1(7)	C62'-C61'-C63'	121.1(14)
B-N2-C34	130.5(7)	C62'-C61'-H61'	98.8(16)
N1-N2-C34	110.3(7)	C63'-C61'-H61'	104.0(13)
Zn1-N3-N4	111.0(5)	C61'-C62'-H62'a	113.3(18)
Zn1-N3-C40	138.7(6)	C61'-C62'-H62'b	114.4(16)
N4-N3-C40	106.6(7)	C61'-C62'-H62'c	100.3(18)
B-N4-N3	120.3(7)	H62'a-C62'-H62'b	109(2)
B-N4-C38	131.4(7)	H62'a-C62'-H62'c	109.5(18)
N3-N4-C38	108.3(7)	H62'b-C62'-H62'c	109(2)
Zn1-N5-N6	110.8(5)	C61'-C63'-H63'a	110.9(11)
Zn1-N5-C44	141.2(6)	C61'-C63'-H63'b	106.4(11)
N6-N5-C44	106.2(7)	C61'-C63'-H63'c	111.1(11)
B-N6-N5	120.3(7)	H63'a-C63'-H63'b	109.5(12)
B-N6-C42	129.0(7)	H63'a-C63'-H63'c	109.5(11)
N5-N6-C42	110.7(7)	H63'b-C63'-H63'c	109.5(11)
N2-C34-C35	108.0(8)	C44'-C64'-C65'	122.7(10)
N2-C34-C37	124.0(9)	C44'-C64'-C69'	118.5(9)
C35-C34-C37	128.0(9)	C65'-C64'-C69'	118.7(10)
C34-C35-C36	105.4(8)	C64'-C65'-C66'	120.3(11)
C34-C35-H35	127.5(10)	C64'-C65'-H65'	120.0(11)
C36-C35-H35	127.0(10)	C66'-C65'-H65'	119.7(12)
N1-C36-C35	109.3(8)	C65'-C66'-C67'	120.3(12)
N1-C36-C46	123.9(8)	C65'-C66'-H66'	122.4(15)
C35-C36-C46	126.8(9)	C67'-C66'-H66'	117.3(13)
C34-C37-H37a	109.0(9)	C66'-C67'-C68'	118.6(12)
C34-C37-H37b	109.3(10)	C66'-C67'-C70'	118.8(15)
C34-C37-H37c	110.1(9)	C68'-C67'-C70'	122.5(14)
H37a-C37-H37b	109.5(10)	C67'-C68'-C69'	123.3(12)
H37a-C37-H37c	109.5(11)	C67'-C68'-H68'	117.3(13)
H37b-C37-H37c	109.5(10)	C69'-C68'-H68'	119.4(14)
N4-C38-C39	109.3(8)	C64'-C69'-C68'	118.8(11)
N4-C38-C41	121.9(9)	C64'-C69'-H69'	120.2(10)
C39-C38-C41	128.8(9)	C68'-C69'-H69'	121.0(11)
C38-C39-C40	105.3(8)	C67'-C70'-C71'	114.7(15)
C38-C39-H39	127.7(9)	C67'-C70'-C72'	116.4(12)
C40-C39-H39	127.0(9)	C67'-C70'-H70'	101.6(14)
N3-C40-C39	110.4(8)	C71'-C70'-C72'	117.2(14)
N3-C40-C55	122.5(8)	C71'-C70'-H70'	100.6(15)
C39-C40-C55	127.1(9)	C72'-C70'-H70'	102.2(17)
C38-C41-H41a	108.5(8)	C70'-C71'-H71'a	110.6(16)
C38-C41-H41b	109.7(9)	C70'-C71'-H71'b	101.9(16)
C38-C41-H41c	110.2(11)	C70'-C71'-H71'c	115.6(18)
H41a-C41-H41b	109.5(13)	H71'a-C71'-H71'b	109.5(20)
H41a-C41-H41c	109.5(10)	H71'a-C71'-H71'c	109.5(16)
H41b-C41-H41c	109.5(9)	H71'b-C71'-H71'c	109.5(18)
N6-C42-C43	107.5(7)	C70'-C72'-H72'a	112.0(13)
N6-C42-C45	124.4(8)	C70'-C72'-H72'b	112.4(14)

C43-C42-C45	128.2(8)	C70'-C72'-H72'c	103.9(15)
C42-C43-C44	105.7(8)	H72'a-C72'-H72'b	109.5(15)
C42-C43-H43	127.3(9)	H72'a-C72'-H72'c	109.5(14)
C44-C43-H43	127.0(9)	H72'b-C72'-H72'c	109.5(13)
N5-C44-C43	109.9(8)	Cl1s-C1s-Cl2s	114.7(8)
N5-C44-C64	124.5(8)	Cl1s-C1s-H1sa	107.0(11)
C43-C44-C64	125.6(8)	Cl1s-C1s-H1sb	109.3(12)
C42-C45-H45a	108.8(8)	Cl2s-C1s-H1sa	107.8(11)
C42-C45-H45b	109.4(8)	Cl2s-C1s-H1sb	108.7(11)
C42-C45-H45c	110.2(8)	H1sa-C1s-H1sb	109.3(13)
H45a-C45-H45b	109.5(9)	C1s-Cl1s-Cl2s	33.5(5)
H45a-C45-H45c	109.5(9)	C1s-Cl1s-H1sa	25.1(5)
H45b-C45-H45c	109.5(9)	C1s-Cl1s-H1sb	24.0(4)
C36-C46-C47	121.8(9)	Cl2s-Cl1s-H1sa	50.25(12)
C36-C46-C51	119.6(8)	Cl2s-Cl1s-H1sb	50.12(11)
C47-C46-C51	118.6(8)	H1sa-Cl1s-H1sb	41.84(8)
C46-C47-C48	120.0(8)	C1s-Cl2s-Cl1s	31.8(5)
C46-C47-H47	119.7(9)	C1s-Cl2s-H1sa	24.0(5)
C48-C47-H47	120.3(9)	C1s-Cl2s-H1sb	23.4(4)
C47-C48-C49	121.0(9)	Cl1s-Cl2s-H1sa	47.79(11)
C47-C48-H48	119.6(10)	Cl1s-Cl2s-H1sb	48.17(12)
C49-C48-H48	119.3(9)	H1sa-Cl2s-H1sb	40.41(6)
C48-C49-C50	118.6(8)	Cl3s-C2s-Cl4s	111.1(16)
C48-C49-C52	120.4(9)	Cl3s-C2s-H2sa	107(3)
C50-C49-C52	121.0(9)	Cl3s-C2s-H2sb	108(2)
C49-C50-C51	121.3(9)	Cl4s-C2s-H2sa	113(2)
C49-C50-H50	118.8(9)	Cl4s-C2s-H2sb	111(3)
C51-C50-H50	119.8(10)	H2sa-C2s-H2sb	104(2)
C46-C51-C50	120.4(9)	C2s-Cl3s-Cl4s	34.0(8)
C46-C51-H51	119.0(9)	C2s-Cl3s-H2sa	24.4(9)
C50-C51-H51	120.6(9)	C2s-Cl3s-H2sb	24.8(9)
C49-C52-C53	109.5(9)	Cl4s-Cl3s-H2sa	51.4(2)
C49-C52-C54	111.8(9)	Cl4s-Cl3s-H2sb	51.3(3)
C49-C52-H52	108.9(9)	H2sa-Cl3s-H2sb	40.52(15)
C53-C52-C54	110.4(10)	C2s-Cl4s-Cl3s	34.9(12)
C53-C52-H52	108.4(10)	C2s-Cl4s-H2sa	23.2(10)
C54-C52-H52	107.7(10)	C2s-Cl4s-H2sb	24.1(11)
C52-C53-H53a	109.2(10)	Cl3s-Cl4s-H2sa	50.5(3)
C52-C53-H53b	108.5(11)	Cl3s-Cl4s-H2sb	50.9(2)
C52-C53-H53c	110.7(11)	H2sa-Cl4s-H2sb	40.12(17)
H53a-C53-H53b	109.5(12)	Cl5s-C3s-Cl6s	113.4(10)
H53a-C53-H53c	109.5(12)	Cl5s-C3s-H3sa	108.7(12)
H53b-C53-H53c	109.5(11)	Cl5s-C3s-H3sb	110.2(13)
C52-C54-H54a	110.8(12)	Cl6s-C3s-H3sa	107.6(13)
C52-C54-H54b	110.2(12)	Cl6s-C3s-H3sb	110.1(14)
C52-C54-H54c	107.4(10)	H3sa-C3s-H3sb	106.6(15)
H54a-C54-H54b	109.5(12)	C3s-Cl5s-Cl6s	32.8(6)
H54a-C54-H54c	109.5(14)	C3s-Cl5s-H3sa	25.3(6)
H54b-C54-H54c	109.5(13)	C3s-Cl5s-H3sb	23.5(6)
C40-C55-C56	120.0(9)	Cl6s-Cl5s-H3sa	49.8(2)
C40-C55-C60	121.7(8)	Cl6s-Cl5s-H3sb	49.4(2)
C56-C55-C60	118.3(9)	H3sa-Cl5s-H3sb	41.11(10)
C55-C56-C57	120.9(10)	C3s-Cl6s-Cl5s	33.9(5)

C55-C56-H56	118.8(10)	C3s-Cl6s-H3sa	26.2(6)
C57-C56-H56	120.3(10)	C3s-Cl6s-H3sb	24.0(6)
C56-C57-C58	121.3(9)	Cl5s-Cl6s-H3sa	51.6(2)
C56-C57-H57	120.4(11)	Cl5s-Cl6s-H3sb	50.8(2)
C58-C57-H57	118.3(10)	H3sa-Cl6s-H3sb	42.13(14)
C57-C58-C59	117.9(9)	C1s-H1sa-Cl1s	47.9(9)
C57-C58-C61	122.9(9)	C1s-H1sa-Cl2s	48.2(8)
C59-C58-C61	119.1(10)	C1s-H1sa-H1sb	34.9(8)
C58-C59-C60	122.4(9)	Cl1s-H1sa-Cl2s	81.96(15)
C58-C59-H59	118.2(10)	Cl1s-H1sa-H1sb	69.58(15)
C60-C59-H59	119.4(10)	Cl2s-H1sa-H1sb	69.70(10)
C55-C60-C59	119.2(9)	C1s-H1sb-Cl1s	46.6(9)
C55-C60-H60	119.9(9)	C1s-H1sb-Cl2s	47.9(9)
C59-C60-H60	120.9(10)	C1s-H1sb-H1sa	35.8(8)
C58-C61-C62	112.6(9)	Cl1s-H1sb-Cl2s	81.70(16)
C58-C61-C63	110.1(9)	Cl1s-H1sb-H1sa	68.58(15)
C58-C61-H61	107.9(10)	Cl2s-H1sb-H1sa	69.89(10)
C62-C61-C63	111.4(9)	C2s-H2sa-Cl3s	47(2)
C62-C61-H61	107.4(10)	C2s-H2sa-Cl4s	43.6(16)
C63-C61-H61	107.2(10)	C2s-H2sa-H2sb	38.2(17)
C61-C62-H62a	109.1(10)	Cl3s-H2sa-Cl4s	78.1(3)
C61-C62-H62b	108.4(10)	Cl3s-H2sa-H2sb	70.39(17)
C61-C62-H62c	110.9(10)	Cl4s-H2sa-H2sb	69.9(3)
H62a-C62-H62b	109.5(11)	C2s-H2sb-Cl3s	47.2(19)
H62a-C62-H62c	109.5(11)	C2s-H2sb-Cl4s	44.3(17)
H62b-C62-H62c	109.5(11)	C2s-H2sb-H2sa	37.1(15)
C61-C63-H63a	109.2(10)	Cl3s-H2sb-Cl4s	77.7(3)
C61-C63-H63b	111.0(11)	Cl3s-H2sb-H2sa	69.1(2)
C61-C63-H63c	108.2(10)	Cl4s-H2sb-H2sa	70.0(3)
H63a-C63-H63b	109.5(11)	C3s-H3sa-Cl5s	46.0(9)
H63a-C63-H63c	109.5(12)	C3s-H3sa-Cl6s	46.2(10)
H63b-C63-H63c	109.5(11)	Cl5s-H3sa-Cl6s	78.6(3)
C44-C64-C65	121.7(9)	C3s-H3sb-Cl5s	46.3(9)
C44-C64-C69	121.3(8)	C3s-H3sb-Cl6s	45.9(11)
C65-C64-C69	116.7(9)	Cl5s-H3sb-Cl6s	79.8(3)

Appendix B Crystallographic Data for Chapter 6

Structure Determination.

(**1(PhNit₂)**).

Red plates of **rfbis** (**1(PhNit₂)**) were crystallized from a diethyl ether/dichloromethane/heptane solution at 22 deg. C. A crystal of dimensions 0.34 x 0.28 x 0.08 mm was mounted on a standard Bruker SMART CCD-based X-ray diffractometer equipped with a LT-2 low temperature device and normal focus Mo-target X-ray tube (λ = 0.71073 A) operated at 2000 W power (50 kV, 40 mA). The X-ray intensities were measured at 118(2) K; the detector was placed at a distance 4.950 cm from the crystal. A total of 3862 frames were collected with a scan width of 0.2° in ω with an exposure time of 30 s/frame. The frames were integrated with the Bruker SAINT software package with a narrow frame algorithm. The integration of the data yielded a total of 37135 reflections to a maximum 2θ value of 56.74° of which 13853 were independent and 9779 were greater than 2σ(I). The final cell constants (Table 1) were based on the xyz centroids of 5636 reflections above 10σ(I). Analysis of the data showed negligible decay during data collection; the data were processed with SADABS, no correction for absorption was necessary. The structure was solved and refined with the Bruker SHELXTL (version 5.10) software package, using the space group P1bar with Z = 4 for the formula $C_{32}H_{41}N_2O_2$. There are two crystallographically independent molecules, one of which is partially disordered. All non-hydrogen atoms were refined anisotropically with the hydrogen atoms placed in idealized positions. Full matrix least-squares refinement based on F^2 converged at R1 = 0.0742 and wR2 = 0.2060 [based on I > 2sigma(I)], R1 = 0.1045 and wR2 = 0.2282 for all data. Additional details are presented in Table 1 and are given as Supporting Information in a CIF file.

Sheldrick, G.M. SHELXTL, v. 5.10; Bruker Analytical X-ray, Madison, WI, 1997.
Sheldrick, G.M. SADABS. Program for Empirical Absorption Correction of Area Detector Data, University of Gottingen: Gottingen, Germany, 1996.
Saint Plus, v. 6.29, Bruker Analytical X-ray, Madison, WI, 2001.

Table S1. Crystal data and structure refinement for rfbis (**1(PhNit₂)**).

Identification code	rfbis
Empirical formula	C32 H41 N2 O2
Formula weight	485.67
Temperature	118(2) K
Wavelength	0.71073 A
Crystal system, space group	Triclinic, P-1
Unit cell dimensions	a = 12.865(3) A; alpha = 108.424(3) deg.
	b = 14.483(3) A; beta = 91.425(4) deg.
	c = 16.875(4) A; gamma = 108.159(3) deg.
Volume	2807.8(10) A^3
Z, Calculated density	4, 1.149 Mg/m^3
Absorption coefficient	0.071 mm^-1
F(000)	1052
Crystal size	0.34 x 0.28 x 0.08 mm
Theta range for data collection	2.66 to 28.49 deg.
Limiting indices	-17<=h<=17, -19<=k<=18, -22<=l<=22
Reflections collected / unique	13853 / 13853 [R(int) = 0.0356]
Completeness to theta =	28.49, 97.2 %
Absorption correction	None
Max. and min. transmission	0.9943 and 0.9763
Refinement method	Full-matrix least-squares on F^2
Data / restraints / parameters	13853 / 0 / 766
Goodness-of-fit on F^2	1.033
Final R indices [I>2sigma(I)]	R1 = 0.0742, wR2 = 0.2060
R indices (all data)	R1 = 0.1045, wR2 = 0.2282
Largest diff. peak and hole	0.735 and -0.579 e.A^-3

(2(PhNit$_2$

Brown needles of **notbu1** (**2(PhNit₂)**) were crystallized from a heptane/dichloromethane solution at 25 deg. C. A crystal of dimensions 0.44 x 0.02 x 0.02 mm was mounted on a standard Bruker SMART CCD-based X-ray diffractometer equipped with a LT-2 low temperature device and normal focus Mo-target X-ray tube (λ = 0.71073 A) operated at 2000 W power (50 kV, 40 mA). The X-ray intensities were measured at 158(2) K; the detector was placed at a distance 4.959 cm from the crystal. A total of 2242 frames were collected with a scan width of 0.3° in ω and phi with an exposure time of 60 s/frame. The frames were integrated with the Bruker SAINT software package with a narrow frame algorithm. The integration of the data yielded a total of 12963 reflections to a maximum 2θ value of 47.92° of which 4193 were independent and 2142 were greater than 2σ(I). The final cell constants (Table 1) were based on the xyz centroids of 1486 reflections above 10σ(I). Analysis of the data showed negligible decay during data collection; the data were processed with SADABS, no correction for absorption was necessary. The structure was solved and refined with the Bruker SHELXTL (version 5.10) software package, using the space group P1bar with Z = 2 for the formula $C_{30}H_{44}N_2O_2$. All non-hydrogen atoms were refined anisotropically with the hydrogen atoms placed in idealized positions. Full matrix least-squares refinement based on F^2 converged at R1 = 0.0544 and wR2 = 0.1252 [based on I > 2sigma(I)], R1 = 0.1127 and wR2 = 0.1303 for all data. Additional details are presented in Table 1 and are given as Supporting Information as a CIF file.

Sheldrick, G.M. SHELXTL, v. 5.10; Bruker Analytical X-ray, Madison, WI, 1997.
Sheldrick, G.M. SADABS. Program for Empirical Absorption Correction of Area Detector Data, University of Gottingen: Gottingen, Germany, 1996.
Saint Plus, v. 6.02, Bruker Analytical X-ray, Madison, WI, 1999.

Table S6. Crystal data and structure refinement for notbu1 (**2(PhNit₂)**).

Identification code	notbu1
Empirical formula	C30 H44 N2 O2
Formula weight	464.67
Temperature	158(2) K
Wavelength	0.71073 A
Crystal system, space group	Triclinic, P-1
Unit cell dimensions	a = 6.1904(11) A alpha = 85.858(8) deg.
	b = 12.730(3) A beta = 80.307(8) deg.
	c = 17.528(4) A gamma = 83.199(9) deg.
Volume	1350.0(4) A^3
Z, Calculated density	2, 1.143 Mg/m^3
Absorption coefficient	0.071 mm^-1
F(000)	508
Crystal size	0.44 x 0.02 x 0.02 mm
Theta range for data collection	1.95 to 23.96 deg.
Limiting indices	-6<=h<=7, -14<=k<=14, 0<=l<=20
Reflections collected / unique	12963 / 4193 [R(int) = 0.0656]
Completeness to theta =	23.96 99.6 %
Absorption correction	None
Refinement method	Full-matrix least-squares on F^2
Data / restraints / parameters	4193 / 0 / 321
Goodness-of-fit on F^2	0.958
Final R indices [I>2sigma(I)]	R1 = 0.0544, wR2 = 0.1127
R indices (all data)	R1 = 0.1252, wR2 = 0.1303
Extinction coefficient	0.027(2)
Largest diff. peak and hole	0.195 and -0.208 e.A^-3

(3(PhNit$_2$)

Crystallography. Crystallographic data for biradical (**3(PhNit$_2$)**): Amber needles of (**3(PhNit$_2$)**) were crystallized from dichloromethane at 23 deg. C. A crystal of dimensions 0.35 x 0.15 x 0.05 mm was mounted on a standard Bruker SMART CCD-based X-ray diffractometer equipped with a LT-2 low temperature device and normal focus Mo-target X-ray tube (λ = 0.71073 A) operated at 2000 W power (50 kV, 40 mA). The X-ray intensities were measured at 158(2) K; the detector was placed at a distance 5.008 cm from the crystal. A total of 4770 frames were collected with a scan width of 0.3° in ω and phi with an exposure time of 30 s/frame. The frames were integrated with the Bruker SAINT software package with a narrow frame algorithm. The integration of the data yielded a total of 25959 reflections to a maximum 2θ value of 52.98° of which 5344 were independent and 4460 were greater that 2σ(I). The final cell constants (Table 1) were based on the xyz centroids of 4032 reflections above 10σ(I). Analysis of the data showed negligible decay during data collection. The data were processed with SADABS, no correction for absorption was necessary. The structure was solved and refined with the Bruker SHELXTL (version 5.10) software package, using the space group P-1 with Z = 2 for the formula C$_{31}$H$_{40}$N$_2$O$_2$. All non-hydrogen atoms were refined anisotropically with the hydrogen atoms placed in idealized positions. Full matrix least-squares refinement based on F^2 converged at R1 = 0.0433 and wR2 = 0.0982 [based on I >

2sigma(I)], R1 = 0.0832 and wR2 = 0.1099 for all data. Additional details are presented in Table 1 and are given as Supporting information as a CIF file.

(3(PhNit$_2$) Table 1. Crystal data and structure refinement for (3(PhNit$_2$)

Empirical formula	$C_{31}H_{40}N_2O_2$
Formula weight	472.65
Temperature, K	158(2)
Wavelength (λ), Å	0.71073
Crystal system	Triclinic
Space group	P-1
a, Å	6.2271(16)
b, Å	12.170(3)
c, Å	17.882(4)
α, °	99.872(5)
β, °	99.659(5)
γ, °	95.631(5)
Volume, Å^3	1304.9(6)
Absorption coefficient, mm^{-1}	0.074
Z	2
Calculated density, Mg/m^3	1.203
F(000)	512
Crystal size, mm	0.35 x 0.15 x 0.05
θ range for data collection,°.	1.71 to 24.71
Limiting indices	-7<=h<=7, -14<=k<=14, -21<=l<=21,
Reflections collected/unique	25959/4460
Absorption correction	None
Data/restraints/parameters	4460/0/324
R1[I>2sigma(I)]*	0.0433
wR2*	0.0982
Largest diff.peak, Å	0.221
GoF	0.896

*based on Fo^2

Structure Determination.

Crystal data of a red plate-like crystal of **3(PhNit)₂** with the approximate dimensions 0.20 x 0.20 x 0.05 mm were collected on a Bruker platform diffractometer equipped with a Smart6000 CCD detector (normal focus sealed tube operated at 50 kV, 45 mA, graphite-monochromated, MoKα = 0.71073 Å). A single crystal was selected and mounted on a 0.1 mm glass capillary with epoxy glue. The crystal was measured at ca. 25(5) K using an open flow He-cryostat. Evaluation of the diffraction data revealed cracking for all tested crystals into several components upon cooling. A total of 1073 frames were collected with an exposure time of 60 s and a scan width of 0.3º in • at a detector to crystal distance of 5.150 cm.

Orientation Matrices for four components were found using Gemini. The data for all four crystal components were integrated simultaneously using SAINT 6.29A. No correction for absorption or decay was applied. A separate integration based on only the orientation matrix of the major component (and thereby containing all reflections originated by component1 – isolated and overlapping) provided a 'HKLF 4' format file, which was used to solve the structure with direct methods in P1bar (SHELXTL 5.1). The structure was refined by full-matrix least squares on F². A refinement on all four components similtaneously converged to R1 = 0.184 (48º cutoff in 2•) for 10 364 reflections with Fo > 4•(Fo) and resulted in batch scale factors of 0.57: 0.20:0.21:0.02. All non-hydrogen atoms were refined with isotropic atomic displacement factors, hydrogen atoms were calculated on idealized positions and treated as riding atoms.

The high R-value is not surprising considering the nature of this cracked crystal, which can be only approximated by a model of four single crystal domains. Not all 'domains' in the cracked crystal are accounted for and some of the indexed ones are obviously not well defined. A home written program was used to separate overlapping and isolated reflections and a better model was obtained by refining on those reflections that originated only from the dominant component. Nitrogen and Oxygen atoms were refined with anisotropic atomic displacement factors, carbon atom were refined isotropically, hydrogen atoms were calculated on idealized positions and treated as riding atoms. The final refinement converged to R1 = 0.0948 (wR2 = 0.2259) for 1129 reflections with Fo > 4•(Fo) and R1 = 0.1031 (wR2 = 0.2323) for all 1254 data.

SMART, Version 5.625, **2001**, Bruker AXS Inc., Madison, Wisconsin, USA.

M. J. Hardie, K. Kirschbaum, A. Martin, A. A. Pinkerton *J. Appl. Cryst.* **1998**, *31*, 815-817.

Gemini 1.02 **2000.** Bruker AXS Inc., Madison, Wisconsin, USA.

Saint 6.29A , **2001** Bruker AXS Inc., Madison, Wisconsin, USA

G.M. Sheldrick, SHELXTL, Version 5.1, **1998,** Bruker AXS Inc., Madison, Wisconsin, USA.

Table S21. Crystal data and structure refinement for abcd3a (**3(PhNit)₂**).

Empirical formula	C31 H40 N2 O2
Formula weight	472.65
Temperature	25(5) K
Wavelength	0.71073 A
Crystal system, space group	triclinic, P1bar
Unit cell dimensions	a=6.2971(5) Å, •=100.563(3)•
	b=11.9668(10) Å, •=96.732(3)•
	c=17.4475(12) Å, •=94.661(3)•
Volume	1276.46(17) Å³
Z, Calculated density	2, 1.230 Mg/m³
Absorption coefficient	0.076 mm⁻¹
F(000)	512
Crystal size	0.20 x 0.20 x 0.02 mm
Theta range for data collection	3.23 to 23.99 deg.
Limiting indices	-5<=h<=6, -5<=k<=12, -18<=l<=18
Reflections collected / unique	1314 / 1254 [R(int) = 0.1085]
Completeness to theta = 23.99	31.4 %
Refinement method	Full-matrix least-squares on F²
Data / restraints / parameters	1254 / 0 / 161
Goodness-of-fit on F²	1.249
Final R indices [I>2sigma(I)]	R1 = 0.0948, wR2 = 0.2259
R indices (all data)	R1 = 0.1031, wR2 = 0.2323
Largest diff. peak and hole	0.236 and -0.211 e.A³

(4(PhNit2)

210

Crystallography. Crystallographic data for biradical **(4(PhNit2)**: Red needles of **(4(PhNit2)** were crystallized from dichloromethane layered with heptane at RT. A crystal of dimensions 0.40 x 0.18 x 0.04 mm was mounted on a Enraf-Nonius CAD4-MACH X-ray diffractometer. The sample was mounted on the end of a glass fiber using a small amount of silicone grease and transferred to the diffractometer. The sample was maintained at a temperature of –125 deg C using a nitrogen cold stream. All X-ray measurements were made on an Enraf-Nonius CAD4-MACH diffractometer. The unit cell dimensions were determined by a fit of 25 well centered reflections and their Friedel pairs with theta 23 deg < 2(theta) < 36 deg. A hemisphere of unique data was collected using the omega scan mode in a non-bisecting geometry. The adoption of a non-bisecting scan mode was accomplished by offsetting psi by 20.00 for each data point collected. This was done to minimize the interaction of the goniometer head with the cold stream. Three standard reflections were measured every 4800 seconds of X-ray exposure time. Scaling the data was accomplished using a 5 point smoothed curved routine fit to the intensity check reflections. The intensity data was corrected for Lorentz and polarization effects. Data were not corrected for absorption.

Structure Solution and Refinement. The data were reduced using routines from the NRCVAX set of programs. The structure was solved using SIR92. All non-H atom positions were recovered from the initial E-map. Hydrogen atoms were included in the model at calculated positions. The hydrogen atom positions and isotropic displacement parameters were allowed to refine. Refinement of the structure was performed using full matrix least-squares based on F. All non-H atoms were allowed to refine with anisotropic displacement parameters (ADP's). The calculated structure factors included corrections for anomalous dispersion from the usual tabulation (International Tables for X-ray Crystallography, Vol. IV, (1974), Table 2.3.1, Kynoch Press, Birmingham, England). A secondary extinction correction was included in the final cycles of refinement. Additional information and relevant literature references can be found in the REPORT.OUT file and the reference section of the Facility's Web page.

Table 1. Crystal data and structure refinement for (4(PhNit2)

Empirical formula	$C_{28}H_{36}N_2O_2$
Formula weight	432.60
Temperature, K	148
Wavelength (λ), Å	0.71073
Crystal system	Triclinic
Space group	P-1
a, Å	6.1933(4)
b, Å	11.4950(10)
c, Å	17.478(2)
α, °	104.577(8)
β, °	99.635(8)
γ, °	94.942(8)

Volume, Å^3	1176.48(19)
Absorption coefficient, mm^{-1}	0.08
Z	2
Calculated density, Mg/m^3	1.221
F(000)	468.25
Crystal size, mm	0.40 x 0.18 x 0.04
θ range for data collection,°.	0.0 to 25.0
Limiting indices	-7<=h<=7, -0<=k<=13, -20<=l<=19,
Reflections collected/unique	4097/4097
Absorption correction	None
Data/restraints/parameters	2809/0/434
RF*	0.051
Rw**	0.053
Largest diff.peak, Å	0.260
GoF(based on Fo)	1.45

*[RF = Σ(Fo-Fc)/ Σ(Fo)]

**(Rw = [Σ(w(Fo-Fc)^2)/ Σ(wFo^2)]$^{-1/2}$)

(6(Nit$_2$))

Structure Determination.

Brown plates of **flat2** (**6(Nit$_2$)**) were crystallized from dichloromethane/pentane at 23 deg. C. A crystal of dimensions 0.24 x 0.12 x 0.06 mm was mounted on a standard Bruker SMART CCD-based X-ray diffractometer equipped with a LT-2 low temperature device and normal focus Mo-target X-ray tube (λ = 0.71073 A) operated at 2000 W power (50 kV, 40 mA). The X-ray intensities were measured at 158(2) K; the detector was placed at a distance 5.058 cm from the crystal. A total of 2862 frames were collected with a scan width of 0.3° in ω and phi with an exposure time of 75 s/frame. The frames were integrated with the Bruker SAINT software package with a narrow frame algorithm. The integration of the data yielded a total of 28025 reflections to a maximum 2θ value of 52.92° of which 3524 were independent and 2083 were greater than 2σ(I). The final cell constants (Table 1) were based on the xyz centroids of 910 reflections above 10σ(I). Analysis of the data showed negligible decay during data collection. The data were processed with SADABS, no correction for absorption was necessary. The structure was solved and refined with the Bruker SHELXTL (version 5.10) software package using the space group P2/c with Z = 4

for the formula $C_{28}H_{36}N_2O_2$. All non-hydrogen atoms were refined anisotropically with the hydrogen atoms placed in idealized positions. Full matrix least-squares refinement based on F^2 converged at R1 = 0.0584 and wR2 = 0.1330 [based on I > 2sigma(I)], R1 = 0.1185 and wR2 = 0.1642 for all data. Additional details are presented in Table 1 and are given as Supporting Information in a CIF file.
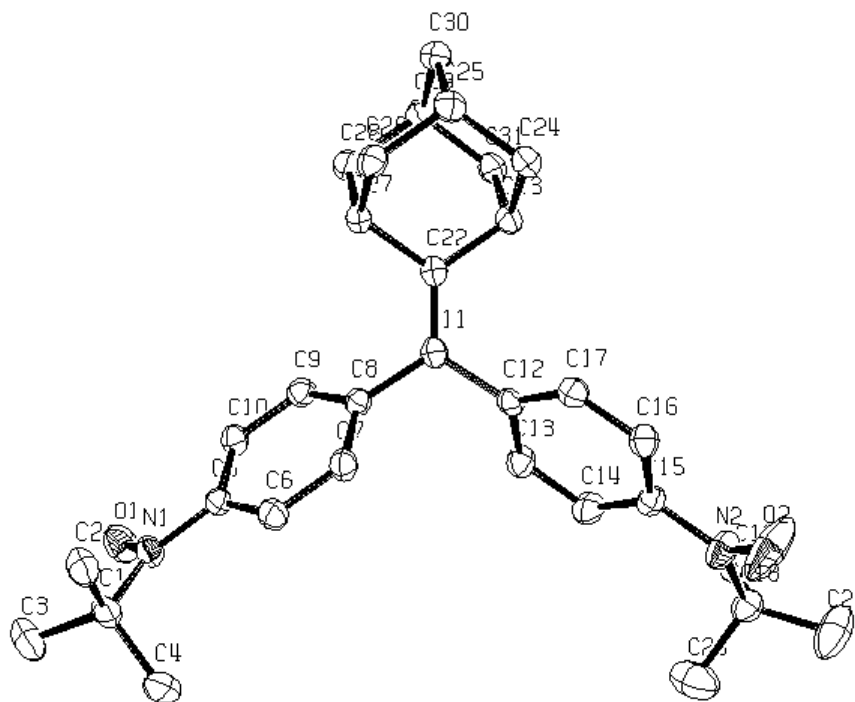
Sheldrick, G.M. SHELXTL, v. 5.10; Bruker Analytical X-ray, Madison, WI, 1997.
Sheldrick, G.M. SADABS. Program for Empirical Absorption Correction of Area Detector Data, University of Gottingen: Gottingen, Germany, 1996.
Saint Plus, v. 6.02, Bruker Analytical X-ray, Madison, WI, 1999.

Table S11. Crystal data and structure refinement for flat2 (**6(Nit$_2$)**).

Identification code	flat2
Empirical formula	C28 H36 N2 O2
Formula weight	432.59
Temperature	158(2) K
Wavelength	0.71073 Å
Crystal system, space group	Monoclinic, P2/c
Unit cell dimensions	a = 15.034(2) Å alpha = 90 deg.
	b = 8.4086(11) Å beta = 94.592(5) deg.
	c = 19.420(3) Å gamma = 90 deg.
Volume	2447.1(6) A^3
Z, Calculated density	4, 1.174 Mg/m^3
Absorption coefficient	0.073 mm^-1
F(000)	936
Crystal size	0.06 x 0.12 x 0.24 mm
Theta range for data collection	2.10 to 23.25 deg.
Limiting indices	-16<=h<=16, -9<=k<=9, -21<=l<=21
Reflections collected / unique	28025 / 3524 [R(int) = 0.0406]
Completeness to theta = 23.25	99.9 %
Absorption correction	None
Refinement method	Full-matrix least-squares on F^2
Data / restraints / parameters	3524 / 0 / 301
Goodness-of-fit on F^2	0.983
Final R indices [I>2sigma(I)]	R1 = 0.0584, wR2 = 0.1330
R indices (all data)	R1 = 0.1185, wR2 = 0.1642
Extinction coefficient	0.038(3)
Largest diff. peak and hole	0.323 and -0.264 e.A^-3

7(PhNit)₂

Structure Determination.
Orange plates of **flor2** (**7(PhNit)₂**) were crystallized from methanol/pentane at 23 deg. C. A crystal of dimensions 0.24 x 0.22 x 0.20 mm was mounted on a standard Bruker SMART CCD-based X-ray diffractometer equipped with a LT-2 low temperature device and normal focus Mo-target X-ray tube (λ = 0.71073 A) operated at 2000 W power (50 kV, 40 mA). The X-ray intensities were measured at 158(2) K; the detector was placed at a distance 5.008 cm from the crystal. A total of 3332 frames were collected with a scan width of 0.3° in ω and phi with an exposure time of 75 s/frame. The frames were integrated with the Bruker SAINT software package with a narrow frame algorithm. The integration of the data yielded a total of 45865 reflections to a maximum 2θ value of 42.0° of which 3007 were independent and 1979 were greater than $2\sigma(I)$. The final cell constants (Table 1) were based on the xyz centroids of 5901 reflections above $10\sigma(I)$. Analysis of the data showed negligible decay during data collection. The data were processed with SADABS, no correction for absorption was necessary. The structure was solved and refined with the Bruker SHELXTL (version 5.10) software package using the space group Pbca with Z = 8 for the formula $C_{33}H_{34}N_2O_2$. All non-hydrogen atoms were refined anisotropically with the hydrogen atoms placed in idealized positions. Full matrix least-squares refinement based on F^2 converged at R1 = 0.0708 and wR2 = 0.1737 [based on I > 2sigma(I)], R1 = 0.1010 and wR2 = 0.1896 for all data. Additional details are presented in Table 1 and are given as Supporting Information in a CIF file.

Sheldrick, G.M. SHELXTL, v. 5.10; Bruker Analytical X-ray, Madison, WI, 1997.
Sheldrick, G.M. SADABS. Program for Empirical Absorption Correction of Area Detector Data, University of Gottingen: Gottingen, Germany, 1996.
Saint Plus, v. 6.02, Bruker Analytical X-ray, Madison, WI, 1999.

Table S16. Crystal data and structure refinement for flor2 (**7(PhNit)₂**).

Identification code	flor2
Empirical formula	C33 H34 N2 O2
Formula weight	490.62
Temperature	158(2) K
Wavelength	0.71073 A

Crystal system, space group	Orthorhombic, Pbca
Unit cell dimensions	a = 12.087(5) A alpha = 90 deg.
	b = 19.740(9) A beta = 90 deg.
	c = 23.655(10) A gamma = 90 deg.
Volume	5644(4) A^3
Z, Calculated density	8, 1.155 Mg/m^3
Absorption coefficient	0.072 mm^-1
F(000)	2096
Crystal size	0.20 x 0.22 x 0.24 mm
Theta range for data collection	1.72 to 21.00 deg.
Limiting indices	-12<=h<=12, -19<=k<=19, -23<=l<=23
Reflections collected / unique	45865 / 3007 [R(int) = 0.0885]
Completeness to theta = 21.00	99.3 %
Absorption correction	None
Refinement method	Full-matrix least-squares on F^2
Data / restraints / parameters	3007 / 0 / 342
Goodness-of-fit on F^2	0.966
Final R indices [I>2sigma(I)]	R1 = 0.0718, wR2 = 0.1737
R indices (all data)	R1 = 0.1010, wR2 = 0.1896
Extinction coefficient	0.0078(11)
Largest diff. peak and hole	0.305 and -0.304 e.A^-3

Structure Determination.

Red plates of **rfbis** (**1(PhNit$_2$)**) were crystallized from a diethyl ether/dichloromethane/heptane solution at 22 deg. C. A crystal of dimensions 0.34 x 0.28 x 0.08 mm was mounted on a standard Bruker SMART CCD-based X-ray diffractometer equipped with a LT-2 low temperature device and normal focus Mo-target X-ray tube (λ = 0.71073 A) operated at 2000 W power (50 kV, 40 mA). The X-ray intensities were measured at 118(2) K; the detector was placed at a distance 4.950 cm from the crystal. A total of 3862 frames were collected with a scan width of 0.2° in ω with an exposure time of 30 s/frame. The frames were integrated with the Bruker SAINT software package with a narrow frame algorithm. The integration of the data yielded a total of 37135 reflections to a maximum 2θ value of 56.74° of which 13853 were independent and 9779 were greater than 2σ(I). The final cell constants (Table 1) were based on the xyz centroids of 5636 reflections above 10σ(I). Analysis of the data showed negligible decay during data collection; the data were processed with SADABS, no correction for absorption was necessary. The structure was solved and refined with the Bruker SHELXTL (version 5.10) software package, using the space group P1bar with Z = 4 for the formula C$_{32}$H$_{41}$N$_2$O$_2$. There are two crystallographically independent molecules, one of which is partially disordered. All non-hydrogen atoms were refined anisotropically with the hydrogen atoms placed in idealized positions. Full matrix least-squares refinement based on F^2 converged at R1 = 0.0742 and wR2 = 0.2060 [based on I > 2sigma(I)], R1 = 0.1045 and wR2 = 0.2282 for all data. Additional details are presented in Table 1 and are given as Supporting Information in a CIF file.

Sheldrick, G.M. SHELXTL, v. 5.10; Bruker Analytical X-ray, Madison, WI, 1997.
Sheldrick, G.M. SADABS. Program for Empirical Absorption Correction of Area Detector Data, University of Gottingen: Gottingen, Germany, 1996.
Saint Plus, v. 6.29, Bruker Analytical X-ray, Madison, WI, 2001.

Table S1. Crystal data and structure refinement for rfbis (**1(PhNit$_2$)**).

Identification code	rfbis
Empirical formula	C32 H41 N2 O2
Formula weight	485.67
Temperature	118(2) K
Wavelength	0.71073 A

Crystal system, space group	Triclinic, P-1
Unit cell dimensions	$a = 12.865(3)$ A; alpha = 108.424(3) deg.
	$b = 14.483(3)$ A; beta = 91.425(4) deg.
	$c = 16.875(4)$ A; gamma = 108.159(3) deg.
Volume	2807.8(10) A^3
Z, Calculated density	4, 1.149 Mg/m^3
Absorption coefficient	0.071 mm^-1
F(000)	1052
Crystal size	0.34 x 0.28 x 0.08 mm
Theta range for data collection	2.66 to 28.49 deg.
Limiting indices	-17<=h<=17, -19<=k<=18, -22<=l<=22
Reflections collected / unique	13853 / 13853 [R(int) = 0.0356]
Completeness to theta =	28.49,97.2 %
Absorption correction	None
Max. and min. transmission	0.9943 and 0.9763
Refinement method	Full-matrix least-squares on F^2
Data / restraints / parameters	13853 / 0 / 766
Goodness-of-fit on F^2	1.033
Final R indices [I>2sigma(I)]	R1 = 0.0742, wR2 = 0.2060
R indices (all data)	R1 = 0.1045, wR2 = 0.2282
Largest diff. peak and hole	0.735 and -0.579 e.A^-3

Table S2. Atomic coordinates (x 10^4) and equivalent isotropic displacement parameters (A^2 x 10^3) for rfbis (**1(PhNit$_2$)**). U(eq) is defined as one third of the trace of the orthogonalized Uij tensor.

_____

	x	y	z	U(eq)
C(1)	3176(2)	1809(2)	4296(1)	20(1)
C(2)	4370(2)	1905(2)	4395(1)	20(1)
C(3)	5175(2)	2581(2)	4114(1)	21(1)
C(4)	6278(2)	2658(2)	4209(1)	23(1)
C(5)	6598(2)	2051(2)	4599(1)	24(1)
C(6)	5808(2)	1384(2)	4894(1)	27(1)
C(7)	4711(2)	1316(2)	4798(1)	25(1)
C(8)	8725(2)	2914(2)	4697(2)	32(1)
C(9)	8636(2)	3943(2)	5248(2)	39(1)
C(10)	9682(2)	2735(2)	5107(2)	45(1)
C(11)	8913(2)	2886(3)	3803(2)	47(1)
C(12)	2915(2)	2624(2)	4983(1)	21(1)
C(13)	3250(2)	3645(2)	4994(1)	29(1)
C(14)	3096(2)	4429(2)	5651(1)	29(1)
C(15)	2585(2)	4215(2)	6328(1)	23(1)
C(16)	2225(2)	3194(2)	6313(1)	23(1)
C(17)	2395(2)	2419(2)	5653(1)	21(1)
C(18)	1938(2)	4996(2)	7763(1)	25(1)
C(19)	2034(2)	6091(2)	8294(2)	36(1)
C(20)	2550(2)	4582(2)	8284(2)	33(1)
C(21)	722(2)	4342(2)	7498(2)	36(1)
C(22)	2434(2)	1065(2)	3660(1)	21(1)
C(23)	1225(2)	971(2)	3608(1)	28(1)
C(24)	702(2)	851(2)	2735(2)	36(1)
C(25)	1456(2)	1467(2)	2261(2)	40(1)

C(26)	2197(2)	920(2)	1755(2)	36(1)
C(27)	3126(2)	816(2)	2258(1)	29(1)
C(28)	2816(2)	341(2)	2955(1)	23(1)
C(29)	2047(2)	-790(2)	2604(1)	30(1)
C(30)	1468(2)	-1222(2)	3256(2)	37(1)
C(31)	405(2)	-987(2)	3440(2)	41(1)
C(32)	537(2)	134(2)	3945(2)	39(1)
C(33)	4941(2)	8000(2)	10650(1)	21(1)
C(34)	3719(2)	7785(2)	10625(1)	22(1)
C(35)	3228(2)	8394(2)	10366(1)	24(1)
C(36)	2103(2)	8204(2)	10322(1)	26(1)
C(37)	1434(2)	7396(2)	10544(1)	30(1)
C(38)	1912(2)	6777(2)	10803(2)	34(1)
C(39)	3036(2)	6966(2)	10836(2)	29(1)
C(40)	-467(2)	7368(2)	9969(2)	39(1)
C(41)	-336(3)	8543(3)	10256(2)	55(1)
C(42)	-1644(2)	6781(3)	10028(2)	57(1)
C(43)	-208(2)	7027(2)	9079(2)	42(1)
C(44)	5258(12)	7249(11)	9991(8)	22(2)
C(45)	5226(5)	7258(4)	9164(4)	30(1)
C(46)	5380(6)	6474(5)	8481(4)	35(1)
C(47)	5595(5)	5663(5)	8636(4)	27(1)
C(48)	5646(4)	5629(3)	9461(3)	25(1)
C(49)	5479(4)	6406(4)	10103(4)	24(1)
C(50)	6337(7)	4755(5)	7283(5)	25(2)
C(51)	7295(12)	4484(14)	7591(11)	118(7)
C(52)	6949(9)	5803(5)	7217(5)	89(3)
C(53)	5710(8)	3930(8)	6461(5)	92(3)
O(4)	5265(5)	3899(3)	8113(3)	65(1)
N(4)	5666(4)	4775(3)	7983(3)	43(1)
C(44A)	5192(11)	7357(10)	9795(6)	16(2)
C(45A)	5540(4)	6550(4)	9738(3)	21(1)
C(46A)	5760(5)	5968(4)	8971(4)	21(1)
C(47A)	5635(4)	6219(4)	8254(3)	20(1)
C(48A)	5238(4)	7035(3)	8310(3)	25(1)
C(49A)	5023(4)	7589(4)	9074(3)	25(1)
C(50A)	6096(6)	4724(6)	7170(4)	18(2)
C(51A)	6170(5)	4395(4)	6230(3)	36(1)
C(52A)	5178(4)	3901(3)	7373(3)	32(1)
C(53A)	7215(7)	4849(6)	7609(5)	37(2)
N(4A)	5897(3)	5725(3)	7451(2)	25(1)
O(4A)	5963(4)	6181(3)	6907(2)	46(1)
C(54)	5685(2)	8736(2)	11291(1)	20(1)
C(55)	5297(2)	9312(2)	12080(1)	25(1)
C(56)	5216(2)	8760(2)	12730(1)	33(1)
C(57)	6304(2)	8757(2)	13121(2)	37(1)
C(58)	7051(2)	8376(2)	12509(2)	34(1)
C(59)	7605(2)	9107(2)	12042(1)	27(1)
C(60)	6911(2)	8985(2)	11239(1)	22(1)
C(61)	7358(2)	9914(2)	10932(1)	27(1)
C(62)	7389(2)	10967(2)	11527(2)	32(1)
C(63)	6298(2)	11031(2)	11842(2)	34(1)
C(64)	5937(2)	10474(2)	12469(1)	30(1)

N(1)	7698(2)	2039(2)	4662(1)	31(1)		
N(2)	2485(2)	5058(1)	6993(1)	31(1)		
N(3)	282(2)	7207(2)	10561(1)	44(1)		
O(1)	7820(2)	1195(2)	4687(1)	50(1)		
O(2)	2902(3)	5956(2)	6937(1)	72(1)		
O(3)	-151(2)	6794(3)	11082(2)	100(1)		

Table S3. Bond lengths [A] and angles [deg] for rfbis (**1(PhNit₂)**).

C(1)-C(22)	1.342(3)	C(36)-C(37)	1.384(3)
C(1)-C(2)	1.499(3)	C(37)-C(38)	1.397(4)
C(1)-C(12)	1.500(3)	C(37)-N(3)	1.423(3)
C(2)-C(3)	1.393(3)	C(38)-C(39)	1.381(3)
C(2)-C(7)	1.403(3)	C(40)-N(3)	1.491(3)
C(3)-C(4)	1.389(3)	C(40)-C(43)	1.506(4)
C(4)-C(5)	1.398(3)	C(40)-C(42)	1.510(4)
C(5)-C(6)	1.390(3)	C(40)-C(41)	1.567(4)
C(5)-N(1)	1.422(3)	C(44)-C(45)	1.399(9)
C(6)-C(7)	1.385(3)	C(44)-C(49)	1.402(13)
C(8)-N(1)	1.504(3)	C(45)-C(46)	1.407(9)
C(8)-C(11)	1.523(4)	C(46)-C(47)	1.384(9)
C(8)-C(10)	1.527(3)	C(47)-C(48)	1.409(7)
C(8)-C(9)	1.528(3)	C(47)-N(4)	1.436(7)
C(12)-C(17)	1.393(3)	C(48)-C(49)	1.371(6)
C(12)-C(13)	1.399(3)	C(50)-N(4)	1.478(9)
C(13)-C(14)	1.383(3)	C(50)-C(53)	1.517(5)
C(14)-C(15)	1.402(3)	C(50)-C(52)	1.519(5)
C(15)-C(16)	1.397(3)	C(50)-C(51)	1.530(5)
C(15)-N(2)	1.416(3)	O(4)-N(4)	1.302(6)
C(16)-C(17)	1.386(3)	C(44A)-C(45A)	1.354(14)
C(18)-N(2)	1.507(3)	C(44A)-C(49A)	1.389(8)
C(18)-C(19)	1.519(3)	C(45A)-C(46A)	1.395(7)
C(18)-C(21)	1.523(3)	C(46A)-C(47A)	1.388(8)
C(18)-C(20)	1.530(3)	C(47A)-C(48A)	1.405(6)
C(22)-C(23)	1.516(3)	C(47A)-N(4A)	1.423(6)
C(22)-C(28)	1.523(3)	C(48A)-C(49A)	1.373(6)
C(23)-C(24)	1.538(3)	C(50A)-N(4A)	1.482(10)
C(23)-C(32)	1.539(3)	C(50A)-C(51A)	1.521(5)
C(24)-C(25)	1.525(4)	C(50A)-C(52A)	1.528(5)
C(25)-C(26)	1.532(4)	C(50A)-C(53A)	1.534(5)
C(26)-C(27)	1.521(3)	N(4A)-O(4A)	1.279(5)
C(27)-C(28)	1.543(3)	C(54)-C(60)	1.516(3)
C(28)-C(29)	1.537(3)	C(54)-C(55)	1.520(3)
C(29)-C(30)	1.531(3)	C(55)-C(64)	1.533(3)
C(30)-C(31)	1.525(4)	C(55)-C(56)	1.537(3)
C(31)-C(32)	1.529(4)	C(56)-C(57)	1.534(3)
C(33)-C(54)	1.344(3)	C(57)-C(58)	1.521(4)
C(33)-C(44)	1.456(17)	C(58)-C(59)	1.528(3)
C(33)-C(34)	1.500(3)	C(59)-C(60)	1.534(3)
C(33)-C(44A)	1.554(13)	C(60)-C(61)	1.545(3)
C(34)-C(39)	1.392(3)	C(61)-C(62)	1.526(3)
C(34)-C(35)	1.395(3)	C(62)-C(63)	1.532(3)
C(35)-C(36)	1.382(3)	C(63)-C(64)	1.522(3)

N(1)-O(1)	1.293(3)	C(30)-C(31)-C(32)	116.4(2)
N(2)-O(2)	1.278(3)	C(31)-C(32)-C(23)	117.1(2)
N(3)-O(3)	1.261(3)	C(54)-C(33)-C(44)	121.4(6)
C(22)-C(1)-C(2)	122.81(18)	C(54)-C(33)-C(34)	123.15(18)
C(22)-C(1)-C(12)	124.57(18)	C(44)-C(33)-C(34)	114.8(6)
C(2)-C(1)-C(12)	112.62(17)	C(54)-C(33)-C(44A)	126.6(5)
C(3)-C(2)-C(7)	117.80(19)	C(44)-C(33)-C(44A)	15.8(5)
C(3)-C(2)-C(1)	122.34(18)	C(34)-C(33)-C(44A)	109.8(5)
C(7)-C(2)-C(1)	119.85(18)	C(39)-C(34)-C(35)	117.7(2)
C(4)-C(3)-C(2)	121.61(19)	C(39)-C(34)-C(33)	121.84(19)
C(3)-C(4)-C(5)	119.68(19)	C(35)-C(34)-C(33)	120.40(18)
C(6)-C(5)-C(4)	119.5(2)	C(36)-C(35)-C(34)	121.8(2)
C(6)-C(5)-N(1)	118.0(2)	C(35)-C(36)-C(37)	120.0(2)
C(4)-C(5)-N(1)	122.4(2)	C(36)-C(37)-C(38)	119.0(2)
C(7)-C(6)-C(5)	120.3(2)	C(36)-C(37)-N(3)	122.2(2)
C(6)-C(7)-C(2)	121.1(2)	C(38)-C(37)-N(3)	118.7(2)
N(1)-C(8)-C(11)	109.2(2)	C(39)-C(38)-C(37)	120.5(2)
N(1)-C(8)-C(10)	106.8(2)	C(38)-C(39)-C(34)	121.0(2)
C(11)-C(8)-C(10)	109.4(2)	N(3)-C(40)-C(43)	111.4(2)
N(1)-C(8)-C(9)	110.20(18)	N(3)-C(40)-C(42)	108.3(2)
C(11)-C(8)-C(9)	112.6(2)	C(43)-C(40)-C(42)	111.3(2)
C(10)-C(8)-C(9)	108.5(2)	N(3)-C(40)-C(41)	109.1(2)
C(17)-C(12)-C(13)	117.36(18)	C(43)-C(40)-C(41)	109.2(2)
C(17)-C(12)-C(1)	122.32(18)	C(42)-C(40)-C(41)	107.5(2)
C(13)-C(12)-C(1)	120.22(18)	C(45)-C(44)-C(49)	115.3(12)
C(14)-C(13)-C(12)	121.7(2)	C(45)-C(44)-C(33)	120.8(9)
C(13)-C(14)-C(15)	120.4(2)	C(49)-C(44)-C(33)	123.5(7)
C(16)-C(15)-C(14)	118.36(19)	C(44)-C(45)-C(46)	123.3(9)
C(16)-C(15)-N(2)	124.11(19)	C(47)-C(46)-C(45)	118.5(6)
C(14)-C(15)-N(2)	117.53(19)	C(46)-C(47)-C(48)	120.1(5)
C(17)-C(16)-C(15)	120.49(19)	C(46)-C(47)-N(4)	123.5(6)
C(16)-C(17)-C(12)	121.71(19)	C(48)-C(47)-N(4)	116.0(5)
N(2)-C(18)-C(19)	107.02(18)	C(49)-C(48)-C(47)	119.1(5)
N(2)-C(18)-C(21)	109.63(19)	C(48)-C(49)-C(44)	123.7(7)
C(19)-C(18)-C(21)	109.11(19)	N(4)-C(50)-C(53)	112.0(7)
N(2)-C(18)-C(20)	110.14(18)	N(4)-C(50)-C(52)	115.3(6)
C(19)-C(18)-C(20)	108.11(19)	C(53)-C(50)-C(52)	114.9(8)
C(21)-C(18)-C(20)	112.66(19)	N(4)-C(50)-C(51)	101.8(8)
C(1)-C(22)-C(23)	120.87(18)	C(53)-C(50)-C(51)	110.4(10)
C(1)-C(22)-C(28)	119.76(18)	C(52)-C(50)-C(51)	100.9(9)
C(23)-C(22)-C(28)	119.29(17)	O(4)-N(4)-C(47)	115.5(4)
C(22)-C(23)-C(24)	114.35(18)	O(4)-N(4)-C(50)	115.3(5)
C(22)-C(23)-C(32)	112.1(2)	C(47)-N(4)-C(50)	127.8(5)
C(24)-C(23)-C(32)	112.0(2)	C(45A)-C(44A)-C(49A)	119.5(9)
C(25)-C(24)-C(23)	115.3(2)	C(45A)-C(44A)-C(33)	120.7(5)
C(24)-C(25)-C(26)	114.2(2)	C(49A)-C(44A)-C(33)	119.8(9)
C(27)-C(26)-C(25)	116.8(2)	C(44A)-C(45A)-C(46A)	120.8(6)
C(26)-C(27)-C(28)	117.36(19)	C(47A)-C(46A)-C(45A)	120.1(5)
C(22)-C(28)-C(29)	116.14(17)	C(46A)-C(47A)-C(48A)	118.9(5)
C(22)-C(28)-C(27)	109.71(17)	C(46A)-C(47A)-N(4A)	125.2(5)
C(29)-C(28)-C(27)	112.61(18)	C(48A)-C(47A)-N(4A)	115.9(4)
C(30)-C(29)-C(28)	115.24(19)	C(49A)-C(48A)-C(47A)	119.6(5)
C(31)-C(30)-C(29)	113.9(2)	C(48A)-C(49A)-C(44A)	121.1(7)

N(4A)-C(50A)-C(51A)	109.7(5)	C(58)-C(59)-C(60)	115.11(18)
N(4A)-C(50A)-C(52A)	110.4(6)	C(54)-C(60)-C(59)	114.54(17)
C(51A)-C(50A)-C(52A)	110.7(5)	C(54)-C(60)-C(61)	110.68(17)
N(4A)-C(50A)-C(53A)	109.9(5)	C(59)-C(60)-C(61)	112.72(18)
C(51A)-C(50A)-C(53A)	106.4(6)	C(62)-C(61)-C(60)	117.08(18)
C(52A)-C(50A)-C(53A)	109.7(6)	C(61)-C(62)-C(63)	116.3(2)
O(4A)-N(4A)-C(47A)	117.3(4)	C(64)-C(63)-C(62)	114.0(2)
O(4A)-N(4A)-C(50A)	116.0(4)	C(63)-C(64)-C(55)	115.54(18)
C(47A)-N(4A)-C(50A)	126.7(4)	O(1)-N(1)-C(5)	116.7(2)
C(33)-C(54)-C(60)	120.51(18)	O(1)-N(1)-C(8)	117.39(19)
C(33)-C(54)-C(55)	119.88(18)	C(5)-N(1)-C(8)	125.91(19)
C(60)-C(54)-C(55)	119.60(17)	O(2)-N(2)-C(15)	116.90(18)
C(54)-C(55)-C(64)	115.80(18)	O(2)-N(2)-C(18)	117.00(18)
C(54)-C(55)-C(56)	110.35(18)	C(15)-N(2)-C(18)	126.10(17)
C(64)-C(55)-C(56)	112.25(18)	O(3)-N(3)-C(37)	116.7(2)
C(57)-C(56)-C(55)	116.70(19)	O(3)-N(3)-C(40)	117.4(2)
C(58)-C(57)-C(56)	116.6(2)	C(37)-N(3)-C(40)	125.7(2)
C(57)-C(58)-C(59)	114.5(2)		

_____

Symmetry transformations used to generate equivalent atoms:

Table S4. Anisotropic displacement parameters (A^2 x 10^3) for rfbis (**1(PhNit$_2$)**). The anisotropic displacement factor exponent takes the form: $-2 \pi^2$ [$h^2 a^{*2} U11 + ... + 2 h k a^* b^* U12$]

_____

	U11	U22	U33	U23	U13	U12
C(1)	21(1)	19(1)	20(1)	4(1)	7(1)	7(1)
C(2)	21(1)	19(1)	16(1)	1(1)	2(1)	7(1)
C(3)	22(1)	20(1)	19(1)	3(1)	2(1)	7(1)
C(4)	21(1)	22(1)	20(1)	3(1)	2(1)	5(1)
C(5)	24(1)	23(1)	19(1)	-2(1)	-2(1)	10(1)
C(6)	32(1)	26(1)	22(1)	5(1)	-1(1)	14(1)
C(7)	29(1)	22(1)	22(1)	6(1)	4(1)	9(1)
C(8)	20(1)	41(1)	27(1)	2(1)	2(1)	12(1)
C(9)	26(1)	36(1)	40(1)	0(1)	4(1)	5(1)
C(10)	26(1)	62(2)	38(1)	1(1)	-4(1)	19(1)
C(11)	34(1)	68(2)	31(1)	6(1)	7(1)	19(1)
C(12)	21(1)	20(1)	20(1)	3(1)	4(1)	9(1)
C(13)	38(1)	24(1)	28(1)	10(1)	17(1)	12(1)
C(14)	39(1)	21(1)	31(1)	9(1)	15(1)	12(1)
C(15)	27(1)	22(1)	21(1)	5(1)	8(1)	12(1)
C(16)	26(1)	23(1)	19(1)	6(1)	7(1)	9(1)
C(17)	21(1)	20(1)	21(1)	5(1)	3(1)	7(1)
C(18)	26(1)	25(1)	20(1)	2(1)	8(1)	10(1)
C(19)	47(2)	29(1)	28(1)	0(1)	12(1)	16(1)
C(20)	31(1)	38(1)	27(1)	7(1)	2(1)	13(1)
C(21)	26(1)	41(1)	35(1)	6(1)	3(1)	11(1)
C(22)	20(1)	20(1)	22(1)	4(1)	6(1)	6(1)
C(23)	19(1)	27(1)	29(1)	0(1)	5(1)	6(1)
C(24)	23(1)	39(1)	38(1)	1(1)	-1(1)	14(1)
C(25)	42(2)	40(1)	40(1)	12(1)	-1(1)	20(1)
C(26)	36(1)	39(1)	28(1)	10(1)	2(1)	11(1)
C(27)	26(1)	33(1)	25(1)	6(1)	8(1)	9(1)

C(28)	20(1)	22(1)	21(1)	-1(1)	4(1)	8(1)
C(29)	31(1)	23(1)	27(1)	-1(1)	3(1)	8(1)
C(30)	42(1)	25(1)	38(1)	8(1)	7(1)	6(1)
C(31)	32(1)	31(1)	45(2)	6(1)	12(1)	-3(1)
C(32)	27(1)	36(1)	41(1)	4(1)	16(1)	1(1)
C(33)	19(1)	20(1)	23(1)	6(1)	6(1)	8(1)
C(34)	20(1)	22(1)	17(1)	1(1)	4(1)	5(1)
C(35)	22(1)	25(1)	20(1)	3(1)	4(1)	7(1)
C(36)	23(1)	37(1)	19(1)	6(1)	4(1)	13(1)
C(37)	18(1)	46(1)	20(1)	7(1)	4(1)	7(1)
C(38)	25(1)	39(1)	33(1)	16(1)	6(1)	1(1)
C(39)	27(1)	30(1)	31(1)	11(1)	5(1)	7(1)
C(40)	21(1)	61(2)	31(1)	9(1)	4(1)	14(1)
C(41)	38(2)	58(2)	52(2)	-4(2)	6(1)	17(1)
C(42)	23(1)	84(2)	57(2)	20(2)	6(1)	13(1)
C(43)	33(1)	57(2)	31(1)	8(1)	0(1)	16(1)
C(44)	19(3)	29(4)	9(5)	2(3)	1(3)	2(2)
C(45)	43(3)	21(3)	30(3)	9(2)	5(2)	15(2)
C(46)	51(4)	32(3)	26(3)	9(3)	7(3)	19(3)
C(47)	33(3)	25(3)	17(3)	1(2)	5(3)	6(2)
C(48)	28(2)	24(2)	27(2)	11(2)	7(2)	11(2)
C(49)	29(2)	23(2)	23(2)	7(2)	8(2)	13(2)
C(50)	22(4)	28(3)	19(3)	0(2)	2(3)	8(2)
C(51)	57(6)	240(20)	97(9)	96(12)	28(6)	68(10)
C(52)	140(8)	45(4)	61(5)	16(3)	50(5)	3(4)
C(53)	79(7)	111(8)	51(5)	-23(5)	-10(4)	36(6)
O(4)	107(4)	26(2)	58(3)	13(2)	41(3)	18(2)
N(4)	71(3)	26(2)	35(2)	9(2)	22(2)	20(2)
C(44A)	16(3)	21(3)	5(5)	1(3)	3(3)	2(2)
C(45A)	23(2)	23(2)	18(2)	7(2)	3(2)	8(2)
C(46A)	24(2)	21(3)	18(3)	2(2)	-1(2)	10(2)
C(47A)	19(2)	19(2)	24(3)	5(2)	7(2)	9(2)
C(48A)	34(2)	26(2)	21(2)	10(2)	8(2)	14(2)
C(49A)	36(3)	23(3)	22(2)	8(2)	8(2)	17(2)
C(50A)	10(3)	23(3)	19(3)	0(2)	-5(2)	10(2)
C(51A)	48(3)	35(3)	28(3)	5(2)	13(2)	21(2)
C(52A)	30(2)	23(2)	36(3)	3(2)	5(2)	7(2)
C(53A)	24(3)	53(3)	26(3)	1(3)	-1(2)	13(3)
N(4A)	33(2)	23(2)	19(2)	6(1)	8(2)	12(2)
O(4A)	83(3)	43(2)	30(2)	21(2)	28(2)	36(2)
C(54)	21(1)	23(1)	20(1)	7(1)	5(1)	11(1)
C(55)	21(1)	33(1)	18(1)	2(1)	3(1)	11(1)
C(56)	25(1)	49(1)	23(1)	12(1)	9(1)	10(1)
C(57)	31(1)	58(2)	24(1)	18(1)	4(1)	13(1)
C(58)	29(1)	44(1)	34(1)	20(1)	3(1)	15(1)
C(59)	20(1)	36(1)	27(1)	10(1)	3(1)	11(1)
C(60)	19(1)	25(1)	21(1)	5(1)	5(1)	9(1)
C(61)	29(1)	27(1)	22(1)	7(1)	9(1)	7(1)
C(62)	33(1)	24(1)	30(1)	5(1)	6(1)	5(1)
C(63)	38(1)	26(1)	32(1)	1(1)	0(1)	13(1)
C(64)	28(1)	31(1)	23(1)	-2(1)	4(1)	13(1)
N(1)	25(1)	31(1)	32(1)	1(1)	-3(1)	14(1)
N(2)	49(1)	20(1)	26(1)	6(1)	17(1)	14(1)

N(3)	20(1)	78(2)	36(1)	28(1)	9(1)	9(1)
O(1)	43(1)	41(1)	68(1)	10(1)	-6(1)	25(1)
O(2)	144(2)	25(1)	52(1)	16(1)	58(2)	31(1)
O(3)	37(1)	197(4)	103(2)	112(3)	27(1)	28(2)

Table S5. Hydrogen coordinates (x 10^4) and isotropic displacement parameters (A^2 x 10^3) for rfbis (**1(PhNit₂)**).

x y z   U(eq)

	x	y	z	U(eq)		x	y	z	U(eq)
H(3A)	4965	2999	3851	25	H(36A)	1789	8627	10139	32
H(4A)	6813	3122	4010	27	H(38A)	1460	6221	10958	41
H(6A)	6021	972	5162	32	H(39A)	3347	6532	11005	35
H(7A)	4181	863	5008	30	H(41A)	-327	8808	10868	83
H(9A)	8102	4121	4953	58	H(41B)	-957	8629	9974	83
H(9B)	9360	4486	5366	58	H(41C)	358	8926	10106	83
H(9C)	8390	3883	5780	58	H(42A)	-1746	6044	9870	86
H(10A)	9556	2742	5679	68	H(42B)	-2150	6882	9645	86
H(10B)	10373	3284	5133	68	H(42C)	-1799	7038	10607	86
H(10C)	9731	2064	4772	68	H(43A)	535	7463	9050	63
H(11A)	8942	2207	3471	70	H(43B)	-748	7093	8699	63
H(11B)	9612	3422	3820	70	H(43C)	-242	6305	8910	63
H(11C)	8305	3013	3543	70	H(45A)	5094	7821	9059	36
H(13A)	3592	3804	4539	35	H(46A)	5337	6501	7927	42
H(14A)	3339	5117	5644	35	H(48A)	5795	5075	9570	30
H(16A)	1861	3029	6758	27	H(49A)	5514	6372	10656	29
H(17A)	2151	1731	5658	25	H(51A)	7009	3803	7654	177
H(19A)	2814	6528	8430	55	H(51B)	7670	5005	8136	177
H(19B)	1720	6087	8816	55	H(51C)	7819	4469	7179	177
H(19C)	1631	6365	7977	55	H(52A)	6419	6077	7028	133
H(20A)	2520	3884	7946	49	H(52B)	7474	5730	6809	133
H(20B)	2199	4562	8790	49	H(52C)	7350	6280	7770	133
H(20C)	3322	5037	8449	49	H(53A)	5107	4119	6267	139
H(21A)	379	4614	7139	54	H(53B)	5405	3265	6549	139
H(21B)	350	4367	8000	54	H(53C)	6212	3872	6035	139
H(21C)	654	3626	7183	54	H(45B)	5635	6378	10227	26
H(23A)	1198	1642	4000	33	H(46B)	5996	5399	8939	26
H(24A)	451	110	2384	43	H(48B)	5119	7202	7822	30
H(24B)	40	1064	2806	43	H(49B)	4754	8140	9111	30
H(25A)	1929	2137	2672	48	H(51D)	6768	4927	6113	55
H(25B)	994	1614	1871	48	H(51E)	5470	4303	5921	55
H(26A)	1724	219	1393	43	H(51F)	6319	3741	6050	55
H(26B)	2529	1300	1377	43	H(52D)	4466	3817	7085	48
H(27A)	3867	1035	2148	35	H(52E)	5162	4114	7983	48
H(28A)	3521	327	3207	27	H(52F)	5318	3242	7180	48
H(29A)	1476	-853	2167	35	H(53D)	7801	5383	7483	56
H(29B)	2484	-1225	2324	35	H(53E)	7356	4191	7405	56
H(30A)	1295	-1980	3052	44	H(53F)	7205	5051	8220	56
H(30B)	1983	-930	3789	44	H(55A)	4524	9251	11904	30
H(31A)	-301	-1509	3251	50	H(56A)	4526	8435	12883	40
H(32A)	209	307	4445	47	H(57A)	6501	8982	13714	45
H(35A)	3679	8955	10217	28	H(58A)	6609	7700	12089	40

H(58B)	7632	8265	12826	40	H(62A)	8047	11550	11693	38
H(59A)	8305	8995	11890	33	H(63A)	6375	11768	12112	41
H(59B)	7794	9827	12432	33	H(63B)	5712	10733	11352	41
H(60A)	6989	8376	10789	27	H(64A)	5469	10806	12831	35
H(61A)	7602	9834	10395	33	H(64B)	6602	10572	12837	35

Brown needles of **notbu1** (**2(PhNit₂)**) were crystallized from a heptane/dichloromethane solution at 25 deg. C. A crystal of dimensions 0.44 x 0.02 x 0.02 mm was mounted on a standard Bruker SMART CCD-based X-ray diffractometer equipped with a LT-2 low temperature device and normal focus Mo-target X-ray tube (λ = 0.71073 A) operated at 2000 W power (50 kV, 40 mA). The X-ray intensities were measured at 158(2) K; the detector was placed at a distance 4.959 cm from the crystal. A total of 2242 frames were collected with a scan width of 0.3° in ω and phi with an exposure time of 60 s/frame. The frames were integrated with the Bruker SAINT software package with a narrow frame algorithm. The integration of the data yielded a total of 12963 reflections to a maximum 2θ value of 47.92° of which 4193 were independent and 2142 were greater than 2σ(I). The final cell constants (Table 1) were based on the xyz centroids of 1486 reflections above 10σ(I). Analysis of the data showed negligible decay during data collection; the data were processed with SADABS, no correction for absorption was necessary. The structure was solved and refined with the Bruker SHELXTL (version 5.10) software package, using the space group P1bar with Z = 2 for the formula $C_{30}H_{44}N_2O_2$. All non-hydrogen atoms were refined anisotropically with the hydrogen atoms placed in idealized positions. Full matrix least-squares refinement based on F^2 converged at R1 = 0.0544 and wR2 = 0.1252 [based on I > 2sigma(I)], R1 = 0.1127 and wR2 = 0.1303 for all data. Additional details are presented in Table 1 and are given as Supporting Information as a CIF file.

Sheldrick, G.M. SHELXTL, v. 5.10; Bruker Analytical X-ray, Madison, WI, 1997.
Sheldrick, G.M. SADABS. Program for Empirical Absorption Correction of Area Detector Data, University of Gottingen: Gottingen, Germany, 1996.
Saint Plus, v. 6.02, Bruker Analytical X-ray, Madison, WI, 1999.

Table S6. Crystal data and structure refinement for notbu1 (**2(PhNit₂)**).

Identification code	notbu1
Empirical formula	C30 H44 N2 O2
Formula weight	464.67
Temperature	158(2) K
Wavelength	0.71073 A
Crystal system, space group	Triclinic, P-1
Unit cell dimensions	a = 6.1904(11) A alpha = 85.858(8) deg.
	b = 12.730(3) A beta = 80.307(8) deg.
	c = 17.528(4) A gamma = 83.199(9) deg.
Volume	1350.0(4) A^3
Z, Calculated density	2, 1.143 Mg/m^3
Absorption coefficient	0.071 mm^-1
F(000)	508
Crystal size	0.44 x 0.02 x 0.02 mm
Theta range for data collection	1.95 to 23.96 deg.
Limiting indices	-6<=h<=7, -14<=k<=14, 0<=l<=20
Reflections collected / unique	12963 / 4193 [R(int) = 0.0656]
Completeness to theta =	23.96, 99.6 %
Absorption correction	None
Refinement method	Full-matrix least-squares on F^2
Data / restraints / parameters	4193 / 0 / 321
Goodness-of-fit on F^2	0.958

Final R indices [I>2sigma(I)]	R1 = 0.0544, wR2 = 0.1127
R indices (all data)	R1 = 0.1252, wR2 = 0.1303
Extinction coefficient	0.027(2)
Largest diff. peak and hole	0.195 and -0.208 e.A^-3

Table S7. Atomic coordinates (x 10^4) and equivalent isotropic displacement parameters (A^2 x 10^3) for notbu1. (**2(PhNit₂)**)
U(eq) is defined as one third of the trace of the orthogonalized
Uij tensor.

	x	y	z	U(eq)		x	y	z	U(eq)
O(1)	7482(4)	4206(2)	3830(1)	36(1)	C(15)	725(5)	7061(2)	21(2)	21(1)
O(2)	-2024(4)	6857(2)	-671(1)	40(1)	C(16)	2790(5)	6767(2)	235(2)	24(1)
N(1)	5397(4)	4279(2)	3814(1)	25(1)	C(17)	3253(5)	7089(2)	917(2)	24(1)
N(2)	53(4)	6719(2)	-644(1)	24(1)	C(18)	1516(5)	6167(2)	-1305(2)	23(1)
C(1)	4118(5)	3426(2)	4260(2)	26(1)	C(19)	2140(6)	5019(3)	-1055(2)	43(1)
C(2)	2091(5)	3934(3)	4766(2)	32(1)	C(20)	176(5)	6200(3)	-1961(2)	40(1)
C(3)	5626(6)	2797(3)	4769(2)	40(1)	C(21)	3549(5)	6749(3)	-1598(2)	32(1)
C(4)	3563(6)	2691(3)	3690(2)	39(1)	C(22)	1897(5)	9044(3)	2408(2)	22(1)
C(5)	4485(5)	5199(2)	3423(2)	22(1)	C(23)	2111(5)	10001(2)	1797(2)	25(1)
C(6)	5742(5)	6054(2)	3267(2)	24(1)	C(24)	3507(5)	9696(3)	1009(2)	32(1)
C(7)	4952(5)	6961(2)	2878(2)	23(1)	C(25)	-66(5)	10575(3)	1607(2)	35(1)
C(8)	2924(5)	7063(2)	2630(2)	21(1)	C(26)	3434(5)	10839(2)	2053(2)	34(1)
C(9)	1751(5)	6179(3)	2754(2)	26(1)	C(27)	1351(5)	9264(2)	3290(2)	25(1)
C(10)	2470(5)	5267(2)	3161(2)	24(1)	C(28)	320(5)	8336(3)	3790(2)	35(1)
C(11)	2151(5)	8036(2)	2168(2)	20(1)	C(29)	-464(5)	10206(3)	3448(2)	35(1)
C(12)	1711(5)	7728(2)	1410(2)	20(1)	C(30)	3351(5)	9468(3)	3656(2)	35(1)
C(13)	-357(5)	7996(2)	1194(2)	22(1)					
C(14)	-848(5)	7679(2)	517(2)	23(1)					

Table S8. Bond lengths [A] and angles [deg] for notbu1 (**2(PhNit₂)**).

O(1)-N(1)	1.288(3)	C(12)-C(17)	1.401(4)
O(2)-N(2)	1.285(3)	C(13)-C(14)	1.372(4)
N(1)-C(5)	1.421(4)	C(14)-C(15)	1.399(4)
N(1)-C(1)	1.513(4)	C(15)-C(16)	1.394(4)
N(2)-C(15)	1.413(4)	C(16)-C(17)	1.376(4)
N(2)-C(18)	1.506(4)	C(18)-C(19)	1.519(4)
C(1)-C(2)	1.515(4)	C(18)-C(20)	1.523(4)
C(1)-C(3)	1.520(4)	C(18)-C(21)	1.532(4)
C(1)-C(4)	1.522(4)	C(22)-C(23)	1.566(4)
C(5)-C(10)	1.391(4)	C(22)-C(27)	1.565(4)
C(5)-C(6)	1.396(4)	C(23)-C(25)	1.531(4)
C(6)-C(7)	1.380(4)	C(23)-C(24)	1.550(4)
C(7)-C(8)	1.385(4)	C(23)-C(26)	1.552(4)
C(8)-C(9)	1.395(4)	C(27)-C(30)	1.543(4)
C(8)-C(11)	1.504(4)	C(27)-C(29)	1.549(4)
C(9)-C(10)	1.384(4)	C(27)-C(28)	1.553(4)
C(11)-C(22)	1.361(4)	O(1)-N(1)-C(5)	116.5(2)
C(11)-C(12)	1.488(4)	O(1)-N(1)-C(1)	117.4(2)
C(12)-C(13)	1.393(4)	C(5)-N(1)-C(1)	125.9(3)

O(2)-N(2)-C(15)	116.6(2)		C(16)-C(15)-C(14)	118.4(3)
O(2)-N(2)-C(18)	116.9(2)		C(16)-C(15)-N(2)	124.3(3)
C(15)-N(2)-C(18)	126.5(3)		C(14)-C(15)-N(2)	117.2(3)
N(1)-C(1)-C(2)	109.6(3)		C(17)-C(16)-C(15)	120.2(3)
N(1)-C(1)-C(3)	107.0(3)		C(16)-C(17)-C(12)	122.0(3)
C(2)-C(1)-C(3)	109.4(3)		N(2)-C(18)-C(19)	109.7(3)
N(1)-C(1)-C(4)	109.1(2)		N(2)-C(18)-C(20)	106.9(2)
C(2)-C(1)-C(4)	112.8(3)		C(19)-C(18)-C(20)	109.0(3)
C(3)-C(1)-C(4)	108.8(3)		N(2)-C(18)-C(21)	111.0(2)
C(10)-C(5)-C(6)	119.1(3)		C(19)-C(18)-C(21)	111.9(3)
C(10)-C(5)-N(1)	123.3(3)		C(20)-C(18)-C(21)	108.0(2)
C(6)-C(5)-N(1)	117.5(3)		C(11)-C(22)-C(23)	120.0(3)
C(7)-C(6)-C(5)	120.0(3)		C(11)-C(22)-C(27)	120.9(3)
C(6)-C(7)-C(8)	122.2(3)		C(23)-C(22)-C(27)	119.1(3)
C(7)-C(8)-C(9)	116.8(3)		C(25)-C(23)-C(24)	105.9(3)
C(7)-C(8)-C(11)	121.2(3)		C(25)-C(23)-C(26)	107.7(3)
C(9)-C(8)-C(11)	121.6(3)		C(24)-C(23)-C(26)	102.0(3)
C(10)-C(9)-C(8)	122.3(3)		C(25)-C(23)-C(22)	115.6(3)
C(9)-C(10)-C(5)	119.5(3)		C(24)-C(23)-C(22)	113.3(2)
C(22)-C(11)-C(12)	125.3(3)		C(26)-C(23)-C(22)	111.3(3)
C(22)-C(11)-C(8)	125.2(3)		C(30)-C(27)-C(29)	108.7(3)
C(12)-C(11)-C(8)	109.6(3)		C(30)-C(27)-C(28)	105.8(3)
C(13)-C(12)-C(17)	116.9(3)		C(29)-C(27)-C(28)	102.8(2)
C(13)-C(12)-C(11)	120.4(3)		C(30)-C(27)-C(22)	114.6(2)
C(17)-C(12)-C(11)	122.5(3)		C(29)-C(27)-C(22)	111.6(2)
C(14)-C(13)-C(12)	121.8(3)		C(28)-C(27)-C(22)	112.6(2)
C(13)-C(14)-C(15)	120.7(3)			

Symmetry transformations used to generate equivalent atoms:

Table S9. Anisotropic displacement parameters (A^2 x 10^3) for notbu1 (**2(PhNit₂)**). The anisotropic displacement factor exponent takes the form: $-2\pi^2 [h^2 a^{*2} U11 + ... + 2 h k a^* b^* U12]$

	U11	U22	U33	U23	U13	U12
O(1)	27(2)	36(2)	45(2)	3(1)	-14(1)	1(1)
O(2)	18(2)	66(2)	39(1)	-18(1)	-9(1)	2(1)
N(1)	25(2)	26(2)	24(2)	-1(1)	-9(1)	0(1)
N(2)	18(2)	30(2)	25(2)	-4(1)	-4(1)	-1(1)
C(1)	30(2)	23(2)	23(2)	2(2)	-3(2)	-3(2)
C(2)	33(2)	39(2)	24(2)	4(2)	-4(2)	-2(2)
C(3)	42(2)	36(2)	38(2)	11(2)	-6(2)	3(2)
C(4)	55(3)	23(2)	39(2)	3(2)	-7(2)	-10(2)
C(5)	26(2)	22(2)	16(2)	-2(2)	-4(2)	2(2)
C(6)	22(2)	29(2)	23(2)	-2(2)	-7(2)	-3(2)
C(7)	24(2)	23(2)	23(2)	-2(2)	-2(2)	-5(2)
C(8)	22(2)	20(2)	21(2)	-4(2)	-4(2)	1(2)
C(9)	26(2)	29(2)	27(2)	-7(2)	-7(2)	-5(2)
C(10)	25(2)	24(2)	24(2)	-1(2)	-7(2)	-6(2)
C(11)	13(2)	25(2)	22(2)	1(2)	-2(1)	-3(2)
C(12)	24(2)	17(2)	19(2)	0(1)	-4(2)	-1(2)
C(13)	19(2)	22(2)	24(2)	3(2)	0(2)	-2(2)

C(14)	19(2)	23(2)	29(2)	1(2)	-6(2)	-3(2)
C(15)	20(2)	21(2)	20(2)	1(2)	-3(2)	-3(2)
C(16)	25(2)	24(2)	24(2)	-3(2)	-6(2)	3(2)
C(17)	18(2)	28(2)	28(2)	3(2)	-7(2)	-2(2)
C(18)	23(2)	22(2)	24(2)	-5(2)	-3(2)	0(2)
C(19)	49(3)	27(2)	47(2)	-1(2)	1(2)	1(2)
C(20)	27(2)	63(3)	32(2)	-21(2)	-3(2)	0(2)
C(21)	29(2)	37(2)	28(2)	1(2)	0(2)	-6(2)
C(22)	12(2)	26(2)	27(2)	0(2)	-3(1)	-3(2)
C(23)	25(2)	20(2)	29(2)	0(2)	-4(2)	-1(2)
C(24)	35(2)	29(2)	32(2)	4(2)	-3(2)	-9(2)
C(25)	33(2)	32(2)	39(2)	6(2)	-10(2)	-1(2)
C(26)	33(2)	24(2)	45(2)	2(2)	-6(2)	-7(2)
C(27)	24(2)	26(2)	26(2)	-5(2)	-1(2)	-4(2)
C(28)	38(2)	36(2)	27(2)	-6(2)	4(2)	-2(2)
C(29)	32(2)	35(2)	35(2)	-9(2)	1(2)	0(2)
C(30)	39(2)	34(2)	32(2)	-7(2)	-11(2)	1(2)

Table S10. Hydrogen coordinates (x 10^4) and isotropic
displacement parameters (A^2 x 10^3) for notbu1 (**2(PhNit₂)**).

x y z   U(eq)

	x	y	z	U(eq)		x	y	z	U(eq)
H(2A)	2513	4481	5060	45(2)	H(21A)	3082	7498	-1713	45(2)
H(2B)	1422	3393	5126	45(2)	H(21B)	4368	6433	-2069	45(2)
H(2C)	1026	4256	4439	45(2)	H(21C)	4497	6690	-1198	45(2)
H(3A)	6929	2461	4442	45(2)	H(24A)	2673	9279	737	45(2)
H(3B)	4835	2251	5083	45(2)	H(24B)	4881	9275	1099	45(2)
H(3C)	6086	3274	5111	45(2)	H(24C)	3848	10340	694	45(2)
H(4A)	2637	3095	3345	45(2)	H(25A)	-863	10080	1388	45(2)
H(4B)	2768	2126	3977	45(2)	H(25B)	238	11168	1230	45(2)
H(4C)	4928	2379	3383	45(2)	H(25C)	-967	10845	2081	45(2)
H(6)	7140	6011	3429	45(2)	H(26A)	3535	11428	1661	45(2)
H(7)	5828	7535	2776	45(2)	H(26B)	4919	10513	2108	45(2)
H(9)	412	6203	2553	45(2)	H(26C)	2682	11104	2551	45(2)
H(10)	1594	4693	3261	45(2)	H(28A)	1462	7741	3831	45(2)
H(13)	-1458	8409	1524	45(2)	H(28B)	-848	8110	3546	45(2)
H(14)	-2271	7881	385	45(2)	H(28C)	-304	8572	4309	45(2)
H(16)	3881	6342	-91	45(2)	H(29A)	-806	10306	4007	45(2)
H(17)	4661	6871	1057	45(2)	H(29B)	-1795	10057	3260	45(2)
H(19A)	2952	4991	-618	45(2)	H(29C)	60	10852	3178	45(2)
H(19B)	3071	4659	-1489	45(2)	H(30A)	2885	9564	4212	45(2)
H(19C)	801	4665	-896	45(2)	H(30B)	3956	10107	3407	45(2)
H(20A)	-1073	5784	-1800	45(2)	H(30C)	4483	8861	3583	45(2)
H(20B)	1112	5903	-2420	45(2)					
H(20C)	-373	6936	-2085	45(2)					

Crystallography. Crystallographic data for biradical **3(PhNit)₂**: Amber needles of **3(PhNit)₂** were crystallized from dichloromethane at 23 deg. C. A crystal of dimensions 0.35 x 0.15 x 0.05 mm was

mounted on a standard Bruker SMART CCD-based X-ray diffractometer equipped with a LT-2 low temperature device and normal focus Mo-target X-ray tube (λ = 0.71073 A) operated at 2000 W power (50 kV, 40 mA). The X-ray intensities were measured at 158(2) K; the detector was placed at a distance 5.008 cm from the crystal. A total of 4770 frames were collected with a scan width of 0.3° in ω and phi with an exposure time of 30 s/frame. The frames were integrated with the Bruker SAINT software package with a narrow frame algorithm. The integration of the data yielded a total of 25959 reflections to a maximum 2θ value of 52.98° of which 5344 were independent and 4460 were greater that $2\sigma(I)$. The final cell constants (Table 1) were based on the xyz centroids of 4032 reflections above $10\sigma(I)$. Analysis of the data showed negligible decay during data collection. The data were processed with SADABS, no correction for absorption was necessary. The structure was solved and refined with the Bruker SHELXTL (version 5.10) software package, using the space group P-1 with Z = 2 for the formula $C_{31}H_{40}N_2O_2$. All non-hydrogen atoms were refined anisotropically with the hydrogen atoms placed in idealized positions. Full matrix least-squares   refinement based on F^2 converged at R1 = 0.0433 and wR2 = 0.0982 [based on I > 2sigma(I)], R1 = 0.0832 and wR2 = 0.1099 for all data. Additional details are presented in Table 1 and are given as Supporting information as a CIF file.

Table 1. Crystal data and structure refinement for 3(PhNit)$_2$

Empirical formula	$C_{31}H_{40}N_2O_2$
Formula weight	472.65
Temperature, K	158(2)
Wavelength (λ), Å	0.71073
Crystal system	Triclinic
Space group	P-1
a, Å	6.2271(16)
b, Å	12.170(3)
c, Å	17.882(4)
α, °	99.872(5)
β, °	99.659(5)
γ, °	95.631(5)
Volume, Å^3	1304.9(6)
Absorption coefficient, mm^{-1}	0.074
Z	2
Calculated density, Mg/m^3	1.203
F(000)	512
Crystal size, mm	0.35 x 0.15 x 0.05
θ range for data collection,°.	1.71 to 24.71
Limiting indices	-7<=h<=7, -14<=k<=14, -21<=l<=21,
Reflections collected/unique	25959/4460
Absorption correction	None
Data/restraints/parameters	4460/0/324
R1[I>2sigma(I)]*	0.0433

wR2[*]		0.0982
Largest diff.peak, Å		0.221
GoF		0.896

[*]based on Fo^2

Table 2. Atomic coordinates (x10^4) and equivalent isotropic displacement parameters (Å^{2}x10^3) for 3(PhNit)$_2$. U(eq) is defined as one-third of the trace of the orthogonalized Uij tensor.

Atoms	x	y	z	U(eq)
O(1)	5464(2)	8799(1)	2618(1)	38(1)
O(2)	16197(3)	2719(2)	4451(1)	79(1)
N(1)	7498(3)	8705(1)	2591(1)	27(1)
N(2)	14263(3)	2911(2)	4543(1)	34(1)
C(1)	9081(4)	9783(2)	2747(1)	30(1)
C(2)	10301(4)	9788(2)	2075(1)	34(1)
C(3)	7719(4)	10758(2)	2799(1)	42(1)
C(4)	10649(4)	9889(2)	3516(1)	44(1)
C(5)	8018(3)	7599(2)	2392(1)	23(1)
C(6)	10155(3)	7309(2)	2513(1)	27(1)
C(7)	10488(3)	6194(2)	2352(1)	26(1)
C(8)	8768(3)	5327(2)	2043(1)	21(1)
C(9)	6657(3)	5634(2)	1914(1)	25(1)
C(10)	6283(3)	6738(2)	2086(1)	24(1)
C(11)	9176(3)	4127(2)	1898(1)	22(1)
C(12)	10440(3)	3769(2)	2585(1)	21(1)
C(13)	9787(3)	3951(2)	3298(1)	28(1)
C(14)	10963(3)	3660(2)	3944(1)	30(1)
C(15)	12894(3)	3185(2)	3903(1)	24(1)
C(16)	13585(3)	3001(2)	3191(1)	27(1)
C(17)	12370(3)	3293(2)	2551(1)	25(1)
C(18)	13741(3)	2883(2)	5333(1)	29(1)
C(19)	11517(4)	2215(2)	5282(1)	48(1)
C(20)	13858(5)	4086(2)	5764(1)	59(1)
C(21)	15467(4)	2324(3)	5761(1)	61(1)
C(22)	8481(3)	3431(2)	1211(1)	20(1)
C(23)	8568(3)	2172(2)	1073(1)	23(1)
C(24)	10043(3)	1857(2)	483(1)	25(1)
C(25)	9165(3)	2235(2)	-271(1)	27(1)
C(26)	9080(3)	3504(2)	-113(1)	26(1)
C(27)	7554(3)	3805(2)	466(1)	23(1)
C(28)	5254(3)	3180(2)	124(1)	26(1)
C(29)	5335(3)	1907(2)	-23(1)	26(1)
C(30)	6844(3)	1612(2)	-601(1)	28(1)
C(31)	6233(3)	1565(2)	745(1)	26(1)

Table 3. Bond lengths [Å] and angles [°] for 3(PhNit)$_2$.

O(1)-N(1)	1.291(2)	C(13)-C(14)	1.380(3)
O(2)-N(2)	1.281(2)	C(14)-C(15)	1.391(3)
N(1)-C(5)	1.415(2)	C(15)-C(16)	1.399(3)
N(1)-C(1)	1.517(3)	C(16)-C(17)	1.383(3)
N(2)-C(15)	1.417(2)	C(18)-C(21)	1.500(3)
N(2)-C(18)	1.507(3)	C(18)-C(19)	1.516(3)
C(1)-C(3)	1.523(3)	C(18)-C(20)	1.522(3)

C(1)-C(4)	1.526(3)	C(22)-C(23)	1.518(3)
C(1)-C(2)	1.526(3)	C(22)-C(27)	1.522(3)
C(5)-C(10)	1.396(3)	C(23)-C(31)	1.535(3)
C(5)-C(6)	1.401(3)	C(23)-C(24)	1.537(3)
C(6)-C(7)	1.381(3)	C(24)-C(25)	1.530(3)
C(7)-C(8)	1.395(3)	C(25)-C(26)	1.530(3)
C(8)-C(9)	1.394(3)	C(25)-C(30)	1.536(3)
C(8)-C(11)	1.494(3)	C(26)-C(27)	1.541(3)
C(9)-C(10)	1.378(3)	C(27)-C(28)	1.529(3)
C(11)-C(22)	1.344(3)	C(28)-C(29)	1.535(3)
C(11)-C(12)	1.499(3)	C(29)-C(30)	1.531(3)
C(12)-C(17)	1.390(3)	C(29)-C(31)	1.534(3)
C(12)-C(13)	1.391(3)		

O(1)-N(1)-C(5)	116.42(16)	C(14)-C(15)-N(2)	124.26(18)
O(1)-N(1)-C(1)	117.29(16)	C(16)-C(15)-N(2)	117.34(18)
C(5)-N(1)-C(1)	126.25(17)	C(17)-C(16)-C(15)	120.24(19)
O(2)-N(2)-C(15)	116.30(17)	C(16)-C(17)-C(12)	121.94(19)
O(2)-N(2)-C(18)	116.39(16)	C(21)-C(18)-N(2)	107.88(17)
C(15)-N(2)-C(18)	127.21(17)	C(21)-C(18)-C(19)	108.5(2)
N(1)-C(1)-C(3)	107.31(18)	N(2)-C(18)-C(19)	111.54(17)
N(1)-C(1)-C(4)	109.91(16)	C(21)-C(18)-C(20)	108.6(2)
C(3)-C(1)-C(4)	108.80(18)	N(2)-C(18)-C(20)	108.75(17)
N(1)-C(1)-C(2)	109.11(16)	C(19)-C(18)-C(20)	111.5(2)
C(3)-C(1)-C(2)	109.52(17)	C(11)-C(22)-C(23)	124.34(17)
C(4)-C(1)-C(2)	112.08(19)	C(11)-C(22)-C(27)	124.53(18)
C(10)-C(5)-C(6)	118.01(18)	C(23)-C(22)-C(27)	111.12(16)
C(10)-C(5)-N(1)	117.81(18)	C(22)-C(23)-C(31)	108.57(16)
C(6)-C(5)-N(1)	124.13(18)	C(22)-C(23)-C(24)	109.83(15)
C(7)-C(6)-C(5)	119.98(19)	C(31)-C(23)-C(24)	108.78(16)
C(6)-C(7)-C(8)	122.46(19)	C(25)-C(24)-C(23)	109.56(16)
C(9)-C(8)-C(7)	116.75(18)	C(26)-C(25)-C(24)	109.80(16)
C(9)-C(8)-C(11)	122.05(18)	C(26)-C(25)-C(30)	109.67(17)
C(7)-C(8)-C(11)	121.12(18)	C(24)-C(25)-C(30)	108.66(16)
C(10)-C(9)-C(8)	121.73(19)	C(25)-C(26)-C(27)	110.27(16)
C(9)-C(10)-C(5)	121.03(19)	C(22)-C(27)-C(28)	110.38(16)
C(22)-C(11)-C(8)	122.97(17)	C(22)-C(27)-C(26)	107.62(15)
C(22)-C(11)-C(12)	122.98(17)	C(28)-C(27)-C(26)	108.71(16)
C(8)-C(11)-C(12)	114.05(16)	C(27)-C(28)-C(29)	109.88(16)
C(17)-C(12)-C(13)	116.95(18)	C(30)-C(29)-C(31)	109.79(16)
C(17)-C(12)-C(11)	121.79(18)	C(30)-C(29)-C(28)	109.40(17)
C(13)-C(12)-C(11)	121.19(18)	C(31)-C(29)-C(28)	108.75(16)
C(14)-C(13)-C(12)	122.19(19)	C(29)-C(30)-C(25)	109.50(16)
C(13)-C(14)-C(15)	120.31(19)	C(29)-C(31)-C(23)	110.11(16)
C(14)-C(15)-C(16)	118.36(18)		

Table 4. Anisotropic displacement parameters ($\text{Å}^2 \text{x} 10^3$) for 3(PhNit)$_2$.
The anisotropic displacement factor exponent takes the form: $-2\rho^2[h^2a^{*2}U_{11}+...+2hka^*b^*U_{12}]$

Atom	U_{11}	U_{22}	U_{33}	U_{23}	U_{13}	U_{12}
O(1)	35(1)	32(1)	50(1)	4(1)	11(1)	13(1)
O(2)	43(1)	169(2)	46(1)	49(1)	18(1)	53(1)
N(1)	32(1)	22(1)	28(1)	5(1)	7(1)	8(1)
N(2)	27(1)	53(1)	28(1)	14(1)	7(1)	15(1)

C(1)	40(1)	19(1)	30(1)	5(1)	8(1)	3(1)
C(2)	41(1)	25(1)	39(1)	9(1)	11(1)	6(1)
C(3)	60(2)	24(1)	49(2)	10(1)	27(1)	11(1)
C(4)	63(2)	26(1)	36(1)	1(1)	-3(1)	-4(1)
C(5)	30(1)	21(1)	20(1)	5(1)	5(1)	6(1)
C(6)	27(1)	22(1)	30(1)	5(1)	2(1)	1(1)
C(7)	24(1)	23(1)	30(1)	7(1)	2(1)	4(1)
C(8)	25(1)	20(1)	19(1)	6(1)	6(1)	3(1)
C(9)	25(1)	24(1)	24(1)	5(1)	2(1)	-1(1)
C(10)	23(1)	24(1)	27(1)	6(1)	5(1)	6(1)
C(11)	21(1)	21(1)	25(1)	8(1)	7(1)	3(1)
C(12)	25(1)	15(1)	23(1)	4(1)	4(1)	0(1)
C(13)	28(1)	32(1)	29(1)	8(1)	8(1)	11(1)
C(14)	33(1)	37(1)	24(1)	8(1)	9(1)	9(1)
C(15)	24(1)	25(1)	23(1)	8(1)	2(1)	2(1)
C(16)	25(1)	28(1)	31(1)	7(1)	7(1)	8(1)
C(17)	26(1)	24(1)	25(1)	4(1)	6(1)	3(1)
C(18)	32(1)	34(1)	23(1)	10(1)	6(1)	5(1)
C(19)	51(2)	58(2)	35(1)	12(1)	9(1)	-6(1)
C(20)	93(2)	41(2)	42(2)	1(1)	23(2)	-1(2)
C(21)	60(2)	98(2)	41(2)	37(2)	14(1)	34(2)
C(22)	19(1)	21(1)	24(1)	8(1)	8(1)	3(1)
C(23)	25(1)	19(1)	25(1)	4(1)	4(1)	3(1)
C(24)	25(1)	21(1)	30(1)	3(1)	6(1)	4(1)
C(25)	25(1)	28(1)	27(1)	4(1)	8(1)	4(1)
C(26)	26(1)	29(1)	25(1)	8(1)	7(1)	4(1)
C(27)	26(1)	20(1)	25(1)	7(1)	4(1)	6(1)
C(28)	28(1)	28(1)	25(1)	6(1)	5(1)	7(1)
C(29)	23(1)	26(1)	27(1)	3(1)	1(1)	0(1)
C(30)	30(1)	27(1)	26(1)	2(1)	3(1)	5(1)
C(31)	27(1)	20(1)	31(1)	6(1)	7(1)	2(1)

Table 5. Hydrogen coordinates (x10^4) and isotropic displacement parameters (Å^{2}x10^3) for 3(PhNit)$_2$.

Atoms	x	y	z	Ueq
H(2A)	11166	9157	2038	43(1)
H(2B)	11283	10497	2162	43(1)
H(2C)	9238	9714	1592	43(1)
H(3A)	6622	10663	2323	43(1)
H(3B)	8684	11468	2867	43(1)
H(3C)	6975	10769	3242	43(1)
H(4A)	9800	9844	3927	43(1)
H(4B)	11590	10615	3633	43(1)
H(4C)	11564	9278	3484	43(1)
H(6)	11374	7879	2705	43(1)
H(7)	11943	6011	2457	43(1)
H(9)	5444	5066	1703	43(1)
H(10)	4821	6915	1995	43(1)
H(13)	8487	4286	3341	43(1)
H(14)	10453	3785	4419	43(1)
H(16)	14893	2673	3148	43(1)
H(17)	12870	3165	2074	43(1)
H(19A)	10365	2584	5018	43(1)

H(19B)	11264	2178	5804	43(1)
H(19C)	11483	1452	4991	43(1)
H(20A)	15341	4480	5815	43(1)
H(20B)	13515	4078	6278	43(1)
H(20C)	12793	4474	5475	43(1)
H(21A)	15510	1574	5464	43(1)
H(21B)	15117	2256	6267	43(1)
H(21C)	16903	2778	5833	43(1)
H(23)	9154	1941	1571	43(1)
H(24A)	11566	2226	692	43(1)
H(24B)	10065	1032	382	43(1)
H(25)	10148	2049	-650	43(1)
H(26A)	8533	3748	-603	43(1)
H(26B)	10577	3905	100	43(1)
H(27)	7503	4635	567	43(1)
H(28A)	4684	3414	-368	43(1)
H(28B)	4248	3373	487	43(1)
H(29)	3823	1501	-237	43(1)
H(30A)	6264	1831	-1097	43(1)
H(30B)	6895	790	-701	43(1)
H(31A)	6256	741	661	43(1)
H(31B)	5263	1763	1119	43(1)

Structure Determination.

Crystal data of a red plate-like crystal of **3(PhNit)$_2$** with the approximate dimensions 0.20 x 0.20 x 0.05 mm were collected on a Bruker platform diffractometer equipped with a Smart6000 CCD detector (normal focus sealed tube operated at 50 kV, 45 mA, graphite-monochromated, MoKα = 0.71073 Å). A single crystal was selected and mounted on a 0.1 mm glass capillary with epoxy glue. The crystal was measured at ca. 25(5) K using an open flow He-cryostat. Evaluation of the diffraction data revealed cracking for all tested crystals into several components upon cooling. A total of 1073 frames were collected with an exposure time of 60 s and a scan width of 0.3° in • at a detector to crystal distance of 5.150 cm.

Orientation Matrices for four components were found using Gemini. The data for all four crystal components were integrated simultaneously using SAINT 6.29A. No correction for absorption or decay was applied. A separate integration based on only the orientation matrix of the major component (and thereby containing all reflections originated by component1 – isolated and overlapping) provided a 'HKLF 4' format file, which was used to solve the structure with direct methods in P1bar (SHELXTL 5.1). The structure was refined by full-matrix least squares on F^2. A refinement on all four components similtaneously converged to R1 = 0.184 (48° cutoff in 2•) for 10 364 reflections with Fo > 4• (Fo) and resulted in batch scale factors of 0.57: 0.20:0.21:0.02. All non-hydrogen atoms were refined with isotropic atomic displacement factors, hydrogen atoms were calculated on idealized positions and treated as riding atoms.

The high R-value is not surprising considering the nature of this cracked crystal, which can be only approximated by a model of four single crystal domains. Not all 'domains' in the cracked crystal are accounted for and some of the indexed ones are obviously not well defined. A home written program was used to separate overlapping and isolated reflections and a better model was obtained by refining on those reflections that originated only from the dominant component. Nitrogen and Oxygen atoms were refined with anisotropic atomic displacement factors, carbon atom were refined isotropically, hydrogen atoms were calculated on idealized positions and treated as riding atoms. The final refinement converged to R1 = 0.0948 (wR2 = 0.2259) for 1129 reflections with Fo > 4• (Fo) and R1 = 0.1031 (wR2 = 0.2323) for all 1254 data.

SMART, Version 5.625, **2001**, Bruker AXS Inc., Madison, Wisconsin, USA.

M. J. Hardie, K. Kirschbaum, A. Martin, A. A. Pinkerton *J. Appl. Cryst*. **1998**, *31*, 815-817.
Gemini 1.02 **2000.** Bruker AXS Inc., Madison, Wisconsin, USA.
Saint 6.29A , **2001** Bruker AXS Inc., Madison, Wisconsin, USA
G.M. Sheldrick, SHELXTL, Version 5.1, **1998,** Bruker AXS Inc., Madison, Wisconsin, USA.

Table S21. Crystal data and structure refinement for abcd3a (**3(PhNit)$_2$**).

Empirical formula	C31 H40 N2 O2
Formula weight	472.65
Temperature	25(5) K
Wavelength	0.71073 A
Crystal system, space group	triclinic, P1bar
Unit cell dimensions	a=6.2971(5) Å, •=100.563(3)•
	b=11.9668(10) Å, •=96.732(3)•
	c=17.4475(12) Å, •=94.661(3)•
Volume	1276.46(17) Å^3
Z, Calculated density	2, 1.230 Mg/m^3
Absorption coefficient	0.076 mm^{-1}
F(000)	512
Crystal size	0.20 x 0.20 x 0.02 mm
Theta range for data collection	3.23 to 23.99 deg.
Limiting indices	-5<=h<=6, -5<=k<=12, -18<=l<=18
Reflections collected / unique	1314 / 1254 [R(int) = 0.1085]
Completeness to theta = 23.99	31.4 %
Refinement method	Full-matrix least-squares on F^2
Data / restraints / parameters	1254 / 0 / 161
Goodness-of-fit on F^2	1.249
Final R indices [I>2sigma(I)]	R1 = 0.0948, wR2 = 0.2259
R indices (all data)	R1 = 0.1031, wR2 = 0.2323
Largest diff. peak and hole	0.236 and -0.211 e.A^3

Table S22. Atomic coordinates (x 10^4) and equivalent isotropic or isotropic displacement parameters (Å^2 x 10^3) for abcd3a (**3(PhNit)$_2$**). U(eq) is defined as one third of the trace of the orthogonalized Uij tensor.

	x	y	z	U(eq)
O(1)	-25036(10)	-11168(6)	-7226(3)	14(2)
O(2)	-13700(10)	-15740(6)	-5370(3)	12(2)
N(1)	-23054(12)	-11248(7)	-7331(3)	12(2)
N(2)	-15630(13)	-16155(7)	-5305(3)	16(2)
C(1)	-21606(15)	-10128(9)	-7148(4)	14(2)
C(2)	-20018(16)	-10100(9)	-7753(4)	20(2)
C(3)	-23023(15)	-9167(9)	-7177(4)	15(2)
C(4)	-20379(15)	-9994(9)	-6304(4)	15(2)
C(5)	-22405(14)	-12331(8)	-7571(4)	12(2)
C(6)	-20309(14)	-12622(8)	-7441(4)	12(2)
C(7)	-19874(15)	-13734(8)	-7637(4)	12(2)
C(8)	-21514(14)	-14622(8)	-7993(3)	8(2)
C(9)	-23603(14)	-14322(8)	-8128(4)	9(2)
C(10)	-24070(15)	-13211(8)	-7929(4)	12(2)
C(11)	-21024(14)	-15836(8)	-8123(4)	12(2)
C(12)	-19755(14)	-16146(8)	-7419(3)	7(2)
C(13)	-20510(14)	-15862(8)	-6682(4)	12(2)

```
C(14)      -19209(14)   -15959(8)    -5994(4)    10(2)
C(15)      -17181(15)   -16284(8)    -6022(4)    11(2)
C(16)      -16460(15)   -16619(8)    -6751(4)    14(2)
C(17)      -17791(14)   -16558(8)    -7441(4)     9(2)
C(18)      -15833(14)   -16976(8)    -4750(4)    10(2)
C(19)      -18142(14)   -17169(8)    -4584(4)    13(2)
C(20)      -14342(14)   -16479(8)    -3991(4)    13(2)
C(21)      -15090(14)   -18105(8)    -5150(4)    14(2)
C(22)      -21609(14)   -16589(8)    -8825(4)    10(2)
C(23)      -21461(14)   -17860(8)    -8930(4)    11(2)
C(24)      -19878(14)   -18207(8)    -9538(4)    12(2)
C(25)      -20705(14)   -17843(8)   -10315(4)    10(2)
C(26)      -20862(15)   -16568(8)   -10177(4)    12(2)
C(27)      -22461(14)   -16215(8)    -9584(3)    10(2)
C(28)      -24673(14)   -16877(8)    -9907(4)    13(2)
C(29)      -24530(15)   -18153(8)   -10039(4)    13(2)
C(30)      -22947(14)   -18497(8)   -10635(4)    13(2)
C(31)      -23692(14)   -18487(8)    -9250(3)    10(2)
```

Table S23. Bond lengths [Å] and angles [•] for abcd3a (**3(PhNit)₂**).

```
O(1)-N(1)               1.292(9)
O(2)-N(2)               1.300(9)
N(1)-C(5)               1.396(12)
N(1)-C(1)               1.518(12)
N(2)-C(15)              1.470(10)
N(2)-C(18)              1.509(13)
C(1)-C(3)               1.517(15)
C(1)-C(2)               1.539(12)
C(1)-C(4)               1.554(10)
C(2)-H(2A)              0.9600
C(2)-H(2B)              0.9600
C(2)-H(2C)              0.9600
C(3)-H(3A)              0.9600
C(3)-H(3B)              0.9600
C(3)-H(3C)              0.9600
C(4)-H(4A)              0.9600
C(4)-H(4B)              0.9600
C(4)-H(4C)              0.9600
C(5)-C(6)               1.396(14)
C(5)-C(10)              1.423(12)
C(6)-C(7)               1.371(13)
C(6)-H(6A)              0.9300
C(7)-C(8)               1.418(12)
C(7)-H(7A)              0.9300
C(8)-C(9)               1.396(13)
C(8)-C(11)              1.492(13)
C(9)-C(10)              1.376(13)
C(9)-H(9A)              0.9300
C(10)-H(10A)            0.9300
C(11)-C(22)             1.372(9)
C(11)-C(12)             1.507(12)
```

```
C(12)-C(17)               1.370(13)
C(12)-C(13)               1.415(10)
C(13)-C(14)               1.401(12)
C(13)-H(13A)              0.9300
C(14)-C(15)               1.369(14)
C(14)-H(14A)              0.9300
C(15)-C(16)               1.401(10)
C(16)-C(17)               1.400(12)
C(16)-H(16A)              0.9300
C(17)-H(17A)              0.9300
C(18)-C(20)               1.522(9)
C(18)-C(19)               1.523(11)
C(18)-C(21)               1.538(13)
C(19)-H(19A)              0.9600
C(19)-H(19B)              0.9600
C(19)-H(19C)              0.9600
C(20)-H(20A)              0.9600
C(20)-H(20B)              0.9600
C(20)-H(20C)              0.9600
C(21)-H(21A)              0.9600
C(21)-H(21B)              0.9600
C(21)-H(21C)              0.9600
C(22)-C(23)               1.510(13)
C(22)-C(27)               1.528(12)
C(23)-C(31)               1.530(12)
C(23)-C(24)               1.563(11)
C(23)-H(23A)              0.9800
C(24)-C(25)               1.544(12)
C(24)-H(24A)              0.9700
C(24)-H(24B)              0.9700
C(25)-C(26)               1.513(13)
C(25)-C(30)               1.547(12)
C(25)-H(25A)              0.9800
C(26)-C(27)               1.554(11)
C(26)-H(26A)              0.9700
C(26)-H(26B)              0.9700
C(27)-C(28)               1.535(12)
C(27)-H(27A)              0.9800
C(28)-C(29)               1.513(14)
C(28)-H(28A)              0.9700
C(28)-H(28B)              0.9700
C(29)-C(30)               1.548(12)
C(29)-C(31)               1.549(12)
C(29)-H(29A)              0.9800
C(30)-H(30A)              0.9700
C(30)-H(30B)              0.9700
C(31)-H(31A)              0.9700
C(31)-H(31B)              0.9700
O(1)-N(1)-C(5)            118.7(7)
O(1)-N(1)-C(1)            115.5(7)
C(5)-N(1)-C(1)            125.8(7)
O(2)-N(2)-C(15)           114.4(6)
O(2)-N(2)-C(18)           117.3(7)
C(15)-N(2)-C(18)          120.3(6)
```

```
C(3)-C(1)-N(1)          107.9(7)
C(3)-C(1)-C(2)          109.3(8)
N(1)-C(1)-C(2)          111.1(6)
C(3)-C(1)-C(4)          109.6(6)
N(1)-C(1)-C(4)          108.2(7)
C(2)-C(1)-C(4)          110.7(7)
C(1)-C(2)-H(2A)         109.5
C(1)-C(2)-H(2B)         109.5
H(2A)-C(2)-H(2B)        109.5
C(1)-C(2)-H(2C)         109.5
H(2A)-C(2)-H(2C)        109.5
H(2B)-C(2)-H(2C)        109.5
C(1)-C(3)-H(3A)         109.5
C(1)-C(3)-H(3B)         109.5
H(3A)-C(3)-H(3B)        109.5
C(1)-C(3)-H(3C)         109.5
H(3A)-C(3)-H(3C)        109.5
H(3B)-C(3)-H(3C)        109.5
C(1)-C(4)-H(4A)         109.5
C(1)-C(4)-H(4B)         109.5
H(4A)-C(4)-H(4B)        109.5
C(1)-C(4)-H(4C)         109.5
H(4A)-C(4)-H(4C)        109.5
H(4B)-C(4)-H(4C)        109.5
C(6)-C(5)-N(1)          125.3(7)
C(6)-C(5)-C(10)         118.5(9)
N(1)-C(5)-C(10)         116.1(8)
C(7)-C(6)-C(5)          120.7(8)
C(7)-C(6)-H(6A)         119.7
C(5)-C(6)-H(6A)         119.7
C(6)-C(7)-C(8)          121.5(9)
C(6)-C(7)-H(7A)         119.2
C(8)-C(7)-H(7A)         119.2
C(9)-C(8)-C(7)          117.4(8)
C(9)-C(8)-C(11)         122.3(8)
C(7)-C(8)-C(11)         119.9(8)
C(10)-C(9)-C(8)         121.8(8)
C(10)-C(9)-H(9A)        119.1
C(8)-C(9)-H(9A)         119.1
C(9)-C(10)-C(5)         120.0(9)
C(9)-C(10)-H(10A)       120.0
C(5)-C(10)-H(10A)       120.0
C(22)-C(11)-C(8)        123.3(8)
C(22)-C(11)-C(12)       123.1(9)
C(8)-C(11)-C(12)        113.6(6)
C(17)-C(12)-C(13)       118.6(7)
C(17)-C(12)-C(11)       123.1(6)
C(13)-C(12)-C(11)       117.8(8)
C(14)-C(13)-C(12)       119.8(9)
C(14)-C(13)-H(13A)      120.1
C(12)-C(13)-H(13A)      120.1
C(15)-C(14)-C(13)       120.7(7)
C(15)-C(14)-H(14A)      119.7
C(13)-C(14)-H(14A)      119.7
```

```
C(14)-C(15)-C(16)        119.8(7)
C(14)-C(15)-N(2)         121.5(6)
C(16)-C(15)-N(2)         118.3(8)
C(17)-C(16)-C(15)        119.2(9)
C(17)-C(16)-H(16A)       120.4
C(15)-C(16)-H(16A)       120.4
C(12)-C(17)-C(16)        121.6(6)
C(12)-C(17)-H(17A)       119.2
C(16)-C(17)-H(17A)       119.2
N(2)-C(18)-C(20)         107.9(8)
N(2)-C(18)-C(19)         111.4(8)
C(20)-C(18)-C(19)        110.5(6)
N(2)-C(18)-C(21)         106.7(6)
C(20)-C(18)-C(21)        109.9(8)
C(19)-C(18)-C(21)        110.3(7)
C(18)-C(19)-H(19A)       109.5
C(18)-C(19)-H(19B)       109.5
H(19A)-C(19)-H(19B)      109.5
C(18)-C(19)-H(19C)       109.5
H(19A)-C(19)-H(19C)      109.5
H(19B)-C(19)-H(19C)      109.5
C(18)-C(20)-H(20A)       109.5
C(18)-C(20)-H(20B)       109.5
H(20A)-C(20)-H(20B)      109.5
C(18)-C(20)-H(20C)       109.5
H(20A)-C(20)-H(20C)      109.5
H(20B)-C(20)-H(20C)      109.5
C(18)-C(21)-H(21A)       109.5
C(18)-C(21)-H(21B)       109.5
H(21A)-C(21)-H(21B)      109.5
C(18)-C(21)-H(21C)       109.5
H(21A)-C(21)-H(21C)      109.5
H(21B)-C(21)-H(21C)      109.5
C(11)-C(22)-C(23)        123.9(8)
C(11)-C(22)-C(27)        122.9(9)
C(23)-C(22)-C(27)        113.2(6)
C(22)-C(23)-C(31)        108.7(8)
C(22)-C(23)-C(24)        109.0(7)
C(31)-C(23)-C(24)        109.1(5)
C(22)-C(23)-H(23A)       110.0
C(31)-C(23)-H(23A)       110.0
C(24)-C(23)-H(23A)       110.0
C(25)-C(24)-C(23)        108.4(7)
C(25)-C(24)-H(24A)       110.0
C(23)-C(24)-H(24A)       110.0
C(25)-C(24)-H(24B)       110.0
C(23)-C(24)-H(24B)       110.0
H(24A)-C(24)-H(24B)      108.4
C(26)-C(25)-C(24)        110.4(5)
C(26)-C(25)-C(30)        109.9(8)
C(24)-C(25)-C(30)        108.5(7)
C(26)-C(25)-H(25A)       109.3
C(24)-C(25)-H(25A)       109.3
C(30)-C(25)-H(25A)       109.3
```

236

```
C(25)-C(26)-C(27)            111.3(7)
C(25)-C(26)-H(26A)           109.4
C(27)-C(26)-H(26A)           109.4
C(25)-C(26)-H(26B)           109.4
C(27)-C(26)-H(26B)           109.4
H(26A)-C(26)-H(26B)          108.0
C(22)-C(27)-C(28)            108.8(7)
C(22)-C(27)-C(26)            106.1(7)
C(28)-C(27)-C(26)            108.7(5)
C(22)-C(27)-H(27A)           111.0
C(28)-C(27)-H(27A)           111.0
C(26)-C(27)-H(27A)           111.0
C(29)-C(28)-C(27)            110.8(8)
C(29)-C(28)-H(28A)           109.5
C(27)-C(28)-H(28A)           109.5
C(29)-C(28)-H(28B)           109.5
C(27)-C(28)-H(28B)           109.5
H(28A)-C(28)-H(28B)          108.1
C(28)-C(29)-C(30)            110.4(7)
C(28)-C(29)-C(31)            109.4(6)
C(30)-C(29)-C(31)            108.4(7)
C(28)-C(29)-H(29A)           109.6
C(30)-C(29)-H(29A)           109.6
C(31)-C(29)-H(29A)           109.6
C(25)-C(30)-C(29)            109.2(5)
C(25)-C(30)-H(30A)           109.8
C(29)-C(30)-H(30A)           109.8
C(25)-C(30)-H(30B)           109.8
C(29)-C(30)-H(30B)           109.8
H(30A)-C(30)-H(30B)          108.3
C(23)-C(31)-C(29)            110.1(7)
C(23)-C(31)-H(31A)           109.6
C(29)-C(31)-H(31A)           109.6
C(23)-C(31)-H(31B)           109.6
C(29)-C(31)-H(31B)           109.6
H(31A)-C(31)-H(31B)          108.2
_____
Symmetry transformations used to generate equivalent atoms:
```

Table S24. Anisotropic displacement parameters (Å^2 x 10^3) for abcd3a (**3(PhNit)₂**).
The anisotropic displacement factor exponent takes the form: $-2 \bullet^2$ [h^2 a^{*2} U11 + ... + 2 h k a* b* U12]

U11	U22	U33	U23	U13	U12	
O(1)	12(4)	11(5)	18(3)	1(2)	−1(2)	−5(3)
O(2)	9(4)	11(5)	14(3)	6(2)	0(2)	−6(3)
N(1)	12(5)	9(6)	13(3)	1(3)	−2(3)	−3(4)
N(2)	15(5)	22(7)	6(3)	1(3)	−1(3)	−10(4)

Table S25. Hydrogen coordinates (x 10^4) and isotropic displacement parameters (Å^2 x 10^3) for abcd3a (**3(PhNit)$_2$**).

x	y	z	U(eq)
H(2A)	−20804	−10184	−8269	29
H(2B)	−19132	−10715	−7740	29
H(2C)	−19126	−9384	−7625	29
H(3A)	−23779	−9251	−7699	23
H(3B)	−22147	−8446	−7041	23
H(3C)	−24039	−9194	−6810	23
H(4A)	−21395	−10014	−5936	23
H(4B)	−19490	−9277	−6170	23
H(4C)	−19496	−10608	−6285	23
H(6A)	−19195	−12054	−7220	15
H(7A)	−18471	−13911	−7533	14
H(9A)	−24709	−14889	−8358	11
H(10A)	−25475	−13035	−8029	14
H(13A)	−21865	−15613	−6655	14
H(14A)	−19729	−15800	−5512	12
H(16A)	−15113	−16879	−6777	17
H(17A)	−17331	−16803	−7925	11
H(19A)	−18585	−16458	−4335	19
H(19B)	−18228	−17711	−4242	19
H(19C)	−19067	−17460	−5069	19
H(20A)	−14815	−15775	−3745	19
H(20B)	−12904	−16337	−4109	19
H(20C)	−14365	−17011	−3642	19
H(21A)	−13635	−17972	−5252	21
H(21B)	−16006	−18399	−5637	21
H(21C)	−15165	−18650	−4810	21
H(23A)	−20945	−18059	−8425	13
H(24A)	−18446	−17830	−9337	14
H(24B)	−19809	−19026	−9629	14
H(25A)	−19712	−18040	−10699	12
H(26A)	−21337	−16350	−10673	14
H(26B)	−19452	−16165	−9974	14
H(27A)	−22549	−15388	−9494	12
H(28A)	−25679	−16674	−9537	16
H(28B)	−25205	−16666	−10399	16
H(29A)	−25958	−18560	−10241	16
H(30A)	−22851	−19314	−10711	15
H(30B)	−23461	−18314	−11138	15
H(31A)	−24678	−18290	−8871	11
H(31B)	−23617	−19306	−9331	11

[1] SMART, Version 5.625, **2001**, Bruker AXS Inc., Madison, Wisconsin, USA.

[1] M. J. Hardie, K. Kirschbaum, A. Martin, A. A. Pinkerton *J. Appl. Cryst*. **1998**, *31*, 815-817.

[1] Gemini 1.02 **2000.** Bruker AXS Inc., Madison, Wisconsin, USA.

[1] Saint 6.29A , **2001** Bruker AXS Inc., Madison, Wisconsin, USA

[1] G.M. Sheldrick, SHELXTL, Version 5.1, **1998,** Bruker AXS Inc., Madison, Wisconsin, USA.

Crystallography. Crystallographic data for biradical **4(PhNit)₂**: Red needles of **4(PhNit)₂** were crystallized from dichloromethane layered with heptane at RT. A crystal of dimensions 0.40 x 0.18 x 0.04 mm was mounted on a Enraf-Nonius CAD4-MACH X-ray diffractometer. The sample was mounted on the end of a glass fiber using a small amount of silicone grease and transferred to the diffractometer. The sample was maintained at a temperature of –125 deg C using a nitrogen cold stream. All X-ray measurements were made on an Enraf-Nonius CAD4-MACH diffractometer. The unit cell dimensions were determined by a fit of 25 well centered reflections and their Friedel pairs with theta 23 deg < 2(theta) < 36 deg. A hemisphere of unique data was collected using the omega scan mode in a non-bisecting geometry. The adoption of a non-bisecting scan mode was accomplished by offsetting psi by 20.00 for each data point collected. This was done to minimize the interaction of the goniometer head with the cold stream. Three standard reflections were measured every 4800 seconds of X-ray exposure time. Scaling the data was accomplished using a 5 point smoothed curved routine fit to the intensity check reflections. The intensity data was corrected for Lorentz and polarization effects. Data were not corrected for absorption.

Structure Solution and Refinement. The data were reduced using routines from the NRCVAX set of programs. The structure was solved using SIR92. All non-H atom positions were recovered from the initial E-map. Hydrogen atoms were included in the model at calculated positions. The hydrogen atom positions and isotropic displacement parameters were allowed to refine. Refinement of the structure was performed using full matrix least-squares based on F. All non-H atoms were allowed to refine with anisotropic displacement parameters (ADP's). The calculated structure factors included corrections for anomalous dispersion from the usual tabulation (International Tables for X-ray Crystallography, Vol. IV, (1974), Table 2.3.1, Kynoch Press, Birmingham, England). A secondary extinction correction was included in the final cycles of refinement. Additional information and relevant literature references can be found in the REPORT.OUT file and the reference section of the Facility's Web page.

Table 1. Crystal data and structure refinement for 4(PhNit)₂

Empirical formula	$C_{28}H_{36}N_2O_2$
Formula weight	432.60
Temperature, K	148
Wavelength (λ), Å	0.71073
Crystal system	Triclinic
Space group	P-1
a, Å	6.1933(4)
b, Å	11.4950(10)

c, Å				17.478(2)
α, °				104.577(8)
β, °				99.635(8)
γ, °				94.942(8)
Volume, Å^3				1176.48(19)
Absorption coefficient, mm^{-1}				0.08
Z				2
Calculated density, Mg/m^3				1.221
F(000)				468.25
Crystal size, mm				0.40 x 0.18 x 0.04
θ range for data collection,°.				0.0 to 25.0
Limiting indices				-7<=h<=7, -0<=k<=13, -20<=l<=19,
Reflections collected/unique				4097/4097
Absorption correction				None
Data/restraints/parameters				2809/0/434
RF*				0.051
Rw**				0.053
Largest diff.peak, Å				0.260
GoF(based on Fo)				1.45

*[RF = Σ(Fo-Fc)/ Σ(Fo)]

**(Rw = [Σ(w(Fo-Fc)^2)/ Σ(wFo^2)]$^{-1/2}$)

Table 2. Atomic coordinates (x10^4) and equivalent isotropic displacement parameters (Å^{2}x10^3) for 4(PhNit)$_2$. U(eq) is defined as one-third of the trace of the orthogonalized Uij tensor.

Atoms	x	y	z	U(eq)
O	.6881(3)	.32090(20)	.46149(12)	.0312(13)
N	.4785(4)	.3019(2)	.46044(13)	.0204(14)
C1	-.0423(4)	.3160(2)	.10274(16)	.0169(15)
C2	-.0246(4)	.3863(2)	.17754(16)	.0166(14)
C3	.0921(4)	.3563(2)	.25043(16)	.0157(14)
C4	.2961(4)	.3107(2)	.25072(16)	.0168(14)
C5	.4154(5)	.2908(2)	.31866(16)	.0182(15)
C6	.3367(4)	.3150(2)	.39078(16)	.0165(14)
C7	.1324(4)	.3593(2)	.39274(17)	.0179(15)
C8	.0161(4)	.3797(2)	.32292(17)	.0187(16)
C9	.0120(5)	.1884(2)	.07062(16)	.0177(14)
C10	-.2017(5)	.1303(3)	.00888(18)	.0207(16)
C11	.1937(5)	.2126(3)	.02385(18)	.0215(16)
C12	.4075(5)	.2710(2)	.53177(16)	.0200(14)
C13	.3897(6)	.3886(3)	.59332(19)	.0274(18)
C14	.5906(5)	.2067(3)	.5677(2)	.0283(18)
C15	.1925(5)	.1843(3)	.5055(2)	.0287(18)
O'	-.5729(3)	.83372(17)	.23851(12)	.0224(11)
N'	-.3641(4)	.84267(20)	.23657(14)	.0177(13)
C3'	-.1100(4)	.5067(2)	.19241(15)	.0160(14)
C4'	-.3297(4)	.5160(2)	.16000(16)	.0167(15)
C5'	-.4095(4)	.6272(2)	.17463(16)	.0163(15)
C6'	-.2711(4)	.7326(2)	.22123(16)	.0158(14)
C7'	-.0534(5)	.7238(2)	.25483(17)	.0173(14)
C8'	.0225(4)	.6122(2)	.24045(16)	.0174(15)

C9'	-.0957(5)	.3428(3)	.02138(16)	.0183(14)
C10'	-.2656(5)	.2344(2)	-.02962(17)	.0206(16)
C11'	.1259(5)	.3248(3)	-.00610(19)	.0223(17)
C12'	-.2540(4)	.9704(2)	.24862(17)	.0189(15)
C13'	-.4005(5)	1.0256(3)	.19101(20)	.0231(17)
C14'	-.2476(6)	1.0380(3)	.33555(20)	.0323(19)
C15'	-.0243(6)	.9750(3)	.2284(3)	.039(2)

Table 3. Bond lengths [Å] and angles [°] for 4(PhNit)$_2$.

O N	1.294(3)	C15 H15a	1.02(4)
N C6	1.426(3)	C15 H15b	1.01(3)
N C12	1.501(4)	C15 H15c	.97(3)
C1 C2	1.334(4)	O' N'	1.295(3)
C1 C9	1.521(4)	N' C6'	1.418(3)
C1 C9'	1.519(4)	N' C12'	1.514(3)
C2 C3	1.490(4)	C3' C4'	1.407(4)
C2 C3'	1.501(4)	C3' C8'	1.391(4)
C3 C4	1.408(4)	C4' C5'	1.389(4)
C3 C8	1.396(4)	C4' H4'	.99(3)
C4 C5	1.371(4)	C5' C6'	1.399(4)
C4 H4	.96(3)	C5' H5'	.94(3)
C5 C6	1.399(4)	C6' C7'	1.400(4)
C5 H5	.96(3)	C7' C8'	1.382(4)
C6 C7	1.406(4)	C7' H7'	.92(3)
C7 C8	1.393(4)	C8' H8'	.98(3)
C7 H7	.98(3)	C9' C10'	1.535(4)
C8 H8	.96(3)	C9' C11'	1.542(4)
C9 C10	1.539(4)	C9' H9'	.93(3)
C9 C11	1.543(4)	C10' H10a'	1.02(3)
C9 H9	.97(3)	C10' H10b'	.97(3)
C10 C10'	1.561(4)	C11' H11a'	.97(3)
C10 H10a	.94(3)	C11' H11b'	.99(3)
C10 H10b	.95(3)	C12' C13'	1.534(4)
C11 C11'	1.572(4)	C12' C14'	1.515(4)
C11 H11a	1.00(3)	C12' C15'	1.521(4)
C11 H11b	.96(3)	C13' H13a'	1.03(3)
C12 C13	1.526(4)	C13' H13b'	.99(3)
C12 C14	1.538(4)	C13' H13c'	.93(3)
C12 C15	1.521(4)	C14' H14a'	1.02(4)
C13 H13a	.97(4)	C14' H14b'	.97(4)
C13 H13b	.97(3)	C14' H14c'	.97(4)
C13 H13c	.99(4)	C15' H15a'	.99(4)
C14 H14a	1.01(4)	C15' H15b'	.94(4)
C14 H14b	.96(3)	C15' H15c'	.99(3)
C14 H14c	1.00(4)		

ONC6	115.6(2)	H15aC15H15b	110(3)
ONC12	118.1(2)	H15aC15H15c	105(3)
C6NC12	126.3(2)	H15bC15H15c	111(2)
C2C1C9	132.1(2)	O'N'C6'	116.4(2)
C2C1C9'	131.4(2)	O'N'C12'	114.80(19)
C9C1C9'	96.2(2)	C6'N'C12'	128.7(2)

C1C2C3	123.3(2)	C2C3'C4'	121.0(2)
C1C2C3'	120.9(2)	C2C3'C8'	121.4(2)
C3C2C3'	115.7(2)	C4'C3'C8'	117.6(2)
C2C3C4	120.6(2)	C3'C4'C5'	121.0(2)
C2C3C8	122.6(2)	C3'C4'H4'	117.1(15)
C4C3C8	116.6(2)	C5'C4'H4'	122.0(15)
C3C4C5	122.0(3)	C4'C5'C6'	120.3(2)
C3C4H4	119.4(14)	C4'C5'H5'	120.9(16)
C5C4H4	118.4(15)	C6'C5'H5'	118.7(16)
C4C5C6	120.6(2)	N'C6'C5'	117.7(2)
C4C5H5	122.0(15)	N'C6'C7'	123.1(2)
C6C5H5	117.1(15)	C5'C6'C7'	119.0(2)
NC6C5	117.3(2)	C6'C7'C8'	119.8(3)
NC6C7	123.4(2)	C6'C7'H7'	118.5(15)
C5C6C7	119.2(2)	C8'C7'H7'	121.7(15)
C6C7C8	118.9(2)	C3'C8'C7'	122.1(2)
C6C7H7	122.1(13)	C3'C8'H8'	121.0(16)
C8C7H7	119.1(13)	C7'C8'H8'	116.8(16)
C3C8C7	122.8(2)	C1C9'C10'	103.6(2)
C3C8H8	118.7(16)	C1C9'C11'	99.5(2)
C7C8H8	118.5(16)	C1C9'H9'	116.7(15)
C1C9C10	100.7(2)	C10'C9'C11'	107.4(2)
C1C9C11	101.1(2)	C10'C9'H9'	115.0(15)
C1C9H9	114.3(14)	C11'C9'H9'	113.2(15)
C10C9C11	108.1(2)	C10C10'C9'	102.7(2)
C10C9H9	115.5(15)	C10C10'H10a'	112.7(16)
C11C9H9	115.3(15)	C10C10'H10b'	111.6(14)
C9C10C10'	103.4(2)	C9'C10'H10a'	112.0(16)
C9C10H10a	111.3(15)	C9'C10'H10b'	110.5(14)
C9C10H10b	111.6(15)	H10a'C10'H10b'	107(2)
C10'C10H10a	113.6(15)	C11C11'C9'	102.8(2)
C10'C10H10b	114.5(15)	C11C11'H11a'	112.2(16)
H10aC10H10b	102(2)	C11C11'H11b'	110.9(16)
C9C11C11'	102.9(2)	C9'C11'H11a'	113.4(16)
C9C11H11a	113.1(18)	C9'C11'H11b'	109.3(16)
C9C11H11b	107.8(17)	H11a'C11'H11b'	108(2)
C11'C11H11a	111.9(18)	N'C12'C13'	106.6(2)
C11'C11H11b	112.5(16)	N'C12'C14'	106.7(2)
H11aC11H11b	108(2)	N'C12'C15'	113.2(2)
NC12C13	108.7(2)	C13'C12'C14'	110.7(2)
NC12C14	106.4(2)	C13'C12'C15'	108.0(3)
NC12C15	110.6(2)	C14'C12'C15'	111.5(3)
C13C12C14	109.8(2)	C12'C13'H13a'	106.8(15)
C13C12C15	112.5(3)	C12'C13'H13b'	111.9(17)
C14C12C15	108.7(2)	C12'C13'H13c'	111.5(18)
C12C13H13a	110.4(18)	H13a'C13'H13b'	111(2)
C12C13H13b	108.3(18)	H13a'C13'H13c'	108(2)
C12C13H13c	112.7(19)	H13b'C13'H13c'	106(3)
H13aC13H13b	107(3)	C12'C14'H14a'	109.3(19)
H13aC13H13c	110(3)	C12'C14'H14b'	107.6(19)
H13bC13H13c	106(3)	C12'C14'H14c'	108.7(18)
C12C14H14a	107.4(19)	H14a'C14'H14b'	109(3)
C12C14H14b	112.4(17)	H14a'C14'H14c'	111(3)

C12C14H14c	106.2(18)	H14b'C14'H14c'	109(3)
H14aC14H14b	105(3)	C12'C15'H15a'	112(2)
H14aC14H14c	113(3)	C12'C15'H15b'	108(2)
H14bC14H14c	112(3)	C12'C15'H15c'	107.8(17)
C12C15H15a	109(2)	H15a'C15'H15b'	111(3)
C12C15H15b	111.2(18)	H15a'C15'H15c'	102(3)
C12C15H15c	108.5(17)	H15b'C15'H15c'	113(3)

Table 4. Anisotropic displacement parameters (Å^2x10^3) for 4(PhNit)$_2$.
   The anisotropic displacement factor exponent takes the form: $-2p^2[h^2a^{*2}U_{11}+...+2hka^*b^*U_{12}]$

Atom	U_{11}	U_{22}	U_{33}	U_{12}	U_{13}	U_{23}
O	.0141(11)	.0522(14)	.0306(12)	.0074(10)	.0046(9)	.0163(11)
N	.0130(13)	.0289(13)	.0195(13)	.0062(10)	.0021(10)	.0066(10)
C1	.0125(14)	.0176(14)	.0228(16)	.0035(11)	.0037(11)	.0086(12)
C2	.0125(14)	.0179(14)	.0223(15)	.0061(11)	.0048(11)	.0085(12)
C3	.0125(14)	.0114(13)	.0215(15)	-.0005(11)	-.0002(11)	.0040(11)
C4	.0192(15)	.0179(14)	.0149(15)	.0054(12)	.0063(12)	.0042(11)
C5	.0137(15)	.0192(14)	.0232(16)	.0058(12)	.0040(12)	.0072(12)
C6	.0152(14)	.0156(14)	.0169(14)	.0010(11)	-.0018(11)	.0048(11)
C7	.0172(15)	.0196(15)	.0188(15)	.0044(12)	.0055(12)	.0063(12)
C8	.0118(14)	.0190(15)	.0269(16)	.0051(12)	.0044(12)	.0075(12)
C9	.0213(15)	.0182(14)	.0161(14)	.0072(12)	.0034(12)	.0077(12)
C10	.0245(17)	.0155(15)	.0224(16)	.0032(12)	.0065(13)	.0043(13)
C11	.0219(17)	.0221(16)	.0228(16)	.0086(13)	.0068(13)	.0069(13)
C12	.0189(15)	.0241(15)	.0171(14)	.0015(12)	.0000(12)	.0082(12)
C13	.0293(19)	.0290(18)	.0244(17)	.0034(15)	.0067(14)	.0075(14)
C14	.0203(18)	.0361(19)	.0301(19)	.0066(15)	-.0012(14)	.0153(16)
C15	.0261(18)	.0297(18)	.0314(19)	-.0007(14)	-.0006(15)	.0158(16)
O'	.0105(10)	.0242(11)	.0333(12)	.0049(8)	.0061(8)	.0075(9)
N'	.0113(12)	.0174(12)	.0241(13)	.0041(9)	.0021(10)	.0054(10)
C3'	.0187(15)	.0172(14)	.0145(14)	.0052(11)	.0040(11)	.0074(11)
C4'	.0146(14)	.0167(14)	.0174(14)	.0010(12)	-.0004(11)	.0047(12)
C5'	.0106(15)	.0196(14)	.0186(15)	.0040(12)	.0008(12)	.0059(12)
C6'	.0155(14)	.0148(13)	.0201(14)	.0055(11)	.0066(12)	.0070(11)
C7'	.0150(15)	.0147(14)	.0205(15)	.0003(12)	.0017(12)	.0036(12)
C8'	.0106(14)	.0200(15)	.0204(15)	.0030(11)	.0011(12)	.0043(12)
C9'	.0195(15)	.0170(15)	.0205(15)	.0073(12)	.0050(12)	.0067(12)
C10'	.0206(16)	.0223(15)	.0192(17)	.0066(12)	.0046(13)	.0047(12)
C11'	.0192(16)	.0254(17)	.0234(17)	.0024(13)	.0037(13)	.0089(13)
C12'	.0127(14)	.0138(13)	.0299(16)	.0019(11)	.0014(12)	.0070(12)
C13'	.0235(18)	.0181(16)	.0274(18)	.0040(13)	.0019(14)	.0072(13)
C14'	.042(2)	.0184(17)	.0293(19)	-.0029(15)	-.0065(16)	.0051(14)
C15'	.0213(18)	.0233(19)	.083(3)	.0043(14)	.0164(19)	.027(2)

Table 5. Hydrogen coordinates (x10^4) and isotropic displacement parameters (Å^2x10^3) for 4(PhNit)$_2$.

Atoms	x	y	z	Ueq
H4	.361(4)	.301(2)	.2040(16)	.010(6)
H5	.562(5)	.268(2)	.3206(15)	.016(7)
H7	.070(4)	.377(2)	.4421(15)	.003(6)
H8	-.120(5)	.413(2)	.3252(16)	.017(7)

H9	.054(4)	.147(2)	.1120(15)	.009(6)
H10a	-.179(4)	.060(2)	-.0286(15)	.010(7)
H10b	-.312(4)	.100(2)	.0337(15)	.010(7)
H11a	.345(6)	.230(3)	.0577(19)	.037(9)
H11b	.187(4)	.142(3)	-.0199(18)	.020(7)
H13a	.351(5)	.371(3)	.642(2)	.034(9)
H13b	.534(5)	.438(3)	.6090(18)	.030(9)
H13c	.283(6)	.437(3)	.571(2)	.045(10)
H14a	.604(6)	.132(3)	.524(2)	.050(11)
H14b	.733(5)	.255(3)	.5811(17)	.026(8)
H14c	.544(5)	.188(3)	.616(2)	.039(9)
H15a	.067(6)	.229(3)	.488(2)	.060(12)
H15b	.203(5)	.111(3)	.4611(19)	.033(9)
H15c	.158(5)	.161(3)	.5520(18)	.023(8)
H4'	-.423(4)	.440(2)	.1254(16)	.016(7)
H5'	-.558(5)	.633(2)	.1554(16)	.017(7)
H7'	.035(4)	.793(2)	.2867(15)	.010(7)
H8'	.176(5)	.611(2)	.2656(16)	.020(7)
H9'	-.138(4)	.419(2)	.0215(15)	.010(7)
H10a'	-.423(5)	.251(2)	-.0274(17)	.022(7)
H10b'	-.252(4)	.216(2)	-.0856(15)	.005(6)
H11a'	.115(4)	.310(2)	-.0639(18)	.018(7)
H11b'	.234(5)	.398(3)	.0211(17)	.024(8)
H13a'	-.330(5)	1.114(3)	.2010(16)	.022(7)
H13b'	-.415(5)	.979(3)	.1338(20)	.033(9)
H13c'	-.543(6)	1.026(3)	.2013(18)	.030(9)
H14a'	-.405(6)	1.036(3)	.346(2)	.049(11)
H14b'	-.160(6)	.997(3)	.369(2)	.044(10)
H14c'	-.177(5)	1.121(3)	.3453(18)	.036(9)
H15a'	.088(6)	.958(3)	.271(2)	.053(11)
H15b'	-.032(6)	.920(3)	.178(2)	.048(12)
H15c'	.027(5)	1.060(3)	.2306(17)	.028(8)

Structure Determination.

Brown plates of **flat2** (**6(Nit$_2$)**) were crystallized from dichloromethane/pentane at 23 deg. C. A crystal of dimensions 0.24 x 0.12 x 0.06 mm was mounted on a standard Bruker SMART CCD-based X-ray diffractometer equipped with a LT-2 low temperature device and normal focus Mo-target X-ray tube (λ = 0.71073 A) operated at 2000 W power (50 kV, 40 mA). The X-ray intensities were measured at 158(2) K; the detector was placed at a distance 5.058 cm from the crystal. A total of 2862 frames were collected with a scan width of 0.3° in ω and phi with an exposure time of 75 s/frame. The frames were integrated with the Bruker SAINT software package with a narrow frame algorithm. The integration of the data yielded a total of 28025 reflections to a maximum 2θ value of 52.92° of which 3524 were independent and 2083 were greater than $2\sigma(I)$. The final cell constants (Table 1) were based on the xyz centroids of 910 reflections above $10\sigma(I)$. Analysis of the data showed negligible decay during data collection. The data were processed with SADABS, no correction for absorption was necessary. The structure was solved and refined with the Bruker SHELXTL (version 5.10) software package using the space group P2/c with Z = 4 for the formula $C_{28}H_{36}N_2O_2$. All non-hydrogen atoms were refined anisotropically with the hydrogen atoms placed in idealized positions. Full matrix least-squares refinement based on F^2 converged at R1 =

0.0584 and wR2 = 0.1330 [based on I > 2sigma(I)], R1 = 0.1185 and wR2 = 0.1642 for all data. Additional details are presented in Table 1 and are given as Supporting Information in a CIF file.

Sheldrick, G.M. SHELXTL, v. 5.10; Bruker Analytical X-ray, Madison, WI, 1997.
Sheldrick, G.M. SADABS. Program for Empirical Absorption Correction of Area Detector Data, University of Gottingen: Gottingen, Germany, 1996.
Saint Plus, v. 6.02, Bruker Analytical X-ray, Madison, WI, 1999.

Table S11. Crystal data and structure refinement for flat2 (**6(Nit$_2$)**).

Identification code	flat2
Empirical formula	C28 H36 N2 O2
Formula weight	432.59
Temperature	158(2) K
Wavelength	0.71073 Å
Crystal system, space group	Monoclinic, P2/c
Unit cell dimensions	a = 15.034(2) Å alpha = 90 deg.
	b = 8.4086(11) Å beta = 94.592(5) deg.
	c = 19.420(3) Å gamma = 90 deg.
Volume	2447.1(6) A^3
Z, Calculated density	4, 1.174 Mg/m^3
Absorption coefficient	0.073 mm^-1
F(000)	936
Crystal size	0.06 x 0.12 x 0.24 mm
Theta range for data collection	2.10 to 23.25 deg.
Limiting indices	-16<=h<=16, -9<=k<=9, -21<=l<=21
Reflections collected / unique	28025 / 3524 [R(int) = 0.0406]
Completeness to theta = 23.25	99.9 %
Absorption correction	None
Refinement method	Full-matrix least-squares on F^2
Data / restraints / parameters	3524 / 0 / 301
Goodness-of-fit on F^2	0.983
Final R indices [I>2sigma(I)]	R1 = 0.0584, wR2 = 0.1330
R indices (all data)	R1 = 0.1185, wR2 = 0.1642
Extinction coefficient	0.038(3)
Largest diff. peak and hole	0.323 and -0.264 e.A^-3

Table S12. Atomic coordinates (x 10^4) and equivalent isotropic displacement parameters (A^2 x 10^3) for flat2 (**6(Nit$_2$)**).

U(eq) is defined as one third of the trace of the orthogonalized Uij tensor.

	x	y	z	U(eq)
O(1)	5551(1)	5053(3)	5579(1)	40(1)
O(2)	666(2)	14226(3)	8479(1)	51(1)
N(1)	4715(2)	4640(3)	5631(1)	31(1)
N(2)	1480(2)	14381(3)	8320(2)	34(1)
C(1)	4549(2)	2926(4)	5808(2)	34(1)
C(2)	3597(2)	2475(5)	5558(2)	54(1)
C(3)	5200(3)	1889(4)	5456(2)	45(1)
C(4)	4699(3)	2747(5)	6591(2)	44(1)
C(5)	4180(2)	5865(4)	5917(2)	29(1)
C(6)	4531(2)	6729(4)	6486(2)	32(1)
C(7)	4041(2)	7925(4)	6762(2)	30(1)
C(8)	3188(2)	8266(4)	6458(2)	27(1)
C(9)	2527(2)	9444(4)	6618(2)	27(1)

C(10)	2410(2)	10695(4)	7115(2)	27(1)
C(11)	2933(2)	11211(4)	7700(2)	30(1)
C(12)	2629(2)	12442(4)	8088(2)	32(1)
C(13)	1810(2)	13163(4)	7900(2)	27(1)
C(14)	1273(2)	12644(4)	7320(2)	28(1)
C(15)	1577(2)	11422(4)	6934(2)	27(1)
C(16)	1119(2)	10625(4)	6281(2)	27(1)
C(17)	1803(2)	9355(4)	6146(2)	28(1)
C(18)	1912(2)	8051(4)	5621(2)	28(1)
C(19)	2840(2)	7400(4)	5876(2)	26(1)
C(20)	3324(2)	6214(4)	5603(2)	28(1)
C(21)	972(2)	11836(4)	5691(2)	34(1)
C(22)	214(2)	9918(4)	6452(2)	32(1)
C(23)	1936(2)	8672(4)	4881(2)	38(1)
C(24)	1199(2)	6736(4)	5641(2)	35(1)
C(25)	1832(2)	16056(4)	8351(2)	31(1)
C(26)	1288(3)	16992(5)	7799(2)	50(1)
C(27)	1696(3)	16713(5)	9062(2)	46(1)
C(28)	2815(2)	16122(5)	8210(2)	48(1)

Table S13. Bond lengths [A] and angles [deg] for flat2 (**6(Nit$_2$)**).

O(1)-N(1)	1.316(3)
O(2)-N(2)	1.292(3)
N(1)-C(5)	1.445(4)
N(1)-C(1)	1.507(4)
N(2)-C(13)	1.423(4)
N(2)-C(25)	1.504(4)
C(1)-C(3)	1.515(5)
C(1)-C(2)	1.522(5)
C(1)-C(4)	1.527(5)
C(5)-C(6)	1.391(5)
C(5)-C(20)	1.409(4)
C(6)-C(7)	1.380(5)
C(7)-C(8)	1.399(4)
C(8)-C(19)	1.410(4)
C(8)-C(9)	1.454(4)
C(9)-C(17)	1.368(4)
C(9)-C(10)	1.447(5)
C(10)-C(11)	1.399(4)
C(10)-C(15)	1.413(4)
C(11)-C(12)	1.380(5)
C(12)-C(13)	1.395(4)
C(13)-C(14)	1.402(4)
C(14)-C(15)	1.372(4)
C(15)-C(16)	1.548(4)
C(16)-C(17)	1.520(5)
C(16)-C(21)	1.534(4)
C(16)-C(22)	1.545(4)
C(17)-C(18)	1.515(5)
C(18)-C(23)	1.531(5)
C(18)-C(19)	1.542(4)

C(18)-C(24)	1.544(5)
C(19)-C(20)	1.367(4)
C(25)-C(26)	1.516(5)
C(25)-C(27)	1.516(5)
C(25)-C(28)	1.525(5)
O(1)-N(1)-C(5)	114.0(3)
O(1)-N(1)-C(1)	116.5(2)
C(5)-N(1)-C(1)	119.1(3)
O(2)-N(2)-C(13)	116.3(3)
O(2)-N(2)-C(25)	115.0(3)
C(13)-N(2)-C(25)	124.0(3)
N(1)-C(1)-C(3)	108.9(3)
N(1)-C(1)-C(2)	109.6(3)
C(3)-C(1)-C(2)	109.8(3)
N(1)-C(1)-C(4)	107.9(3)
C(3)-C(1)-C(4)	110.1(3)
C(2)-C(1)-C(4)	110.6(3)
C(6)-C(5)-C(20)	120.7(3)
C(6)-C(5)-N(1)	119.3(3)
C(20)-C(5)-N(1)	120.0(3)
C(7)-C(6)-C(5)	120.6(3)
C(6)-C(7)-C(8)	119.1(3)
C(7)-C(8)-C(19)	120.1(3)
C(7)-C(8)-C(9)	132.1(3)
C(19)-C(8)-C(9)	107.9(3)
C(17)-C(9)-C(10)	110.7(3)
C(17)-C(9)-C(8)	109.9(3)
C(10)-C(9)-C(8)	139.3(3)
C(11)-C(10)-C(15)	119.8(3)
C(11)-C(10)-C(9)	132.7(3)
C(15)-C(10)-C(9)	107.5(3)
C(12)-C(11)-C(10)	119.2(3)
C(11)-C(12)-C(13)	120.5(3)
C(12)-C(13)-C(14)	121.0(3)
C(12)-C(13)-N(2)	120.2(3)
C(14)-C(13)-N(2)	118.7(3)
C(15)-C(14)-C(13)	118.4(3)
C(14)-C(15)-C(10)	121.1(3)
C(14)-C(15)-C(16)	128.8(3)
C(10)-C(15)-C(16)	110.1(3)
C(17)-C(16)-C(21)	113.4(3)
C(17)-C(16)-C(22)	112.7(3)
C(21)-C(16)-C(22)	109.8(3)
C(17)-C(16)-C(15)	100.5(3)
C(21)-C(16)-C(15)	110.6(3)
C(22)-C(16)-C(15)	109.4(3)
C(9)-C(17)-C(18)	111.5(3)
C(9)-C(17)-C(16)	111.1(3)
C(18)-C(17)-C(16)	137.4(3)
C(17)-C(18)-C(23)	113.4(3)
C(17)-C(18)-C(19)	100.7(3)
C(23)-C(18)-C(19)	109.5(3)
C(17)-C(18)-C(24)	112.8(3)

C(23)-C(18)-C(24)	109.6(3)
C(19)-C(18)-C(24)	110.5(3)
C(20)-C(19)-C(8)	120.9(3)
C(20)-C(19)-C(18)	129.1(3)
C(8)-C(19)-C(18)	110.0(3)
C(19)-C(20)-C(5)	118.7(3)
N(2)-C(25)-C(26)	106.8(3)
N(2)-C(25)-C(27)	107.8(3)
C(26)-C(25)-C(27)	110.6(3)
N(2)-C(25)-C(28)	111.7(3)
C(26)-C(25)-C(28)	109.2(3)
C(27)-C(25)-C(28)	110.7(3)

Symmetry transformations used to generate equivalent atoms:

Table S14. Anisotropic displacement parameters (A^2 x 10^3) for flat2. (**6(Nit₂)**)
The anisotropic displacement factor exponent takes the form: -2 pi^2 [h^2 a*^2 U11 + ... + 2 h k a* b* U12]

	U11	U22	U33	U23	U13	U12
O(1)	14(1)	47(2)	57(2)	-7(1)	-4(1)	2(1)
O(2)	22(2)	63(2)	71(2)	-21(2)	10(1)	-7(1)
N(1)	16(2)	39(2)	35(2)	-2(1)	-4(1)	4(1)
N(2)	13(2)	44(2)	44(2)	-5(2)	-1(1)	-2(1)
C(1)	18(2)	34(2)	49(2)	2(2)	-9(2)	-3(2)
C(2)	36(2)	45(3)	77(3)	11(2)	-19(2)	-14(2)
C(3)	47(3)	36(2)	52(3)	-7(2)	-6(2)	6(2)
C(4)	38(2)	44(2)	50(3)	4(2)	-1(2)	5(2)
C(5)	17(2)	34(2)	36(2)	-4(2)	-3(2)	2(2)
C(6)	15(2)	42(2)	38(2)	-4(2)	-9(2)	4(2)
C(7)	19(2)	36(2)	34(2)	-3(2)	-9(2)	3(2)
C(8)	14(2)	32(2)	34(2)	0(2)	-5(2)	3(2)
C(9)	15(2)	36(2)	29(2)	0(2)	-5(2)	-1(2)
C(10)	14(2)	34(2)	31(2)	0(2)	-4(2)	2(2)
C(11)	15(2)	41(2)	33(2)	-2(2)	-9(2)	1(2)
C(12)	19(2)	42(2)	31(2)	-3(2)	-9(2)	0(2)
C(13)	18(2)	33(2)	31(2)	-7(2)	0(2)	0(2)
C(14)	17(2)	34(2)	33(2)	-1(2)	-3(2)	1(2)
C(15)	19(2)	30(2)	32(2)	6(2)	-3(2)	-4(2)
C(16)	15(2)	33(2)	33(2)	-2(2)	-4(2)	-1(2)
C(17)	16(2)	36(2)	31(2)	1(2)	-4(2)	-1(2)
C(18)	13(2)	38(2)	30(2)	0(2)	-9(2)	5(2)
C(19)	13(2)	31(2)	34(2)	-1(2)	-5(2)	-1(2)
C(20)	20(2)	33(2)	30(2)	-5(2)	-7(2)	-1(2)
C(21)	23(2)	41(2)	36(2)	4(2)	-5(2)	2(2)
C(22)	14(2)	41(2)	39(2)	-1(2)	-5(2)	-1(2)
C(23)	28(2)	46(2)	38(2)	-4(2)	-9(2)	10(2)
C(24)	19(2)	43(2)	42(2)	-8(2)	-5(2)	0(2)
C(25)	26(2)	29(2)	37(2)	-1(2)	-3(2)	0(2)
C(26)	42(3)	57(3)	48(3)	8(2)	-10(2)	7(2)
C(27)	45(3)	47(3)	43(2)	-8(2)	-6(2)	1(2)
C(28)	25(2)	42(2)	75(3)	2(2)	2(2)	-4(2)

Table S15. Hydrogen coordinates (x 10^4) and isotropic displacement parameters (A^2 x 10^3) for flat2 (**6(Nit$_2$)**).

	x	y	z	U(eq)
H(2A)	3178	3131	5796	51(2)
H(2B)	3496	1351	5660	51(2)
H(2C)	3503	2653	5059	51(2)
H(3A)	5099	2014	4954	51(2)
H(3B)	5110	774	5580	51(2)
H(3C)	5812	2207	5606	51(2)
H(4A)	5293	3148	6748	51(2)
H(4B)	4654	1622	6716	51(2)
H(4C)	4245	3357	6813	51(2)
H(6)	5113	6493	6686	51(2)
H(7)	4281	8509	7153	51(2)
H(11)	3491	10720	7829	51(2)
H(12)	2979	12800	8487	51(2)
H(14)	711	13128	7197	51(2)
H(20)	3089	5635	5210	51(2)
H(21A)	1545	12305	5595	51(2)
H(21B)	569	12677	5827	51(2)
H(21C)	707	11301	5276	51(2)
H(22A)	-60	9354	6046	51(2)
H(22B)	-183	10777	6578	51(2)
H(22C)	309	9174	6839	51(2)
H(23A)	1354	9130	4727	51(2)
H(23B)	2070	7792	4575	51(2)
H(23C)	2398	9490	4868	51(2)
H(24A)	1186	6340	6114	51(2)
H(24B)	1345	5861	5336	51(2)
H(24C)	613	7173	5484	51(2)
H(26A)	1389	16560	7343	51(2)
H(26B)	1471	18111	7822	51(2)
H(26C)	653	16911	7875	51(2)
H(27A)	1062	16658	9144	51(2)
H(27B)	1895	17823	9090	51(2)
H(27C)	2044	16083	9413	51(2)
H(28A)	3171	15540	8572	51(2)
H(28B)	3012	17233	8206	51(2)
H(28C)	2893	15636	7760	51(2)

Structure Determination.

Orange plates of **flor2** (**7(PhNit)$_2$**) were crystallized from methanol/pentane at 23 deg. C. A crystal of dimensions 0.24 x 0.22 x 0.20 mm was mounted on a standard Bruker SMART CCD-based X-ray diffractometer equipped with a LT-2 low temperature device and normal focus Mo-target X-ray tube (λ = 0.71073 A) operated at 2000 W power (50 kV, 40 mA). The X-ray intensities were measured at 158(2) K; the detector was placed at a distance 5.008 cm from the crystal. A total of 3332 frames were collected with a scan width of 0.3° in ω and phi with an exposure time of 75 s/frame. The frames were integrated with the Bruker SAINT software package with a narrow frame algorithm. The integration of the data yielded a total of 45865 reflections to a maximum 2θ value of 42.0° of which 3007 were independent and 1979 were

greater than 2σ(I). The final cell constants (Table 1) were based on the xyz centroids of 5901 reflections above 10σ(I). Analysis of the data showed negligible decay during data collection. The data were processed with SADABS, no correction for absorption was necessary. The structure was solved and refined with the Bruker SHELXTL (version 5.10) software package using the space group Pbca with Z = 8 for the formula $C_{33}H_{34}N_2O_2$. All non-hydrogen atoms were refined anisotropically with the hydrogen atoms placed in idealized positions. Full matrix least-squares refinement based on F^2 converged at R1 = 0.0708 and wR2 = 0.1737 [based on I > 2sigma(I)], R1 = 0.1010 and wR2 = 0.1896 for all data. Additional details are presented in Table 1 and are given as Supporting Information in a CIF file.

Sheldrick, G.M. SHELXTL, v. 5.10; Bruker Analytical X-ray, Madison, WI, 1997.

Sheldrick, G.M. SADABS. Program for Empirical Absorption Correction of Area Detector Data, University of Gottingen: Gottingen, Germany, 1996.

Saint Plus, v. 6.02, Bruker Analytical X-ray, Madison, WI, 1999.

Table S16. Crystal data and structure refinement for flor2 (**7(PhNit)₂**).

Identification code	flor2
Empirical formula	C33 H34 N2 O2
Formula weight	490.62
Temperature	158(2) K
Wavelength	0.71073 A
Crystal system, space group	Orthorhombic, Pbca
Unit cell dimensions	a = 12.087(5) A alpha = 90 deg.
	b = 19.740(9) A beta = 90 deg.
	c = 23.655(10) A gamma = 90 deg.
Volume	5644(4) A^3
Z, Calculated density	8, 1.155 Mg/m^3
Absorption coefficient	0.072 mm^-1
F(000)	2096
Crystal size	0.20 x 0.22 x 0.24 mm
Theta range for data collection	1.72 to 21.00 deg.
Limiting indices	-12<=h<=12, -19<=k<=19, -23<=l<=23
Reflections collected / unique	45865 / 3007 [R(int) = 0.0885]
Completeness to theta = 21.00	99.3 %
Absorption correction	None
Refinement method	Full-matrix least-squares on F^2
Data / restraints / parameters	3007 / 0 / 342
Goodness-of-fit on F^2	0.966
Final R indices [I>2sigma(I)]	R1 = 0.0718, wR2 = 0.1737
R indices (all data)	R1 = 0.1010, wR2 = 0.1896
Extinction coefficient	0.0078(11)
Largest diff. peak and hole	0.305 and -0.304 e.A^-3

Table S17. Atomic coordinates (x 10^4) and equivalent isotropic displacement parameters (A^2 x 10^3) for flor2 (**7(PhNit)₂**).

U(eq) is defined as one third of the trace of the orthogonalized Uij tensor.

	x	y	z	U(eq)
N(1)	5492(3)	1884(2)	7226(2)	46(1)
N(2)	7992(3)	690(2)	3502(2)	50(1)
O(1)	6286(3)	1469(2)	7382(2)	79(1)
O(2)	8813(3)	1115(2)	3540(2)	77(1)
C(1)	5333(4)	2512(2)	7604(2)	45(1)
C(2)	4091(4)	2612(3)	7730(2)	66(2)
C(3)	5848(4)	3133(2)	7299(2)	56(1)

C(4)	5954(4)	2386(2)	8161(2)	57(1)
C(5)	5040(3)	1772(2)	6677(2)	38(1)
C(6)	5347(3)	1166(2)	6387(2)	39(1)
C(7)	5074(3)	1082(2)	5819(2)	38(1)
C(8)	4459(3)	1574(2)	5513(2)	38(1)
C(9)	4078(3)	2138(2)	5835(2)	39(1)
C(10)	4347(3)	2235(2)	6395(2)	38(1)
C(11)	4216(3)	1503(2)	4878(2)	37(1)
C(12)	5207(3)	1213(2)	4538(2)	38(1)
C(13)	6303(4)	1432(2)	4660(2)	41(1)
C(14)	7195(3)	1246(2)	4321(2)	43(1)
C(15)	7037(3)	839(2)	3839(2)	40(1)
C(16)	5962(3)	613(2)	3711(2)	43(1)
C(17)	5066(3)	806(2)	4052(2)	40(1)
C(18)	8171(4)	56(2)	3144(2)	47(1)
C(19)	7604(4)	135(2)	2575(2)	72(2)
C(20)	7758(4)	-575(2)	3478(2)	62(2)
C(21)	9432(4)	-21(2)	3048(2)	70(2)
C(22)	3912(4)	2198(2)	4597(2)	40(1)
C(23)	4561(4)	2781(2)	4564(2)	47(1)
C(24)	4119(4)	3355(2)	4287(2)	52(1)
C(25)	3074(4)	3329(2)	4042(2)	51(1)
C(26)	2422(4)	2745(2)	4072(2)	48(1)
C(27)	2854(3)	2172(2)	4354(2)	42(1)
C(28)	2350(3)	1495(2)	4478(2)	40(1)
C(29)	1308(4)	1230(2)	4340(2)	49(1)
C(30)	1050(4)	569(2)	4513(2)	53(1)
C(31)	1828(4)	175(2)	4806(2)	49(1)
C(32)	2871(3)	440(2)	4944(2)	44(1)
C(33)	3138(3)	1101(2)	4775(2)	36(1)

Table S18. Bond lengths [A] and angles [deg] for flor2 (**7(PhNit)₂**).

N(1)-O(1)	1.316(4)
N(1)-C(5)	1.426(5)
N(1)-C(1)	1.540(5)
N(2)-O(2)	1.303(4)
N(2)-C(15)	1.434(5)
N(2)-C(18)	1.526(5)
C(1)-C(4)	1.537(6)
C(1)-C(2)	1.543(6)
C(1)-C(3)	1.553(6)
C(5)-C(10)	1.408(5)
C(5)-C(6)	1.428(5)
C(6)-C(7)	1.393(6)
C(7)-C(8)	1.420(5)
C(8)-C(9)	1.426(6)
C(8)-C(11)	1.539(6)
C(9)-C(10)	1.378(6)
C(11)-C(33)	1.544(6)
C(11)-C(12)	1.553(6)
C(11)-C(22)	1.567(6)
C(12)-C(17)	1.412(5)

C(12)-C(13)	1.423(6)
C(13)-C(14)	1.394(6)
C(14)-C(15)	1.407(6)
C(15)-C(16)	1.407(6)
C(16)-C(17)	1.404(6)
C(18)-C(19)	1.519(6)
C(18)-C(21)	1.548(6)
C(18)-C(20)	1.556(6)
C(22)-C(23)	1.396(6)
C(22)-C(27)	1.402(6)
C(23)-C(24)	1.413(6)
C(24)-C(25)	1.391(6)
C(25)-C(26)	1.399(6)
C(26)-C(27)	1.414(6)
C(27)-C(28)	1.496(6)
C(28)-C(29)	1.403(6)
C(28)-C(33)	1.418(6)
C(29)-C(30)	1.402(6)
C(30)-C(31)	1.404(6)
C(31)-C(32)	1.404(6)
C(32)-C(33)	1.403(5)
O(1)-N(1)-C(5)	116.0(3)
O(1)-N(1)-C(1)	115.4(3)
C(5)-N(1)-C(1)	127.3(3)
O(2)-N(2)-C(15)	116.3(3)
O(2)-N(2)-C(18)	117.3(3)
C(15)-N(2)-C(18)	126.3(3)
C(4)-C(1)-N(1)	107.8(3)
C(4)-C(1)-C(2)	109.2(4)
N(1)-C(1)-C(2)	109.7(4)
C(4)-C(1)-C(3)	109.3(4)
N(1)-C(1)-C(3)	108.4(3)
C(2)-C(1)-C(3)	112.3(4)
C(10)-C(5)-N(1)	123.9(4)
C(10)-C(5)-C(6)	118.0(4)
N(1)-C(5)-C(6)	118.0(4)
C(7)-C(6)-C(5)	120.2(4)
C(6)-C(7)-C(8)	122.2(4)
C(7)-C(8)-C(9)	115.6(4)
C(7)-C(8)-C(11)	122.4(4)
C(9)-C(8)-C(11)	122.1(4)
C(10)-C(9)-C(8)	123.1(4)
C(9)-C(10)-C(5)	120.4(4)
C(8)-C(11)-C(33)	111.2(3)
C(8)-C(11)-C(12)	113.1(3)
C(33)-C(11)-C(12)	112.3(3)
C(8)-C(11)-C(22)	112.3(3)
C(33)-C(11)-C(22)	100.7(3)
C(12)-C(11)-C(22)	106.5(3)
C(17)-C(12)-C(13)	116.8(4)
C(17)-C(12)-C(11)	122.5(4)
C(13)-C(12)-C(11)	120.0(4)
C(14)-C(13)-C(12)	121.5(4)

C(13)-C(14)-C(15)	120.8(4)
C(16)-C(15)-C(14)	118.8(4)
C(16)-C(15)-N(2)	123.9(4)
C(14)-C(15)-N(2)	117.3(4)
C(17)-C(16)-C(15)	120.1(4)
C(16)-C(17)-C(12)	121.9(4)
C(19)-C(18)-N(2)	110.1(3)
C(19)-C(18)-C(21)	108.9(4)
N(2)-C(18)-C(21)	107.6(3)
C(19)-C(18)-C(20)	112.7(4)
N(2)-C(18)-C(20)	109.2(4)
C(21)-C(18)-C(20)	108.2(4)
C(23)-C(22)-C(27)	121.4(4)
C(23)-C(22)-C(11)	127.8(4)
C(27)-C(22)-C(11)	110.8(4)
C(22)-C(23)-C(24)	118.3(4)
C(25)-C(24)-C(23)	120.5(4)
C(24)-C(25)-C(26)	121.3(4)
C(25)-C(26)-C(27)	118.4(4)
C(22)-C(27)-C(26)	120.1(4)
C(22)-C(27)-C(28)	109.0(4)
C(26)-C(27)-C(28)	130.9(4)
C(29)-C(28)-C(33)	120.9(4)
C(29)-C(28)-C(27)	130.9(4)
C(33)-C(28)-C(27)	108.2(3)
C(30)-C(29)-C(28)	118.6(4)
C(29)-C(30)-C(31)	120.8(4)
C(30)-C(31)-C(32)	120.6(4)
C(33)-C(32)-C(31)	119.2(4)
C(32)-C(33)-C(28)	119.8(4)
C(32)-C(33)-C(11)	128.9(4)
C(28)-C(33)-C(11)	111.2(3)

Symmetry transformations used to generate equivalent atoms:

Table S19. Anisotropic displacement parameters (A^2 x 10^3) for flor2 (**7(PhNit)₂**).
The anisotropic displacement factor exponent takes the form: -2 pi^2 [h^2 a*^2 U11 + ... + 2 h k a* b* U12]

	U11	U22	U33	U23	U13	U12
N(1)	43(2)	25(2)	70(3)	2(2)	-4(2)	7(2)
N(2)	32(2)	28(2)	89(3)	-11(2)	14(2)	-6(2)
O(1)	90(3)	49(2)	97(3)	-10(2)	-28(2)	30(2)
O(2)	46(2)	45(2)	138(3)	-21(2)	31(2)	-24(2)
C(1)	37(3)	36(3)	63(3)	-6(2)	6(2)	2(2)
C(2)	50(4)	72(4)	75(4)	-4(3)	6(3)	9(3)
C(3)	37(3)	35(3)	94(4)	1(2)	-6(3)	-6(2)
C(4)	57(3)	48(3)	66(3)	-9(2)	-6(3)	3(3)
C(5)	27(3)	29(3)	59(3)	5(2)	-2(2)	2(2)
C(6)	30(3)	20(2)	66(3)	4(2)	2(2)	2(2)
C(7)	26(3)	21(2)	69(3)	0(2)	1(2)	-1(2)
C(8)	19(2)	23(2)	71(3)	2(2)	3(2)	-1(2)

C(9)	27(3)	27(2)	64(3)	3(2)	5(2)	9(2)
C(10)	23(2)	29(2)	62(3)	-5(2)	6(2)	1(2)
C(11)	26(3)	23(2)	62(3)	2(2)	1(2)	6(2)
C(12)	30(3)	22(2)	62(3)	1(2)	-1(2)	5(2)
C(13)	33(3)	22(2)	68(3)	-3(2)	-3(2)	1(2)
C(14)	26(3)	25(2)	79(3)	2(2)	-1(2)	0(2)
C(15)	29(3)	24(2)	68(3)	-1(2)	5(2)	1(2)
C(16)	33(3)	24(2)	71(3)	-7(2)	0(2)	1(2)
C(17)	27(3)	29(2)	65(3)	-1(2)	-1(2)	1(2)
C(18)	35(3)	33(3)	74(3)	-6(2)	10(2)	2(2)
C(19)	73(4)	63(3)	81(4)	-14(3)	7(3)	13(3)
C(20)	53(3)	32(3)	101(4)	-10(2)	20(3)	-1(2)
C(21)	43(3)	53(3)	115(4)	-17(3)	15(3)	4(3)
C(22)	33(3)	28(3)	60(3)	-5(2)	2(2)	7(2)
C(23)	33(3)	30(3)	77(3)	-3(2)	5(2)	3(2)
C(24)	44(3)	27(3)	84(3)	1(2)	8(3)	10(2)
C(25)	44(3)	34(3)	74(3)	4(2)	6(3)	13(3)
C(26)	34(3)	35(3)	74(3)	2(2)	-2(2)	18(2)
C(27)	28(3)	36(3)	63(3)	-6(2)	1(2)	8(2)
C(28)	24(3)	30(3)	65(3)	-3(2)	1(2)	2(2)
C(29)	32(3)	45(3)	71(3)	-4(2)	-4(2)	6(2)
C(30)	28(3)	45(3)	85(4)	-4(3)	-4(3)	-7(2)
C(31)	35(3)	31(3)	79(3)	1(2)	3(3)	-11(3)
C(32)	31(3)	31(3)	72(3)	-4(2)	2(2)	-5(2)
C(33)	23(3)	23(3)	63(3)	-4(2)	4(2)	0(2)

Table S20. Hydrogen coordinates (x 10^4) and isotropic displacement parameters (A^2 x 10^3) for flor2 (**7(PhNit)₂**).

	x	y	z	U(eq)
H(2A)	3728	2813	7400	70(3)
H(2B)	4005	2914	8056	70(3)
H(2C)	3752	2172	7815	70(3)
H(3A)	6624	3038	7209	70(3)
H(3B)	5805	3531	7546	70(3)
H(3C)	5440	3223	6949	70(3)
H(4A)	5659	1978	8343	70(3)
H(4B)	5855	2776	8412	70(3)
H(4C)	6743	2323	8082	70(3)
H(6)	5738	820	6581	70(3)
H(7)	5307	682	5629	70(3)
H(9)	3616	2462	5655	70(3)
H(10)	4064	2617	6592	70(3)
H(13)	6429	1712	4981	70(3)
H(14)	7918	1395	4416	70(3)
H(16)	5843	329	3392	70(3)
H(17)	4343	658	3954	70(3)
H(19A)	6803	169	2631	70(3)
H(19B)	7770	-259	2338	70(3)
H(19C)	7874	546	2389	70(3)
H(20A)	8114	-587	3850	70(3)
H(20B)	7946	-987	3268	70(3)

H(20C)	6954	-548	3525	70(3)
H(21A)	9712	376	2845	70(3)
H(21B)	9574	-430	2824	70(3)
H(21C)	9807	-60	3414	70(3)
H(23)	5281	2793	4725	70(3)
H(24)	4539	3761	4268	70(3)
H(25)	2798	3716	3850	70(3)
H(26)	1705	2733	3908	70(3)
H(29)	787	1492	4134	70(3)
H(30)	341	386	4431	70(3)
H(31)	1646	-276	4912	70(3)
H(32)	3389	175	5150	70(3)

Bibliography

References Chapter 1.
(1) Jakubovics, J. P. *Magnetism and Magnetic Materials*; Second ed.; Univeristy Press: Cambridge, 1994.
(2) Gatteschi, D., Ed. *Molecular Magnetic Materials*; Kluwer Academic Publishers: Amsterdam, 1991.
(3) Turnbull, M. M.; Sugimoto, T.; Thompson, L. K., Eds. *Molecule-Based Magnetic Materials. Theory, Techniques, and Applications*; ACS: Washington, DC, 1996.
(4) Mattis, D. C. *The Theory of Magnetism*; Harper & Row: New York, 1965.
(5) Drago, R. S. *Physical Methods*.
(6) Kahn, O. *Molecular Magnetism*, 1993.
(7) *Magnetism I - Fundamentals*; Kluwer Academic Publishers: Norwell, 2002.
(8) *Magnetic Molecular Materials*; Kluwer Academic Publishers: Boston, 1991; Vol. 198.
(9) Curie, P. *Ann. Chim. Phys.* **1895**, 289.
(10) Weiss, P. *J. de Phys.* **1907**, 661.
(11) Borden, W. T.; Iwamura, H.; Berson, J. A. *Acc. Chem. Res.* **1994**, *27*, 109.
(12) Borden, W. T., Ed. *Diradicals*; Wiley: New York, 1982.
(13) Gatteschi, D.; Sessoli, R. *J. Magn. Magn. Mat.* **1992**, *104*, 2092.
(14) Iwamura, H. *Pure Appl. Chem.* **1987**, *59*, 1595.
(15) Rajca, A. *Chem. Rev.* **1994**, *94*, 871.
(16) Rajca, A.; Wongsriratanakul, J.; Rajca, S. *Science* **2001**, *294*, 1503.
(17) Gatteschi, D.; Caneschi, A.; Laugier, J.; Rey, P. *J. Am. Chem. Soc.* **1987**, *109*, 2191.
(18) Iwamura, H.; Inoue, K.; Hayamizu, T. *Pure Appl. Chem.* **1996**, *68*, 243.
(19) Caneschi, A.; Gatteschi, D.; Sessoli, R. *Acc. Chem. Res.* **1989**, *22*, 392.
(20) Dougherty, D. A. *Acc. Chem. Res.* **1991**, *24*, 88.
(21) Baclay, T. M.; Hicks, R. G.; Lemaire, M. T.; Thompson, L. K. *Inorg. Chem.* **2003**, *42*, 2261.
(22) Hicks, R. G. *Aust. J. Chem.* **2001**, *54*, 597.
(23) Hicks, R. G.; Lemaire, M. T.; Thompson, L. K.; Baclay, T. M. *J. Am. Chem. Soc.* **2000**, *122*, 8077.
(24) Brook, D. J. R.; Fornell, S.; Stevens, J. E.; Noll, B.; Koch, T. H.; Eisfeld, W. *Inorg. Chem.* **2000**, *39*, 562.
(25) Brook, D. J. R.; Fox, H. H.; Lynch, V.; Fox, M. A. *J. Phys. Chem.* **1996**, *100*, 2066.
(26) Pierpont, C. G.; Attia, A. S. *Coll. Czech. Chem. Comm.* **2001**, *66*, 33.
(27) Pierpont, C. G.; Buchanan, R. M. *Coord. Chem. Rev.* **1981**, *38*, 45.
(28) Pierpont, C. G.; Lange, C. W. *Prog. Inorg. Chem.* **1994**, *41*, 331.

References Chapter 2.
(1) Kahn, O. *Molecular Magnetism*, 1993.
(2) Rajca, A. *Chem. Rev.* **1994**, *94*, 871.

(3) Lowe, J. P. *Quantum Chemistry*; 2nd ed.; Academic Press: New York, 1993.

(4) Alberty, R. A.; Silbey, R. J. *Physical Chemistry*; John Wiley & Sons, Inc.: New York, 1992.

(5) Borden, W. T.; Iwamura, H.; Berson, J. A. *Acc. Chem. Res.* **1994**, *27*, 109.

(6) Hadfield, D. *Permanent Magnets and Magnetism*; Iliffe Books, LTD.: New York, 1962.

(7) Lahti, P. M., Ed. *Magnetic Properties of Organic Materials*; Marcel Dekker: New York, 1999.

(8) Dougherty, D. A. *Acc. Chem. Res.* **1991**, *24*, 88.

(9) Longuett Higgins, H. C. *J. Chem. Phys.* **1950**, *18*, 265.

(10) Borden, W. T.; Davidson, E. R. *J. Am. Chem. Soc.* **1977**, *99*, 4587.

(11) Phelan, N. F. *J. Chem. Ed.* **1968**, *45*, 633.

(12) Berson, J. A., Ed. *The Chemistry of the Quinonoid Compounds, Vol. II*; John Wiley & Sons: New York, 1988.

(13) Kuhn, R.; Trischmann, H. *Angew. Chem., Int. Ed. Eng.* **1963**, *2*, 155.

(14) Kuhn, R.; Neugebauer, F. A.; Trischmann, H. *Angew. Chem., Int. Ed. Eng.* **1964**, *3*, 232.

(15) Hicks, R. G. *Aust. J. Chem.* **2001**, *54*, 597.

(16) Brook, D. J. R.; Fox, H. H.; Lynch, V.; Fox, M. A. *J. Phys. Chem.* **1996**, *100*, 2066.

(17) Fico, R. M., Jr.; Hay, M. F.; Reese, S.; Hammond, S.; Lambert, E.; Fox, M. A. *J. Org. Chem.* **1999**, *64*, 9386.

(18) Pierpont, C. G.; Lange, C. W. *Prog. Inorg. Chem.* **1994**, *41*, 331.

(19) Pierpont, C. G.; Attia, A. S. *Coll. Czech. Chem. Comm.* **2001**, *66*, 33.

(20) Pierpont, C. G.; Buchanan, R. M. *Coord. Chem. Rev.* **1981**, *38*, 45.

(21) Shultz, D. A.; Fico, R. M., Jr.; Bodnar, S. H.; Kumar, R. K.; Vostrikova, K. E.; Kampf, J. W.; Boyle, P. D. **2003**, submitted.

(22) Volodarsky, L. B.; Reznikov, V. A.; Ovvharenko, V. I. *Synthetic Chemistry of Stable Nitroxides*; CRC Press: Boca Raton, 1994.

(23) Shultz, D. A.; Fico, R. M., Jr.; Lee, H.; Kampf, J. W.; Kirschbaum, K.; Pinkerton, A. A.; Boyle, P. D. *J. Am. Chem. Soc.* **2003**, *125*, in press.

References Chapter 3
(1) Gerson, F. *High Resolution E.S.R. Spectroscopy*; John Wiley & Sons Ltd.: New York, 1970; Vol. 1.

(2) Atherton, N. M. *Electron Spin Resonance*; John Wiley & Sons Inc.: New York, 1973.

(3) Assenheim, H. M. *Introduction to Electron Spin Resonance*; Hilget & Watts Ltd.: London, 1966.

(4) Wertz, J. E.; Bolton, J. R. *Electron Spin Resonance*; Chapman and Hall: New York, 1986.

(5) Drago, R. R. *Physical Methods for Chemists*; 2nd ed. ed.; HBJ Saunders: Orlando, 1992.

(6) Rajca, A. *Chem. Rev.* **1994**, *94*, 871.

(7)   Duling, D.; Version 0.96 ed.; Public EPR Software Tools, National Institute of
        Environmental Health Sciences, National Institutes of Health: Triangle Park, NC,
        1996.

(8)   Hanna, M. *Quantum Mechanics in Chemistry*; Hanna, M. Quantum Mechanics in
        Chemistry; The Benjamin/Cummings Publishing Company, Inc.: Menlo Park,
        CA, 1981: Menlo Park, CA, 1981.

(9)   Bersohn, M.; Baird, J. C. *An Introduction to Electron Paramagnetic Resonance*;
        W. A. Benjamin, Inc.: New York, 1966.

(10)   Angiolillo, P. J.; Lin, V. S.-Y.; Vanderkooi, J. M.; Therien, M. J. *J. Am. Chem.
        Soc.* **1995**, *117*, 12514.

(11)   Bruker; 1.25, Shareware Version ed.; Brüker Analytische Messtechnik GmbH,
        1996.

(12)   Berson, J. A., Ed. *The Chemistry of the Quinonoid Compounds, Vol. II*; John
        Wiley & Sons: New York, 1988.

(13)   McElfresh, M. "Fundamentals of Magnetism and Magnetic Measurements,"
        Quantum Design, 1994.

(14)   Jacobs, S. J. In *Chemistry*; California Institute of Technology: Pasadena, 1994.

(15)   Onnes, H. K. "Nobel Prize in Physics," 1913.

(16)   Bardeen, J.; Cooper, N. L.; Schrieffer, J. R. "Nobel Prize in Physics," 1972.

(17)   Josephson, B.; Esaki, I.; Giaever, I. "Nobel Prize in Physics," 1973.

(18)   *Magnetism I - Fundamentals*; Kluwer Academic Publishers: Norwell, 2002.

(19)   Gatteschi, D., Ed. *Molecular Magnetic Materials*; Kluwer Academic Publishers:
        Amsterdam, 1991.

(20)   Gatteschi, D.; Sessoli, R. *J. Magn. Magn. Mat.* **1992**, *104*, 2092.

(21)   Jakubovics, J. P. *Magnetism and Magnetic Materials*; Second ed.; University
        Press: Cambridge, 1994.

(22)   Kahn, O. *Molecular Magnetism*; VCH: New York, 1993.

(23)   Lahti, P. M., Ed. *Magnetic Properties of Organic Materials*; Marcel Dekker: New
        York, 1999.

(24)   Mattis, D. C. *The Theory of Magnetism*; Harper & Row: New York, 1965.

(25)   O'Connor, C. J. *Prog. Inorg. Chem.* **1982**, *29*, 203.

(26)   Turnbull, M. M.; Sugimoto, T.; Thompson, L. K., Eds. *Molecule-Based Magnetic
        Materials. Theory, Techniques, and Applications*; ACS: Washington, DC, 1996.

(27)   Carlin, R. L. *Magnetochemistry*; Springer-Verlag: New York, 1986.

(28)   Curie, P. *Ann. Chim. Phys.* **1895**, 289.

(29)   Van Vleck, J. H. *The Theory of Electric and Magnetic Susceptibilities*; Oxford
        University Press: Oxford, 1932.

(30)   Caneschi, A.; Dei, A.; Mussari, C. P.; Shultz, D. A.; Sorace, L.; Vostrikova, K. E.
        Inorg. Chem. **2002**, *41*, 1086.

References Chapter 4.
(1)   Fico, R. M., Jr.; Hay, M. F.; Reese, S.; Hammond, S.; Lambert, E.; Fox, M. A. *J.
        Org. Chem.* **1999**, *64*, 9386.

(2)   Brook, D. J. R.; Fox, H. H.; Lynch, V.; Fox, M. A. *J. Phys. Chem.* **1996**, *100*, 2066.
(3)   Borden, W. T.; Davidson, E. R. *J. Am. Chem. Soc.* **1977**, *99*, 4587.
(4)   Brook, D. J. R.; Fox, H. H.; Lynch, V.; Fox, M. A. *J. Phys. Chem.* **1996**, *100*, 2066.
(5)   Fischer, H. H. *Tetrahedron* **1967**, *23*, 1939.
(6)   Mukai, K.; Azuma, N.; Shikata, H.; Ishizu, K. *Bull. Chem. Soc. Jpn.* **1970**, *43*, 3958.
(7)   Azuma, N.; Ishizu, K.; Mukai, K. *J. Chem. Phys.* **1974**, *61*, 2294.
(8)   Dowd, P.; Chang, W.; Paik, Y. H. *J. Am. Chem. Soc.* **1987**, *109*, 5284.
(9)   Roth, W. R.; Ruhkamp, J.; Lennartz, H. W. *Chem. Ber.* **1991**, *124*, 2047.
(10)   Roth, W. R.; Kowalczik, U.; Maier, G.; Reisenaur, H. P.; Sustmann, R.; Müller, W. *Angew. Chem., Int. Ed. Eng.* **1987**, *26*, 1285.
(11)   Alies, F.; Luneau, D.; Laugier, J.; Rey, P. *J. Phys. Chem.* **1993**, *97*, 2922.
(12)   Ullmann, E. F.; Boocock, D. G. B. *Chem. Comm.* **1969**, 1161.
(13)   Berson, J. A. *The Chemistry of the Quinonoid Compounds*; Wiley, 1988; Vol. 2, Chapter 10.
(14)   Neugebauer, F. A.; Fischer, H. *Angew. Chem. Int. Ed. Eng.* **1980**, *19*, 724.
(15)   Kuhn, R.; Trischmann, H. *Angew. Chem. Int. Ed. Eng.* **1963**, *2*, 155.
(16)   Katritzky, A. R.; Belyakov, S. A.; Durst, H. D.; Xu, R.; Dalal, N. S. *Can. J. Chem.* **1994**, *72*, 1849.
(17)   Neugebauer, F. A. *Angew. Chem., Int. Ed. Eng.* **1973**, *12*, 455.
(18)   Kuhn, R.; Neugebaur, F. A.; Trischmann, H. *Monatsch.* **1966**, *97*, 525.
(19)   Neugebauer, F. A. *Tetrahedron* **1970**, *26*, 4853.
(20)   Dormann, E.; Winter, H.; Dyakonow, W.; Gotschy, B.; Lang, A.; Naarmann, H.; Walker, N. *Ber. Bunsenges. Phys. Chem.* **1992**, *96*, 922.
(21)   Neugebauer, F. A.; Fischer, H.; Krieger, C. *J. Chem. Soc., Perkin Trans. 2* **1993**, 535.
(22)   Neugebauer, F. A.; Fischer, H.; Siegel, R. *Chem. Ber.* **1988**, *121*, 815.
(23)   Neugebauer, F. A.; Fischer, H.; Krieger, C. *Chem. Ber.* **1983**, *116*, 3461.
(24)   Jaworski, J. S. *Electroanal. Chem.* **1991**, *300*, 167.
(25)   Jaworski, J. S.; Krawczyk, I. *Monatsh. Chem.* **1992**, *123*, 43.
(26)   Forrester, A. R.; Hay, J. M.; Thomson, R. H. *Organic Chemistry of Stable Free Radicals*; Academic Press: London, 1968.
(27)   Wertz, J. E.; Bolton, J. R. *Electron Spin Resonance*.
(28)   Bruker; 1.25, Shareware Version ed.; Brüker Analytische Messtechnik GmbH, 1996.
(29)   Wasserman, E.; Snyder, L. C.; Yager, W. A. *J. Chem. Phys.* **1964**, *41*, 1763.
(30)   Raphaelian, L.; Hooks, H.; Ottmann, G. *Angew. Chem. Int. Ed. Engl.* **1967**, *6*, 363.
(31)   Knorr, A. *Funktionalisierte Fluoreszenzfarbstoffe auf Anthracen-und Pyrenbasis*; University of Regensburg: Regensburg, 1995.

References Chapter 5.

(1)   Shultz, D. A.; Fico, R. M., Jr.; Bodnar, S. H.; Kumar, R. K.; Vostrikova, K. E.; Kampf, J. W.; Boyle, P. D. *J. Am. Chem. Soc.* **2003**, *125*, 11761.

(2)   Shultz, D. A.; Lee, H.; Fico, R. M., Jr. *Tetrahedron* **1999**, *55*, 12079.

(3)   Borden, W. T.; Davidson, E. R. *J. Am. Chem. Soc.* **1977**, *99*, 4587.

(4)   Dougherty, D. A. *Acc. Chem. Res.* **1991**, *24*, 88.

(5)   Rajca, A. *Chem. Rev.* **1994**, *94*, 871.

(6)   Lahti, P. M., Ed. *Magnetic Properties of Organic Materials*; Marcel Dekker: New York, 1999.

(7)   For work on substiuent and conformation effects on biradicals using computational chemistry and EPR spectroscopy, see the following: West, A. P., Jr.; Silverman, S. K.; Dougherty, D. A. *J. Am. Chem. Soc.* **1996**, *118*, 1452; Silverman, S. K.; Dougherty, D. A. *J. Phys. Chem.* **1993**, *97*, 13273.

(8)   West, A. P., Jr.; Silverman, S. K.; Dougherty, D. A. *J. Am. Chem. Soc.* **1996**, *118*, 1452.

(9)   For electronic modulation of *J* for singlet ground-state biradicals, see: Berson, J. A. Structural Determinants of the Chemical and Magnetic Properties of Non-Kekule Molecules. In *Magnetic Properties of Organic Materials*; Lahti, P. M., Ed.; Marcel Dekker: New York, 1999, pp 7.

(10)   Shultz, D. A.; Bodnar, S. H.; Lee, H.; Kampf, J. W.; Incarvito, C. D.; Rheingold, A. L. *J. Am. Chem. Soc.* **2002**, *124*, 10054.

(11)   Shultz, D. A. *Conformational Exchange Modulation in Trimethylenemethane (TMM)-Type Biradicals*; In *Magnetic Properties of Organic Materials*; Lahti, P., Ed.; Marcel Dekker, Inc.: New York, 1999.

(12)   Dei, A.; Gatteschi, D.; Sangregorio, C.; Sorace, L.; Vaz, M. G. F. *Inorg. Chem.* **2003**, *42*, 1701.

(13)   Fujita, J.; Tanaka, M.; Suemune, H.; Koga, N.; Matsuda, K.; Iwamura, H. *J. Am. Chem. Soc.* **1996**, *118*, 9347.

(14)   Okada, K.; Imakura, T.; Oda, M.; Murai, H.; Baumgarten, M. *J. Am. Chem. Soc.* **1996**, *118*, 3047.

(15)   Adam, W.; van Barneveld, C.; Bottle, S. E.; Engert, H.; Hanson, G. R.; Harrer, H. M.; Heim, C.; Nau, W. M.; Wang, D. *J. Am. Chem. Soc.* **1996**, *118*, 3974.

(16)   Fang, S.; Lee, M.-S.; Hrovat, D. A.; Borden, W. T. *J. Am. Chem Soc.* **1995**, *117*, 6727.

(17)   Silverman, S. K.; Dougherty, D. A. *J. Phys. Chem.* **1993**, *97*, 13273.

(18)   Kanno, F.; Inoue, K.; Koga, N.; Iwamura, H. *J. Am. Chem. Soc.* **1993**, *115*, 847.

(19)   Dvolaitzky, M.; Chiarelli, R.; Rassat, A. *Angew. Chem., Int. Ed. Engl.* **1992**, *31*, 180.

(20)   Shultz, D. A.; Boal, A. K.; Lee, H.; Farmer, G. T. *J. Org. Chem.* **1999**, *64*, 4386.

(21)   Shultz, D. A.; Boal, A. K.; Lee, H.; Farmer, G. T. *J. Org. Chem.* **1998**, *63*, 9462.

(22)   Ruf, M.; Noll, B. C.; Groner, M. D.; Yee, G. T.; Pierpont, C. G. *Inorg. Chem.* **1997**, *36*, 4860.

(23)   Scheeren, J. W.; Ooms, P. H. J.; Nivard, R. J. F. *Synthesis* **1973**, 149.

(24)   Shultz, D. A.; Bodnar, S. H.; Kampf, J. W. *Chem. Commun.* **2001**, 93.

(25)   Pierpont, C. G.; Lange, C. W. *Prog. Inorg. Chem.* **1994**, *41*, 331.
(26)   Ruf, M.; Lawrence, A. M.; Noll, B. C.; Pierpont, C. G. *Inorg. Chem.* **1998**, *37*, 1992.
(27)   Shultz, D. A.; Bodnar, S. H.; Kumar, R. K.; Lee, H.; Kampf, J. W. *Inorg. Chem.* **2001**, *40*, 546.
(28)   Wasserman, E.; Snyder, L. C.; Yager, W. A. *J. Chem. Phys.* **1964**, *41*, 1763.
(29)   Some of the g=2 signal is a double-quantum transition as shown by power dependence studies, see: deGroot, M. S.; van der Waals, J. H. *Physica* **1963**, *29*, 1128.
(30)   Bruker; 1.25, Shareware Version ed.; Brüker Analytische Messtechnik GmbH, 1996.
(31)   Shultz, D. A.; Boal, A. K.; Farmer, G. T. *J. Am. Chem. Soc.* **1997**, *119*, 3846.
(32)   Berson, J. A., Ed. *The Chemistry of the Quinonoid Compounds, Vol. II*; John Wiley & Sons: New York, 1988.
(33)   Shultz, D. A.; Boal, A. K.; Driscoll, D. J.; Farmer, G. T.; Hollomon, M. G.; Kitchin, J. R.; Miller, D. B.; Tew, G. N. *Mol. Cryst. Liq. Cryst.* **1997**, *305*, 303.
(34)   Kahn, O. *Molecular Magnetism*; VCH: New York, 1993.
(35)   Bleaney, B.; Bowers, K. D. *Proc. R. Soc. London* **1952**, *A214*, 451.
(36)   O'Connor, C. J. *Prog. Inorg. Chem.* **1982**, *29*, 203.
(37)   Caneschi, A.; Dei, A.; Mussari, C. P.; Shultz, D. A.; Sorace, L.; Vostrikova, K. E. *Inorg. Chem.* **2002**, *41*, 1086.
(38)   Ullmann, E. F.; Boocock, D. G. B. *Chem. Comm.* **1969**, 1161.
(39)   Mukai, K.; Tamaki, T. *Bull. Chem. Soc. Jpn.* **1977**, *50*, 1239.
(40)   Sandberg, K. A.; Shultz, D. A. *J. Phys. Org. Chem.* **1998**, *11*, 819.
(41)   We were unsuccessful at calculating the ZFS parameters for our biradicals using the methods described in Sandberg, K. A.; Shultz, D. A. *J. Phys. Org. Chem.* **1998**, *11*, 819., possibly due to the fact several of the biradicals are between the extremes of disjoint and nondisjoint.
(42)   Hatfield, W. E. *Chapter 7. Properties of Condensed Compounds (Compounds with Spin Exchange)*; In *Theory and applications of molecular paramagnetism*; Boudreaux, E. A., Mulay, L. N., Eds.; Wiley Interscience: New York, 1976, pp 381.
(43)   Anderson, P. W. *Phys. Rev.* **1959**, *115*, 2.
(44)   Karplus, M. *J. Am. Chem. Soc.* **1963**, *85*, 2870.
(45)   Streitwieser, A., Jr. *Molecular Orbital Theory for Organic Chemists*; In *Molecular Orbital Theory for Organic Chemists*; Wiley & Sons: New York, 1961, p 16.
(46)   The same qualitative result is also obtained from a $\cos(f_1)\cos(f_2)$ function.
(47)   Wenthold, P. G.; Hu, J.; Squires, R. R.; Lineberger, W. C. *J. Am. Chem. Soc.* **1996**, *118*, 475.
(48)   Wenthold, P. G.; Kim, J. B.; Lineberger, W. C. *J. Am. Chem. Soc.* **1997**, *119*, 1354.
(49)   Shultz, D. A.; Fico, R. M., Jr.; Lee, H.; Kampf, J. W.; Kirschbaum, K.; Pinkerton, A. A.; Boyle, P. D. *J. Am. Chem. Soc.* **2003**, *125*, in press.

(50)   Shultz, D. A.; Fico, R. M., Jr.; Boyle, P. D.; Kampf, J. W. *J. Am. Chem. Soc.* **2001**, *123*, 10403.

(51)   Shultz, D. A.; Farmer, G. T. *J. Org. Chem.* **1998**, *63*, 6254.

(52)   Shultz, D. A.; Bodnar, S. H. *Inorg. Chem.* **1999**, *38*, 591.

References Chapter 6.

(1)   Shultz, D. A.; Fico, R. M., Jr.; Lee, H.; Kampf, J. W.; Kirschbaum, K.; Pinkerton, A. A.; Boyle, P. D. *J. Am. Chem. Soc.* **2003**, *Accepted*.

(2)   Shultz, D. A.; Fico, R. M., Jr.; Boyle, P. D.; Kampf, J. W. *J. Am. Chem. Soc.* **2001**, *123*, 10403.

(3)   Shultz, D. A. *Conformational Exchange Modulation in Trimethylenemethane (TMM)-Type Biradicals*; In *Magnetic Properties of Organic Materials*; Lahti, P., Ed.; Marcel Dekker, Inc.: New York, 1999.

(4)   Dei, A.; Gatteschi, D.; Sangregorio, C.; Sorace, L.; Vaz, M. G. F. *Inorg. Chem.* **2003**, *42*, 1701.

(5)   Fujita, J.; Tanaka, M.; Suemune, H.; Koga, N.; Matsuda, K.; Iwamura, H. *J. Am. Chem. Soc.* **1996**, *118*, 9347.

(6)   Okada, K.; Imakura, T.; Oda, M.; Murai, H.; Baumgarten, M. *J. Am. Chem. Soc.* **1996**, *118*, 3047.

(7)   Adam, W.; van Barneveld, C.; Bottle, S. E.; Engert, H.; Hanson, G. R.; Harrer, H. M.; Heim, C.; Nau, W. M.; Wang, D. *J. Am. Chem. Soc.* **1996**, *118*, 3974.

(8)   Fang, S.; Lee, M.-S.; Hrovat, D. A.; Borden, W. T. *J. Am. Chem Soc.* **1995**, *117*, 6727.

(9)   Silverman, S. K.; Dougherty, D. A. *J. Phys. Chem.* **1993**, *97*, 13273.

(10)   Kanno, F.; Inoue, K.; Koga, N.; Iwamura, H. *J. Am. Chem. Soc.* **1993**, *115*, 847.

(11)   Dvolaitzky, M.; Chiarelli, R.; Rassat, A. *Angew. Chem., Int. Ed. Engl.* **1992**, *31*, 180.

(12)   Kaftory, M.; Nugiel, D. A.; Biali, S. E.; Rappoport, Z. *J. Am. Chem. Soc.* **1989**, *111*, 8181.

(13)   Dougherty, D. A. *Acc. Chem. Res.* **1991**, *24*, 88.

(14)   Rajca, A. *Chem. Rev.* **1994**, *94*, 871.

(15)   Shultz, D. A.; Fico, R. M., Jr.; Bodnar, S. H.; Kumar, R. K.; Vostrikova, K. E.; Kampf, J. W.; Boyle, P. D. *J. Am. Chem. Soc.* **2003**, *125*, 11761.

(16)   Borden, W. T.; Davidson, E. R. *J. Am. Chem. Soc.* **1977**, *99*, 4587.

(17)   Borden, W. T., Ed. *Diradicals*; Wiley: New York, 1982.

(18)   Borden, W. T.; Iwamura, H.; Berson, J. A. *Acc. Chem. Res.* **1994**, *27*, 109.

(19)   Shultz, D. A.; Boal, A. K.; Lee, H.; Farmer, G. T. *J. Org. Chem.* **1999**, *64*, 4386.

(20)   Wenthold, P. G.; Hu, J.; Squires, R. R.; Lineberger, W. C. *J. Am. Chem. Soc.* **1996**, *118*, 475.

(21)   Wenthold, P. G.; Kim, J. B.; Lineberger, W. C. *J. Am. Chem. Soc.* **1997**, *119*, 1354.

(22)   Streitwieser, A., Jr. *Molecular Orbital Theory for Organic Chemists*; In *Molecular Orbital Theory for Organic Chemists*; Wiley & Sons: New York, 1961, p 16.

(23)   The same qualitative result is also obtained from a $\cos(f_1)\cos(f_2)$ function.

(24)   Anderson, P. W. *Phys. Rev.* **1959**, *115*, 2.

(25)   Hatfield, W. E. *Chapter 7. Properties of Condensed Compounds (Compounds with Spin Exchange)*; In *Theory and applications of molecular paramagnetism*; Mulay, L. N., Ed.; Wiley Interscience: New York, 1976, pp 381.

(26)   Matsumoto, T.; Koga, N.; Iwamura, H. *J. Am. Chem. Soc.* **1992**, *114*, 5448.

(27)   Matsumoto, T.; Ishida, T.; Koga, N.; Iwamura, H. *J. Am. Chem. Soc.* **1992**, *114*, 9952.

(28)   Mugnoli, A.; Simonetta, M. *J. Chem. Soc. Perkin Trans. 2* **1976**, 1831.

(29)   Shultz, D. A.; Boal, A. K.; Farmer, G. T. *J. Am. Chem. Soc.* **1997**, *119*, 3846.

(30)   Aurich, H. G.; Hahn, K.; Stork, K.; Weiss, W. *Tetrahedron* **1977**, *33*, 969.

(31)   Kahn, O. *Molecular Magnetism*; VCH: New York, 1993.

(32)   Bleaney, B.; Bowers, K. D. *Proc. R. Soc. London* **1952**, *A214*, 451.

(33)   O'Connor, C. J. *Prog. Inorg. Chem.* **1982**, *29*, 203.

(34)   Caneschi, A.; Dei, A.; Mussari, C. P.; Shultz, D. A.; Sorace, L.; Vostrikova, K. E. *Inorg. Chem.* **2002**, *41*, 1086.

(35)   Georges, R.; Borras-Almenar, J. J.; Coronado, E.; Curely, J.; Drillon, M. *One-dimensional Magnetism: An Overview of the Models*; In *Magnetism: Molecules to Materials, Models and Experiments*; Drillon, M., Ed.; Wiley-VCH: New York, 2001, pp 1.

(36)   Karplus, M. *J. Am. Chem. Soc.* **1963**, *85*, 2870.

(37)   Shultz, D. A.; Gwaltney, K. P.; Lee, H. *J. Org. Chem.* **1998**, *63*, 769.

(38)   Wheeler, D. E.; Rodriquez, J. H.; McCusker, J. K. *J. Phys. Chem. A* **1999**, *103*, 4101.

(39)   Jacobs, S. J.; Shultz, D. A.; Jain, R.; Novak, J.; Dougherty, D. A. *J. Am. Chem. Soc.* **1993**, *115*, 1744.

(40)   Rajca, A. *High-Spin Polyradicals*; In *Magnetic Properties of Organic Materials*; Lahti, P., Ed.; Marcel Dekker, Inc.: New York, 1999, pp 345.

References Chapter 7.

(1)   Shultz, D. A.; Fico, R. M., Jr.; Bodnar, S. H.; Kumar, R. K.; Vostrikova, K. E.; Kampf, J. W.; Boyle, P. D. *J. Am. Chem. Soc.* **2003**, *125*, 11761.

(2)   Fico, R. M., Jr.; Hay, M. F.; Reese, S.; Hammond, S.; Lambert, E.; Fox, M. A. *J. Org. Chem.* **1999**, *64*, 9386.

(3)   Shultz, D. A.; Lee, H.; Fico, R. M., Jr. *Tetrahedron* **1999**, *55*, 12079.

(4)   Shultz, D. A.; Fico, R. M., Jr.; Boyle, P. D.; Kampf, J. W. *J. Am. Chem. Soc.* **2001**, *123*, 10403.

(5)   Shultz, D. A.; Fico, R. M., Jr.; Lee, H.; Kampf, J. W.; Kirschbaum, K.; Pinkerton, A. A.; Boyle, P. D. *J. Am. Chem. Soc.* **2003**, *125*, in press.

(6)   Borden, W. T.; Iwamura, H.; Berson, J. A. *Acc. Chem. Res.* **1994**, *27*, 109.

(7)   Bush, L. C.; Heath, R. B.; Feng, X. W.; Wang, P. A.; Maksimovic, L.; Song, A. I.; Chung, W.-S.; Berinstain, A. B.; Scaiano, J. C.; Berson, J. A. *J. Am. Chem. Soc.* **1997**, *119*, 1406.

(8)   Caneschi, A.; Gatteschi, D.; Sessoli, R.; Rey, P. *Acc. Chem. Res.* **1989**, *22*, 392.

(9)   Carlin, R. L. *Magnetochemistry*; Springer-Verlag: New York, 1986.

(10)   Dougherty, D. A. *Acc. Chem. Res.* **1991**, *24*, 88.

(11)   Gatteschi, D., Ed. *Molecular Magnetic Materials*; Kluwer Academic Publishers: Amsterdam, 1991.

(12)   Gatteschi, D.; Sessoli, R. *J. Magn. Magn. Mat.* **1992**, *104*, 2092.

(13)   Iwamura, H.; Koga, N. *Acc. Chem. Res.* **1993**, *26*, 346.

(14)   Kahn, O. *Molecular Magnetism*; VCH: New York, 1993.

(15)   Lahti, P. M., Ed. *Magnetic Properties of Organic Materials*; Marcel Dekker: New York, 1999.

(16)   Rajca, A. *Chem. Rev.* **1994**, *94*, 871.

(17)   Hicks, R. G. *Aust. J. Chem.* **2001**, *54*, 597.

(18)   Pierpont, C. G.; Buchanan, R. M. *Coord. Chem. Rev.* **1981**, *38*, 45.

(19)   Pierpont, C. G.; Lange, C. W. *Prog. Inorg. Chem.* **1994**, *41*, 331.

(20)   Pierpont, C. G.; Attia, A. S. *Coll. Czech. Chem. Comm.* **2001**, *66*, 33.

(21)   Amabilino, D. B.; Veciana, J. *Nitroxide-based Organic Magnets*; In *Magnetism: Molecules to Materials II: Molecule-Based Materials*; Miller, J. S., Drillon, M., Eds.; Wiley-VCH: New York, 2001, pp 1.

(22)   Berson, J. A., Ed. *The Chemistry of the Quinonoid Compounds, Vol. II*; John Wiley & Sons: New York, 1988.

(23)   Karplus, M. *J. Am. Chem. Soc.* **1963**, *85*, 2870

VITA

To start at the beginning, Rosario Mario Fico Jr. was born in Buffalo, NY in May 1971. The family moved to New Haven, CT where one mitten was lost into a radiation bath. This is his first know laboratory experiment. His stay in New Haven was brief, and so are his memories. In 1st grade he moved west into the wild wilderness of unincorporated northern Illinios. After graduating from Zion Benton Township High School, home of the ZeeBees, he attended Illinois State University. Home of the Redbirds. He graduated with his B.S. in Chemistry in 1994. He remained at ISU earning his Master's in hopes of getting into a better Ph.D. program than his undergraduate grades would otherwise allow. For his Master's, he worked with Professor Cheryl Stevenson on "Thermolysis and Chiral Effects involving the Substituted and Unsubstituted Cyclooctatetraene Dianions." Rosario graduated with his Master's in Chemistry in 1996. His plan of using his Master's as a stepping-stone for his Ph.D career worked. From there he moved to the University of Texas, at Austin. Home of the Longhorns, which is by far one of the best schools around. There he worked with Chancellor Marye Anne Fox, where he was able to build upon his work studying monoradicals, by studying biradicals. After his first few years his advisor moved to North Carolina State University, home of the Wolfpack. Rosario chose to move also, in part because of the opportunity to work with Professor David Shultz. While at NCSU Rosario learned that there was a sport more important than football, namely basketball. Basketball, however, did not appeal to him so he continued studying biradicals with Dr. Shultz. Rosario is thankful for his time at NCSU, partly because the Department reminds him of the Department at ISU. He is also thankful for his time at NCSU, because he was able to continue studying biradicals.

Permanent address: 3617 Marcom St., Raleigh, North Carolina 27606

This dissertation was typed by the author after taking typing lessons.